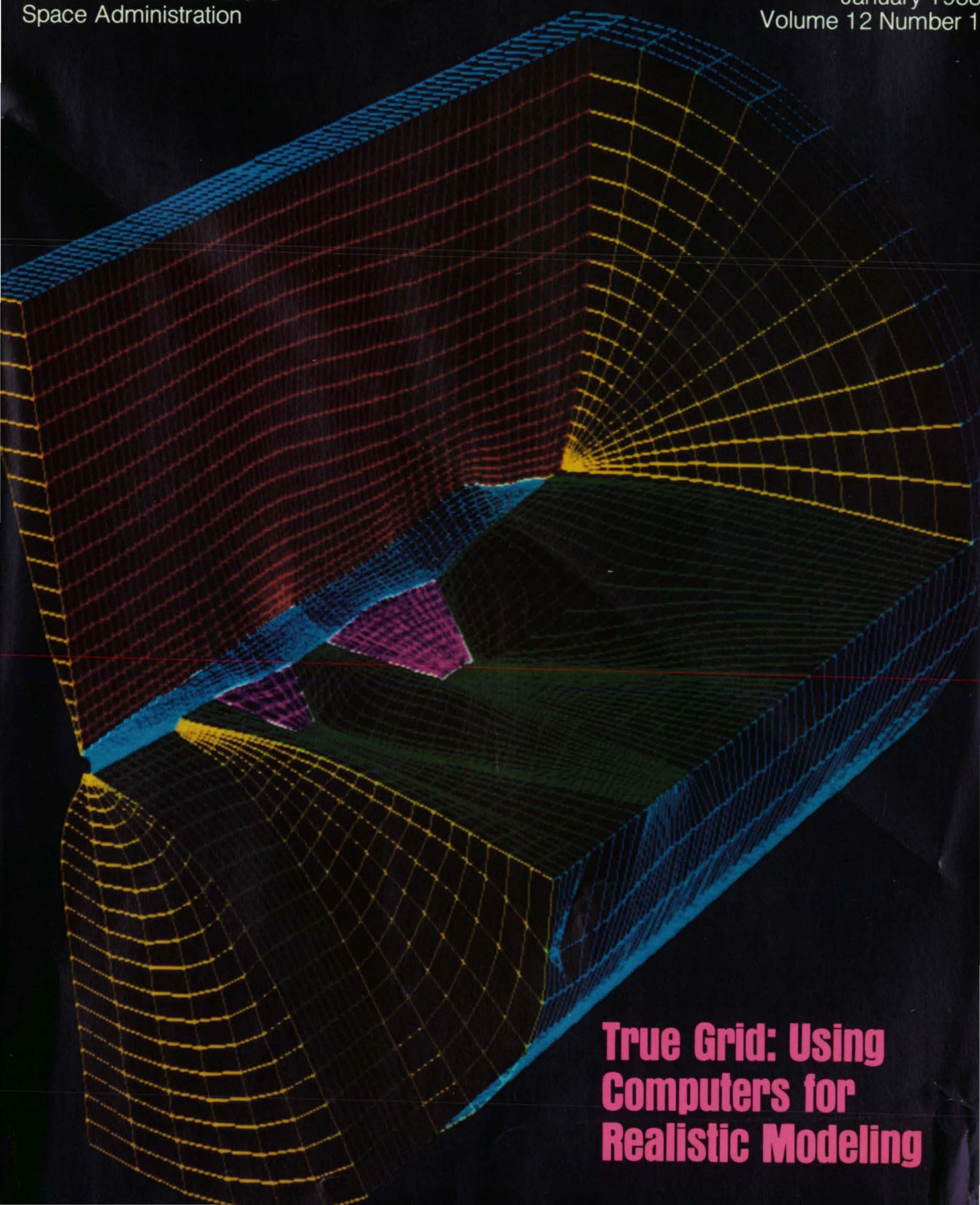
NASA Tech Briefs

National Aeronautics and Space Administration

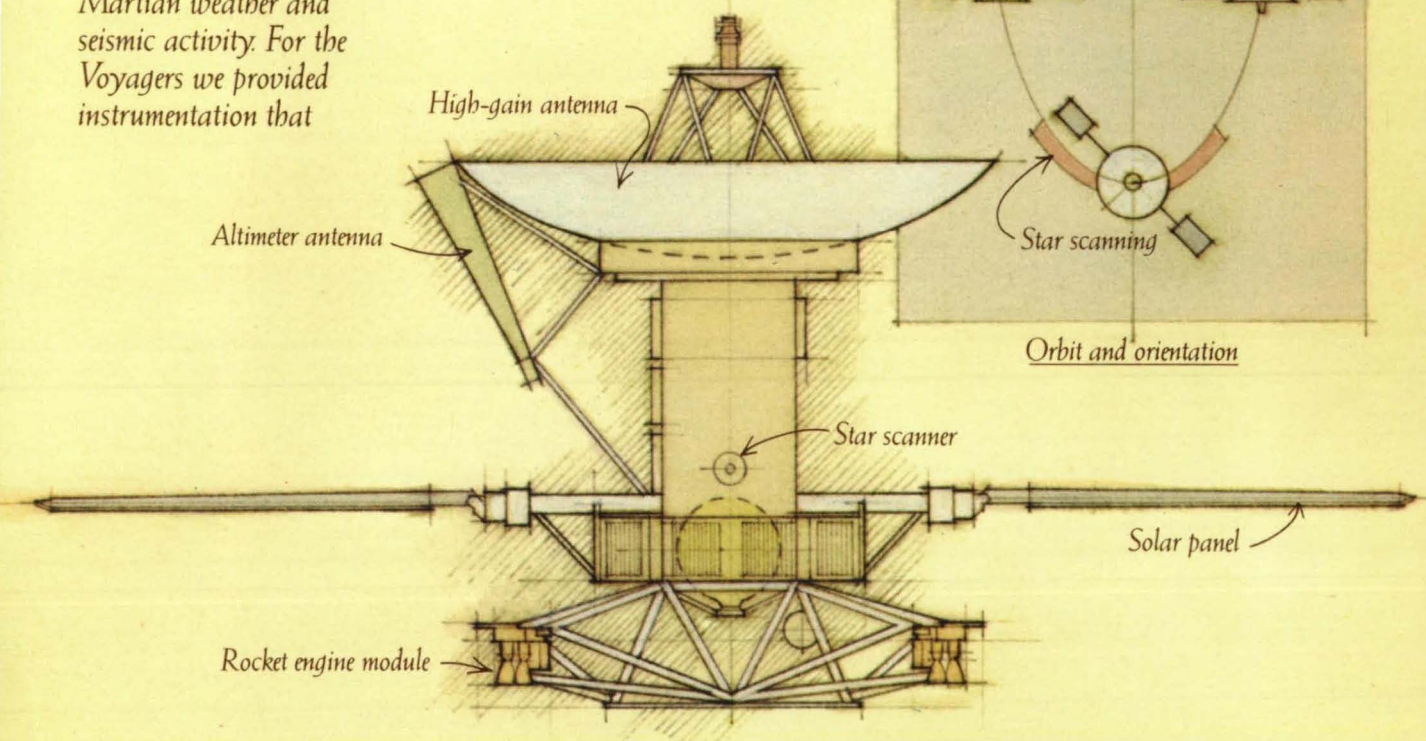
January 1988
Volume 12 Number 1



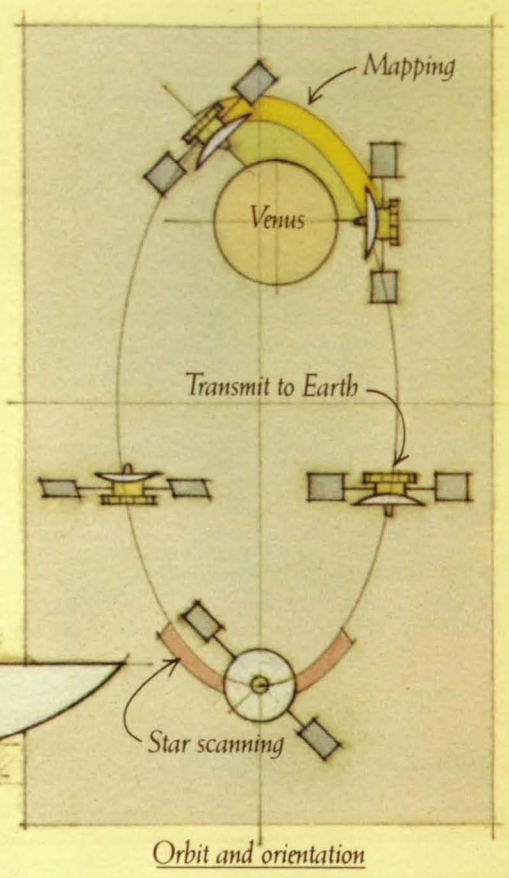
True Grid: Using Computers for Realistic Modeling

In space: looking back to look forward.

What can the nature and origin of the universe tell us about the future of Earth? To help answer that question, we make craft and instruments for traveling billions of miles in space and seeing as far as 15 billion years back in time. Martin Marietta was the integrator and builder of two Viking landers, which sent back remarkable photos of the surface of Mars, examined soil samples, and studied Martian weather and seismic activity. For the Voyagers we provided instrumentation that reported on electromagnetic activity near Jupiter and Saturn–Voyager 2 went on to Uranus, some 2 billion miles from Earth. That was nine years after launch; next destination, Neptune, in 1989. These are but a few results of Martin Marietta's ability to create survivable, mystery-solving craft and their instruments–from concept through mission completion.



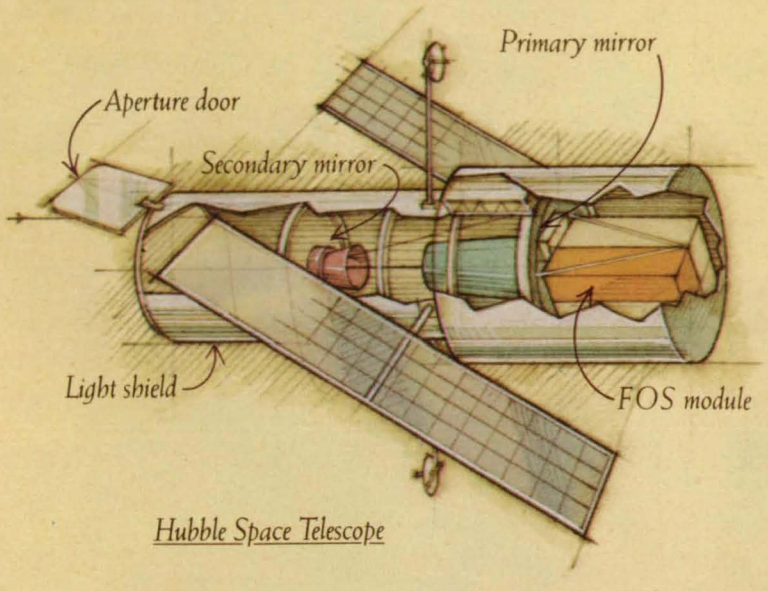
Magellan Spacecraft



Orbit and orientation

Mission: map Venus.

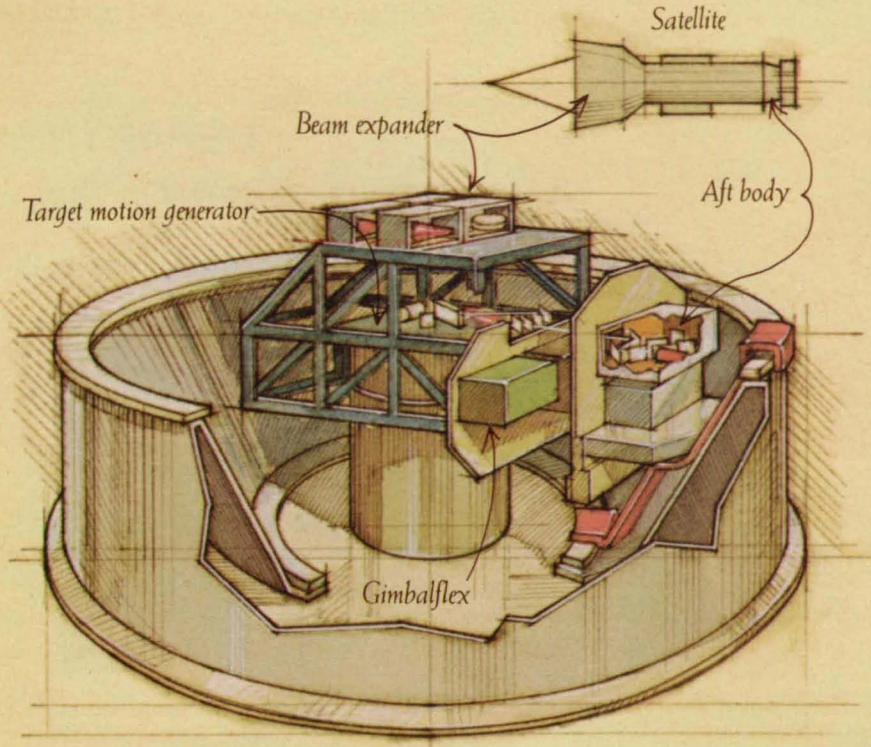
From orbit, Magellan's radar will penetrate the planet's thick, gaseous cloud cover and send back photo-like images of nearly 90% of its surface. Our role: design, integrate, build and test the craft.



Hubble Space Telescope

Viewing the infant universe.

For the Hubble Space Telescope we are providing the Faint Object Spectrograph (FOS), which will see objects up to 15 billion light-years away. Since the universe is estimated to be 18-20 billion years old, astronomers will witness events close to its birth.



Fine Pointing Simulator

The fine points of fine pointing.

Precisely controlled, space-spanning energy delivery and collection systems create difficult pointing and retargeting challenges, which we can now simulate. This new lab is working toward the precision to zero in on a football-size object 3,000 miles away, in support of the Strategic Defense Initiative research program.

Masterminding tomorrow's technologies

MARTIN MARIETTA

6801 Rockledge Drive, Bethesda, Maryland 20817, USA

NASA Tech Briefs

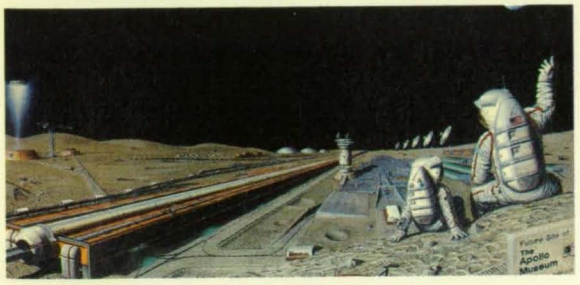
National Aeronautics and Space Administration

JANUARY 1988
Volume 12 Number 1

ABP BPA

SPECIAL FEATURES

A New Era In Technology Utilization 10

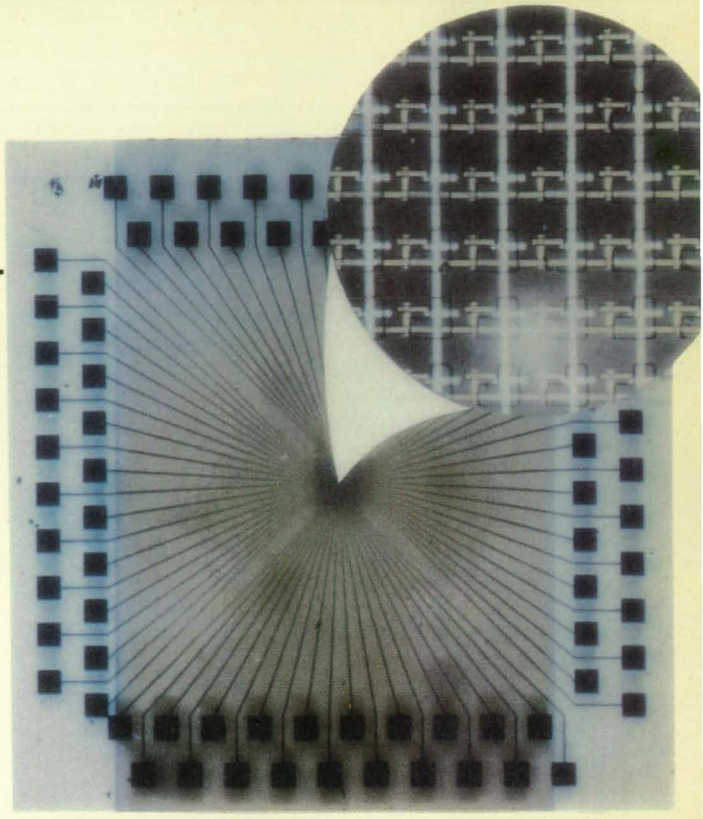


An artist's conception of a moon-based factory of the future (courtesy of the Lunar and Planetary Institute). A special report on emerging space opportunities, written by James T. Rose, NASA's new Assistant Administrator for Commercial Programs, appears on page 10.

Electronic Neurocomputers 12
Mission Accomplished 104

TECHNICAL SECTION

New Product Ideas 14
NASA TU Services 16
Electronic Components and Circuits 18
Electronic Systems 42
Physical Sciences 58
Materials 61
Computer Programs 68
Mechanics 80
Machinery 87
Fabrication Technology 93
Mathematics and Information Sciences 96
Life Sciences 78
Subject Index 101



Promising to bring machine minds leagues closer to the efficiency of the human brain, neural networks are a hot research area. At NASA's Jet Propulsion Laboratory, researchers are using advanced thin film techniques to implement 1600-synapse neural networks on a 4mm by 4mm area, as shown in the photo above. For more information about neural network developments, see page 12, and related technical briefs on pages 35, 36, 38 and 42.

DEPARTMENTS

New On The Market 100
Advertiser's Index 103

Our cover shows a cutaway view of a computer-generated grid about a simplified F-16 aircraft model. Computational fluid dynamic simulations of air flow properties are obtained at the grid intersections. Color distinguishes the different surfaces. The simulation was generated by Reese L. Sorenson, of Ames Research Center, whose tech brief on the subject appears on page 97.



How did NASA-derived technology change this young boy's life? See page 104.

This document was prepared under the sponsorship of the National Aeronautics and Space Administration. Neither Associated Business Publications Co., nor anyone acting on behalf of Associated Business Publications Co., nor the United States Government nor any person acting on behalf of the United States Government assumes any liability resulting from the use of the information contained in this document, or warrants that such use will be free from privately owned rights. The U.S. Government does not endorse any commercial product, process, or activity identified in this publication.

Permissions: Authorization to photocopy items for internal or personal use, or the internal or personal use of specific clients, is granted by Associated Business Publications, provided that the flat fee of $3.00 per copy is paid directly to the Copyright Clearance Center (21 Congress St., Salem, MA 01970). For those organizations that have been granted a photocopy license by CCC, a separate system of payment has been arranged. The fee code for users of the Transactional Reporting Service is: ISSN 0145-319X/88 $3.00 + .00

NASA Tech Briefs, ISSN 0145-319X, USPS 750-070, copyright © 1988 in U.S., is published monthly except July/August and November/December (10x per year) by Associated Business Publications Co., 41 E. 42nd St., New York, NY 10017-5391. The copyrighted information does not include the individual Tech Briefs which are supplied by NASA. Editorial, sales, production and circulation offices at 41 E. 42nd Street, New York, NY 10017-5391. Subscriptions for non-qualified subscribers in the U.S., Panama Canal Zone, and Puerto Rico, $75.00 for 1 year; $125.00 for 2 years; $200 for 3 years. Single copies $15.00. Remit by check, draft, postal or express orders. Other remittances at sender's risk. Address all communications for subscriptions or circulation to NASA Tech Briefs, 41 E. 42nd Street, New York, NY 10017-5391. Second-class postage paid at New York, NY and additional mailing offices.

POSTMASTER: please send address changes to NASA Tech Briefs, 41 E. 42nd Street, Suite 921, New York, NY 10017-5391.



The shortest distance between two points just became shorter.

DCS Announces its NEW Programmable Universal Demodulator.

DCS brings to existing, field-proven technology a new twist in innovative thinking.

The result is an FM demodulator that is a quantum leap beyond competition. For one thing, this computer controlled advance is menu-driven, with keypad entry, and stored formats. It can discriminate all 50 standard IRIG channels as well as non-standard configurations. And when you consider that the complete system is packed in a single housing and priced substantially below other units, you can understand our pride.

Innovation is not new at Data-Control Systems. For thirty years, we have been extending the leading edge in telemetry systems. Our specialty is solving problems. In fact, we've just shortened the shortest distance between two points.



DCS Universal FM Tunable Demodulator
Full 2 MHz bandwidth / Accuracy to 1 HZ / Programmable low pass filter / Tape speed compensation / Spectral display / All formats PBW, CBW-LP, CA / Large alphanumeric display / Multiple computer interfaces

Quanta Systems Corporation
Data-Control Systems
CompuDyne Defense
Electronics Group

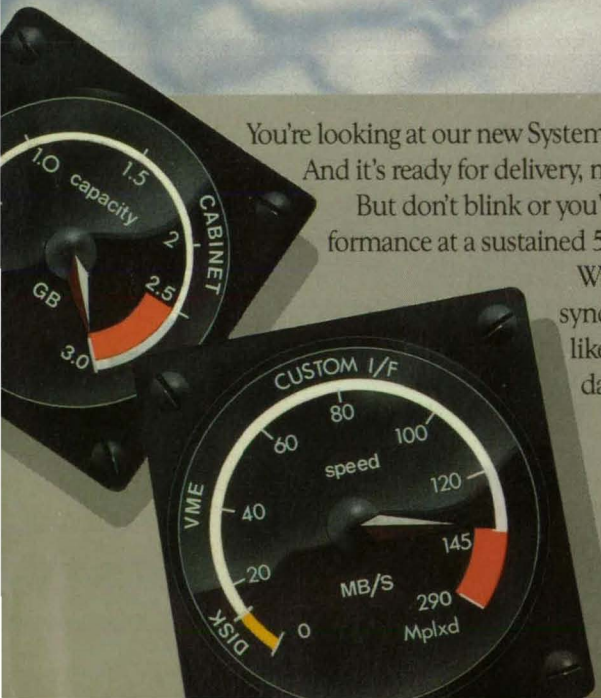
1455 Research Boulevard
Rockville, MD 20850
(301) 279-8798
TWX (710) 828-9785

8291 Westminster Ave., Suite 150
Westminster, CA 92683
(714) 984-4471
TWX (910) 596-1802

Circle Reader Action No. 371

No speed





You're looking at our new System 93 PLUS,™ the fastest solid state mass storage subsystem on the market. And it's ready for delivery, now.

But don't blink or you'll miss the Zitel 145 Megabyte/sec block transfer rate for custom bus performance at a sustained 55 nsec cycle time for 64 bit words. And there's no need to refresh.

With up to 512 Megabyte capacity per chassis based on 1 Megabit DRAMS and synchronous/asynchronous modes, our new 93 PLUS is ideal for applications like flight simulation, radar processing, uplinks/downlinks, or any high-speed data capture and buffering requirement.

There's also an off-the-shelf VME interface with a sustained 40 Megabyte/sec transfer rate.

And it does it all without hitting any speed bumps.

It's completely solid state and backed by a fully operational temperature test that's part of our continuing stringent Quality Assurance Program to ensure trouble-free system integration.



Tri-port ruggedized syste meets Mil Spec 810-C

bumps.

System 93 PLUS is a trademark of Zitel. Zitel Corporation is a public company traded on the NASDAQ National Market System.

And you'll easily avoid the biggest speed bumps of all, development time. Talk to us about our Turnkey Interface Program and we'll shift into high gear, helping you move product to market in no time.

So when you're ready to find out more about the fastest mass storage subsystem, our superior Quality Assurance Program and how a Zitel partnership works with you, simply call our toll-free number. We'll respond with a copy of "Designing for Performance with System 93."

Our engineers would like to show you how to avoid the speed bumps imposed by slower, more cumbersome solutions.



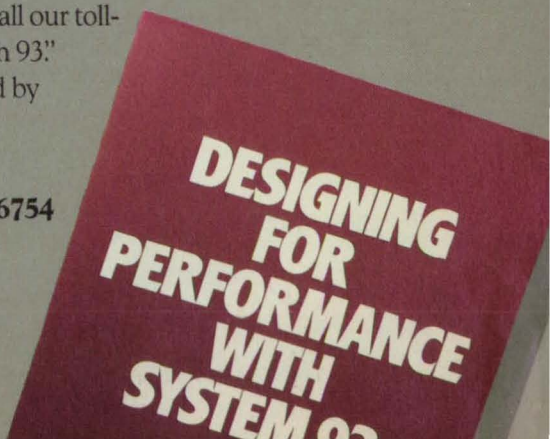
Tri-port commercial system.

Toll-free: 1-800-622-5020
In California (collect): (408) 946-9600 FAX: (408) 262-6754
TWX: 910-338-0567 TLX: 171607 ZITEL SNJ

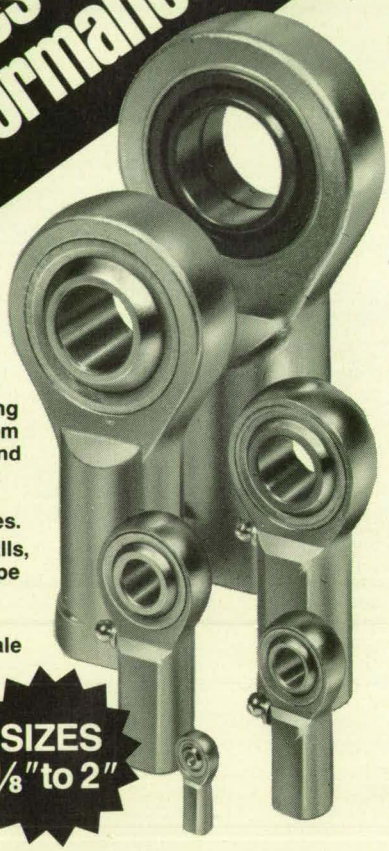
630 Alder Drive
Milpitas, CA 95035

zitel *Memories of the future*

Circle Reader Action No. 555



ROD ENDS- Across-the-Board AURORA Quality Improves Your Product Performance!



- Rod ends and bearing in standard or custom design for regular and special applications for aerospace and most other industries.
- Precision ground balls, single piece race type construction.
- High misalignment units available in male and female models.

SIZES 1/8" to 2"

Aurora Bearing Company offers a complete line of quality rod ends and linkages to provide nearly trouble-free performance. Expertly designed and competitively priced, you'll find that they will improve the life and important functions of your products.



NEW!

Write for FREE 36-page catalog.

Aurora Bearing—the MOTION TRANSFER SPECIALISTS!

AURORA BEARING COMPANY
970 South Lake Street
Aurora, Illinois 60506 • Ph. 312 859-2030
TELEX: 280079 AUR BRGS/FAX #8590971

NASA Tech Briefs

National Aeronautics and Space Administration

ABP VBPA

NASA Tech Briefs:

Published by ..... **Associated Business Publications**
Editor-in-Chief ..... **Bill Schnirring**
Publisher ..... **Thomas H. King**
Associate Publisher ..... **Frank Nothaft**
Associate Publisher ..... **Robin J. DuCharme**
Managing Editor ..... **R. J. Laer**
Associate Editor ..... **Leo D. Kluger**
Associate Editor ..... **Joseph T. Pramberger**
Technical Advisor ..... **Dr. Robert E. Waterman**
Production Manager ..... **Rita Nothaft**
Traffic Manager ..... **James E. Cobb**
Circulation Director ..... **Anita Weissman**
Controller ..... **Neil B. Rose**
Awards Manager ..... **Evelyn Mars**
Reader Service Manager ..... **Arlene Berrios**

Technical Staff:

Briefs prepared for National Aeronautics and Space Administration by **Logical Technical Services Corp.**, NY, NY
Technical/Managing Editor ..... **Ted Selinsky**
Art Director ..... **Ernest Gillespie**
Administrator ..... **Elizabeth Texeira**
Chief Copy Editor ..... **Lorne Bullen**
Staff Editors ..... **Dr. James Boyd, Dr. Larry Gruenberger, Jordan Randjelovich, George Watson, Oden Browne, Joseph Renzler**
Graphics ..... **Luis Martinez, Vernald Gillman, Charles Sammartano**
Editorial & Production **Bill Little, Frank Ponce, Ivonne Valdes, Paul Marcus**

NASA:

NASA Tech Briefs are provided by the National Aeronautics and Space Administration, Technology Utilization Division, Washington, DC:
Administrator ..... **Dr. James C. Fletcher**
Assistant Administrator for Commercial Programs ..... **James T. Rose**
Deputy Assistant Administrator (Programs) ..... **Henry J. Clarks**
Deputy Director TU Division (Publications Manager) ..... **Leonard A. Ault**

Associated Business Publications
41 East 42nd Street, Suite 921, New York, NY 10017-5391
(212) 490-3999

President ..... **Bill Schnirring**
Executive Vice President ..... **Frank Nothaft**
Vice President Marketing ..... **Mark J. Seltman**
Vice President ..... **John K. Abely**

Advertising:

New York Office: (212) 490-3999
Sales Manager ..... **Robin DuCharme**
Account Executive (Mid-Atlantic) ..... **Dick Soule**
Account Executive (Midwest) ..... **Michelle Larsen**
Advertising Coordination Manager ..... **Erving Dockery, Jr.**
Account Executives (Eastern MA, NH, ME, RI) ... **Lee Arpin** at (617) 899-5613; **Bill Doucette** at (617) 278-7792
Account Executive (Western MA, CT, VT) .... **George Watts** at (413) 596-4747
Account Executives (No. Calif., UT) ..... for Area Code 415—**Janice Richey King** and for Area Code 408—**Richard Cassidy** at (415) 656-3613
Account Executives (So. Calif., AZ, NV, NM) ..... for Area Codes 818/213/805—**Thomas Stillman** or **Dana Gindoff** and for Area Codes 619/714—**Leslie Alley** at (213) 541-4699

NTBM-Research Center

Project Director ..... **Mark J. Seltman**
Account Supervisor ..... **Lourdes Del Valle**



LP4000 with
Multi-pen Changer

Here's what to look for when you want great value

IOLINE plotters are designed to give you more flexibility and features for less cost than any other machine of their kind.

For example, our plotters draw not only on A through E sizes of media, but also plot on hundreds of in-between sizes from 1.5″×1.5″ up to 37″ wide roll stock. This saves you time and money by allowing you to make "check plots" on small, low-cost paper before committing to full-size media for final work.

It's easy also to set paper size, pen speed, micro-calibration, plot rotation—everything exactly as you want—by just tapping a few keys on the plotter's intelligent keypad. Plus, up to 3 sets of personalized defaults can be saved in its non-volatile memory.

They're fast, too. Our high-performance LP4000™ draws at speeds selectable up to 20 inches per second (ips) axially with .001″ resolution. For less demanding applications, our economical LP3700™ plots up to 10 ips axially with .0025″ resolution.

Another feature is compatibility. IOLINE plotters emulate both HP-GL and DM/PL plotter languages so they work with a host of software like AutoCAD, VersaCAD, and CADKEY, to name a few.

Furthermore, our Multi-pen Changer™ option holds up to 20 pens and, with our hyperBUFFER™ option, you can dramatically increase plotting throughput with intelligent vector sorting and compression buffering of up to 1MB of plot data.

Now here's the clincher: Our top-gun LP4000 costs just $5,495* less options. And there are other models priced even lower!

Why wait? Call us now at **1-206-775-7861.** Or, circle our reader service number and we'll gladly send you our brochure.

Remember, getting your money's worth—that's what IOLINE plotters are all about.

IOLINE™

LARGE-FORMAT PEN PLOTTERS

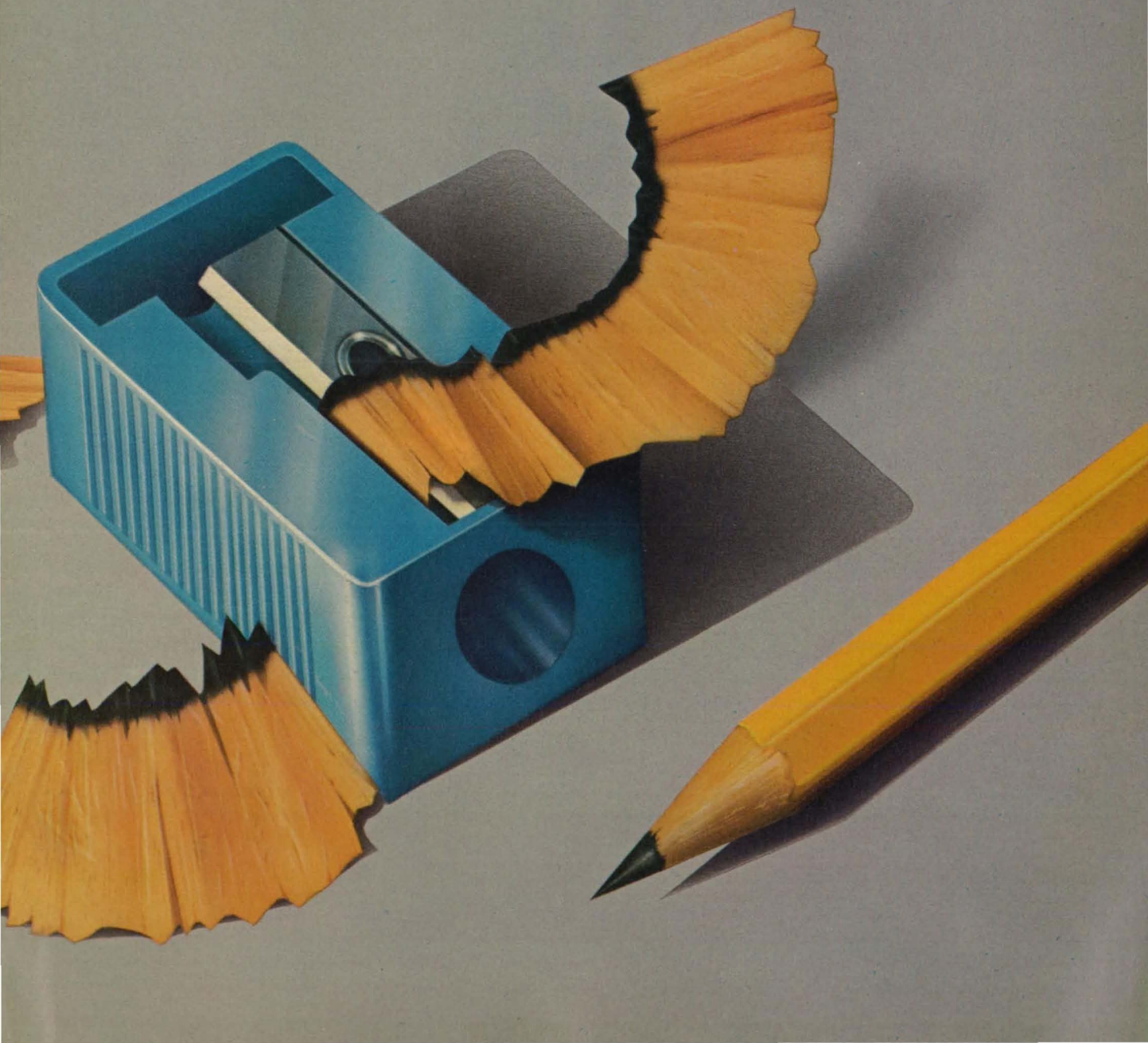
Circle Reader Action No. 472

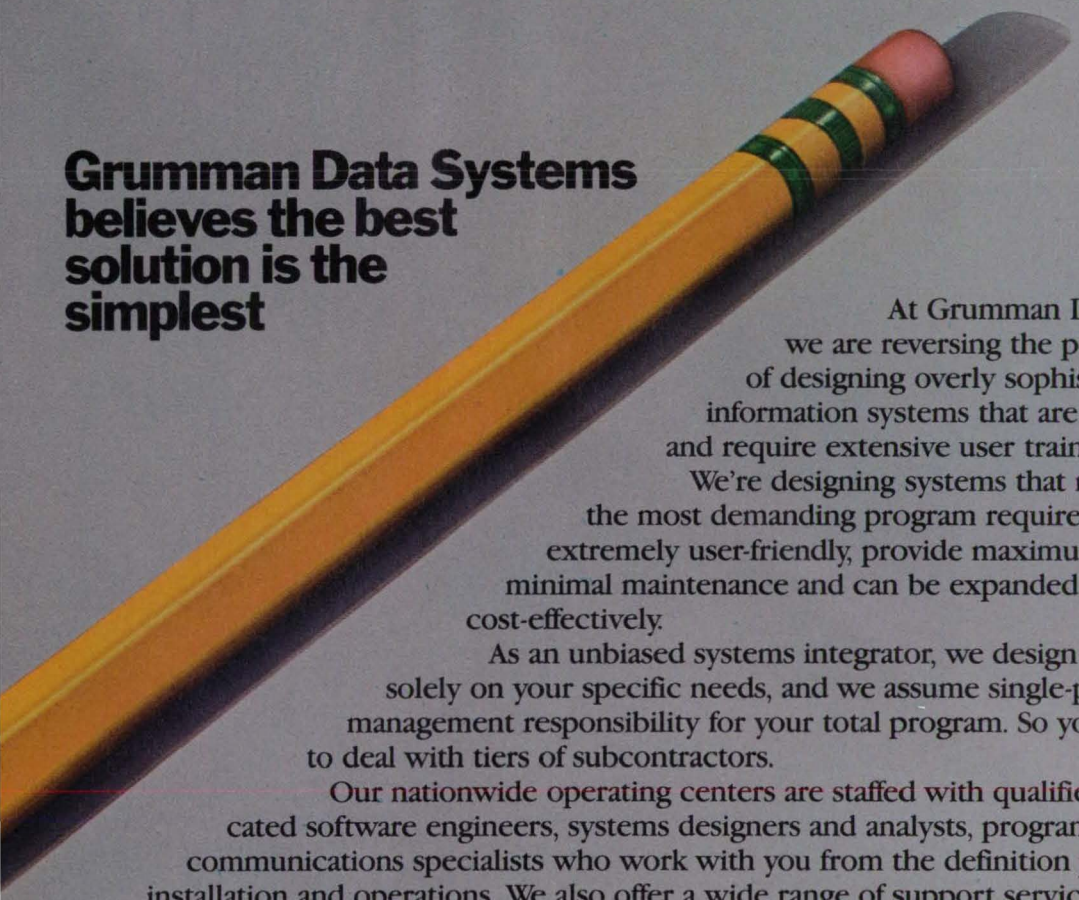
IOLINE CORPORATION 19417-36TH AVE. W LYNNWOOD, WASH. 98036 (206) 775-7861 TELEX 4949856 IC UI FAX (206) 775-2818

LP4000, LP3700, Multi-pen Changer, and hyperBUFFER are trademarks of Ioline Corporation. AutoCAD is a registered trademark of Auto Desk Inc. VersaCAD is a registered trademark of T&W Systems. CADKEY is a registered trademark of MicroControl Systems, Inc. *Suggested U.S. List price.

AVAILABLE ON GSA CONTRACT

A GREAT SOLUTION DOESN'T HAVE TO BE COMPLICATED





Grumman Data Systems believes the best solution is the simplest

At Grumman Data Systems, we are reversing the popular trend of designing overly sophisticated information systems that are costly to build and require extensive user training.

We're designing systems that not only meet the most demanding program requirements, but are extremely user-friendly, provide maximum up-time with minimal maintenance and can be expanded easily and cost-effectively.

As an unbiased systems integrator, we design our systems solely on your specific needs, and we assume single-point management responsibility for your total program. So you don't have to deal with tiers of subcontractors.

Our nationwide operating centers are staffed with qualified and dedicated software engineers, systems designers and analysts, programmers and communications specialists who work with you from the definition phase through installation and operations. We also offer a wide range of support services, including training, facilities management, systems maintenance, automated publishing and micrographics.

So if you have a systems integration problem, bring it to Grumman Data Systems. We'll solve it on time and within budget. It's that simple. For more information, contact Wesley R. Stout, Director, Technical Services, Grumman Data Systems, 1000 Woodbury Road, Woodbury, NY 11797. (516) 682-8500.

® Grumman is a registered trademark of Grumman Corporation

GRUMMAN®

Circle Reader Action No. 363



A New Era In Technology Utilization

by James T. Rose

James T. Rose is NASA's new Assistant Administrator for Commercial Programs. Mr. Rose began his aerospace career at NASA's Langley Research Center in 1957. He later served as Director of McDonnell Douglas' Electrophoresis Operations in Space Program, where he pioneered space industrial manufacturing. In 1986 he left industry to rejoin NASA.

After 25 years of remarkable achievement in fostering the application of aerospace technology to earthbound industry, a new era of technology utilization is emerging in the form of commercial space ventures. NASA research and development activities in the coming age of Space Station, advanced space transportation, and expansion into the solar system will offer U.S. industry new commercial opportunities with potential for strengthening the U.S. economy and securing a leadership position in global competition.

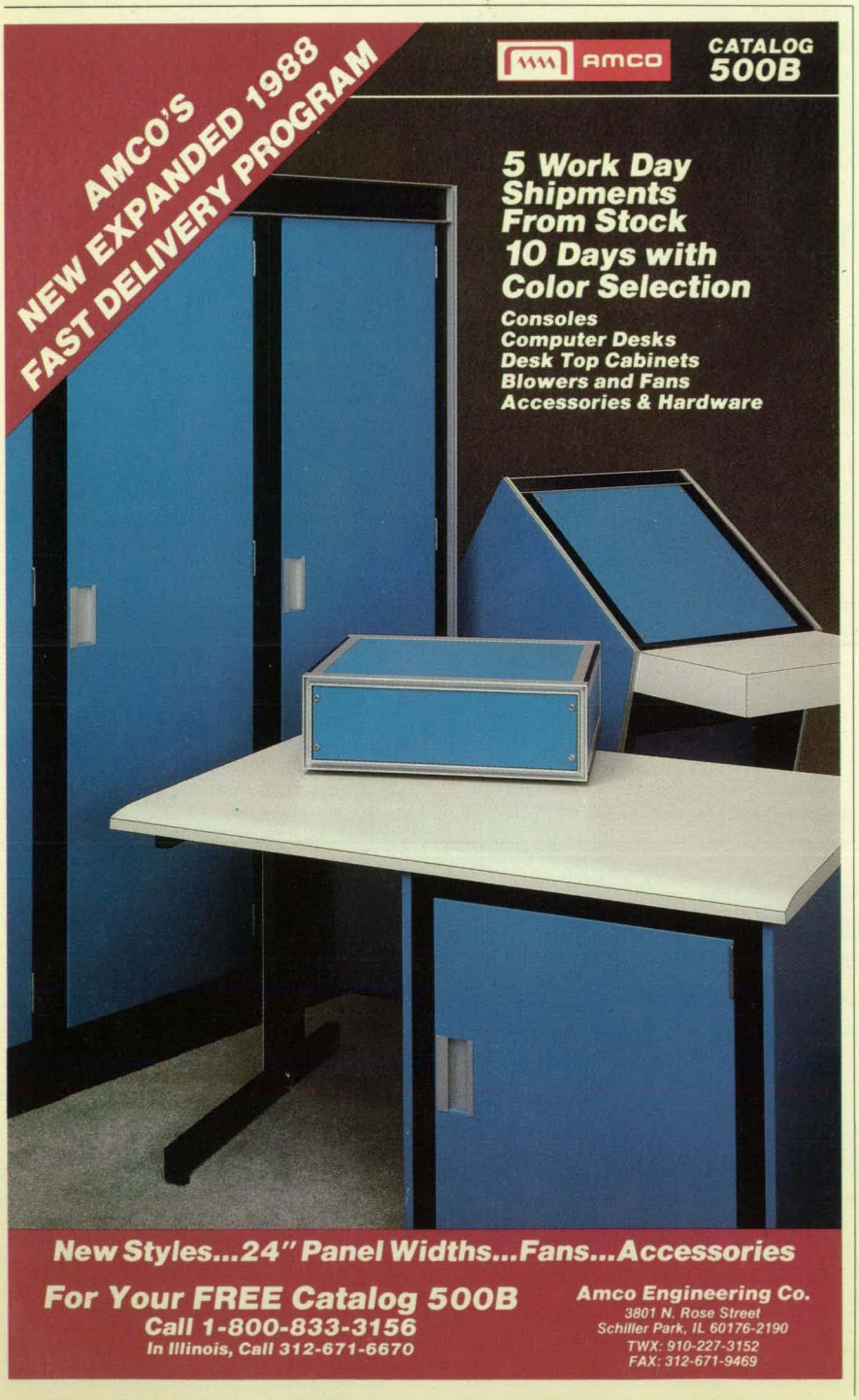
We in the NASA Office of Commercial Programs believe that greater involvement by the private sector is essential to keep America competitive in the harvesting of space resources. Our mission is to encourage the maximum commercial use of space and to promote NASA technology applications by U.S industry. To accomplish this, we have developed a series of new initiatives:

- The formation of an advisory committee to insure industry is provided the mechanism to identify and recommend to NASA the activities most likely to encourage commercial development;
- A fresh look at pricing structures for industry's use of government transportation and on-orbit services;
- A new pricing policy for start-up companies and emerging industries that will be broad enough to cover the entire range of commercial possibilities, yet flexible enough to work on a case by case basis depending on the nature of the enterprise;
- A streamlining of the process by which NASA concludes cooperative agreements with private companies, thereby shortening the time it takes to reach such agreements.

Of paramount concern to emerging commercial ventures is access to space. Our office is developing a plan to optimize the 28 percent commercial allocation for Space Shuttle secondary payloads. We'll encourage companies to develop payload-of-opportunity experiments which can be quickly substituted in the event of an unexpected payload opening. We also plan to tap the creative talents of America's small business entrepreneurs, asking them to propose and explore new concepts for commercial space uses.

In the area of technology utilization, our office is working to create a national network to promote and support public use of NASA technology. We plan to strengthen the technology tranfer process within NASA by encouraging collaboration among federal laboratories, state and local governments, universities, and the private sector in bringing this technology to the marketplace. In addition, we want to increase participation by the NASA laboratories and field centers in technology sharing programs.

These initiatives are driven in no small measure by the challenge of global competition. It's no secret that foreign development of commercial space markets is determined, formidable, and expanding. We must meet these challenges and collectively come to realize that space is the next frontier in which to expand our economic base. □



NOVESPACE

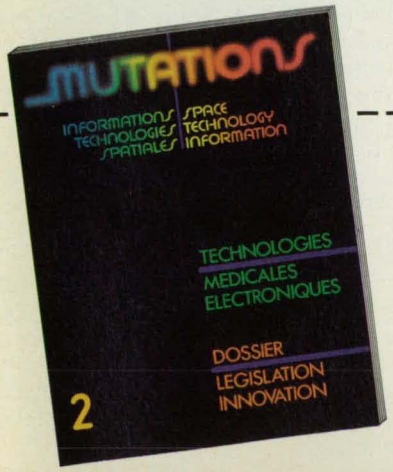


The Foremost Consultancy Company for the Transfer and Utilization of Space Technologies.

NOVESPACE main goal is to transfer technologies or products developed for space programs to non-space industries.
Therefore, **NOVESPACE**
Collects information about technologies or products available for transfer under the form of licenses or partnership agreements;
Edits a catalog of these technologies : MUTATIONS, published twice a year and sent to 20,000 executives around the world;
Is in touch with many innovative companies in France, in Europe; in Japan and in the USA;
Advises companies in negotiating agreements and in finding financial resources for transfers.

What we can do with your company :

We can look for the best partners or licensees in the European Community for your high-tech products.
We can work out marketing studies, financial schemes.
We can help in the negotiation of licensing, partnership or joint-venture agreements.
We can also propose you licenses for technologies, coming from several European aerospace companies, in sectors as varied as electronics, medical instrumentation, materials, optics, software etc.



To receive more information about NOVESPACE and to get a free copy of our catalog « MUTATIONS », please fill this coupon.

NAME : _____ TITLE : _____

COMPANY NAME : _____

ADDRESS : _____

CITY : _____ COUNTRY / STATE : _____

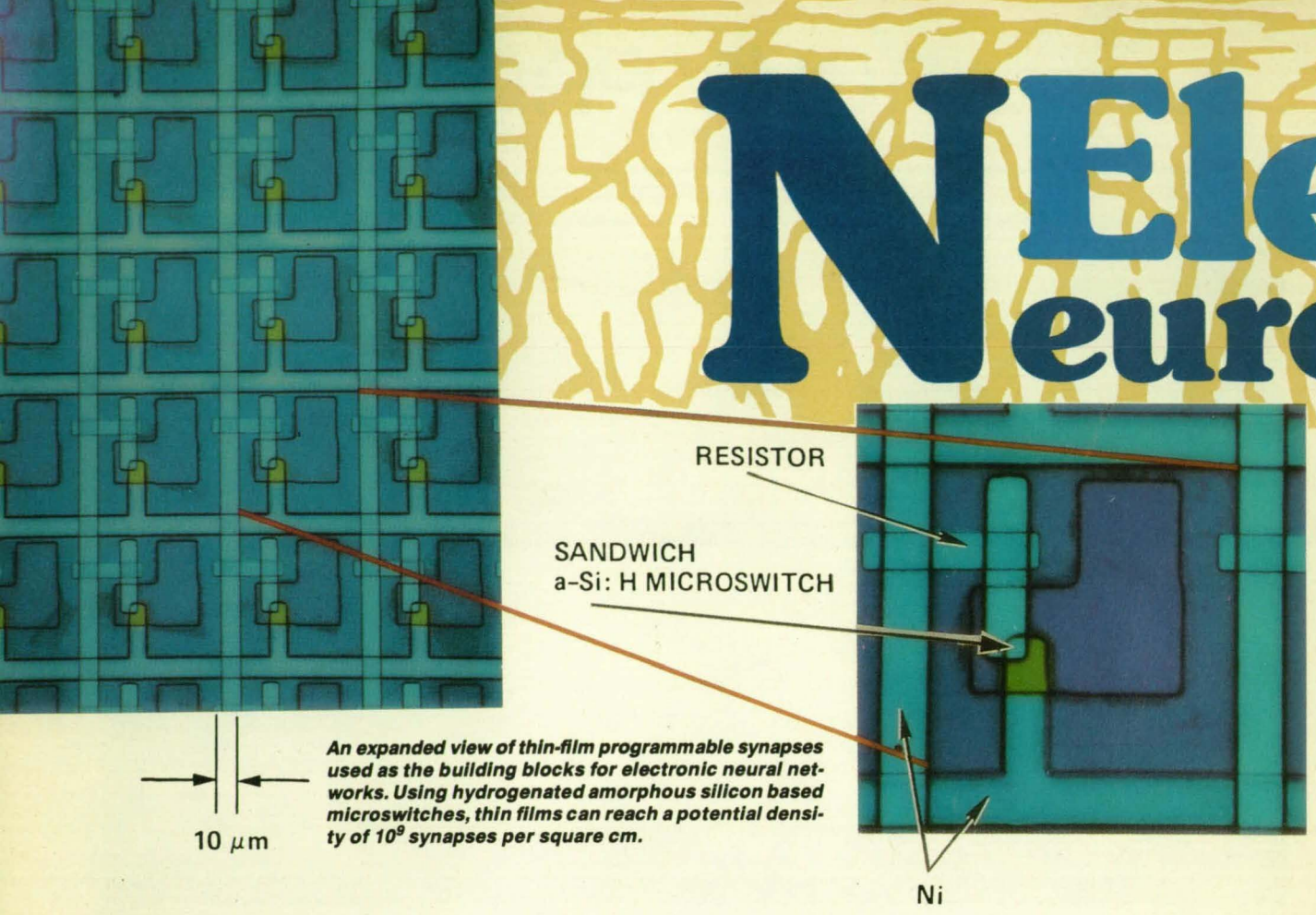
ZIP CODE : _____ TEL NUMBER : _____

NOVESPACE

15, rue des Halles - 75001 PARIS - FRANCE - Tel. : 33 (1) 42.33.41.41 - Telex : 214 674

Circle Reader Action No. 554

NEle
euro



An expanded view of thin-film programmable synapses used as the building blocks for electronic neural networks. Using hydrogenated amorphous silicon based microswitches, thin films can reach a potential density of 10^9 synapses per square cm.

Not even the fastest computer can compete with the human brain in image recognition, language comprehension, or combinatorial optimization. This is primarily because of the fundamental difference in the sequential processing of a digital computer and the parallel computation of the human brain. Neuroscientists have discovered that the human brain's massive parallelism and computational richness derives from global and dense interconnections among the neurons, a large number of almost identical logic elements connected to each other in varying strengths by a complex network of synapses. Man-made neural network models share a common structure: a collection of simple processing elements, representing neurons, interacting through a highly interconnected synaptic network.

A neural network stores "intelligence" or "knowledge" as the connection strengths or synaptic weights among the neurons. The state of the system is described by the activity pattern of the output neurons. When the network is provided with a problem, each neuron receives input signals from its neighbors and asynchronously adjusts its output over time. The system evolves into a steady activity pattern, a solution to the input problem.

Software simulation of network architectures offers researchers the ability to conveniently study neural network models. However, simulation of even a moderately large neural network—a few hundred neurons or more—requires an immense amount of computation, making this approach expensive and time consuming.

A hardware approach is the most efficient way to allow large sets of "neurons" to orchestrate their operations simultaneously. Hardware-based networks can not only provide high speed research tools to study a sysem's emerging behavior, but they also offer a baseline for designing application-specific architectures for real-life problems. At JPL, we have recently fabricated a programmable chip that can be used as the building block for truly parallel, hardware-based neural networks. Work is also under way developing novel thin-film-based neural networks

Analog-Digital Hybrid Neurocomputer

A fully parallel hardware computer is an ideal research tool to investigate the dynamics, associative recall properties, and computational capabilities of neural networks. However, the size of such networks has been limited by the rapid increase in circuit complexity as the number of synaptic interconnections rises. We've designed and built an electronic neurocomputer based on a semi-parallel analog-digital hybrid architecture that significantly reduces hardware complexity. The architecture has two parts: it uses high density digital random access memories to store information, and it takes advantage of the high speed capability of analog hardware (neurons) to process the information. Since complete physical connections between neurons are not required, the hybrid neurocomputer can easily be expanded to simulate networks with several hundred neurons.

The architecture of JPL's hybrid neurocomputer promises an effective processing speed of *100 million* connections per second for a 1000-neuron system. A particularly attractive feature of this neurocomputer is that the system activity can be "frozen" at any time during its evolution. This provides a convenient way to study neural networks with all their static and dynamic eccentricities, generally difficult to simulate in software systems.

The Leading Edge

Very Large Scale Integrated Circuit (VLSI) technology plays an increasingly important role in the development of electronic neural networks. At JPL, we've fabricated à VLSI chip to serve as the basic building block for large

By Dr. Anilkumar P. Thakoor and Dr. Alex Moopenn

ctronic computers

synaptic arrays. The chip features complete programmability of the 32 X 32 "resistive" binary connections (synapses) and cascadability for expansion up to a 512X512 matrix. As a research tool, a neural network system based on such a matrix has significant speed advantages over software-based neural net simulations since convergence time is expected to be only a few microseconds. A prototype system based on one of these chips connects to an array of 32 discrete neurons. Since each connection is fully programmable, the system can easily be configured for a variety of test applications.

Novel thin film materials and modern submicron lithographic techniques have paved the way for the development of ultra-high density synaptic interconnects for electronic neural networks. These techniques have led to a nonvolatile, associative memory that promises an information storage density of 10^9 bits/cm^2. Information storage takes place in "memory cells," consisting of two terminal, passive synaptic connections. These connections have to be unusually "weak," in the range of a megaohm, to limit the current in the wires. This helps avoid electromigration and limits overall power dissipation. We are also developing fully programmable, reversible, non-volatile, resistive synapses in thin-film form. These will be useful for "self-learning" and adaptive networks in hardware-based expert systems.

Applications

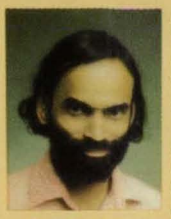
Neural networks have unique dynamic and collective properties, particularly suited for associative recall of stored information. Since system convergence time is governed by the response time of the neurons, high-speed parallel recall of information is achieved even when a large number of memories are stored in a synaptic matrix.

Several other features of thin-film-based neural networks makes them attractive: Their lack of moving parts gives robust and reliable operation, information storage in simple non-volatile synaptic connections brings high speed and a significant reduction in active electronics, and, just as a web keeps its shape even with a number of strands destroyed, neural networks are generally damage insensitive and have superior fault-tolerance.

In addition to associative memory applications, neural networks are well suited for solving computationally intensive optimization problems. In decision making for real-life complex situations, the absolute best answer can not always be calculated within the allotted time frame. In some applications, it's better to have any answer rather than none, and that answer should be made based on the best computations and logic operations possible. Neural networks, like the human brain, are well suited to finding these "at a reflex" solutions, rapidly providing one of several relatively "very good" solutions to a particular situation.

A variety of model application problems in the fields of large database management, automation and robotics, pattern recognition, real-time situation analysis, process optimization, and self-organization and learning are currently under investigation at JPL. An autonomous system consisting of digital and neural components lies in the not-too-distant future. Such a system will have fault-tolerant associative, neural memory along with digital data storage. Neural logic-processor modules will allow the system to independently learn and adapt to new, unforseen situations and to make rapid optimal decisions. Such systems will be particularly attractive for remote—space—or hostile environment applications.

Massively parallel networks of simple neuron-like processing elements seem to hold a key to some very important aspects of intelligence not captured by existing digital and AI technology. As a step in the direction of their original and foremost goal, neural net models may actually have scratched the surface of the mysterious workings of the elegant biological machine: the human brain. □



Dr. Anilkumar P. Thakoor *is a Member of the Technical Staff and Group Supervisor of the Solid State Science Group at JPL. He received his BSc and MSc from the University of Poona, India, and his PhD in Physics from the Indian Institute of Technology, New Delhi, India. His research interests include amorphous materials, photovoltaics, artificial neural networks for information processing, and thin film implementations of neural network architectures.*



Dr. Alex Moopenn *is a Member of the Technical Staff in the Solid State Science Group at JPL. He received his BA from San Francisco State University in 1976, and his PhD from the University of California, Davis, in 1983, both in physics. His research interests include thin film and solid state devices, artificial neural networks for computing, and electronic implementations of neural networks.*

A Peek at Software-Based Neural Network Research

Although hardware-based neural networks are just beginning to take shape, numerous software applications are under intensive development. At Johns Hopkins University, Terry Sejnowski has developed NETtalk, a program that converts English text to speech. The program converts letters to phonemes without direct human intervention after several training sessions.

Dr. Jerry Soloman, at JPL, is studying the applicability of neural networks to perform spectral pattern recognition for imaging spectrometer data analysis. A group headed by Nevin Bryant, also at JPL, is assessing the applicability of neural network technology to increase the efficiency and sophistication of mapped and geocoded data integration and analysis. Allied to this study is a neural network implementation of "all-source-correlation-algorithms" for solving multi-parameter, computation-intensive optimization problems. This will allow fast decision-making based on information gathered from different sources and sensor systems.

Reinhold Mann at Oak Ridge Laboratory uses neural networks to allow a computer to recognize the essence of any alphabetical character. His research will eventually allow a computer to decipher even the most ragged of handwriting.

Neural networks are also finding applications in optimizing the performance of advanced concurrent processing systems. For example, Geoffrey Fox and Jacob Barhen at the California Institute of Technology are developing neural network algorithms for dynamic load balancing in hypercube supercomputers. □

New Product Ideas

New Product Ideas are just a few of the many innovations described in this issue of *NASA Tech Briefs* and having promising commercial applications. Each is discussed further on the referenced page in the appropriate section in this issue. If you are interested in developing a product from these or other NASA innovations, you can receive further technical information by requesting the TSP referenced at the end of the full-length article or by writing the Technology Utilization Office o the sponsoring NASA center (s page 16). NASA's patent-licens program to encourage comme cial development is described page 16.

Unified Robot-Control System

A robot controller uses only one microprocessor to control as many as 16 joint-actuating motors. Use of the single joint-control processor results in fewer components, lower cost, and simpler architecture than are required in existing systems of comparable performance. The single processor can correlate events on different joints. (See page 44).

Public-Facilities Locator for the Blind

A proposed optoelectronic system assists the blind in locating restrooms, water fountains, stairways, emergency exits, elevators, and other key places. The concept calls for a wall-mounted infrared-pulse transmitter at each important location. A compact circuit worn by the user would receive the signals and convert them to synthetic-voice announcements. (See page 49).

Coatings Boost Solar-Cell Outputs

The electrical outputs of thin solar photovoltaic cells made of dendritic-web silicon are increased by a combination of reflective back-surface contact made of Al/Ti/Pd/Ag and front antireflection coating layer of ZnSe topped by a layer of MgF_2. Experiments at visible and near-infrared wavelengths showed increased short-circuit cell current by as much as 50 percent. (See page 27).

Arc-Jet Power Supply and Starting Circuit

A lightweight circuit for starting arc jets and controlling them is capable of high power efficiency. The circuit has an output averaging inductor that doubles for ignition as the high-voltage pulse transformer, eliminating heavy, expensive magnetic components. No external high-voltage power supplies or blocking diodes are needed to start the arc. The starting circuit minimizes electrode erosion during initiation of the arc. (See page 22).

Tool Removes Arc-Light Reflectors

A new tool makes installation, adjustment, and removal of self-clamping arc-light reflectors on welding torches easy and simple. The tool has two arms that reach around from the back of the torch. A lip on each arm hooks into the arc-light reflector clamp. When the tool handles are squeezed, the clamp of the arc-light reflector is spread, and the reflector is easily removed without damage. (See page 93).

THE FIRST FAMILY IN LINEAR MOTION:



AUTOMATION GAGES, INC. BALL AND ROLLER SLIDES

NOW 63 MODELS AVAILABLE FROM STOCK FOR IMMEDIATE DELIVERY!

When it comes to smooth, precise linear motion, come to the original: Automation Gages. We're the experts in ball and roller slide assemblies. In fact, AG invented the patented single wedge pre-load adjustment technique which permits perfect adjustment with one screw and eliminates all play and backlash. For durability, repeatability, and long term value, AG ball and roller slides have no competition.

AG offers nine basic lines and a total of 63 models available from stock. Travels range from ½" to 15" for light, medium and heavy duty applications. And if AG doesn't have exactly what you need, we'll design and manufacture it for you to your specifications.

In addition to ball and roller slides, AG has positioning and measuring stages and accessories, all available with a phone call. For the best in linear motion, call the first family, Automation Gages, first.

WRITE OR CALL FOR FREE CATALOG

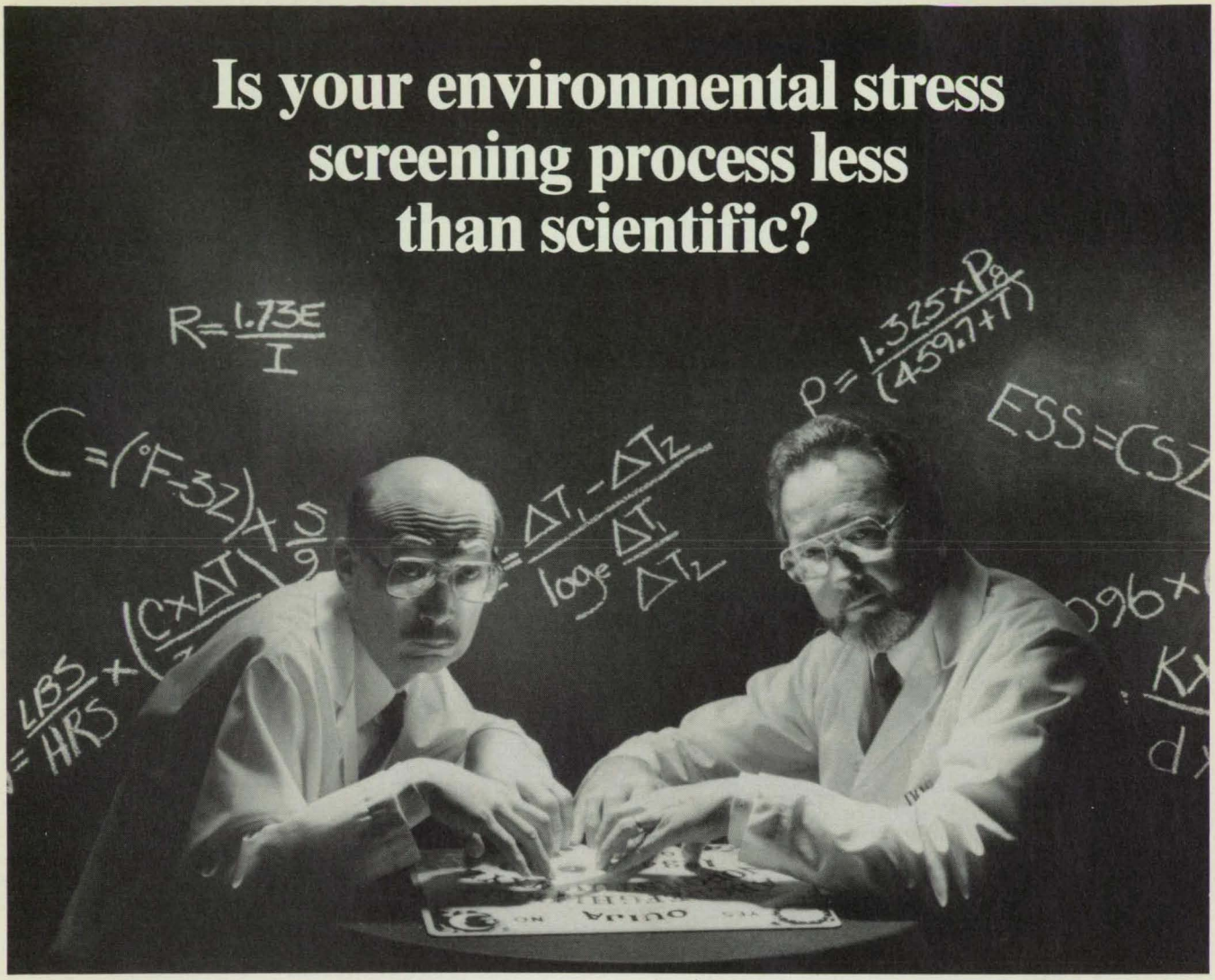
"got a problem...call"

1-800-922-0329. IN NEW YORK STATE, CALL 716-544-0400

Dept. 246

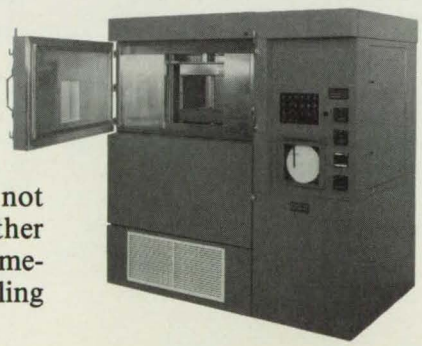
AUTOMATION GAGES, INC. 850 HUDSON AVENUE ROCHESTER, NY 14621

Is your environmental stress screening process less than scientific?



Is your ESS process more mystical than mathematical? Are inferior chambers reducing your stress screening to a game of chance? Do your expert engineers cross their fingers and hope? After all your stress screening efforts, are you still unsure how your product will perform in the field?

Step out of the Dark Ages. Cincinnati Sub-Zero's Thermal Shock Chambers achieve temperature extremes in seconds, not minutes or hours, like other standard chambers. Immediate temperature cycling establishes reliable ESS criteria, assuring a legitimate test for a product's future performance.



Take the guesswork out of ESS with CSZ's Thermal Shock Chambers and relax with their ease of set-up, trouble-free performance and accurate screening results. And CSZ chambers have the best warranty in the business, insuring solid performance for years to come.

For Thermal Shock Chambers ready for immediate delivery or chambers built to any specification, contact Cincinnati Sub-Zero. And take the guess out of ESS.

CSZ
Cincinnati Sub-Zero

12011 Mosteller Road, Cincinnati, Ohio 45241 • (513) 772-8810 • TLX 62395420 SUB ZERO

Circle Reader Action No. 528

HOW YOU CAN BENEFIT FROM NASA'S TECHNOLOGY UTILIZATION SERVICES

If you're a regular reader of TECH BRIEFS, then you're already making use of one of the low- and no-cost services provided by NASA's Technology Utilization (TU) Network. But a TECH BRIEFS subscription represents only a fraction of the technical information and applications/engineering services offered by the TU Network as a whole. In fact, when all of the components of NASA's Technology Utilization Network are considered, TECH BRIEFS represents the proverbial tip of the iceberg.

We've outlined below NASA's TU Network—named the participants, described their services, and listed the individuals you can contact for more information relating to your specific needs. We encourage you to make use of the information, access, and applications services offered by NASA's Technology Utilization Network.

How You Can Utilize **NASA's Industrial Applications Centers**—A nationwide network offering a broad range of technical services, including computerized access to over 100 million documents worldwide.

You can contact NASA's network of Industrial Applications Centers (IACs) for assistance in solving a specific technical problem or meeting your information needs. The "user friendly" IACs are staffed by technology transfer experts who provide computerized information retrieval from one of the world's largest banks of technical data. Nearly 500 computerized data bases, ranging from NASA's own data base to Chemical Abstracts and INSPEC, are accessible through the nine IACs located throughout the nation. The IACs also offer technical consultation services and/or linkage with other experts in the field. You can obtain more information about these services by calling or writing the nearest IAC. User fees are charged for IAC information services.

Aerospace Research Applications Center (ARAC)
Indianapolis Center for Advanced Research
611 N. Capitol Avenue
Indianapolis, IN 46204
Dr. F. Timothy Janis, Director
(317) 262-5036

Central Industrial Applications Center/NASA (CIAC)
Southeastern Oklahoma State U.
Station A, Box 2584
Durant, OK 74701
Dickie Deel, Acting Director
(405) 924-6822

North Carolina Science and Technology Research Center (NC/STRC)
Post Office Box 12235
Research Triangle Park, NC 27709
J. Graves Vann, Jr., Director
(919) 549-0671

NASA Industrial Applications Ctr. 823 William Pitt Union
University of Pittsburgh
Pittsburgh, PA 15260
Paul A. McWilliams, Exec. Director
(412) 648-7000

NASA/Southern Technology Applications Center
P. O. Box 24
Progress Ctr., One Progress Blvd.
Alachua, FL 32615
J. Ronald Thornton, Director
(904) 462-3913
(800) 354-4832 (FL only)
(800) 225-0308 (toll-free US)

NASA/UK Technology Applications Center
University of Kentucky
109 Kinkead Hall
Lexington, KY 40506-0057
William R. Strong, Director
(606) 257-6322

NERAC, Inc.
One Technology Drive
Tolland, CT 06084
Daniel U. Wilde, President
(203) 872-7000

Technology Application Center (TAC)
University of New Mexico
Albuquerque, NM 87131
Stanley A. Morain, Director
(505) 277-3622

NASA Industrial Applications Center (WESRAC)
University of Southern California
Research Annex
3716 South Hope Street, Room 200
Los Angeles, CA 90007
Radford G. King, Acting Director
(213) 743-8988
(800) 642-2872 (CA only)
(800) 872-7477 (toll-free US)

NASA/SU Industrial Applications Center
Southern University Department of Computer Science
Baton Rouge, LA 70813
John Hubbell, Director
(504) 771-2060

If you represent a public sector organization with a particular need, you can contact NASA's Application Team for technology matching and problem solving assistance. Staffed by professional engineers from a variety of disciplines, the Application Team works with public sector organizations to identify and solve critical problems with existing NASA technology. **Technology Application Team, Research Triangle Institute, P.O. Box 12194, Research Triangle Park, NC 27709. *Doris Rouse, Director,* (919) 541-6980**

How You Can Access Technology Transfer Services At NASA Field Centers:

Technology Utilization Officers & Patent Counsels—Each NASA Field Center has a Technology Utilization Officer (TUO) and a Patent Counsel to facilitate technology transfer between NASA and the private sector.

If you need further information about new technologies presented in *NASA Tech Briefs*, request the Technical Support Package (TSP). If a TSP is not available, you can contact the Technology Utilization Officer at the NASA Field Center that sponsored the research. He can arrange for assistance in applying the technology by putting you in touch with the people who developed it. If you want information about the patent status of a technology or are interested in licensing a NASA invention, contact the Patent Counsel at the NASA Field Center that sponsored the research. Refer to the NASA reference number at the end of the Tech Brief.

Ames Research Ctr.
Technology Utilization Officer: Laurance Milov
Mail Code 223-3
Moffett Field, CA 94035
(415) 694-6471
Patent Counsel: Darrell G. Brekke
Mail Code 200-11
Moffett Field, CA 94035
(415) 694-5104

Lewis Research Center
Technology Utilization Officer: Daniel G. Soltis
Mail Stop 7-3
21000 Brookpark Road
Cleveland, OH 44135
(216) 433-5567
Patent Counsel: Gene E. Shook
Mail Code 301-6
21000 Brookpark Road
Cleveland, OH 44135
(216) 433-5753

National Space Technology Laboratories
Technology Utilization Officer: Robert M. Barlow
Code GA-00
NSTL Station, MS 39529
(601) 688-1929

John F. Kennedy Space Center
Technology Utilization Officer: Thomas M. Hammond
Mail Stop PT-TPO-A
Kennedy Space Center, FL 32899
(305) 867-3017
Patent Counsel: James O. Harrell
Mail Code PT-PAT
Kennedy Space Center, FL 32899
(305) 867-2544

Langley Research Ctr.
Technology Utilization Officer: John Samos
Mail Stop 139A
Hampton, VA 23665
(804) 865-3281
Patent Counsel: George F. Helfrich
Mail Code 279
Hampton, VA 23665
(804) 865-3725

Goddard Space Flight Center
Technology Utilization Officer: Donald S. Friedman
Mail Code 702
Greenbelt, MD 20771
(301) 286-6242
Patent Counsel: R. Dennis Marchant
Mail Code 204
Greenbelt, MD 20771
(301) 286-7351

Jet Propulsion Lab.
Technology Utilization Mgr.: Norman L. Chalfin
Mail Stop 156-211
4800 Oak Grove Drive
Pasadena, CA 91109
(818) 354-2240

NASA Resident
Technology Utilization Officer: Gordon S. Chapman
Mail Stop 180-801
4800 Oak Grove Drive
Pasadena, CA 91109
(818) 354-4849
Patent Counsel: Paul F. McCaul
Mail Code 180-801
4800 Oak Grove Drive
Pasadena, CA 91109
(818) 354-2734

George C. Marshall Space Flight Center
Technology Utilization Officer: Ismail Akbay
Code AT01
Marshall Space Flight Center,
AL 35812
(205) 544-2223
Patent Counsel: Leon D. Wofford, Jr.
Mail Code CC01
Marshall Space Flight Center,
AL 35812
(205) 544-0024

Lyndon B. Johnson Space Center
Technology Utilization Officer: Dean C. Glenn
Mail Code EA4
Houston, TX 77058
(713) 483-3809
Patent Counsel: Edward K. Fein
Mail Code AL3
Houston, TX 77058
(713) 483-4871

NASA Headquarters
Technology Utilization Officer: Leonard A. Ault
Code IU
Washington, DC 20546
(202) 453-1920
Assistant General Counsel for Patent Matters: Robert F. Kempf, Code GP
Washington, DC 20546
(202) 453-2424

A Shortcut To Software: **COSMIC®**— For software developed with NASA funding, contact COSMIC, NASA's Computer Software Management and Information Center. New and updated programs are announced in the Computer Programs section. COSMIC publishes an annual software catalog. For more information call or write: **COSMIC®**, 382 East Broad Street, Athens, GA 30602 *John A. Gibson, Dir.,* (404) 542-3265

If You Have a Question . . . **NASA Scientific & Technical Information Facility** can answer questions about NASA's Technology Utilization Network and its services and documents. The STI staff supplies documents and provides referrals. Call, write or use the feedback card in this issue to contact: **NASA Scientific and Technical Information Facility,** Technology Utilization Office, P.O. Box 8757, Baltimore, MD 21240-0757. *Walter M. Heiland, Manager,* (301) 859-5300, Ext. 242, 243

NEW CAPABILITIES

CAPTURE IT



Capture data at fast trigger rates—internal or external—with the new Model 194A High Resolution Digitizer. Here are the advantages:

Faster, More Thorough Testing.

NOW—With the Model 194A High Speed Digitizer, you can acquire samples with external trigger pulses. Capture discrete samples synchronized to changes in position, distance, angle, log (time), a stimulus level, or other events. With trigger rates up to 1MHz, you can take more data in less time. That means more complete testing at lower cost.

Resolution of 16 bits. At rates up to 100kHz.

The Model 194A's 16-bit (4½-digit) resolution lets you detect 1 part in 32,000—far better than most digitizing devices. For higher frequency waveforms—up to 1MHz—the 194A samples with 8-bit resolution. And its 64k bytes of memory is up to 8 times that of other digitizers.

Add the 1944A Channel 2 option and acquire two different waveforms simultaneously, in time sync, or asynchronously. Each channel is independent, isolated, fully programmable, and has 64k bytes of memory.

The 194A provides 5 trigger options for initiating a measurement. Pre- and post-trigger data can be stored.

Analyze and Automate

The 194A directly displays key waveform parameters such as integration, RMS, average, and peak-peak. With two channels installed you can compute ratio or difference between channels.

All functions are IEEE-488 bus programmable. And our exclusive, built-in TRANSLATOR software reduces bus transfer time and simplifies documentation.

At **$4095**, you won't find better performance. And the optional second channel for just **$1995** doubles acquisition capability. For complete details contact the **Product Information Center, Keithley Instruments, Inc., 28775 Aurora Road, Cleveland, Ohio 44139, (216) 248-0400.**

KEITHLEY

Circle Reader Action No. 536

Electronic Components & Circuits

Hardware, Techniques, and Processes

18 Adjustable, Audible Continuity Tester for Delicate Circuits
20 Optical Rotary Joint for Data Transfer
22 Arc-Jet Power Supply and Starting Circuit
23 Difference-Equation/Flow-Graph Circuit Analysis
26 Dual-Band Microstrip Antenna With Reactive Loading
27 Wide-Band, Wide-Scan Antenna for Circular Polarization
27 Coatings Boost Solar-Cell Outputs
30 Compact Sun-Position Sensor
32 Designing a Microwave Band-Stop Filter
35 Electronic Neural-Network Simulator
35 Programmable Synaptic Arrays for Electronic Neural Networks
36 Blanket Gate Would Address Blocks of Memory
38 Integrated Circuit for Simulation of Neural Network
40 Three-Waveguide Beam and Polarization Splitter

Computer Programs

68 Computing Radiation Characteristics of Phased Arrays

Adjustable, Audible Continuity Tester for Delicate Circuits

The unit is adjustable to resistances up to 35 ohms.

Goddard Space Flight Center, Greenbelt, Maryland

An adjustable, audible electrical-continuity tester gives an audible indication, making it unnecessary for the user to look directly at the instrument to observe a meter reading. The user's eyes can be kept on the circuit board being tested; there is therefore little risk that the user would let the tester probes slip from the terminals under test and cause false indications or damage the circuit or components.

In addition, the current and voltage of the tester are strictly limited. It can apply no more than 0.6 volts dc and no more than 3 mA through the probes. It can therefore be used safely on circuit boards in which semiconductor components have been installed, and on complementary metal oxide/semiconductor integrated circuits, which are highly susceptible to damage during testing.

The tester is compact (see Figure 1), and its circuit is simple (see Figure 2). It can

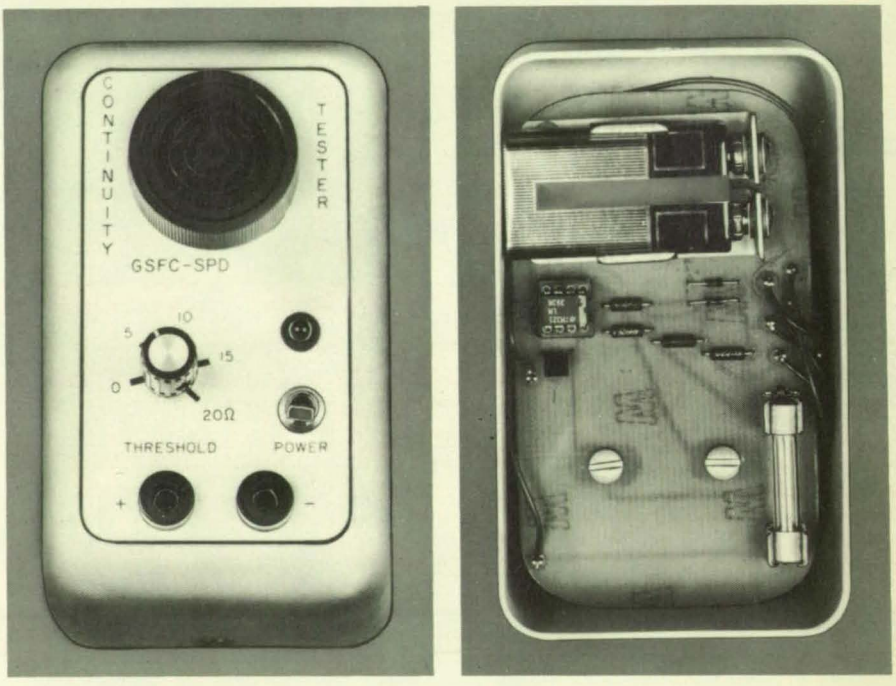


Figure 1. The **Continuity Tester** is mounted on a small circuit board in a compact enclosure.

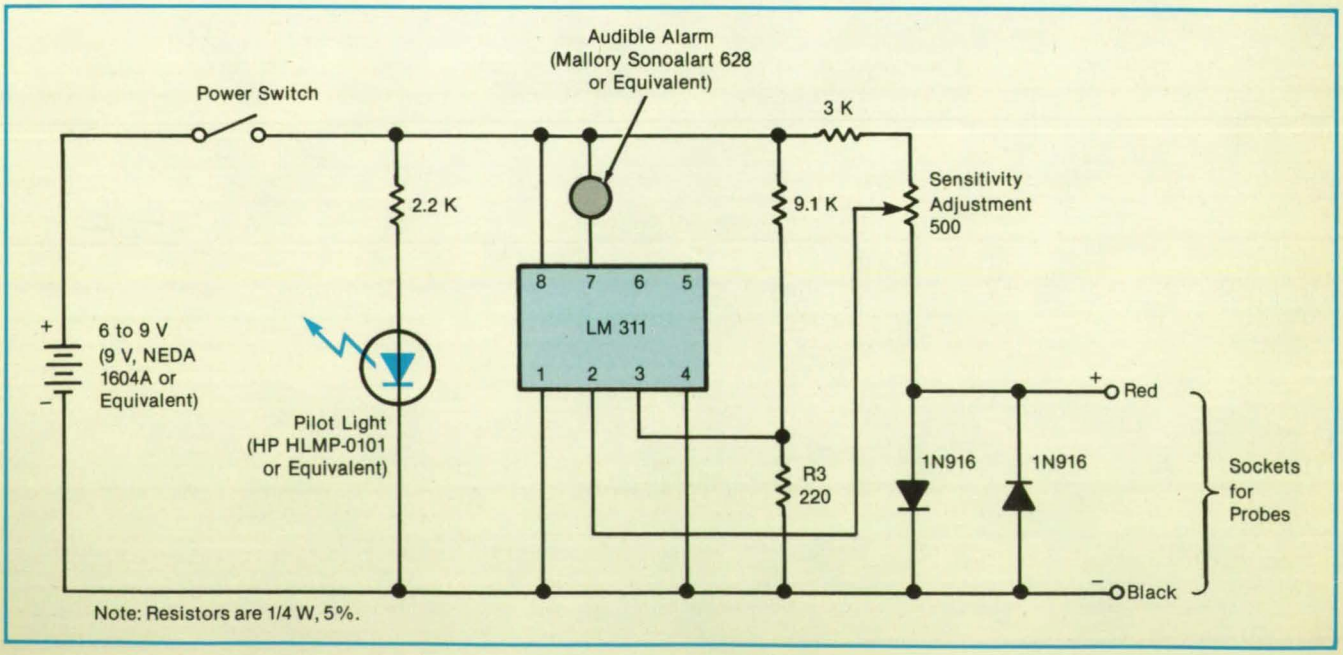


Figure 2. The **Tester Circuit** consists of only a few components. The 500-Ω potentiometer sets the threshold (maximum) resistance that will trigger the alarm. The circuit is housed in a compact enclosure on a small circuit board.

Check coupon for FREE BROCHURE "Fun with Superconductors"

FLUORAMICS, INC. IS PROUD TO ANNOUNCE

SUPERCONDUCTORS FOR SALE

ISTORY WAS MADE THIS YEAR AND YOU CAN BE PART OF IT!

no would ever have expected that a black ceramic aterial would revolutionize the world of science d be the source of a whole new class of super-nductors?

NOW FOR THE FIRST TIME IN THE HISTORY OF SCIENCE

en the first reports describing these amazing ceramic perconductors appeared, our research director followed m with great interest. The equipment and skills required fit lab to a tee. Now, after months of intensive work, we would to make the results of our efforts available. Experimentors o would like to evaluate the new superconductors but don't ve the time, personnel or facilities to make them, can now go work. A multitude of applications will no doubt appear. All you ed is a bottle of Liquid Nitrogen and the usual electronic skills.

od luck, we hope you get lots of patents and find dozens of plications for this new remarkable technology.

EACH SUPERCONDUCTOR TESTED BY THE SCIENTIST WHO MADE IT

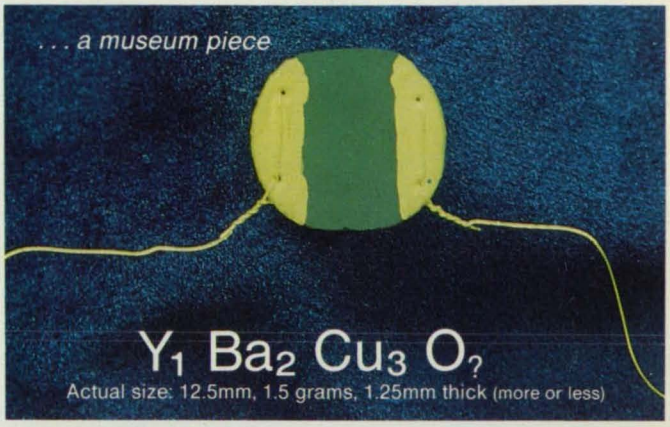


ach Fluoramics' superconductor is carefully drilled with 4 les. Copper wire is threaded in place. Conductive silver paste hand-painted to assure uniform area contact. Meissner vitation and transition curves are run on representative mples from each lot.

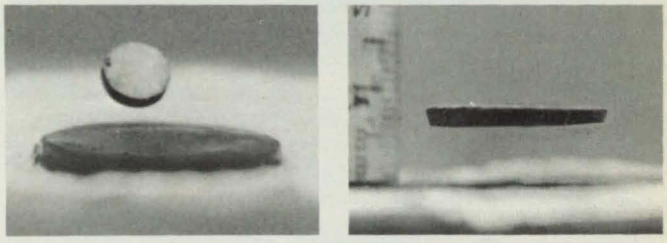
A ceramic with zero electrical resistance? See for yourself!

s the temperature is lowered, the super-nductor's resistance drops slowly until out 90° kelvin (that's -280° below zero renheit—very hot in the world of supercon-uctors). Then it falls as if on a ride over iagara Falls in a barrel . . . to zero ohms or early so (77° kelvin or -320° F Liquid itrogen Temperature).

SPECTACULAR SIGHT! A small cobalt marium magnet resting on its surface will agically float up and levitate at the same ne, demonstrating the Meissner effect.



HERE'S WHAT YOU'LL SEE

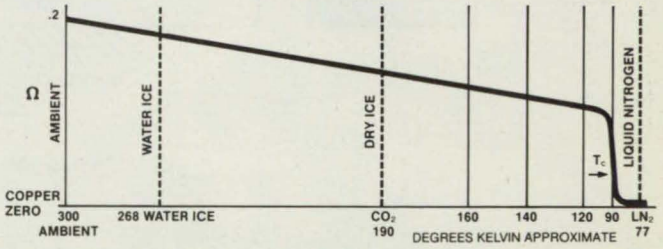


THE MEISSNER EFFECT

A rare earth magnet levitates over Fluoramics' superconductor that's been cooled with Liquid Nitrogen.

A superconductor floats ¼" or more over a nest of 4 magnets. It'll stay up about 30 seconds before it warms and settles.

TYPICAL SUPERCONDUCTOR TRANSITION CURVE
$Y_1\ Ba_2\ Cu_3\ O_?$ CERAMIC



PLEASE SEND A.S.A.P.

TO ORDER:
CALL TOLL FREE
1-800-922-0075
OR SEND IN THE ORDER FORM BELOW

Limited Quantity

Laboratory test superconductors for the introductory price of . .

18K Gold Wire Painted Gold Electrodes	Copper Wire Painted Silver Electrodes	Rare Earth Magnets
____ (1) $100.00	____ (1) $ 95.00	____ (1) small disc $25.00 each
____ (2) $150.00	____ (2) $142.50	
____ (3) $170.00	____ (3) $165.50	

____ (2) $100.00 No electrode blanks for Meissner Effect
____ FREE BROCHURE "Fun with Superconductors"

Call for volume prices.

Fluoramics, Inc. N-188
103 Pleasant Avenue
Upper Saddle River, N.J. 07458

My check or money order for $ ____ is enclosed
Charge my credit card:
☐ Am.Express ☐ MasterCard ☐ Visa

Card No. _____
Exp. Date _____
P.O. # _____
Name _____
Address _____
City _____
State _____ Zip _____

(N.J. residents please add 6% sales tax.)

Circle Reader Action No. 541

See NASA Tech Briefs for our award-winning ads of 1986 and 1987 "TUFOIL, The Transistor of Lubrication"

be built from inexpensive standard components available from retail outlets.

The tester can be adjusted to indicate continuity below any resistance value up to 35 ohms. For example, if the user sets the tester to 30 ohms, the unit will emit an audible tone whenever the resistance between the probes is 30 ohms or less; if, for example, the resistance is 30.2 ohms, the unit will remain silent.

This work was done by William B. McAlister of **Goddard Space Flight Center**. *No further documentation is available.*
GSC-13102

Optical Rotary Joint for Data Transfer

A proposed joint would increase bandwidth and reduce errors.

Lyndon B. Johnson Space Center, Houston, Texas

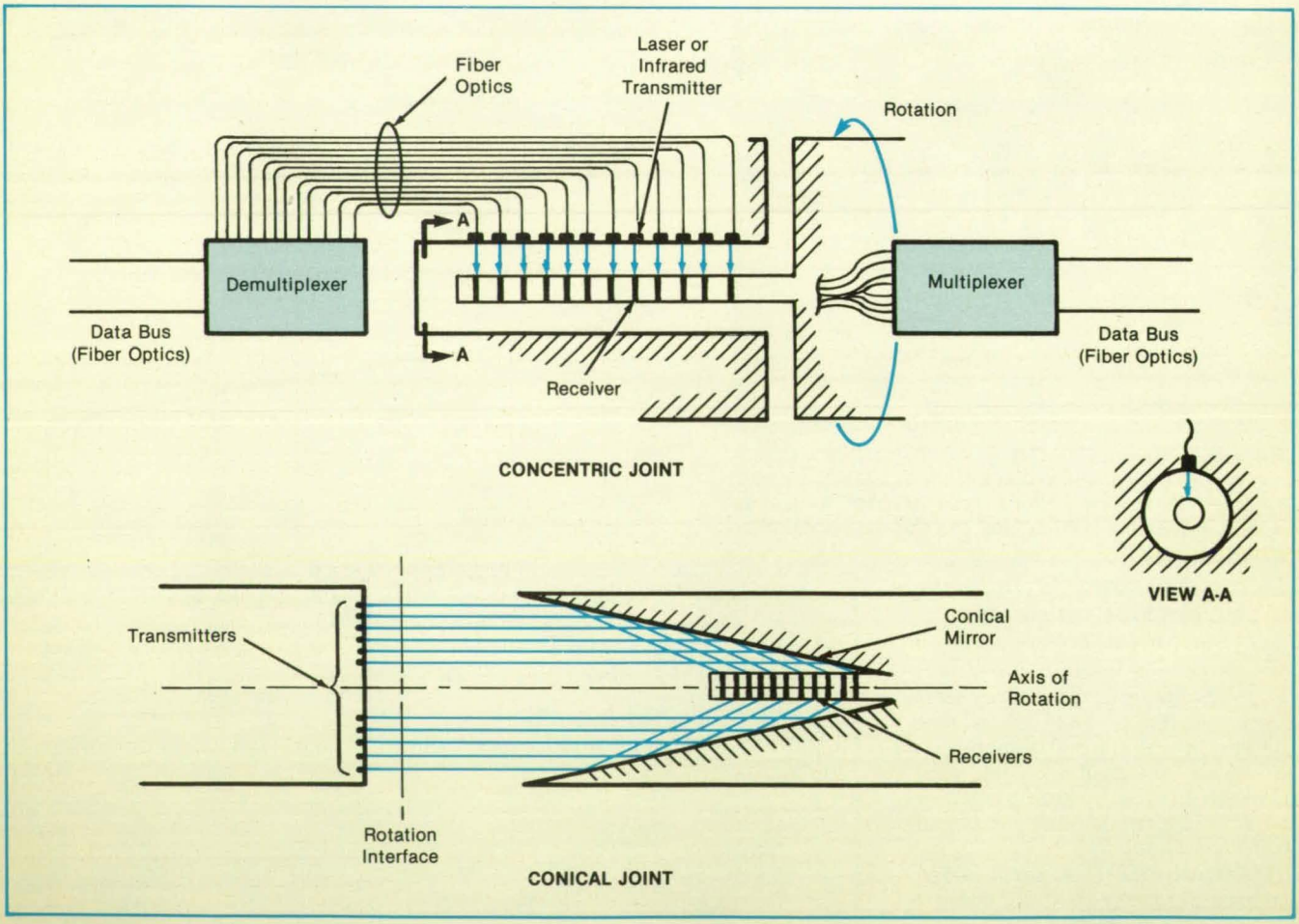
A scheme for transferring digital data across a rotary joint would use light instead of electrical signals. The optical joint would offer greater bandwidth than that of conventional electrical sliprings and would probably operate at a considerably lower error rate. According to an estimate, a highly reliable, compact joint could be built for less than $1 per channel and could accommodate one or several channels, each with a 1-MHz bandwidth. The concept could be applied to the transfer of high-speed data to rotating antennas or across the joints of robots and manipulators in automated manufacturing.

The concept calls for a row of laser or light-emitting-diode transmitters on the outside member of a cylindrical joint and a series of corresponding photodiode receivers on the inner member (see figure). The receivers would be arranged as a stack of rings. A transmitter would continually beam light at its receiver ring as the latter rotates. Instead of facing each other across the gap, the transmitting and receiving diodes could be located away from the gap, connected to the transmission points and the receiving rings by optical fibers.

The joint could be made as long as necessary to accommodate the requisite number of transmitter/receiver pairs for each channel. For bidirectional data flow, a combination of transmitters and receivers would be mounted on both sides of the joint. There would be no mechanical contact between transmitters and receivers and, therefore, no wear.

In a variation of the concept (also shown in the figure), transmitters would be arrayed along a radius of a flat disk, and receiver rings would be arrayed along a pole surrounded by a conical mirror. The mirror would reflect light from the lasers — the only suitable transmitters in this case — into the receiving photodiodes.

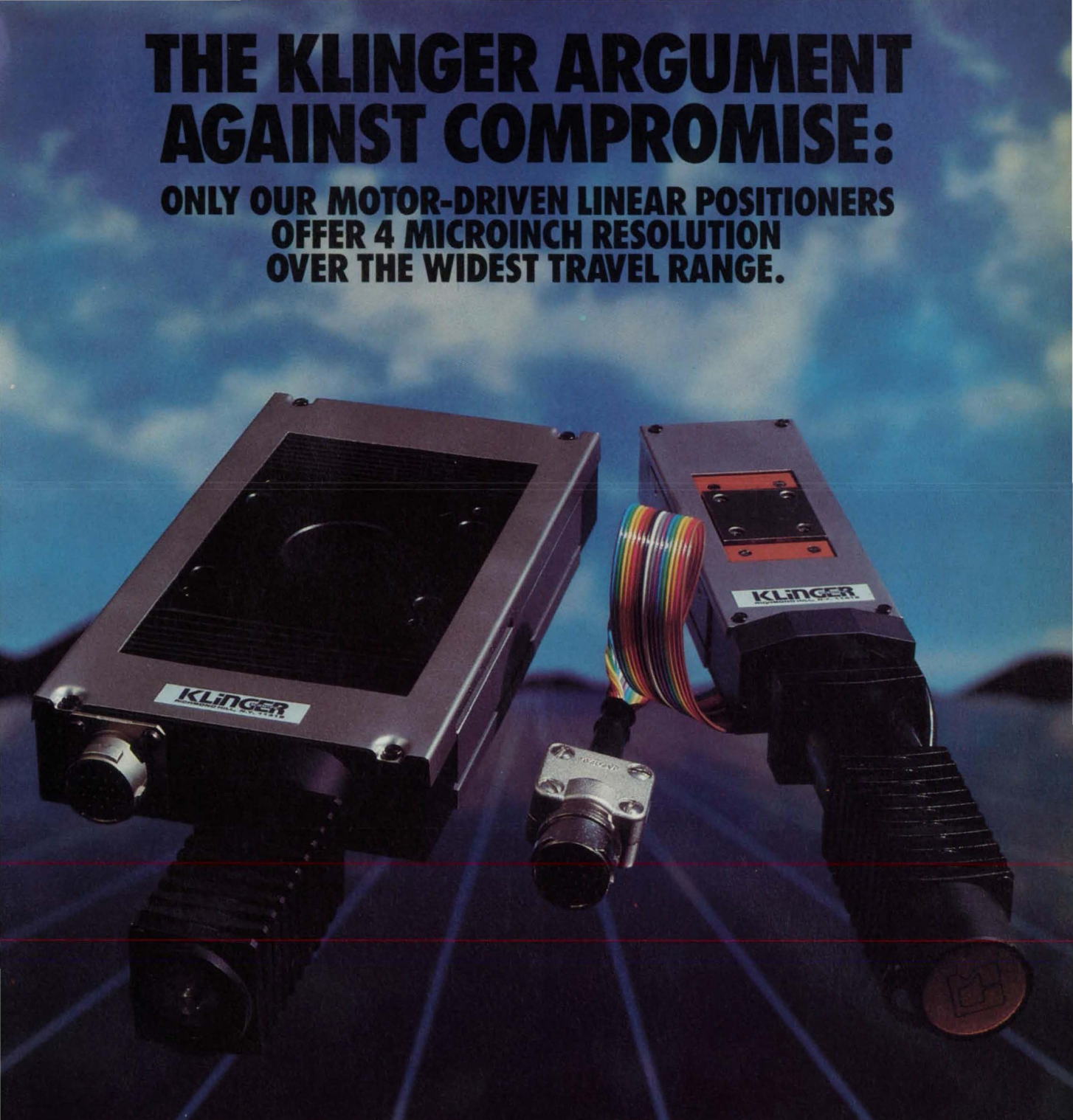
This work was done by Fred J. Becker of McDonnell Douglas Corp. for **Johnson Space Center**. *For further information, Circle 84 on the TSP Request Card.*
MSC-21182



Light Pulses Would Be Transmitted across the gap of the rotary optical data joint. The conical form of the joint would be useful when one of the members must have a flat surface.

THE KLINGER ARGUMENT AGAINST COMPROMISE:

ONLY OUR MOTOR-DRIVEN LINEAR POSITIONERS OFFER 4 MICROINCH RESOLUTION OVER THE WIDEST TRAVEL RANGE.



Whether your work involves laser machining, automated fiber optic alignment, semiconductor research or any high precision application, Klinger's wide selection of motor-driven linear stages will deliver unmatched precision.

All our linear stages can be used in combination to create XY or XYZ positioning systems. Incremental encoders for position verification are available. Other options include homing, clean room and vacuum preparation.

Don't compromise. The best is always a bargain. Klinger standards of engineering and manufacturing, as exemplified by our linear positioning stages, have made us the world leader in micropositioning systems. Get our free 212-page micropositioning handbook for complete specifications on these and thousands of other components.

Write or phone Klinger Scientific Corporation, 110-20 Jamaica Avenue, Richmond Hill, NY 11418. (718) 846-3700.

KLINGER SCIENTIFIC

Worldwide Network to Meet Your Needs • **France:** Micro Controle, Evry, (tel.) 64.97.98.98 • **England:** Micro Controle, Newbury, (tel.) 44/635.521.757 • **Italy:** Nachet Italia, Milano, (tel.) 02/9233.315 • **West Germany:** Spindler & Hoyer, Gottingen, (tel.) 49/0/551/69.350 • **Belgium:** Micro Controle, Bruxelles • **Switzerland:** G.M.P.S.A., Lausanne, (tel.) 46/21/33/3328 • **Sweden:** Martinsson & Co., Hagersten, (tel.) 08/744/03/00 • **Japan:** Hakuto Co. Ltd., Tokyo, (tel.) 03/341/2611 • **Canada:** Optikon Corp. Ltd., Waterloo, Ontario, (tel.) 519/885/2551 • **Taiwan ROC:** Pan-Co International Ltd., Taipei, (tel.) 886-2.391.46.42 • **Korea:** Sam Joong Corp., Seoul, (tel.) 82-2.548.0732 or 33

Arc-Jet Power Supply and Starting Circuit

Power efficiency is high, current is regulated, and starting is automatic.

Lewis Research Center, Cleveland, Ohio

An arc jet operates by heating a gas with an electric arc and expanding the heated gas through a nozzle to provide thrust. Typically, the arc-discharge voltage decreases with increasing current. This arc characteristic requires some form of current limiting to prevent the destruction of the thruster. Previously, power for arc jets in the laboratory was obtained from a high-voltage power supply with a ballast resistor in series with the thruster arc. The resistor wastes power, and the power supply does not act as a constant-current source.

Some means must be provided to initiate the arc discharge. At present, there are three basic methods for starting arc jets; each has advantages and disadvantages. In one mechanical method, the electrodes are momentarily brought together. In another method, the propellant-gas pressure or composition is adjusted until a Paschen discharge is established. In a third method, a high voltage (about 1 kV) is applied between the electrodes until the arc starts.

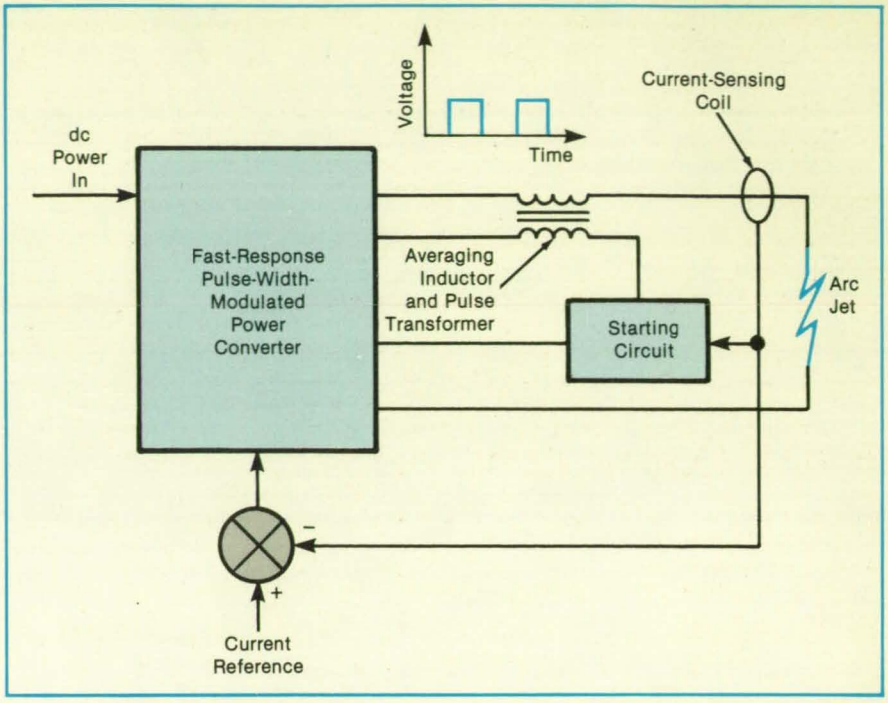


Figure 1. A **Feedback Control System** keeps the arc-jet current nearly constant, once the arc has been struck by the starting pulse.

A new circuit for starting arc jets and controlling them in steady operation is capable of high power efficiency and can be constructed in a lightweight form. The design comprises a pulse-width-modulated power converter, which is configured in a closed control loop for fast current control.

A functional diagram of the circuit is shown in Figure 1. Figure 2 is a detailed schematic diagram. The arc-jet power supply is a current regulator with fast response. The series averaging inductor maintains nearly constant current during rapid voltage changes and thereby allows

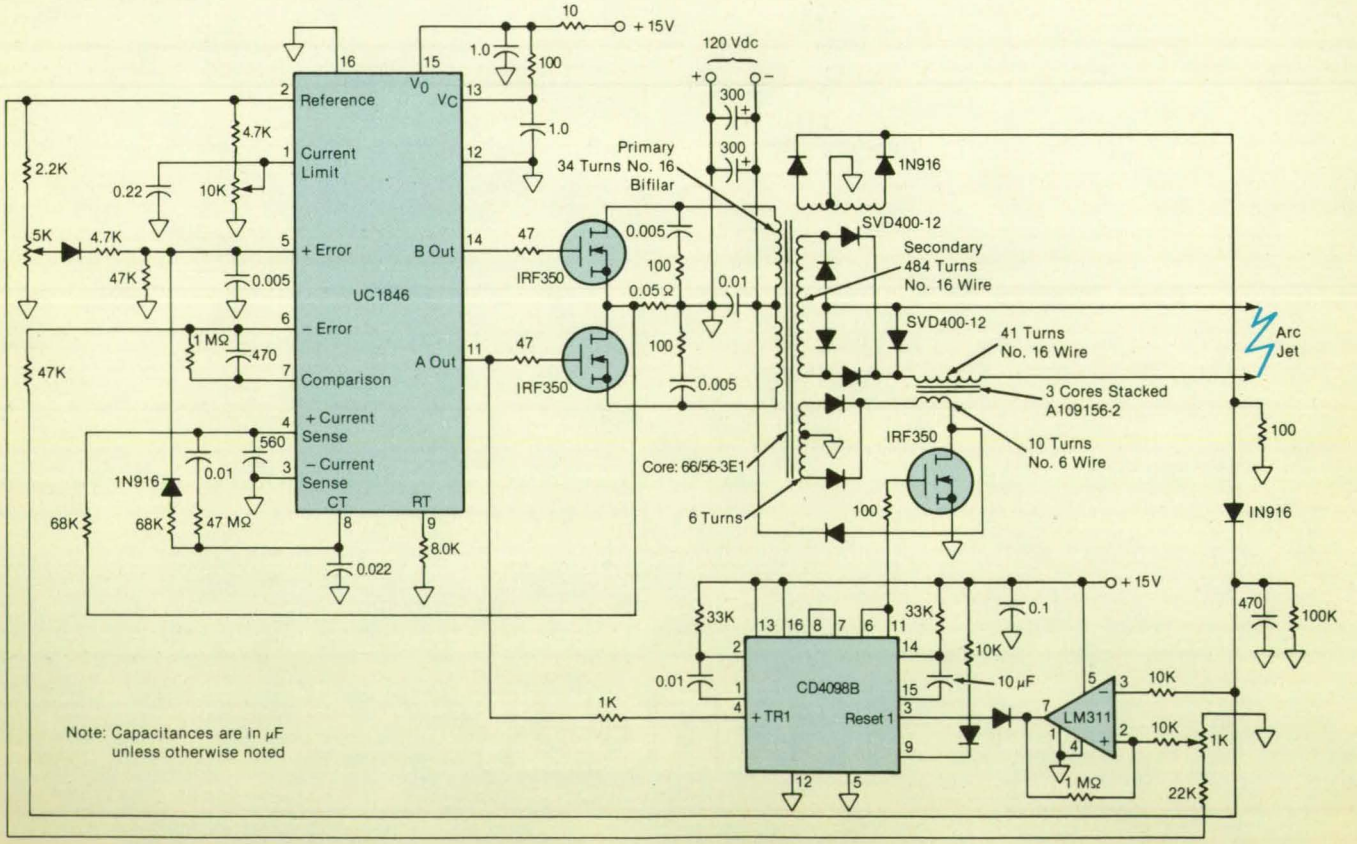


Figure 2. The **Circuit of Figure 1** is made of commercially available components. This design is capable of high power efficiency.

time for the fast-response regulator to adjust its pulse width to accommodate load-voltage changes.

An important feature of the circuit is that the output averaging inductor doubles as the high-voltage pulse transformer for ignition. This is significant because magnetic components are heavy and expensive. In addition, no external high-voltage power supplies or blocking diodes are needed to start the arc. Another advantage is that the limited-energy and limited-maximum-current features of the starting circuit minimize electrode erosion during initiation of the arc.

The starting circuit operates according to the same principle as that of an automobile ignition coil. Current flows through a low-voltage winding. When the current is interrupted by a transistor switch, the inductor magnetic field collapses, and a high-voltage pulse is produced. The pulse is initiated every 0.25 second until arc current is detected. Then the pulser is automatically turned off.

This work was done by Robert P. Gruber of **Lewis Research Center**. *Further information may be found in NASA TM-87340 [N86-25409/NSP], "Power Electronics for a 1-Kilowatt Arcjet Thruster."*

Copies may be purchased [prepayment required] from the National Technical Information Service, Springfield, Virginia 22161, Telephone No. (703) 487-4650. Rush orders may be placed for an extra fee by calling (800) 336-4700.

This invention is owned by NASA, and a patent application has been filed. Inquiries concerning nonexclusive or exclusive license for its commercial development should be addressed to the Patent Counsel, Lewis Research Center [see page 16]. Refer to LEW-14374.

Difference-Equation/Flow-Graph Circuit Analysis

Solutions are reached quickly on small computers.

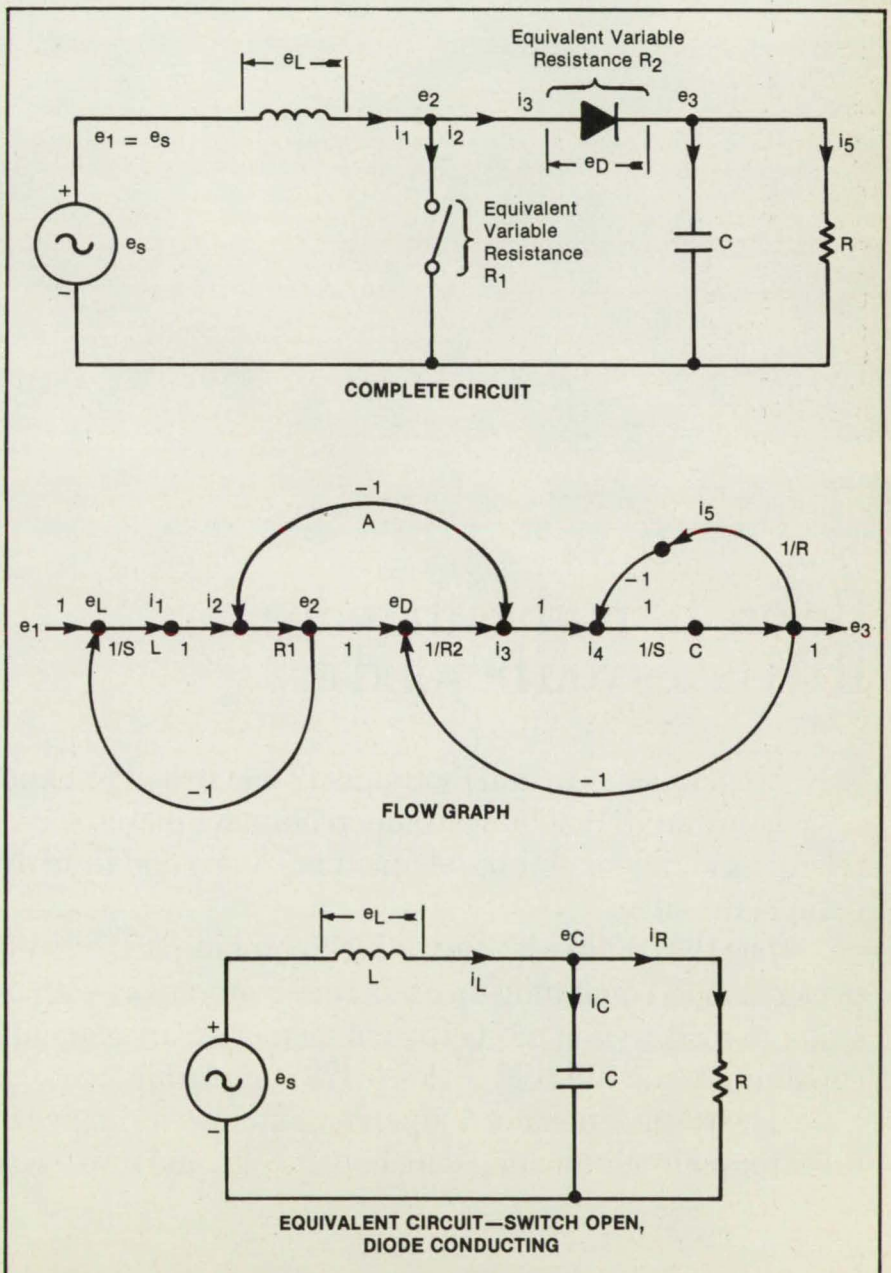
Marshall Space Flight Center, Alabama

A numerical technique enables rapid, approximate analyses of electronic circuits that contain linear and nonlinear elements. The technique can be practiced in a variety of computer languages on large and small computers; for circuits that are simple enough, programmable hand calculators can be used. Although some combinations of circuit elements can make the numerical solutions diverge, the technique enables the quick identification of divergence and the correction of circuit models to make the solutions converge.

A circuit to be analyzed by the technique can optionally be depicted by a signal-flow graph. The voltages at the circuit nodes and the currents between the nodes are represented in terms of the standard equations of nodal analysis. Using the flow graph of the schematic circuit diagram, one propagates a voltage signal forward mathematically from a first node to a second node via the equation for the current between them. Because the voltage at the second node affects the voltage at the first node, the voltage signal is also propagated backward by the iteration of nodal equations, using the forward-propagated voltage at the second node in the subsequent iteration for the voltage at the first node.

Finite-timestep difference equations are used to approximate the differential equations for transient voltages and currents in the presence of inductance or capacitance. Such nonlinear circuit elements as switches and diodes can be represented by time-, current-, or voltage-dependent resistances or changes of circuit configuration.

The technique can be illustrated by reference to the "boost" charging circuit of the figure. The signal is mathematically propagated from voltage source $e_S(t)$ rightward to resistor R. To avoid mathematical divergences caused by the treatment of



This **"Boost" Charging Circuit** resonantly charges capacitor C from the energy stored in inductor L during the preceding charging cycle. The voltage across C and R can exceed e_S.

Before he pushes the edge, IBM takes you beyond it.

From miles away and thousands of feet below, you know exactly what he's feeling.

Using an IBM 3090 with supercomputer power, you've pushed your design through relentless iterations of finite element modeling and fluid dynamics analysis. You've defined the edge.

The IBM 3090 with Vector Facility, for its part, has redefined supercomputer performance, combining up to six vector processors with one of the industry's fastest scalar processors and most efficient memory management systems, parallel processing capabilities, and full IBM System/370 compatibility.

The result is balanced supercomputer performance that can improve your job turnaround by eliminating data bottlenecks, and save the added expense of a separate



front-end processor. Plus, the IBM Vector Facility's modular design lets you start with just the computer power you need today, and make economical in-field upgrades as your needs grow. And that gives the IBM 3090VF a big edge over more expensive and less flexible vector processors.

IBM's integrated system approach combines the power of the IBM 3090VF with the advantages of a single operating environment, low entry cost, low software and maintenance costs, a wide variety of application programs, and IBM support to create a winner in total cost-of-computing.

To find out more, or to arrange to have your IBM Marketing Representative contact you, simply call 1-800-IBM-2468, ext. 20.

IBM®

© IBM 1987

Circle Reader Action No. 551

the diode and switch as time-varying resistances, the circuit is mathematically reconfigured and new equations written for each of the four distinct combinations of diode and switch states. For example, when the switch is open and the diode is conducting, the algorithm and equations for the voltages and currents are the following, where t = time, and Δt = the increment of time:

- $e_L(t) = e_S(t) - e_C(t - \Delta t)$,
- $i_L(t) = i_L(t - \Delta t) + e_L \Delta t / L$,
- $i_C(t) = i_L(t) - i_R(t - \Delta t)$,
- $e_C(t) = e_C(t - \Delta t) + i_C(t) \Delta t / C$, and
- $i_R(t) = e_C(t) / R$
- Increment time by Δt and return to step 1.

(Note that R_1 and R_2 are nonlinear resistors and can cause loop A not to converge.)

This work was done by I. M. McVey of Rockwell International Corp. for **Marshall Space Flight Center**. *For further information, Circle 51 on the TSP Request Card.*
MFS-29245

Dual-Band Microstrip Antenna With Reactive Loading

An effective but bulky coaxial stub is replaced.

Lyndon B. Johnson Space Center, Houston, Texas

A short-circuited microstrip transmission line serves as a reactive loading element for a microstrip antenna. Constructed integrally with the stripline radiating element, the shorted line preserves the low microstrip profile and enables tuning of the antenna for two-band operation: previously, such tuning required a coaxial loading stub, which protruded into the space above the circuit board.

The loading element (see Figure 1) overcomes the inherent narrow bandwidth of the antenna, splitting the resonance into two different frequencies. The change in resonant frequency is affected by the stub length, L; the insert distance, S; the gap width, G; the strip width, W; and the thickness and permeability of the dielectric.

As G is increased, the lower resonant frequency decreases, but the upper resonant frequency is hardly affected. As S is increased, the two resonant frequencies are brought closer together. L is set according to theoretical predictions of the stub lengths that cause dual resonance. Thus, the antenna can be made to resonate at two specified frequencies by a suitable choice of radiator and loading-element dimensions, as shown for example in Figure 2.

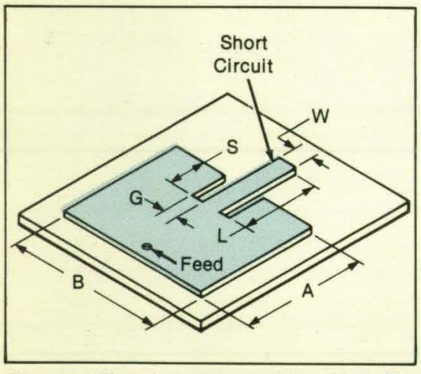


Figure 1. The **Antenna and Loading Element** are made as a unitary microstrip.

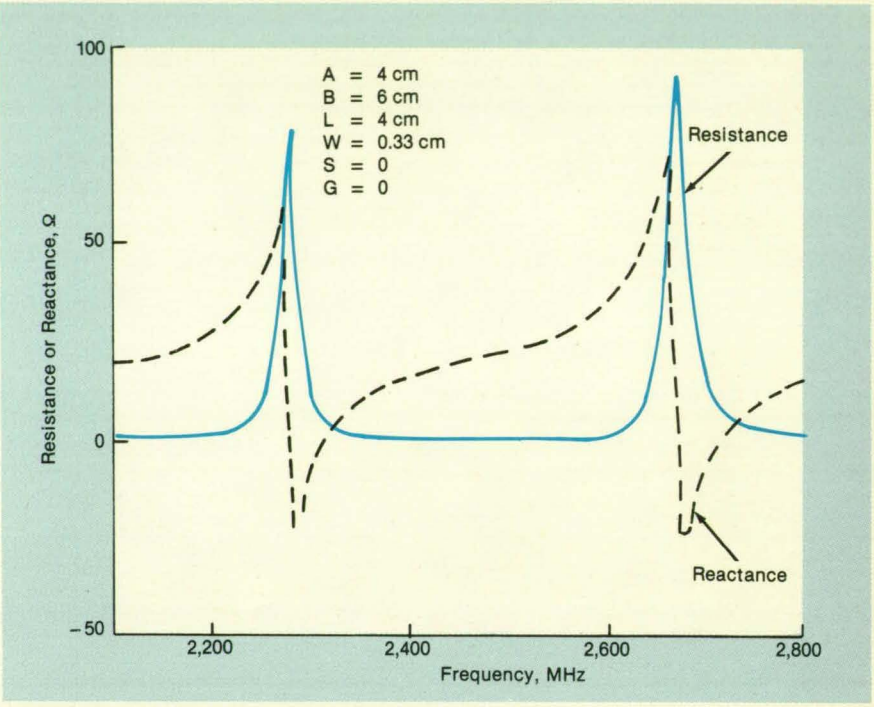


Figure 2. **Two Resonances** are exhibited by a unit like that shown in Figure 1.

This work was done by Shayla E. Davidson of **Johnson Space Center**. *For further information, Circle 94 on the TSP Request Card.*
MSC-21118

Wide-Band, Wide-Scan Antenna for Circular Polarization

Circular polarization is generated by linearly polarized elements.

NASA's Jet Propulsion Laboratory, Pasadena, California

Circularly polarized radio waves are generated by an array of linearly polarized elements composed of subarrays of four balanced elements. Within each subarray, the angular orientations and phases of the elements are 0°, 90°, 180°, and 270°, respectively. The axial-ratio bandwidth of such an array is greater than that of conventional circularly polarized antennas, and the main beam can be scanned to relatively wide angles without seriously degrading the circular polarization. A microstrip antenna based on this concept weighs less, has a less complex feed system, and has lower loss than does a conventional antenna for circular polarization.

In the microstrip version shown in the figure, the orthogonal sets of patches generate orthogonal electromagnetic fields, while the different phases of the feeds provide the 90° phase difference needed for circular polarization. At beam angles other than broadside (that is, other than perpendicular to the plane of the array) in the x-z and y-z planes, the spatial phase delays among elements do not degrade the circular polarization because the phases change by the same amount for both of the component linearly polarized waves. To an observer far away, the radiation appears to

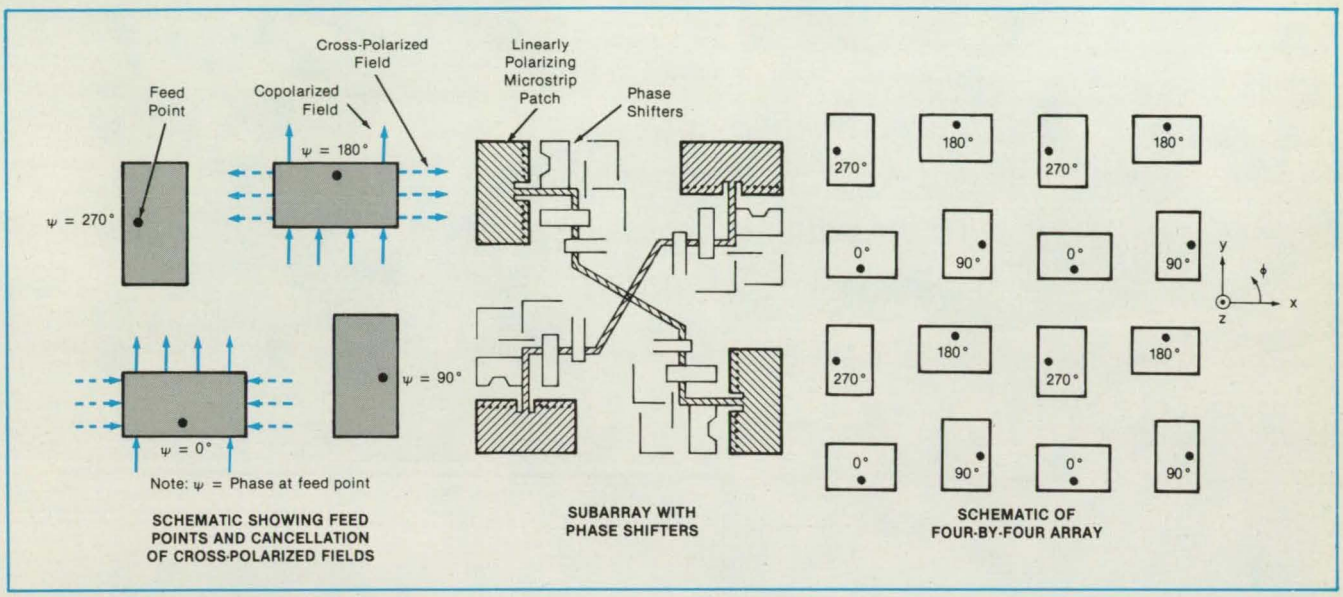
emanate from two circularly polarized sources.

In the broadside direction, the copolarized components from different radiating elements reinforce each other, while the cross-polarized radiation impurities cancel each other. This is a particular advantage in microstrip arrays having thick substrates, which generate undesired higher-order modes. The cancellation of the cross-polarized components results in large axial-ratio bandwidth.

In principle, the undesired fields do not cancel in beam directions outside the principal planes. In practice, however, the beam-narrowing and averaging effects in large arrays do suppress the radiation of spatial field impurities, with the result that the polarization is nearly circular over a wide range of beam directions in all planes. Another advantage of the spatial arrangement of elements is that the mutual coupling of this type of array is less than that of a conventional array: the orthogonality allows very little coupling between immediate neighboring elements.

Arrays of 2×2, 4×4, and 2×8 elements have been tested sucessfully. Although the development efforts have thus far concentrated on microstrip versions, the concept should be applicable to arrays of rod dipole or other radiating elements. Antennas of this general type should prove useful in communications and phased-array radar.

This work was done by John Huang of Caltech for **NASA's Jet Propulsion Laboratory**. *For further information, Circle 90 on the TSP Request Card.*
NPO-16831



The **Basic Two-by-Two Subarray** of antenna elements can be made of microstrip patches. The patches are arranged in an orthogonal pattern. The patches are fed through different phase shifters so that the signals at their feed points have the same orthogonal relationship in phase.

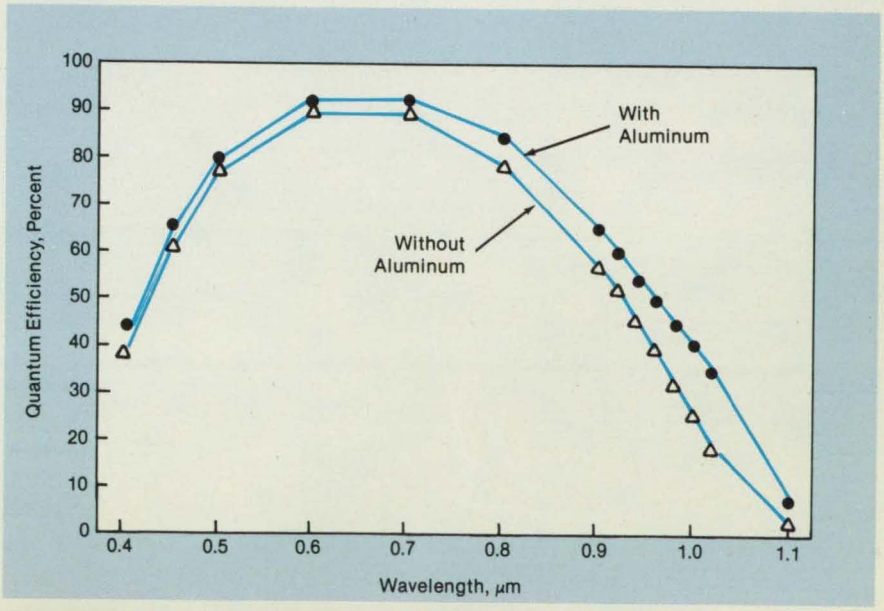
Coatings Boost Solar-Cell Outputs

Efficiencies are increased by more-complete utilization of incident light.

NASA's Jet Propulsion Laboratory, Pasadena, California

The electrical outputs of thin solar photovoltaic cells made of dendritic-web silicon are increased by a combination of front-surface, antireflective coatings and back-surface, reflective coatings. Although the use of such coatings is well established, improvements have been achieved recently through theoretical and experimental studies of ways to optimize the coatings for the particular wavelengths of incident light, cell thicknesses, and cell materials.

If the thickness of the cell is less than or comparable to the photon-absorption length, then an appreciable fraction of the incident light reaches the back surface unused. For example, at wavelengths greater than 0.9 μm, a 125-μm-thick dendritic-web-silicon cell absorbs only 93 percent of the usable photons. In that case, a back-surface reflective coating sends unused light back into the cell, enabling more of it to be converted to electrical energy on the second pass.



The **Internal Quantum Efficiency** of a photovoltaic cell is increased by the use of a more-reflective back-surface contact made with aluminum.



Copyright © 1987, Tektronix, Inc. All rights reserved. SAA-626

BUILT FOR THE BENCH.

The Tek 2750 Series of Laboratory Spectrum Analyzers. Configuration flexibility. Optioned to your application. From the powerful, fully programmable new 2756—at 325 GHz—to the VHF/UHF 2753, Tektronix sets a better-value standard in laboratory spectrum analysis.

Only Tek makes it so cost-effective to optimize spectrum analysis to your set of requirements and value criteria, whether your primary need is high-end performance—for research and development—or repeatability and throughput for manufacturing test.

You'll find a perfect fit for your bench, systems and budget needs. A choice of seven lab analyzers makes it possible for Tek to meet your needs precisely—at any frequency—with the right measure of economy and outstanding ease of use.

A built-in precision counter, Macro programming and signal processing intelligence are just a few ways to optimize the 2750 Series for your own use. Look at Tek features like marker frequency accuracy of 10^{-9} and automatic signal tracking. And with TekSPANS® software—available for IBM PC, Tek and HP controllers—you can automate complex measurements, including EMI tests.

What you can count on is more performance for the dollar than you've ever seen, including superior optionability: Tek waveguide mixers, preselectors, MATE compatibility, 75-ohm input, rackmount, computer packages and software for your system needs, and more.

Get the facts! Discover the Tek value differential before you make another buy. Contact your Tek Sales Engineer or call direct: 1-800-TEK-SPEC, Ext. 23. In Oregon: 235-7315, Ext. 10.

TEKTRONIX 2750 SERIES LAB SPECTRUM ANALYZERS

Tektronix®
COMMITTED TO EXCELLENCE

Circle Reader Action No. 329

The Ti/Pd/Ag back metal ordinarily used on solar cells is a poor reflector of photons with wavelengths greater than 0.9 μm. However, aluminum reflects 90 to 95 percent at these wavelengths, and a reflective back-surface contact can be made of Al/Ti/Pd/Ag. Measurements of the output of a cell at visible and near-infrared wavelengths showed that the inclusion of aluminum in the back-surface coating produces a small increase in efficiency (see figure).

The front antireflection coating increases the cell output further by enabling more light to enter the cell. According to calculations, an improved antireflection coating can be made by thermally evaporating a 548-Å layer of ZnSe, followed by a 1,040-Å layer of MgF_2, on the bare silicon surface. If the cell has a passivating surface layer of silicon dioxide, then the layer thicknesses must be changed to 398 Å and 1,080 Å, respectively. With these thicknesses, the predicted increase in short-circuit cell current is 51.7 percent. Experiments with coated cells showed increases of as much as 50 percent. The discrepancy between the prediction and the measurements is probably due to absorption in the ZnSe film.

This work was done by Ajeet Rohatgi, Robert B. Campbell, T. W. O'Keefe, Posenjit Rai-Choudbury, and Richard A. Hoffman of Westinghouse Electric Corp. for **NASA's Jet Propulsion Laboratory**. *For further information, Circle 121 on the TSP Request Card.*
NPO-16819

Compact Sun-Position Sensor

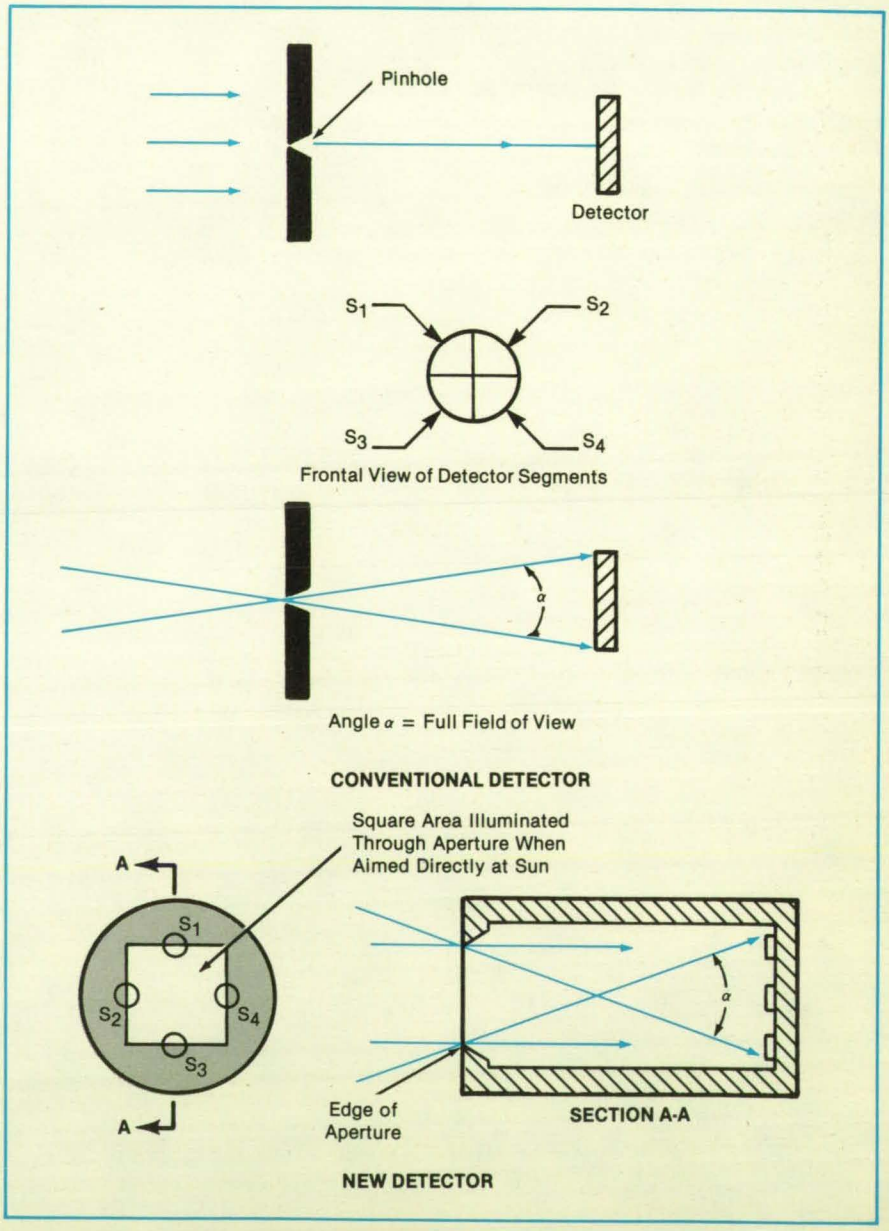
A single device finds and tracks the Sun.

Ames Research Center, Moffett Field, California

A light sensor combines a wide field of view with high resolution so that it can be used for both finding and tracking a moving light source like the Sun. The sensor was developed as a smaller, lighter, and simpler replacement for an instrument that employed two sensors — one with coarse resolution and a wide field for finding the Sun and one with fine resolution and a narrow field for following the moving Sun after it has been found. Previously, the integration of the two types of sensors introduced mechanical and electronic complexity.

A conventional Sun-position sensor (see top of figure) includes a single photodetector divided into four quadrants, on which a spot of light is projected from a pinhole aperture. To increase the field of view, the diameter of the detector can be increased, or the distance between the aperture and detector can be decreased. However, the diameter should be small to keep noise and response time short. Moreover, decreasing the aperture distance makes the detector less sensitive to changes in spot position. Thus, a wide field of view is incompatible with high resolution.

The new sensor contains four photodetectors spaced 90° apart on a circle opposite the square aperture of a small cylindrical chamber (see bottom of figure). The aperture casts equal shade on the detectors when the cylinder axis points directly at the center of the Sun. Upward or downward movement of the Sun places one of the vertical-motion detectors in more shade and the other in less shade. The difference in the outputs of the two vertical-motion detectors S_1 and S_3 is therefore an elevation-error signal. Similarly, sideways motion of the Sun changes the shade on each of the horizontal detectors relative to the other so that S_2 and S_4 generate an azimuth-error signal. The detectors can be photovoltaic cells or photoresistors.



The **Conventional Sensor** (above) can have a wide field of view or high angular resolution but not both. The new sensor (below) has both a wide field of view and high angular resolution when its axis is within a few degrees of the line to the Sun.

Only one video camera can be any video camera you want it to be.

Available on GSA Contract GSOOK87AGS0101.



Imagine being able to design a camera to suit your every need. You can with the Panasonic® WV-D5000 because it's totally modular. Just choose the ENG, EFP, or studio configuration that's right for you.

The WV-D5000 is even more versatile. You can use some of the world's finest photographic lenses. Lenses you may already own. Lenses from Canon, Pentax, Minolta, Olympus and Nikon. Wide angle lenses. Long lenses. Lenses for telescopy and microscopy.

And if that isn't impressive enough, the WV-D5000 has a strobe-effect shutter speed of 1/1000th of a second. That means you can shoot high-speed action like a roller coaster and during VCR playback actually see the excitement on a child's face.

But whether the action is fast or slow, the WV-D5000's CCD pickup element provides clear, stable video images with a minimum of blooming and burn-in. Horizontal resolution is a hefty 380 lines while S/N is a quiet 46dB. And when it comes to light, you need only 0.7 footcandles at f1.4.



You'd expect a camera of this caliber to be fully flexible, and the WV-D5000 fulfills your every expectation. With auto-tracing white balance, intermittent recording as well as audio and video fade-in and fade-out.

The Panasonic WV-D5000. It's the one video camera you can customize to be any video camera.

Panasonic
Professional/Industrial Video

For more information and your copy of the Authorized Communications Schedule Price List contact your local Panasonic Industrial Video dealer or call (703) 486-5533 (FTS: (202) 486-5533) or write to Government Marketing Dept., Panasonic AVSG, Suite 901, 1215 Jefferson Davis Highway, Arlington, VA 22202-4302.

Circle Reader Action No. 380

This work was done by Yutaka Matsumoto and Cesar Mina of **Ames Research Center**. *No further documentation is available.*

Inquiries concerning rights for the commercial use of this invention should be addressed to the Patent Counsel, Ames Research Center [see page 16]. Refer to ARC-11696.

Designing a Microwave Band-Stop Filter

Lumped-circuit design techniques are applied to iris-coupled cavities.

NASA's Jet Propulsion Laboratory, Pasadena, California

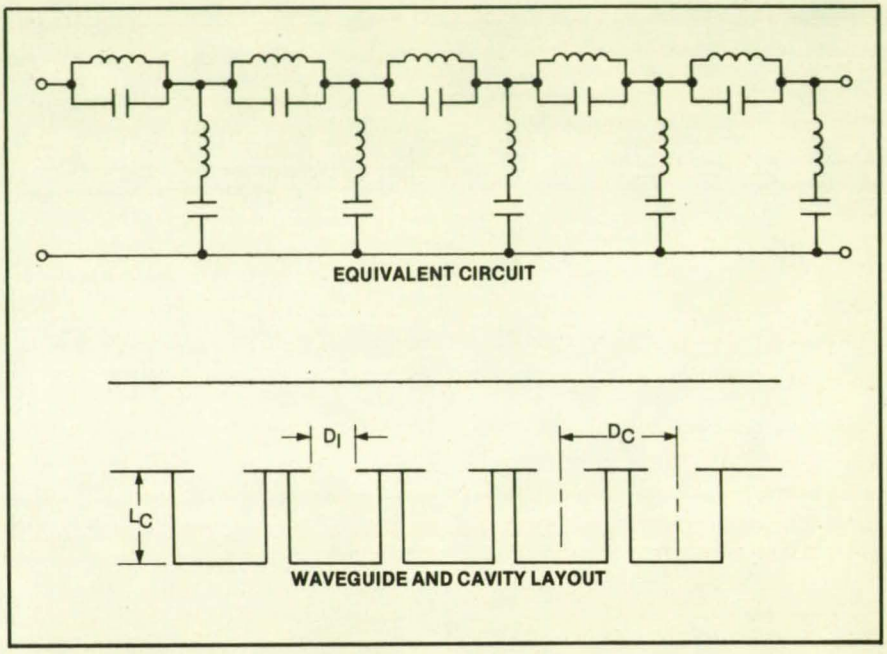
A band-stop filter for use with a maser preamplifier in an X-band receiver consists of five resonant cavities coupled through irises to a waveguide (see figure). The design specification calls for the filter to provide 70 dB of rejection at frequencies of 7.145 to 7.235 GHz to protect the maser from a 20-kW transmitted signal, while allowing signals received at 8.4 to 8.5 GHz to pass to the maser with no more than 0.5 dB of insertion loss.

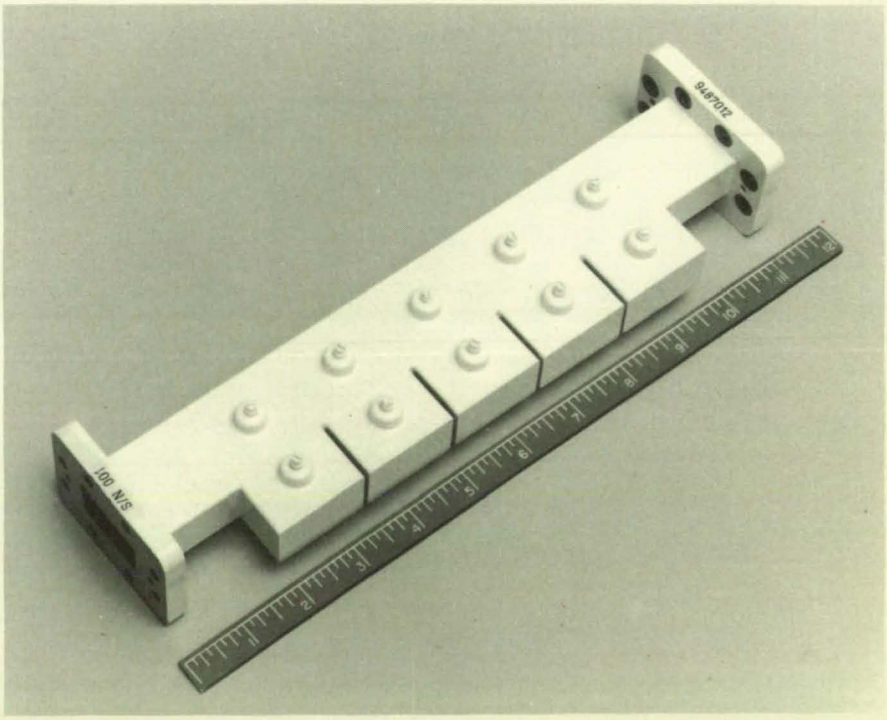
To obtain data to start the design procedure, the return loss and the transmission loss of a one-cavity filter were measured as a function of frequency in and about the stopband for several values of the iris diameter (D_I) and cavity length (L_C). With the help of a computer program, these measurements were fit to the response of an equivalent combination of series and parallel inductances and capacitances representing the cavity/waveguide junctions: it is possible to do this because, over narrow frequency bands, cavity/waveguide filters behave like lumped-element resonant circuits.

From the measurements, curves were obtained to show the variation of the band-stop resonant frequency as a function of D_I and L_C. An infinite number of combinations of D_I and L_C give the same resonant frequency. However, the insertion loss and the transmission loss both increase with D_I. Consequently, the optimum combination of D_I and L_C is the one with the smallest D_I that will still provide the required stop-band transmission loss.

The optimum pair of D_I and L_C was selected by the use of the equivalent inductances and capacitances in a computer program that simulated the characteristics of the five-cavity filter. This program also found the optimum cavity spacing (D_C) for each pair of D_I and L_C. The optimum values for the filter were found to be L_C = 0.82 in. (2.08 cm), D_I = 0.78 in. (1.98 cm), and D_C = 1.58 in. (4.01 cm). These values correspond to a resonant frequency of 7.240 GHz. A tuning screw in each cavity enables fine adjustment of the band-stop resonance frequency to the specified value of 7.190 GHz. A tuning screw at each cavity/waveguide junction is used to adjust the pass-band voltage standing-wave ratio to no more than the specified maximum of 1.05:1.

This work was done by F. Manshadi of **Caltech** *for* **NASA's Jet Propulsion Laboratory**. *For further information, Circle 106 on the TSP Request Card.* *NPO-16945*





PRODUCTION UNIT

The **Waveguide/Cavity Filter** imitates lumped series and parallel combinations of inductance and capacitance over a narrow stopband centered at 7.190 GHz. The filter is made of standard WR125 waveguide stock.

Electronic Neural-Network Simulator

Experimental circuits are faster than simulation programs run on digital computers.

NASA's Jet Propulsion Laboratory, Pasadena, California

A hybrid analog/digital neurocomputer made of standard components aids research in neural-network computing. It is used to study such neural-network concepts as those described in the following article.

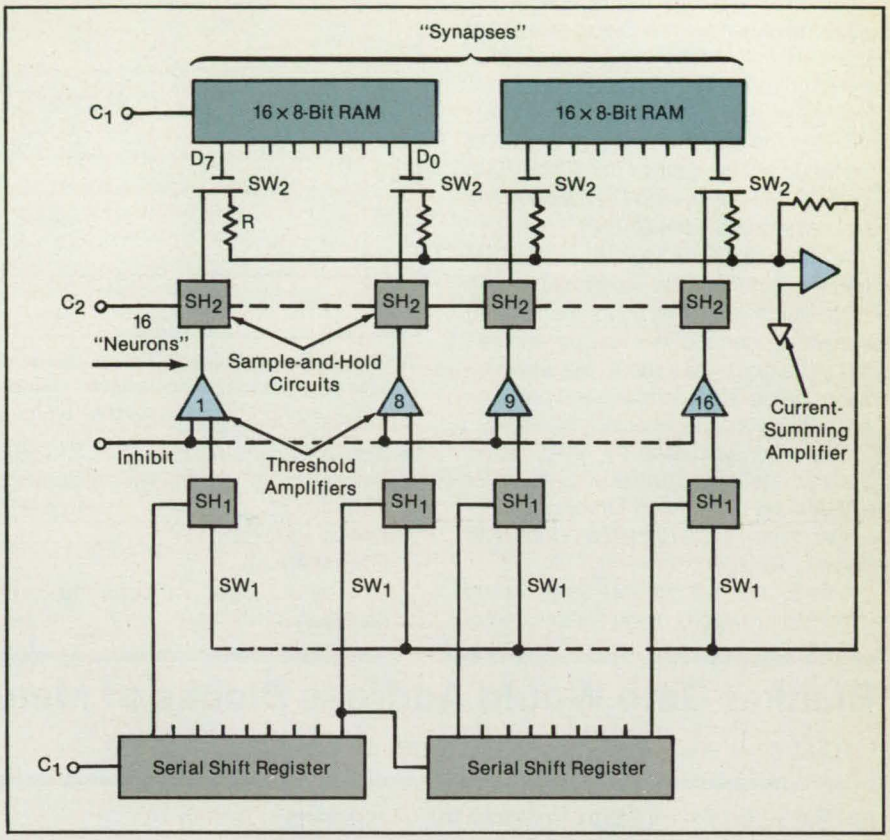
The computer contains a digital random-access memory that stores binary synaptic information and an array of analog threshold amplifiers with input and output sample-and-hold circuits that simulate neurons. The computer is faster than the software simulations previously used to experiment with electronic neural networks.

The computer is controlled by two clock signals, C_1 and C_2. The rate of clock C_2 is N times that of C_1, where N is the number of neurons. In the figure, there are 16 neurons, so that in this case, C_2 is 16 times as fast as C_1.

On each cycle of C_1, a serial shift register selects a neuron input for updating and sampling by one of the sample-and-hold circuits in group SH_1. The neuron input signal is determined by two factors: the current neuron output state at the outputs of the sample-and-hold circuits in group SH_2 and the synaptic information at the memory outputs that control pass-transistor array SW_2.

The updating process is repeated at each cycle of C_1, each neuron being checked in turn as directed by the serial shift registers. On each cycle of C_2, the neuron outputs — as determined by the updated inputs and the inhibiting signal — are sampled by the circuits in group SH_2, completing one system cycle. Thus, the system throughput and cycle time are set by the update-clock rate and the number of neurons. To prevent an update from being interrupted, the two clocks are not permitted to overlap.

The neurocomputer offers a significant reduction in hardware complexity over a fully-parallel electronic neural network. It is easily expandable and can be configured to simulate neural networks with either a feedback or feed-forward architecture. Furthermore, synapses with multiple quantized gray levels can be implemented with the incorporation of additional digital random-access memories.



A Serial Shift Register Routes Clock Pulses C_1 to neurons in sequence. Clock pulses C_2 interrogate the neurons. The neuron interconnection information is stored in the simulated synapses (the memory chips). The system shown here contains 16 neurons and 256 binary synaptic nodes. It can readily be expanded to greater complexity.

This work was done by Alex W. Moopenn, Anilkumar P. Thakoor, and John J. Lambe of Caltech for **NASA's Jet Propulsion Laboratory**. *For further information, Circle 67 on the TSP Request Card.*

This invention is owned by NASA, and a patent application has been filed. Inquiries concerning nonexclusive or exclusive license for its commercial development should be addressed to the Patent Counsel, NASA Resident Office-JPL [see page 16]. Refer to NPO-17058.

Programmable Synaptic Arrays for Electronic Neural Networks

High resistances prevent hotspots in parallel input and output operation.

NASA's Jet Propulsion Laboratory, Pasadena, California

A nonvolatile computer memory combines ultrahigh storage density with extremely-low power dissipation. It can accommodate about 1 billion bits in a square centimeter of surface area. A bit can be written with an expenditure of less than 1 nanojoule of energy and can be read with even lower energy.

The memory was developed for parallel input and output operation such as that in the Hopfield neural network, which is patterned after biological memories. In a neural-network memory, the memorized data do not reside in assigned locations but are widely distributed. The information is found by content rather than by address. Thus, many adjoining memory cells dissipate heat simultaneously as they are read from, and written to, in parallel. Hotspots of excessive dissipation would ordinarily result.

In the new memory, however, the energy released is so small that temperatures stay low even though the cells are densely packed. The cells are thin-film switching

elements, the ON resistances of which are high — about 1 MΩ — and the OFF resistances of which are even larger — about 1 GΩ. These extremely high resistances keep current and energy dissipation low when the elements change state.

A cell contains a film of hydrogenated amorphous silicon (or germanium) about 0.2 μm thick sandwiched between a pair of crossed thin-film conducting lines of nickel or indium tin oxide (see figure). A 1-μs voltage pulse applied through the contact changes the resistance of the portion of the film under the contact from $2\times10^9\,\Omega$ to $2\times10^4\,\Omega$, thereby turning ON the portion of the element under the contact.

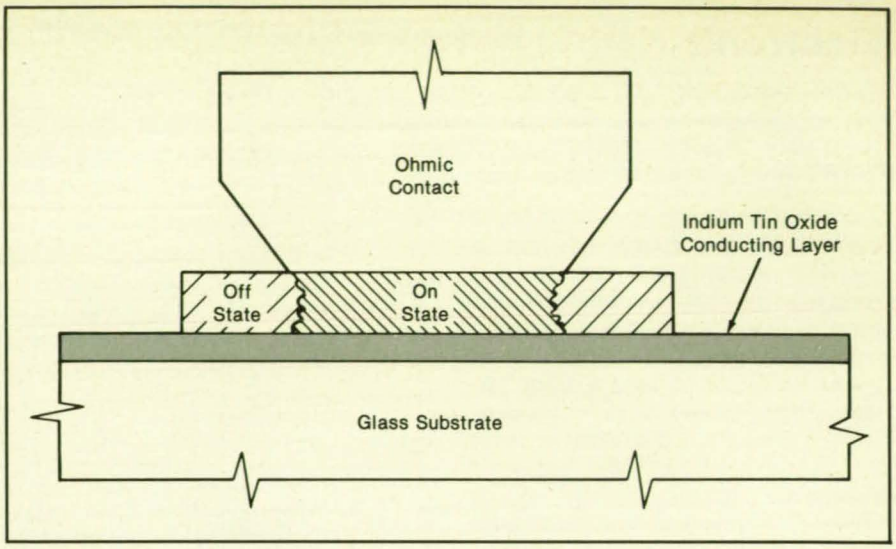
A large, stable, 1-MΩ thin-film ballast resistor connected in series with each microswitch (synapse) limits the reading and writing current. The resistor ensures that the energy delivered to the semiconductor cell is well controlled and prevents destructive runaway effects.

This work was done by Anilkumar P. Thakoor and John Lambe of Caltech for **NASA's Jet Propulsion Laboratory**. *For further information, Circle 68 on the TSP Request Card.*

Title to this invention has been waived under the provisions of the National Aeronautics and Space Act [42 U.S.C. 2457(f)], to the Caltech/JPL. Inquiries concerning licenses for its commercial development should be addressed to

Edward Ansell,
Director of Patents and Licensing
Mail Stop 301-6
California Institute of Technology
1207 East California Boulevard
Pasadena, CA 91125.

Refer to NPO-16674, volume and number of this NASA Tech Briefs *issue, and the page number.*



A **Memory Cell** includes an amorphous semiconductor film on a conducting thin-film wire on a glass substrate. An electrical lead makes contact with an area about 1 μm wide on the surface of the amorphous semiconductor film. The thickness of the conducting layer is 0.2 μm.

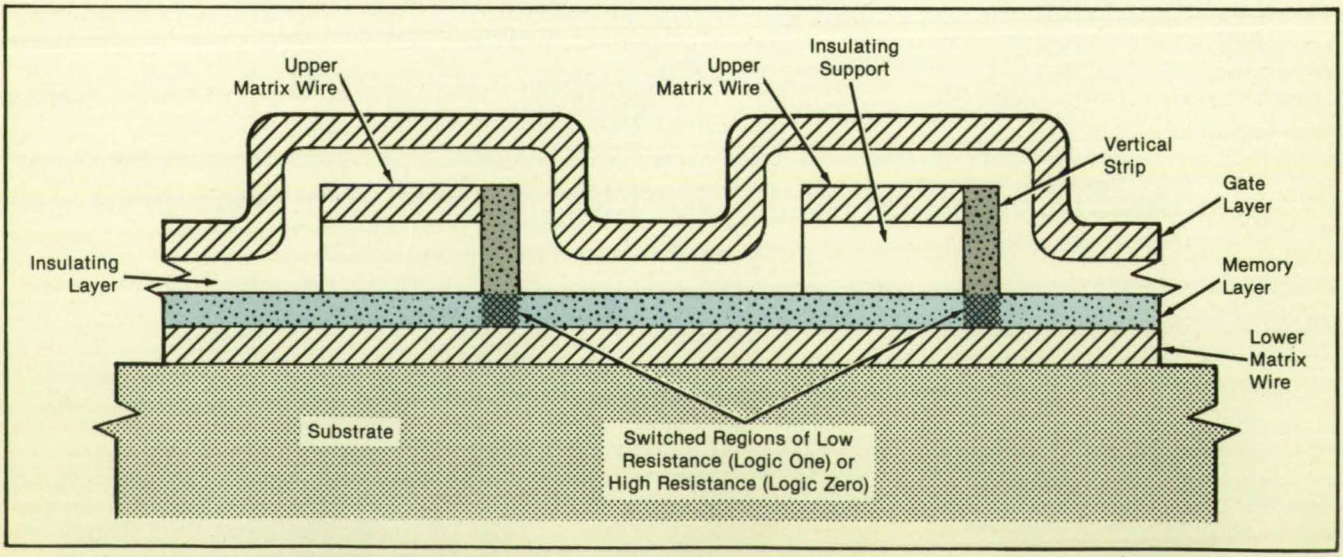
Blanket Gate Would Address Blocks of Memory

Circuit-chip area would be used more efficiently.

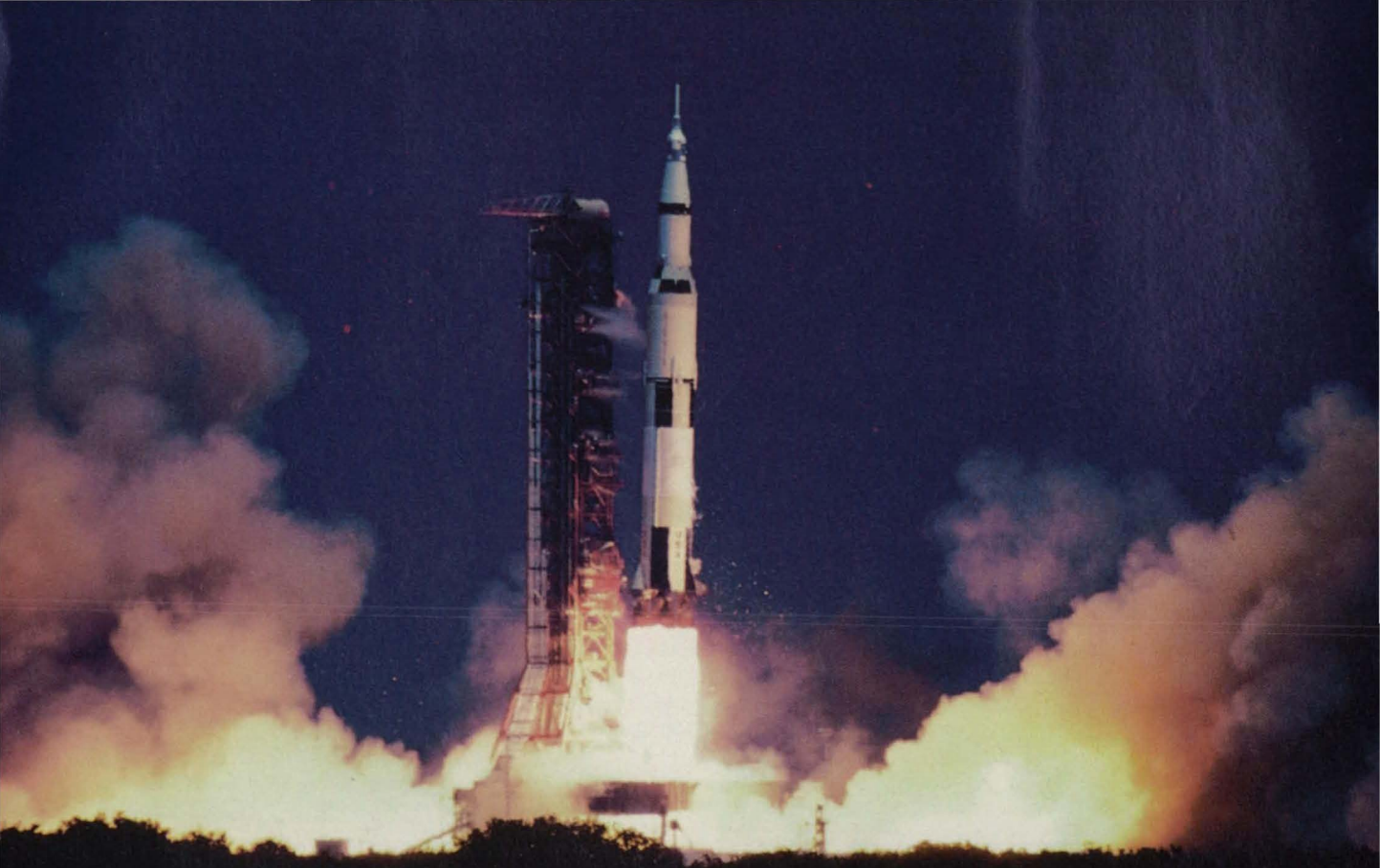
NASA's Jet Propulsion Laboratory, Pasadena, California

A proposed gate structure would selectively allow and restrict access to blocks of memory in an electronic neural-type network. By breaking the memory into independent blocks, the gate would greatly simplify the problem of reading from and writing to memory. For example, since the blocks would not be used simultaneously, they could share the operational amplifiers that prompt and read information stored in the memory cells. Far fewer operational amplifiers would be needed, and the chip area they occupy would be reduced correspondingly. The cost per bit would drop as a result.

The gate would overlie an array of thin-film amorphous silicon memory cells like those described in the preceding article. Instead of being discrete cells, however, the array of resistors would lie in a single continuous layer in which the extremely high resistivity of the material would isolate the cells from each other. Each block of cells would be provided with its own blan-



The **Blanket Gate Layer** would overlay the memory cells in a block. (Two cells are shown here.) A voltage on the gate layer would inhibit reading and writing throughout the block. The inhibiting mechanism is much like that in an insulated-gate transistor.



America's largest travel service plans the space industry's more conventional flights.

Even the space industry is not immune to the high cost of conventional travel here on earth. That's why they have their travel managed by Ask Mr. Foster.

Only Ask Mr. Foster offers such an extensive selection of money-saving travel management programs. Including our guarantee of the lowest available airfares everytime, the finest hotel program in the business with exceptional discounts at over 13,000 hotels worldwide, special car rental savings plus a host of other services.

It's travel management programs like these that explain why Ask Mr. Foster has been Corporate America's most dependable traveling companion for 100 years.

The next time you make travel plans, call Ask Mr. Foster at 1-800-FOSTER-5. We'll help you with your conventional travel plans, as well as something unconventional: saving money.

You can expect the world of us.℠

Ask Mr. Foster® Travel
Since 1888

Circle Reader Action No. 527

ket gate.

Within a blanket gate, memory cells would lie between matrix wires running at right angles to each other in parallel planes (see figure). At each cell, the upper matrix wire would be connected to a vertical strip that makes contact with the memory layer. Like the memory layer, the vertical strips would be made of amorphous hydrogenated silicon or germanium. (The vertical strip replaces both the ballast resistor and the contact described in the preceding article.) A voltage applied between a strip and its lower matrix wire would change the local resistance of the memory film from high to relatively low, thereby switching the memory cell on (changing its logic state from zero to one). The change would be permanent; that is, the memory would be nonvolatile.

The gate structure would include an insulating layer and a conducting gate layer that blankets the cells in a block. A voltage could be applied to the gate layer to deplete the carriers in all the vertical strips in the block. The strips thus could be prevented from conducting pulses fed to them by the upper and lower matrix wires, and both writing and reading of the memory cells would thereby be prevented. The block of memory cells would thus be cut off from the rest of the system. When the blocking voltage on the gate layer is removed, the block would be reconnected to the rest of the system.

Conventional fabrication methods would be used; fine-line lithography would not be necessary. The lower wire matrix would be deposited on a substrate, followed by the amorphous silicon memory layer. Insulating supports would be deposited on each row of cell sites through a mask, and the upper matrix wires would be deposited on the supports. The vertical strips would be deposited on the sides of the supports by evaporation from a silicon source.

In a content-addressable memory, each block of cells would be associated with a class or subclass of contents. For example, a block might be dedicated to data on people whose surnames begin with the letter J. When searching for data on one such person, the controlling and encoding microprocessor would send out a signal to all other blanket gates so that only the J block could be read.

Although the memory array for the blanket gate would not be as densely packed as the discrete-cell memory in the preceding article would be, the bit density would still be quite high — about 10 times that in conventional semiconductor memories. This is because the decrease in cell density would be more than offset by the elimination of the large circuit-chip area that would otherwise be required for duplicate operational amplifiers.

This work was done by John Lambe, Alexander Moopenn, and Anilkumar P. Thakoor of Caltech for **NASA's Jet Propulsion Laboratory**. *For further information, Circle 66 on the TSP Request Card.*

Title to this invention has been waived under the provisions of the National Aeronautics and Space Act [42 U.S.C. 2457(f)], to the Caltech/JPL. Inquiries concerning licenses for its commercial development should be addressed to

Edward Ansell,
Director of Patents and Licensing
Mail Stop 301-6
California Institute of Technology
1207 East California Boulevard
Pasadena, CA 91125.

Refer to NPO-16682, volume and number of this NASA Tech Briefs *issue, and the page number.*

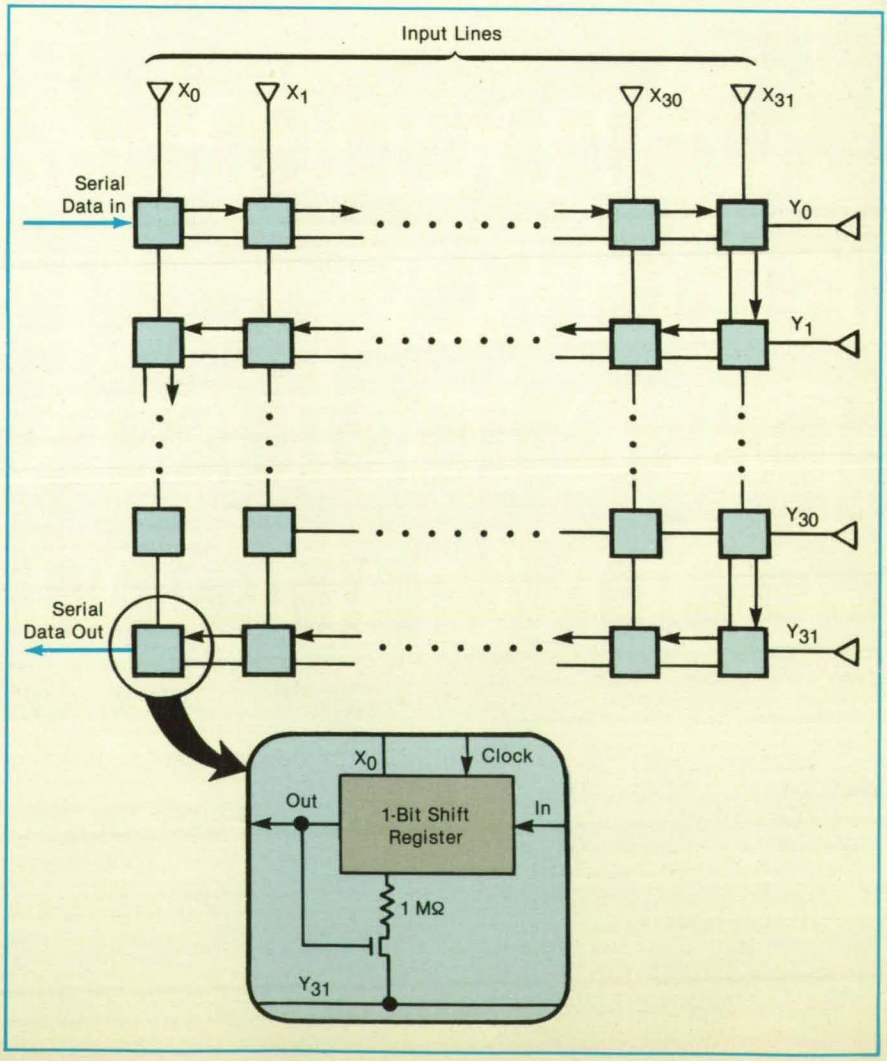
Integrated Circuit for Simulation of Neural Network

Ballast resistors are deposited on top of the circuit structure.

NASA's Jet Propulsion Laboratory,
Pasadena, California

A cascadable, programmable binary connection matrix is fabricated in VLSI form as a basic building block for assembly of like units into content-addressable electronic memory matrices that operate somewhat like networks of neurons. In such a matrix, connections are formed during the storage of data, and the data are recalled from memory by prompting the matrix with approximate or partly erroneous signals. In many cases, redundancy in the pattern of connections causes the matrix to respond with the correct stored data.

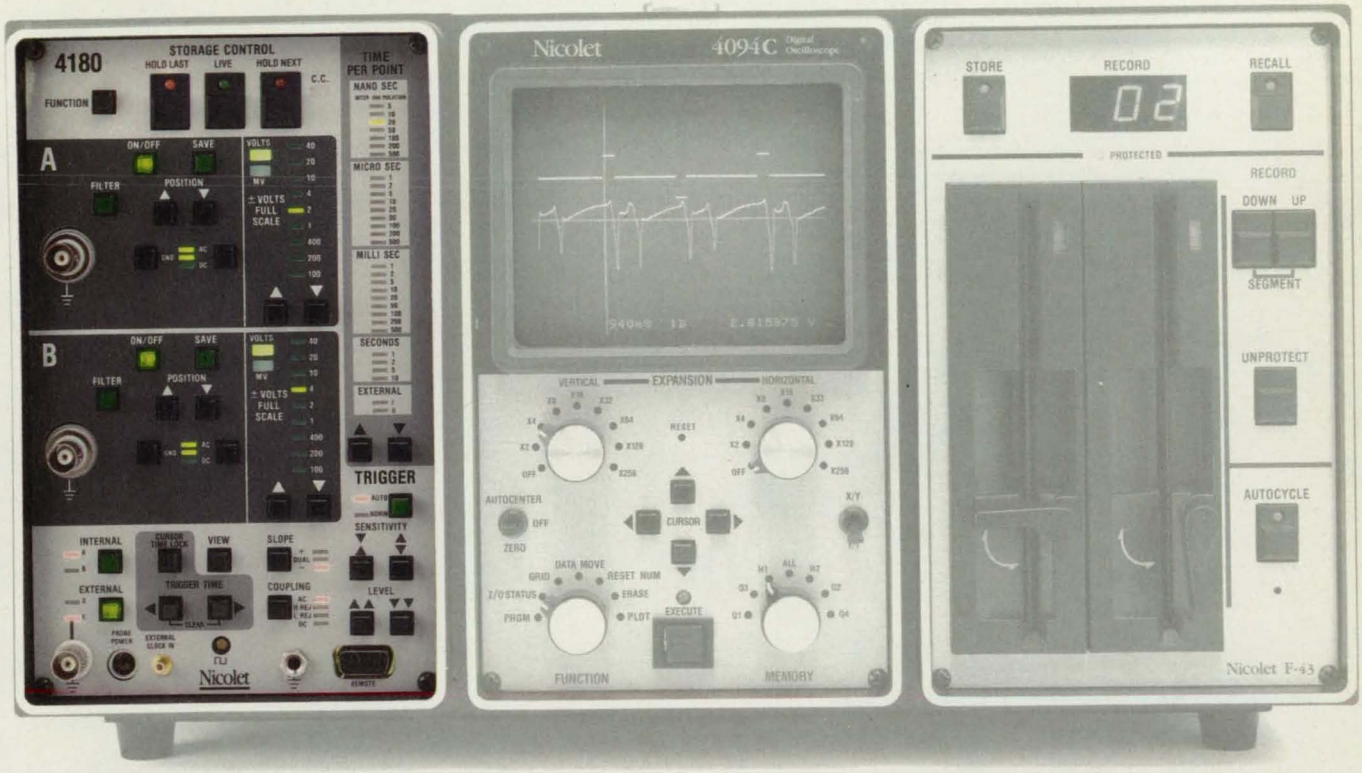
The matrix is an integrated circuit, the active elements of which are complementary metal-oxide/semiconductor (CMOS) devices. Each circuit chip includes 32 input ("X") lines and 32 output ("Y") lines (see figure). Each node of the matrix includes an analog switch that is turned on or off ac-



A **Cascadable, Programmable, VLSI(32 × 32) Synaptic Chip** based on the neural network architecture provides a basic building block for larger (e.g., 512 × 512) neural network embodiments.

The New 4180 Plug-In

SPEED TRIALS.



- *Multi-channel: two or four channel configurations.*
- *Unmatched single-shot capabilities.*
- *High speed, 200 MHz digitizing.*
- *100 MHz analog input bandwidth.*
- *Real-time math functions.*

- *For your Free Speed Trial call: 800-356-3090 or 608-273-5008*

Nicolet Test Instruments Division
P.O. Box 4288
5225-2 Verona Road
Madison, WI 53711-0288

Nicolet Digital Oscilloscopes

Speed. Using the latest designs in ADC technology, your input signal can be digitized at speeds up to 200 MHz (5ns per data point) and saved for analysis. The wide band input amplifiers allow signals up to the 100 MHz Nyquist limit to be input without distortion. Sophisticated trigger setup displays allow you to accurately set the level, sensitivity, and slope to make one-shot transients easy to catch; eliminating the usual hit or miss guesswork. For multi-channel applications two 4180's can operate together in one mainframe producing a four channel scope with no degradation in speed or performance.



Real-Time Math. In addition to the extensive post-processing capabilities in the mainframe, the 4180 has several useful routines which present computed results as live, real-time displays: *FFT, MAX/MIN, A+B, A−B, A×B, A/B,* and *AVERAGING.*

Nicolet
INSTRUMENTS OF DISCOVERY

Circle Reader Action No. 350

cording to the output of the associated stage of a 1-bit serial shift register connected in cascade. The shift register is controlled by its input line; the binary connection data is serially shifted into the matrix along the input line at the rate of 1 bit per clock cycle.

To keep the static and dynamic power consumption below a maximum acceptable level, a 1-MΩ ballast resistor is connected in series with each analog switch. The active circuit elements are formed by conventional CMOS fabrication processes. Contact windows are opened in the metalization layer of the CMOS chip to enable the deposition of a patterned layer of suitable resistive material. In comparison with conventional CMOS processes for very-large-scale integrated circuits, this process lends itself more readily to the attainment of the required 5-percent precision in the ballast resistances.

A representative 512- by 512-node matrix would be made by assembling a 16-by-16 array of such chips. At a practical clock rate of 1 MHz, the connection pattern could be shifted into this matrix in a time of 0.262 s.

This work was done by Anilkumar P. Thakoor, Alexander W. Moopenn, and Satish K. Khanna of Caltech for **NASA's Jet Propulsion Laboratory**. *For further information, Circle 70 on the TSP Request Card.*

NPO-17059

Three-Waveguide Beam and Polarization Splitter

Different modes are guided to different output ports.

NASA's Jet Propulsion Laboratory, Pasadena, California

A monolithic ensemble of three waveguides splits an input signal beam into three output beams according to the polarization components. The waveguides are made of titanium diffused in lithium niobate. Before the diffusion step, the titanium is deposited to form an inner (middle) waveguide and outer waveguides on both sides of the inner one.

The gap between each outer waveguide and the inner waveguide is made very small over a predetermined part of the total length. The length of this region of proximity and the size of the gap are selected in conjunction with the diffusion conditions to be used, with a view toward obtaining the desired beam- and polarization-splitting functions. A field plate is placed over each waveguide along at least the portion of its length in the region of proximity to the adjacent waveguide.

In operation, the plates over the outer waveguides are energized with like voltages, while the plate over the inner waveguide is energized with a different voltage. If a signal that has transverse electric and transverse magnetic components is fed into one end of the middle waveguide, then a pure transverse electric signal emerges from the other end of the middle waveguide, while equal transverse magnetic signals emerge from the other ends of the outer waveguides.

This work was done by Gail A. Bogert of AT&T Technologies, Inc., for **NASA's Jet Propulsion Laboratory**. *For further information, Circle 109 on the TSP Request Card.*

NPO-16986



Circle Reader Action No. 537

Is your subscription about to expire?

Check the expire date. If it is less than 6 months now is the time to fill out a new qualification form before your subscription expires.

The NEW Alsys Cross-Development System

AdaNOW

Real-Time Embedded, Bare-Board Ada Now Targeted To Entire iAPX86 Family.

Efficient, compact, production quality Ada code. Efficient, application-tailored Run Time system. On an 8 MHz 286, a pure synchronization rendezvous in 250 microseconds.

Real-time Ada has come of age.

The new Alsys cross-development system is now available. And, of course, validated. It is hosted on an IBM PC AT or compatible, and targets every member of the Intel iAPX86 family.

The system contains two compilers and a toolset. First, a validated Ada cross-compiler to bare 8086, 80186, 80286, 80386 and other boards. Second, a validated self-hosted Ada compiler on the AT that allows you to generate code for the target that can be tested on the host.

And the tools. First, AdaProbe, Alsys' unique debugger and program viewer for the host, and Cross-AdaProbe for the target. And then, a complete and uniquely powerful multi-library system, binder, AdaReformat, AdaXref, AdaMake, downloading utilities, configurability interface, and utilities supporting PROM-burning.

The new cross-development system is based on the new Alsys Version 3 "root" representing a quantum leap forward in Ada technology. If you thought Ada wasn't ready for real-time, you owe it to yourself to call.

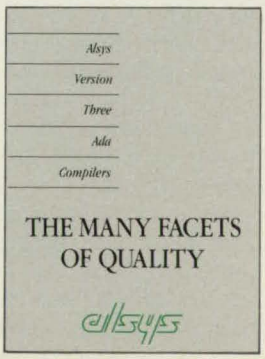
alsys

In the US: Alsys Inc., 1432 Main St., Waltham, MA 02154 Tel: (617) 890-0030
In the UK: Alsys Ltd., Partridge House, Newtown Rd., Henley-on-Thames, Oxon RG9 1EN Tel: 44 (491) 579090
In the rest of the world: Alsys SA, 29 Avenue de Versailles, 78170 La Celle St. Cloud, France Tel: 33 (1) 3918.12.44

Send me: _____New Brochure on Ada Real-Time
_____Data Sheet on Cross-Compiling to the iAPX86
_____New Brochure on V. 3 "Quality"

Name_____
Company_____
Address_____
City_____State_____Zip_____
Phone_____

Alsys, Inc. • 1432 Main Street • Waltham, MA 02154



*Ada is a registered trademark of the U.S. Government (AJPO).

Circle Reader Action No. 341

Electronic Systems

Hardware, Techniques, and Processes

42 Electronic Neural Networks
44 Unified Robot-Control System
46 The Mark III Hypercube-Ensemble Computers
47 Dual Pilot-Tone Calibration Technique
49 Public-Facilities Locator for the Blind
49 Automatically Inspecting Thin Ceramics for Pinholes
50 Millimeter-Wave Radiometer Imager
54 Position and Force Control for Multiple-Arm Robots
55 Lightweight Video-Camera Head
56 Television-and-Laser Range-Measuring System

Books and Reports

57 Minimum-Time Control for Robotic Manipulators

Electronic Neural Networks

A memory based on neural network models is content-addressable and fault-tolerant.

NASA's Jet Propulsion Laboratory, Pasadena, California

An experimental memory system behaves like a biological memory in several respects: It retrieves data when stimulated by imperfect input, it is redundant enough to continue functioning when a memory cell fails and the stored data are addressed by the form of the data themselves, rather than by location as in conventional electronic memories.

The system (see Figure 1) includes an electronic equivalent of a synaptic network; in particular, a matrix of programmable binary switching elements over which the data are distributed. The switches are programmed in parallel by the outputs of serial-input/parallel-output shift registers (not shown). The input and output terminals of a bank of high-gain nonlinear amplifiers (representing neurons) are connected in a nonlinear-feedback configuration by the switches and by memory-prompting shift registers.

An input-data vector is encoded by a microprocessor or other small computer, then fed to the serial-input/parallel-output shift registers. To recall stored data, the prompting shift registers interrogate the matrix with a pattern of ones and zeros that approximates the information sought. If the recalling approximation is sufficiently close, the electronic neurons turn on and present the exact stored data.

The circuits based on discrete electronic components and architectures derived from the neural net concepts display several unique features, including fast associative recall of information, parallel input/output, and intrinsic fault-tolerance. Development of thin-film-based, nonvolatile, programmable, binary synaptic arrays (matrices of resistive microswitches) for high-density associative memory systems is currently in progress.

The example of Figure 2 illustrates the writing and reading of information in a 4-by-4 matrix of switched resistors. To insure that the reading of a memory does not cause spurious writing, the writing voltage must be double the reading voltage. In this

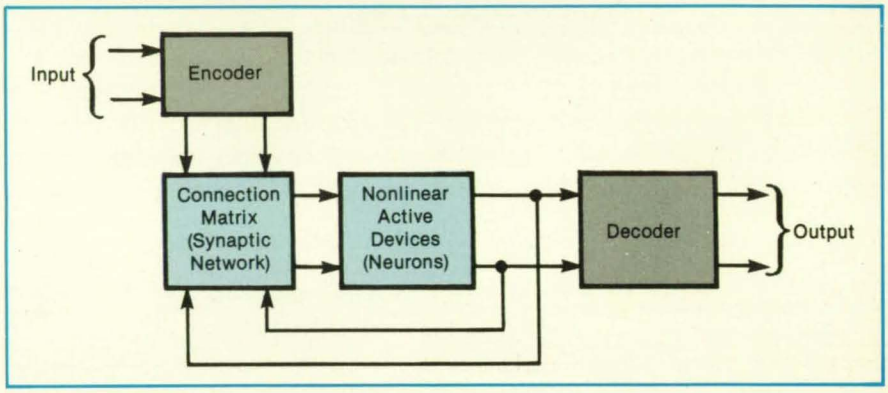


Figure 1. The **Memory System** includes a connection matrix of switching elements (representing a synaptic network) and a bank of nonlinear feedback amplifiers that mimic somewhat the behavior of neurons.

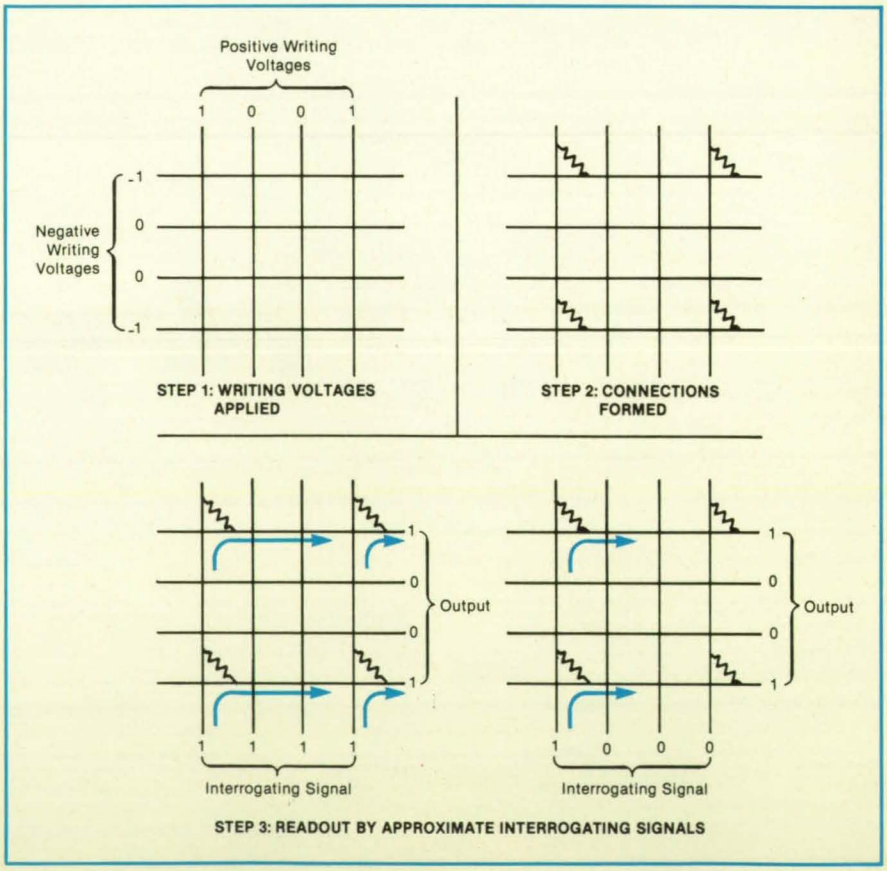


Figure 2. A **Small Switching Matrix** illustrates the approximate-input/exact-output and fault tolerance of the simulated neuron network.

VisionLab II. The Vision To Understand The Unknown.

VisionLab II breaks the time barrier, with more real-time image processing features. And it breaks the price barrier, with big system performance on an economical, compatible microcomputer system.



Image analysis

New from 3M Comtal, VisionLab II's advanced design delivers exceptional true color, 60Hz, flicker-free performance, plus:

- Real-time continuous roam and zoom.
- Near real-time region of interest processing, spatial processing, convolutions, histograms and filtering.



Contrast enhancement

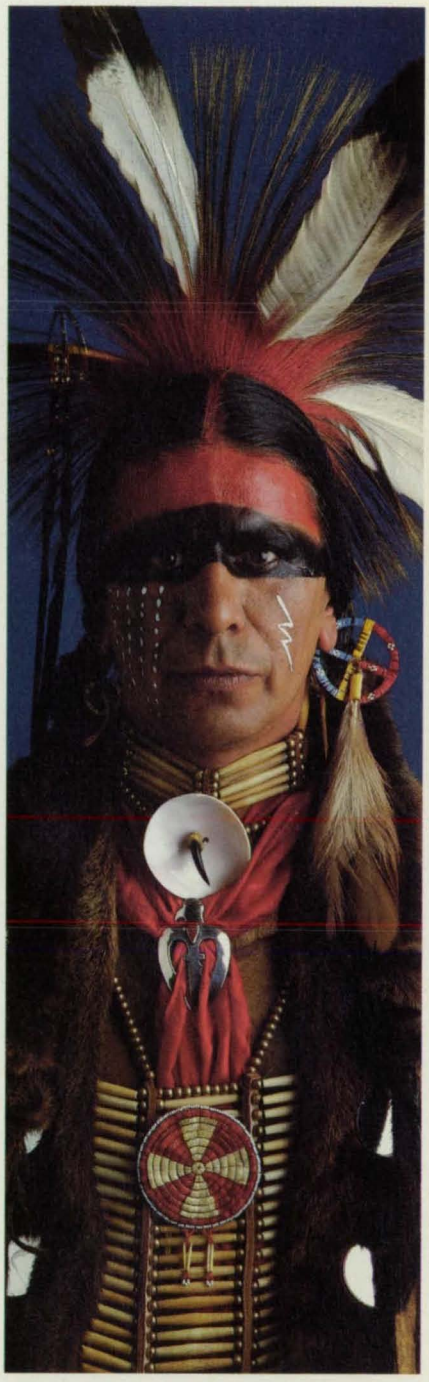
- A unique separate video bus, with an image-transfer rate of 36MPixels/second.
- Standard configuration of four 512 x 512 x 8-bit memory planes, plus 640 x 512 x 1-bit overlay for graphics and icons.
- Dynamic allocation for RGB true color operation, YMCK four color operation, or 1024 x 1024 x 8-bit, with real-time continuous zoom and overview.
- Standard and non-standard video inputs including RS170/330, NTSC and TTL.
- Genloc, with up to four programmable video inputs.
- Standard real-time data capture and optional real-time true color capture.



Zoom and pseudocolor

- Real-time spatial data compression, variable windowing, aspect ratio correction and contrast and gamma correction.

Plus much more. VisionLab II has the power and the performance to revolutionize how you utilize digital imaging. It's the kind of breakthrough you'd expect from 3M Comtal, pioneers in a New World of image processing technology.



VisionLab II

Expanding the Powers of Perception

3M Comtal
For information call today:
(800) 423-4166 · CA: (818) 441-1900

3M

Circle Reader Action No. 319

example, the binary number 1001 is to be stored. A unit positive voltage is therefore impressed on the first and fourth vertical lines and a unit negative voltage on the first and fourth horizontal lines. The ancillary switching circuitry detects the double-unit voltage difference at the intersections of the lines with the +1 and −1 voltages and responds by switching in the resistors at these four intersections. The resistors remain after the writing voltage is turned off.

The data can be read out, for instance, by interrogating with signals on the vertical lines and detecting currents on the horizontal lines. In this example, if the interrogating signal is 1111, it causes currents representing 1001 to flow out of the horizontal lines. The 1111 reading signal is only an approximation of the data; yet it causes the precise 1001 value to be read out. A reading signal of 1000, 0001, 1101, 1011, or 1001 would also produce the correct result.

Since the number 1001 is effectively recorded in two places in the matrix, the correct readout can be obtained with one or two resistors missing, depending on the interrogating signal. If two diagonally located resistors are missing, an interrogation by 1111, 1001, 1101, or 1011 still gives an output of 1001. If only the upper right resistor is missing, a correct output will still be obtained as long as the interrogating signal includes a 1 on the leftmost vertical line.

The fault-tolerant, content-addressable memory concept has great potential for use in large interactive memories. Applications may include the next generation of computers, expert systems, and artificial intelligence. If constructed as very-large-scale integrated circuits, these memories may be denser and more reliable than those now in use.

This work was done by John Lambe, Alexander Moopen, and Anilkumar P. Thakoor of Caltech for **NASA's Jet Propulsion Laboratory**. *For further information, Circle 69 on the TSP Request Card.*

Title to this invention has been waived under the provisions of the National Aeronautics and Space Act [42 U.S.C. 2457(f)], to the Caltech/JPL. Inquiries concerning licenses for its commercial development should be addressed to

Edward Ansell,
Director of Patents and Licensing
Mail Stop 301-6
California Institute of Technology
1207 East California Boulevard
Pasadena, CA 91125.

Refer to NPO-16680, volume and number of this NASA Tech Briefs *issue, and the page number.*

Unified Robot-Control System

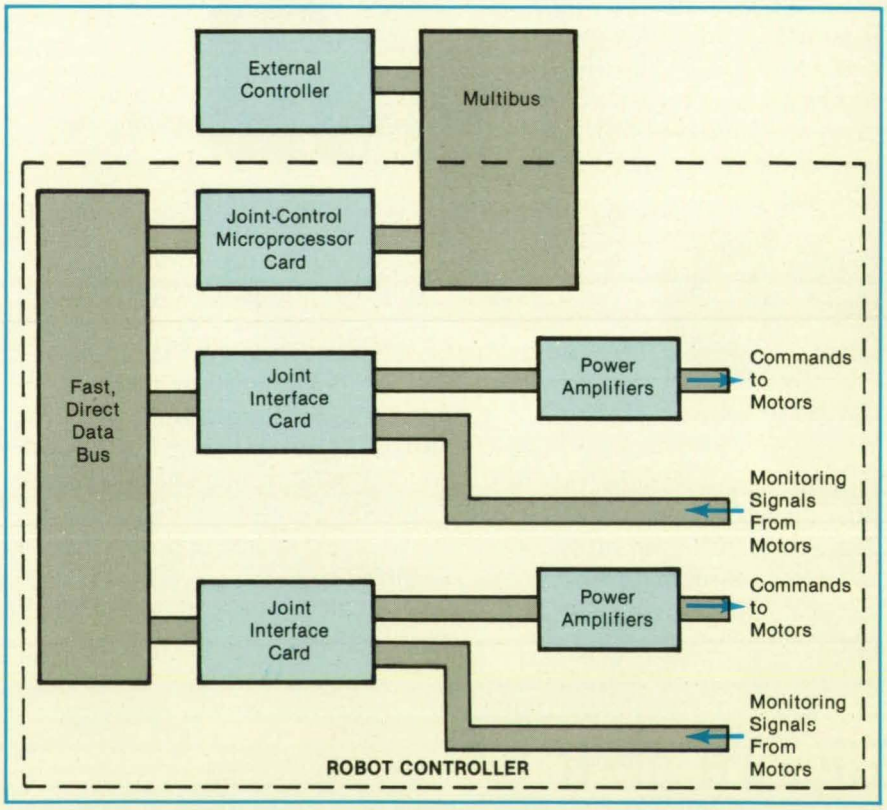
Robot-joint motors are integrated with a control computer or computers.

NASA's Jet Propulsion Laboratory, Pasadena, California

A robot controller uses only 1 microprocessor to control as many as 16 joint-actuating motors. The control system uses a high-speed bus to communicate with the joint-interface circuits, an addressing scheme that makes it possible to write commands to several motors simultaneously, and an efficient assembly-language servo code. These features enable the control of the 16 joints at a 1-kHz servo rate. In contrast, commercial robot controllers include separate microprocessors for each joint to achieve the same rate. The new system is suitable for the control of motors in numerically-controlled manufacturing systems.

The use of a single joint-control processor results in fewer components, lower cost, and simpler architecture than are required in existing systems of comparable performance. Moreover, the single processor can correlate events on different joints — an impossible feat if a separate processor is assigned to each joint.

The joint-control microprocessor is the NS32016 (or equivalent), a 32-bit linear-address-space microprocessor. It is mounted on the joint-level processor circuit card, which also contains a floating-point arithmetic unit; an interruption-controlling unit; a 32K read-only memory; a 128K random-access memory; two serial ports; a parallel data interface; an interface between the fast, direct data bus and the joint interface cards; and an interface with the multibus (a standard data bus) that links the controller to an external controller (see figure). The controller card supplies control signals to the joint interface cards and accepts feedback signals from them. The card contains about 100 integrated circuits and costs about $400 (at 1986 prices).



A **Fast, Direct Data Bus** carries digital signals between the controller card and the joint interface cards. The joint interface cards supply digital motor-control signals to the motors through power amplifiers and provide digital monitoring signals to the controller card.

Each of the joint interface cards (one card for four joints) contains an interface with the fast, direct data bus; pulse-width modulation (PWM) generators; interfaces with the quadrature angle encoders on the motors; digital tachometers; analog-to-digital converters; and an electronically-erasable, programmable read-only memory. A joint interface card applies digital control signals from the controller card to the PWM generators that in turn provide motor-drive pulses to the power amplifiers.

What the PC did for computing, GoldWorks™ now does for expert system building.

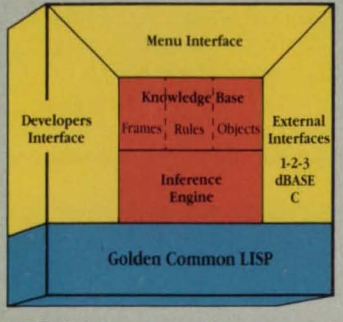
Remember computing before the PC?

Climate-controlled rooms behind "Restricted Area" signs. DP gurus speaking a language nobody else knew. Mystified end-users. Then technology evolved, the PC emerged and serious desktop computing became affordable. The economics of computing changed forever.

Now, GoldWorks uses PCs to transform the economics of expert system building.

On your 286- or 386-based PC, **GoldWorks** offers the functionality and power of high-end expert system tools, plus the ease of use and low cost of PC shells. With **GoldWorks**, you can *develop and deliver* serious expert systems *cost-effectively.*

"...allows us to leverage thousands of installed PCs..."
–Dr. David Shpilberg, Coopers & Lybrand



GoldWorks is the most powerful expert system tool available on PCs.

With GoldWorks, you don't have to compromise.

Easy-to-use shells run on PCs, but lack real functionality. Powerful high-end tools can't integrate with existing PC applications or deliver expert systems on PCs. GoldWorks combines the best features of both.

"...a powerful combination of expert system development and end-user support."
–Bruce M. Gras, Arthur D. Little, Inc.

It's as easy to use as a shell...

The Menu Interface lets you prototype and build expert system applications fast, without knowing the underlying programming environment. On-line help and tutorials make you productive quickly.

...and as function-rich as a high-end tool.

GoldWorks offers frames, rules, object programming and powerful control mechanisms, just like the high-end tools. And GoldWorks runs on advanced PCs, so expert systems you build can be *delivered* cost-effectively to end-users.

"...power comparable to ART or KEE..."
–Kenneth Levine, Lekton, Inc.

GoldWorks lets you integrate with existing PC programs.

You can integrate expert systems with dBASE III, Lotus 1-2-3 and C...plus build and deliver expert systems in network environments.

See this powerful, flexible tool for yourself. Order the GoldWorks Demonstration Kit.

You'll get an 18-minute videotape, showcasing many GoldWorks features in a sample application. You'll also receive a copy of the actual 282-page Expert System User's Guide that comes with **GoldWorks**. We'll credit your $49 to your **GoldWorks** purchase.

"Any Fortune 1000 organization can easily cost-justify...this tool."
–Randy Reiter, Athena Group

For more information, or to order, call toll-free:

1-800-242-5477.

In Mass., call (617) 492-2071.

GoldWorks from Gold Hill. The expert in AI on PCs.

GOLD HILL™

Gold Hill Computers, Inc.
163 Harvard Street
Cambridge, MA 02139

Copyright 1987, Gold Hill Computers, Inc. Golden Common LISP is a registered trademark and GoldWorks is a trademark of Gold Hill Computers, Inc. Lotus is a registered trademark and 1-2-3 is a trademark of Lotus Development Corporation. dBASE is a trademark of Ashton-Tate. KEE is a trademark of Intellicorp. ART is a trademark of Inference Corporation.

Circle Reader Action No. 465

Direct digital control of the PWM generators, instead of the usual analog control, eliminates digital-to-analog conversion and its nonlinearity and drift with temperature. With a loss of energy of only 5 percent, as compared with up to 50 percent for analog control, direct digital control is also more efficient.

Each power amplifier contains power transistors, driver circuits, a short-circuit detector, and current-feedback resistors. The cost of the components of the power amplifiers is less than $100 per motor (1986 prices).

The analog-to-digital converters accept signals that represent shaft positions, motor currents, inductive freewheeling currents, and power-supply voltages. They furnish this information to the controller card in digital form. Acting in concert with the quadrature encoder interfaces, the digital tachometers measure the angular velocities of the motor shafts so accurately and quickly that instantaneous motor accelerations can be calculated reliably from any two consecutive velocity measurements — impossible with analog tachometers. Moreover, because the digital tachometers use the outputs of the angle encoders, they do not require the installation of additional equipment on the motors.

The controller determines the torques, back-electromotive-force constants, electrical resistances, and winding temperatures of the motors; the loads upon the motors; and the status of the power supply. The controller can also identify and act on the following problems:

- Open or short motor circuits,
- Broken encoder wires or constant voltages in encoder inputs,
- Malfunctions of potentiometers,
- Insufficient power to drive the motors, and
- Failures of components on the joint interface cards.

In response, the controller can apply the proper voltages to the motors, open the motor circuits where necessary, provide regenerative damping through any motor in either direction, and apply or release electromagnetic brakes.

The controller contains a code-generator software so that it can adapt to the particular motors and sensors used. After robot hookup, the motor, encoder, potentiometer polarities can be changed from software. The control method used can be different on every motor. The code generator writes highly optimized assembly code.

This work was done by Zoltan F. Szakaly of Caltech for **NASA's Jet Propulsion Laboratory**. *For further information, Circle 62 on the TSP Request Card.*

This invention is owned by NASA, and a patent application has been filed. Inquiries concerning nonexclusive or exclusive license for its commercial development should be addressed to the Patent Counsel, NASA Resident Office-JPL [see page 16]. Refer to NPO-17134.

The Mark III Hypercube-Ensemble Computers

Concurrent processors will operate at high speed.

NASA's Jet Propulsion Laboratory, Pasadena, California

The Mark III Hypercube concept is being applied in the development of a series of increasingly powerful computers. When fully developed, the Mark III computers will be especially useful for the solution of physical problems with spatially and temporally varying quantities. Disciplines that will benefit from the speed and memory capacity of the Mark III Hypercube include astrophysics, geophysics, chemistry, weather, high-energy physics, applied mechanics, image processing, oil exploration, aircraft design, and microcircuit design.

As in previous hypercube networks, each of $N = 2^k$ identical concurrent processors is located at a node that corresponds to a corner of a k-dimensional cube. Each processor is connected to its k nearest neighbors along the topological equivalents of the k edges that meet at that corner. The prototype contained 4 nodes; two additional 32-node models were built and are operational. A subsequent 1 gigaflop 128-node model is now under construction and will be operational by the end of 1988.

The Mark III concept includes very powerful nodes connected by high-speed communication links. The processor at each node is composed of three subprocessors that are tightly coupled through a 4-Mbyte main node memory on a common bus (see figure). The peak rate of data transfer between the main memory and each subprocessor is 12 Mbytes/s. To minimize the degradation of performance caused by simultaneous attempts of the subprocessors to gain access to the main node memory, each subprocessor is also provided with a high-speed local memory. The main subprocessor arbitrates the memory contentions.

The input/output control subprocessor includes an MC68020 microprocessor, 64 Kbytes of high-speed local memory, and a direct-memory-access channel-support module. This subprocessor is capable of an input/output-channel transfer rate up to 68 Mbits/s.

The main subprocessor is also based on the MC68020 and operates at over 2 million instructions per second. It includes a 32-bit arithmetic and logic unit and a full 32-bit address generator. The local memory of 128 Kbytes has faster access than does the shared main memory; this allows the microprocessor to reach its full execution speed.

The high-speed floating-point subprocessor is a peripheral unit attached to the node board by a daughter-board connector. This subprocessor is responsible for heavy floating-point arithmetic: it can increase the speed of such computations to as much as 50 times that achievable with the floating-point coprocessor that is part of the main subprocessor.

The shared main memory is partitioned into four address-interleaved dynamic memory modules, each having its own dynamic memory controller. Circuitry is included to correct one-bit data errors in memory and to signal (but not to correct) two-bit errors; in the latter case, the main subprocessor is interrupted. The read/write memory cycle is 200 ns from a valid address strobe.

The success of the Mark III Hypercube concept will depend on the development of software to tap the high-speed potential of concurrent processing. In particular, it will be necessary to spread the computational work load as evenly as possible among all the nodes and to reduce the need for data transfers among the nodes.

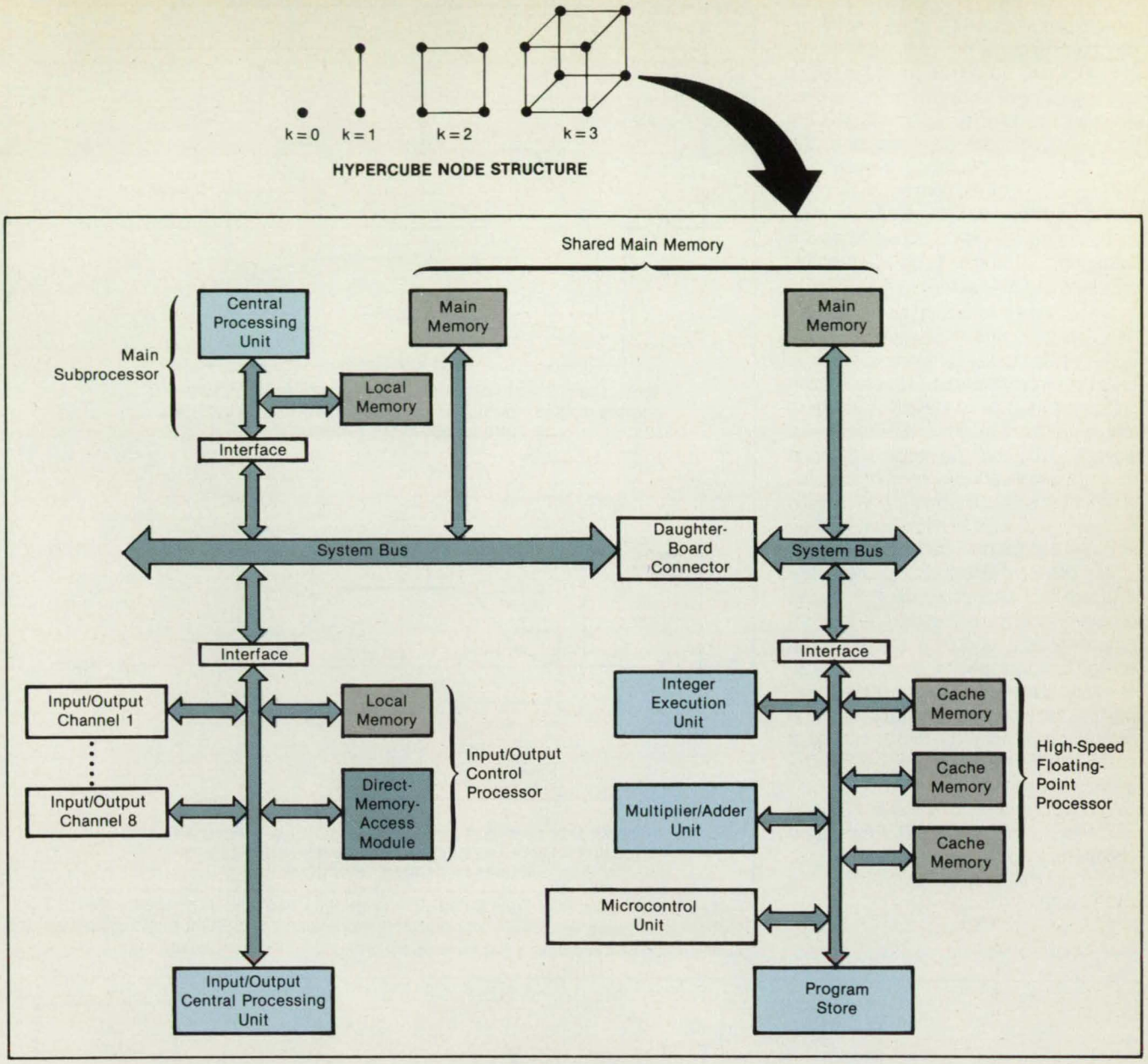
The lack of good software — both at the operating system and application level — is the main issue holding back the development of parallel computers. Work is also being applied to the development of useful "parallel supercomputer software tools" on the basis of the experience in using "real parallel machines" to solve "real problems."

This work was done by John C. Peterson, Jesus O. Tuazon, Don Lieberman, and Moshe Pniel of Caltech for **NASA's Jet Propulsion Laboratory**. *For further information, Circle 14 on the TSP Request Card.*

In accordance with Public Law 96-517, the contractor has elected to retain title to this invention. Inquiries concerning rights for its commercial use should be addressed to

Edward Ansell,
Director of Patents and Licensing
Mail Stop 301-6
California Institute of Technology
1207 East California Boulevard
Pasadena, CA 91125

Refer to NPO-16772, volume and number of this NASA Tech Briefs *issue, and the page number.*



NODE PROCESSOR

The **Processor of Each Node** of Mark III Hypercube ensemble is a specialized computer that contains three subprocessors and a shared main memory. The hypercube ensemble solves a problem quickly by simultaneously processing a part of the problem at each such node and passing the combined results to a host computer.

Dual Pilot-Tone Calibration Technique

The signal-to-noise ratio would be increased.

NASA's Jet Propulsion Laboratory, Pasadena, California

A proposed phase-shift-keying scheme for the radio transmission of digital signals would include two pilot tones, one near each edge of the frequency band (see Figure 1). As in other pilot-tone techniques, the pilot tones would be used to compensate for the effects of multipath fading on the amplitude and phase of the received signal.

The tone-calibration techniques rely on the assumption that the pilot-tone and data components of the transmitted signal are both degraded in the same way by fading. In practice, this is assured by setting the pilot-tone frequencies as close as possible to the data frequency band. After suitable processing, the pilot tones would be used as coherent references in a synchronous data detector to remove the fading phase component and to normalize the fading amplitude component.

By the placement of the pilot tones near the band edges, the dual pilot-tone technique eliminates the guard bands on both sides of a single carrier-frequency pilot tone. Consequently, the data bandwidth and the overall bandwidth can be reduced somewhat. However, near the band edges the pilot tones are more sensitive to frequency shifts and more susceptible to adjacent-channel interference.

A dual-pilot-tone-calibrated receiver is illustrated in Figure 2. The incoming signal is filtered through a bandpass filter. Part of the initially filtered signal z(t), where t = time, is sent to the synchronous detec-

tor and part to each of two filters with narrow passbands at the pilot frequencies. The outputs $C_+(t)$ and $C_-(t)$, of the upper and lower tone-frequency filters, respectively, are multiplied to obtain a signal $C'(t)$. This signal includes components at the sum of the two pilot-tone frequencies (which equal twice the carrier frequency f_o) and at the difference between the two pilot-tone frequencies (which equals twice the frequency difference f_p between either pilot tone and the carrier).

$C'(t)$ is filtered to obtain the $2f_o$ component, which is used in the calibration subsystem, and the $2f_p$ component, which is used in a bit synchronizer. In the calibration subsystem, $C'(t)$ is divided by a squared, low-pass-filtered version of itself to obtain a signal $C_o'(t)$ that has the phase of $C'(t)$ and an amplitude inversely proportional to that of $C'(t)$. $C_o'(t)$ is halved in frequency to obtain $C_o(t)$, which is used to demodulate coherently the bandpass-filtered input.

The dual-pilot-tone technique has been evaluated for various phase-shift keying schemes in terms of the average bit-error probability as a function of the ratio of bit energy to noise spectral density. The calculations show an effective 3-dB improvement in the signal-to-noise ratio, which is likely to overshadow the disadvantages of adjacent-channel interference and frequency offsets.

This work was done by Marvin K. Simon of Caltech for **NASA's Jet Propulsion Laboratory**. *For further information, Circle 164 on the TSP Request Card.*
NPO-16930

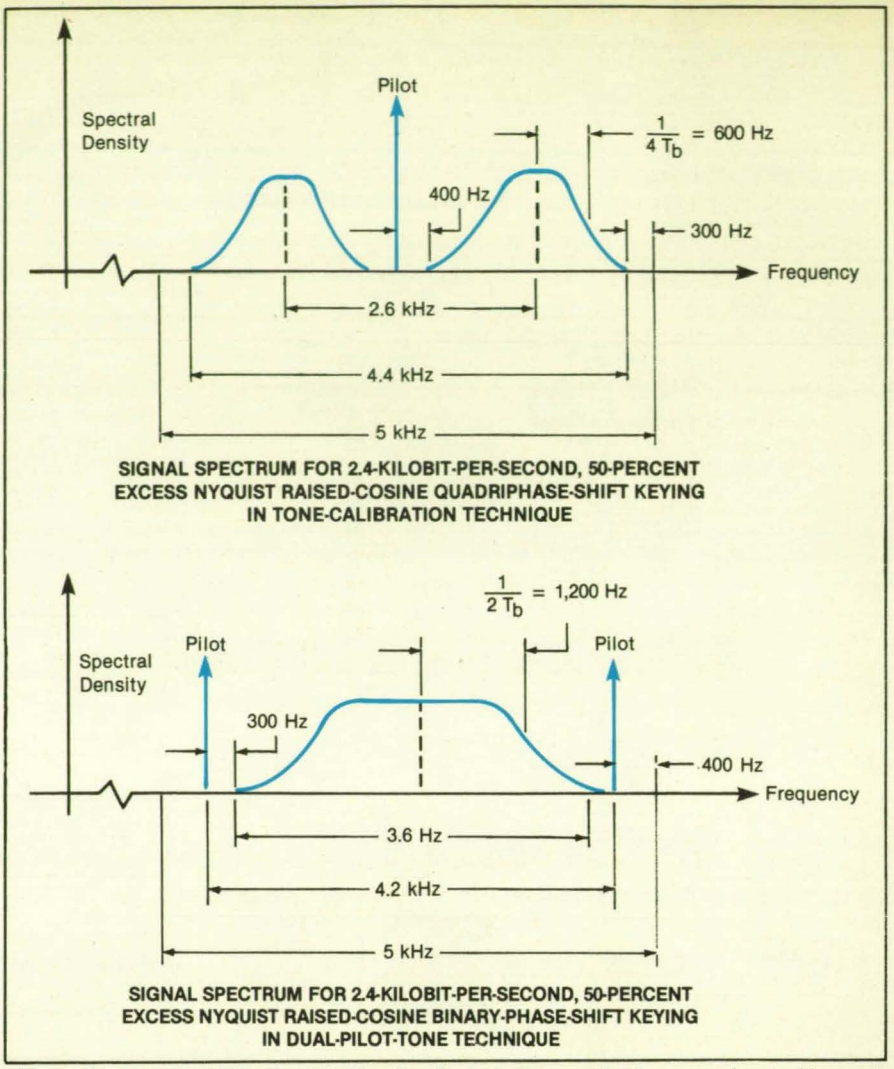


Figure 1. In the **Dual Pilot-Tone Calibration Technique**, two pilot tones are located just outside the sidebands, whereas in an older single-tone method, the pilot tone lies between the sidebands. The bandwidths shown here are typical and for comparison only.

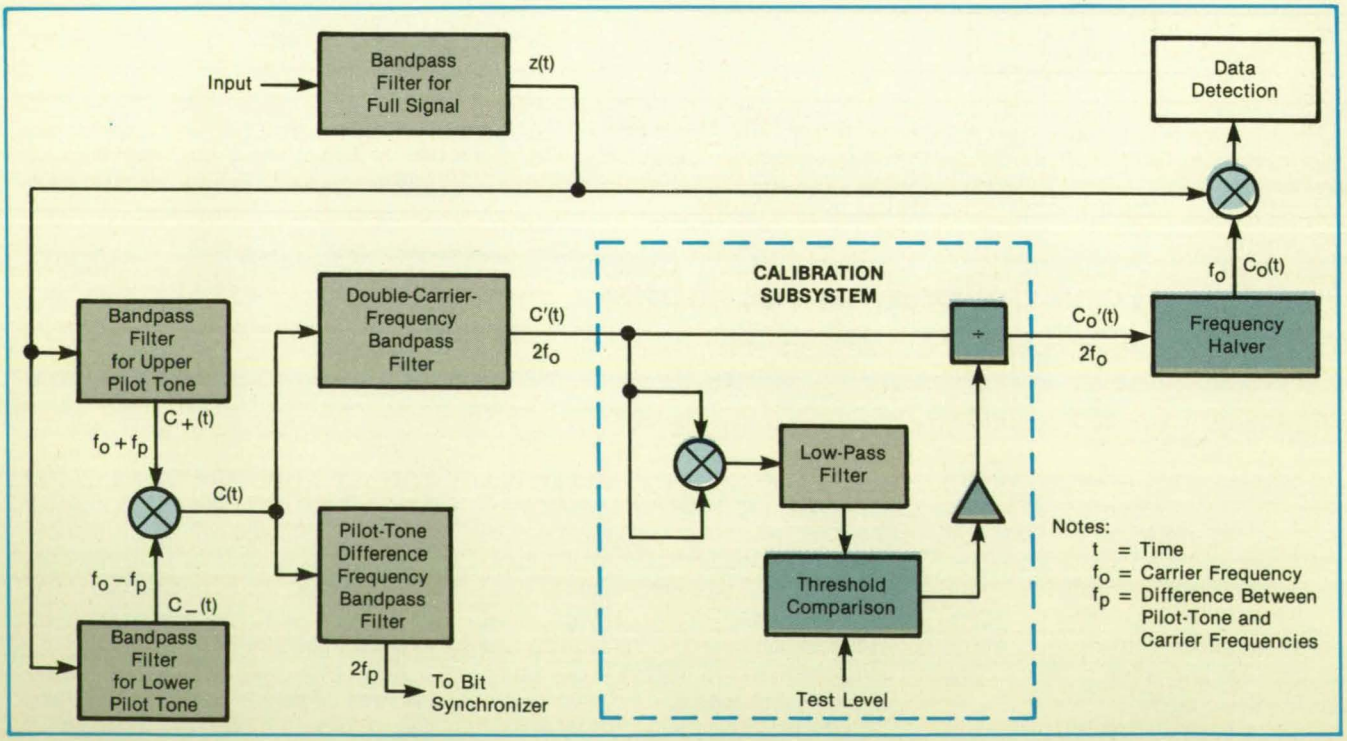


Figure 2. A **Carrier Frequency Is Synthesized** from the two pilot-tone frequencies in the dual-pilot-tone-calibrated receiver. An effective composite carrier signal derived from the pilot tones is used to demodulate coherently the data portion of the received signal.

Public-Facilities Locator for the Blind

An optoelectronic system would enable blind people to find key places without assistance.

Lyndon B. Johnson Space Center, Houston, Texas

A proposed optoelectronic system (see figure) would guide blind people to important locations in public buildings. With the system, a sightless person could easily determine the directions and distances of restrooms, water fountains, stairways, emergency exits, and elevators, for example.

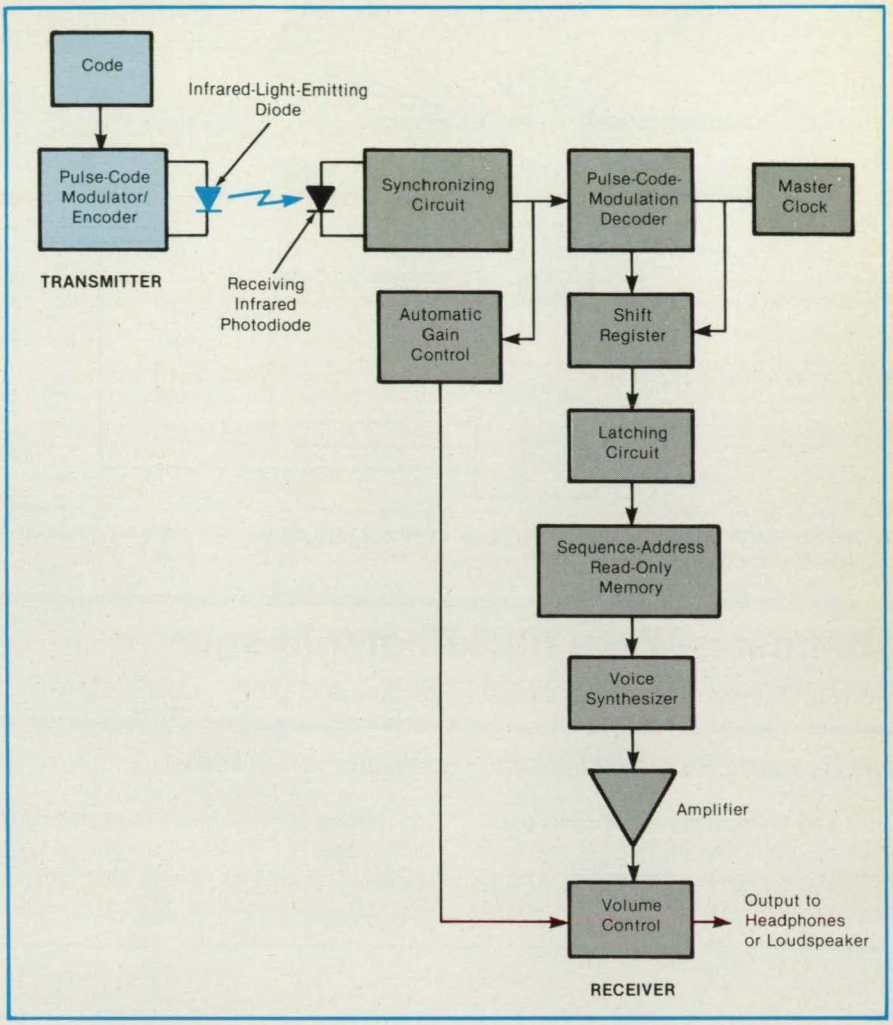
The concept calls for a wall-mounted infrared-pulse transmitter at each of the important locations. A compact circuit worn by the user would receive the infrared signals and convert them to synthetic-voice announcements. The sequence of infrared pulses would be unique for each type of location. The receiver could thus translate a sequence into a specific message in the user's earphone. The loudness of the announcement would increase with the received infrared power, so that the closer the user would come to the location, the louder the announcement would grow.

A 4-bit binary gray code has been tentatively selected for pulse-code-modulating the infrared signal. In this code, three consecutive zeros never occur. The code is easy to implement, and encoding and decoding can each be done by a single silicon integrated-circuit chip.

A transmitter would give out two identifying bursts in rapid sequence — for example, "men's room, men's room" — and would repeat the sequence continually at an even cadence. The repetition rate would be timed so that a person moving at 1 m/s would not miss an announcement when walking through the infrared beam.

In the receiver, codes would be detected by an infrared photodiode and separated by a synchronizing circuit. After decoding, a signal would pass to a shift register having serial input and parallel output. A latching circuit would hold the parallel decoded data briefly before transferring them to a sequence-address read-only memory (ROM).

The ROM would release appropriate phoneme signals to a voice synthesizer. The volume of the amplified synthesizer output would be controlled by an automatic gain controller according to the intensity of the received infrared signal and would thus increase in magnitude with a decrease in the distance to the transmitter. Finally, the synthetic-voice signal would be applied to headphones.



The **Circuitry Is Uncomplicated and Inexpensive**, in both the transmitter and the receiver. Readily-available light-emitting diodes, photodiodes, and integrated-circuit chips would be used to build the locator aid for the blind.

Infrared is preferable to radio-frequency energy as the transmission medium for several reasons: It does not interfere with other electronic equipment, it fades faster with increasing distance and thus gives a better indication of distance, and it is less subject to noise and errors.

This work was done by Kevin D. Moore of Lockheed Engineering & Management Services Co., Inc., for **Johnson Space Center**. *For further information, Circle 115 on the TSP Request Card.*
MSC-21197

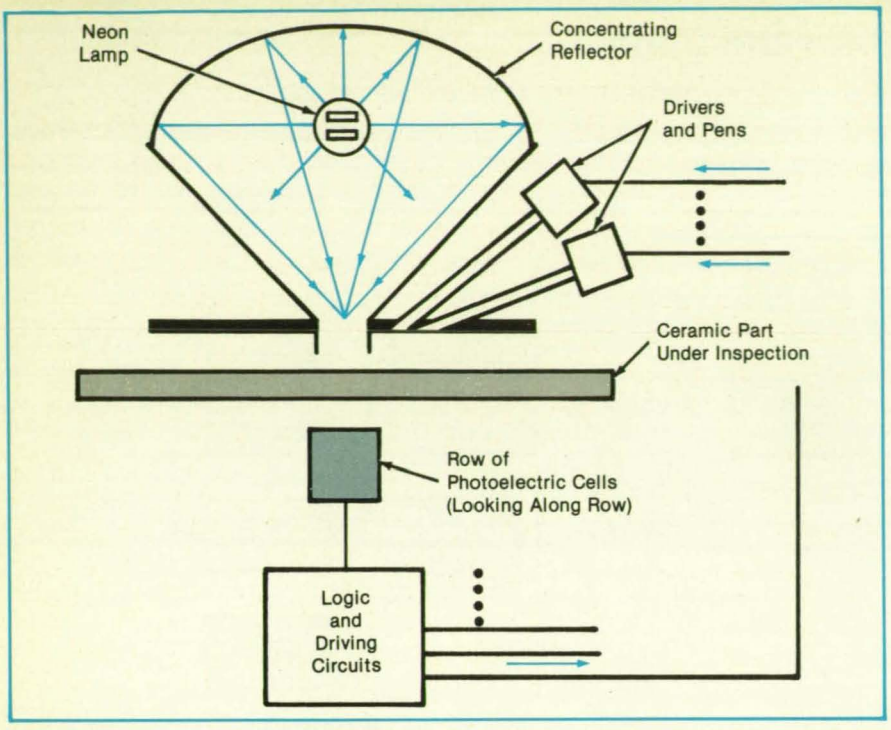
Automatically Inspecting Thin Ceramics for Pinholes

Flaws would be located and marked.

Lyndon B. Johnson Space Center, Houston, Texas

A proposed apparatus for inspecting prefired ceramic materials would detect minute flaws that might escape ordinary visual inspections. The method would not only detect flaws but would also mark their locations. The method is intended for such thin ceramic parts as insulation in capacitors and some radio-frequency filters.

According to the concept, a neon lamp



A **Ceramic Wafer** would be inspected optoelectronically for pinholes. The pinholes would be marked by felt-tipped pens.

in a reflecting chamber would direct intense light through a narrow slot onto the surface of the prefired ceramic. A row of photoelectric cells on the opposite side of the ceramic would sense light transmitted through flaws (see figure).

If a photocell sensed light as the ceramic was moved under the illuminated slot, the photocell output would be amplified and applied to a logic circuit. The circuit would activate an electromechanical marker, which would push a felt-tip pen onto the ceramic to mark the site of the flaw.

The method would enable the automatic nondestructive testing of ceramic parts. It could be made of inexpensive, off-the-shelf components.

This work was done by James R. Honaker of Rockwell International Corp. **Johnson Space Center**. *For further information, Circle 72 on the TSP Request Card. MSC-21091*

Millimeter-Wave Radiometer Imager

Terrain is viewed through clouds, smoke, and dust.

NASA's Jet Propulsion Laboratory, Pasadena, California

A 3-mm radiometer system with a mechanically scanned antenna has been built for use on a small aircraft or helicopter to produce near-real-time moderate-resolution images of the ground. One of the main advantages of this passive imaging sensor is that it is able to provide information through clouds, smoke, and dust when visual and infrared (IR) systems are unusable. This millimeter-wave imaging sensor can be used also for a variety of remote-sensing applications such as measure-

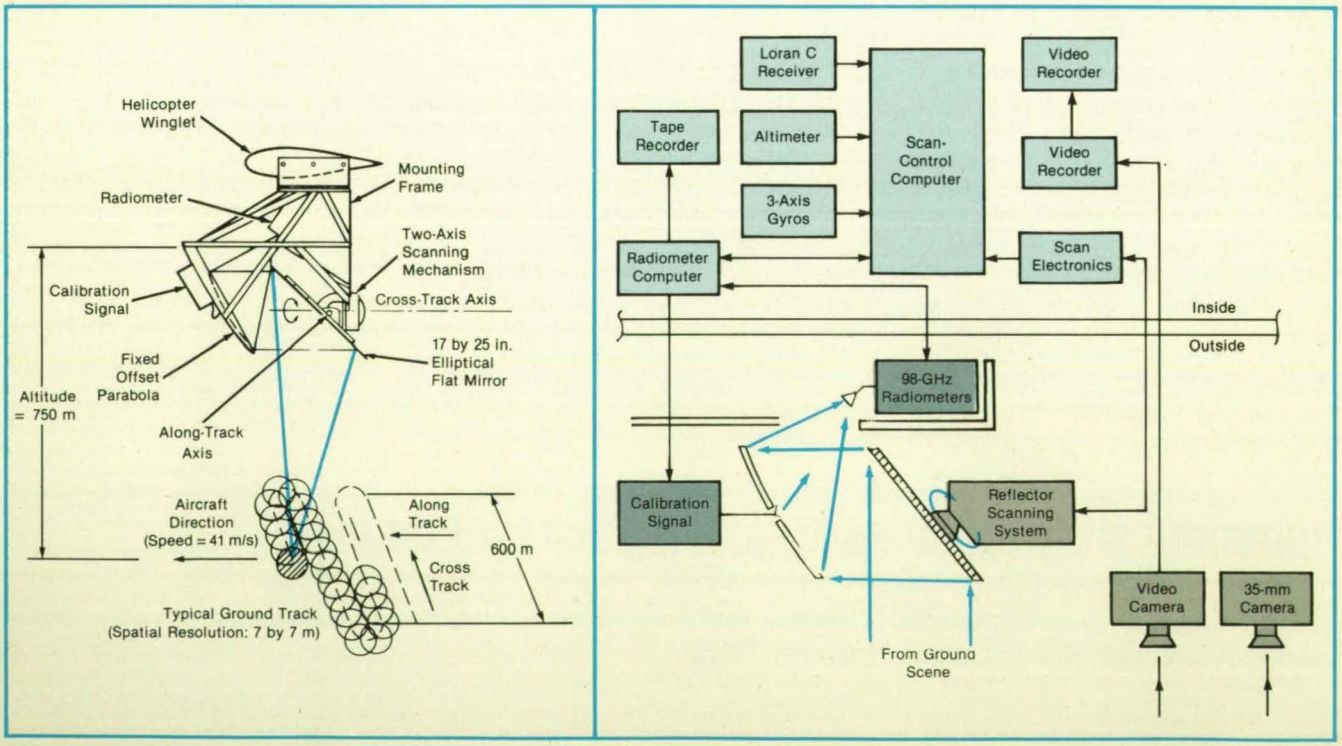


Figure 1. The **Millimeter-Wave Imaging-Sensor System** is shown in the aircraft configuration (left) and as the block diagram (right).

ments of surface moisture, snow cover, vegetation type and extent, mineral type and extent, surface temperature, and thermal inertia. It is also possible to map fires and volcanic lava flows through obscuring clouds and smoke. The fact that the millimeter-wave sensor observes different physical phenomena makes it a valuable addition to visual and IR imaging systems.

When a millimeter-wave sensor observes a ground scene from above, the received signal is composed of thermal emission from objects in the antenna beam, sky emission reflected from these objects, and emission from the atmosphere below the radiometer. The temperature of the signal received from an object in the antenna beam is proportional to the product of physical temperature and the surface emissivity of the object. The surface emissivity is a function of the material and roughness, and ranges from near zero for reflectors to near unity for rough absorbers. Thus millimeter-wave scenes can show large contrasts with reflecting objects, such as metal vehicles, buildings, or wet areas — appearing much colder than the surrounding rough background.

The system configuration and block diagram are shown in Figure 1. A lightweight flat reflector is mechanically scanned crosstrack ±20° at a 4-Hz rate. A two-axis scanner, controlled by a microcomputer with inputs from both rate and angle gyros, is used to scan the reflector and to correct for aircraft movement due to turbulence. This provides line-of-sight stabilization without the use of a conventional stabilized platform. The two-axis scanner also uses a butterfly scanning pattern to compensate for the forward aircraft motion to produce a linear raster-scan pattern on the ground. The signal from the ground is reflected from the flat scanning mirror onto a 16-in. (40-cm) offset parabolic antenna, which focuses the received signal on the feed horn of the radiometer.

Two linearly polarized 98-GHz superheterodyne radiometers are used to provide polarization information and to improve the measurement sensitivity. A broadband orthomode junction splits the received signal into two orthogonal linearly polarized signals, and the two radiometers use balanced mixers with beam-lead diodes. A Gunn-diode oscillator, tuned to 98 GHz, is split with a hybrid tee and used to provide 2 mW of local-oscillator power for each mixer. Each mixer is followed by a low-noise GaAs FET IF amplifier centered at 3 GHz.

The detected output signals from the radiometer are recorded on a digital cartridge tape along with system-status information. Ground-truth data are given by a 35-mm camera, a video camera, and an IR sensor. Because the data are taken with a stabilized-raster pattern, the ground minicomputer system can immediately play back and display the data in false colors on

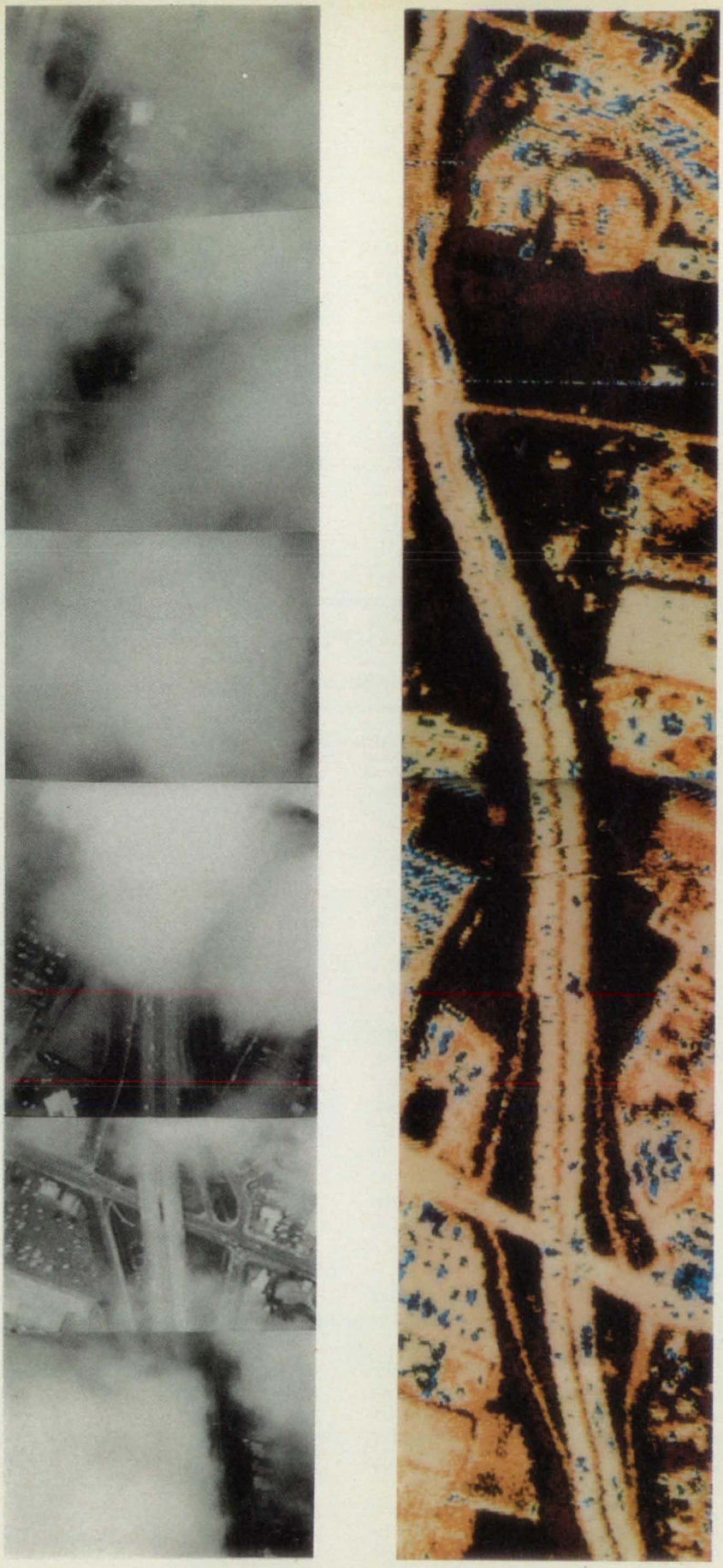


Figure 2. Photographs show the **Comparison of the Visual-Wavelength and Millimeter-wave Images** of a section of freeway South of Carlsbad, California, taken on a rainy day. The sensor was flown over a layer of broken clouds, as seen on the left. The area pictured is 0.4 by 1.9 km.

a video monitor. The features that make this system different from previous airborne millimeter-wave imaging sensors are its high resolution, small size, stabilization, and computer processing, which provide near-real-time calibrated images.

Test flights of the millimeter-wave imaging sensor were made with the sensor mounted on a commercial helicopter. Most of the flights were near an altitude of 750 m (2,500 ft) and an airspeed of ~90 km/h. The objectives of these test flights were to verify the capabilities of this sensor with respect to signal-to-noise ratio and operation with clouds, and to get millimeter-wave imaging data on a variety of areas and objects. These tests were very successful, and a sample of the data is shown in Figure 2.

The photograph shows the visual and millimeter-wave images taken during a rainy day. During that day, the millimeter-wave sensor was flown at 2,500 ft over a layer of broken clouds that for large areas completely obscured the visual images. On the millimeter-wave image the freeways, vehicles, parking lots, and buildings are shown clearly as colder targets, reflecting the cooler sky. Vehicles on the freeway, traveling in the same direction as that of the helicopter, have been stretched, while those traveling in the opposite direction were compressed. This picture shows the ability of the millimeter-wave imager to provide information on the ground scene when the video image is obscured by clouds.

One of the most interesting things about the millimeter-wave images is that there are many recognizable objects (i.e., reflective objects, such as bodies of water, metal structures, highways, and buildings) that stand out from the background clutter. A study of many images leads to the conclusion that it is rarely necessary to expand the temperature range per color step beyond 3 K: this range is ~4 times larger than the radiometer noise, since the scene clutter is ≈2 K. It is also interesting that, by properly choosing the range of temperatures and the order of colors, different features within a scene can be made to stand out or blend in. Other image-processing and -enhancement techniques also can be used to improve the detection of objects.

This work was done by W. J. Wilson, R. J. Howard, A. C. Ibbott, G. S. Parks, and W. B. Ricketts of Caltech for **NASA's Jet Propulsion Laboratory**. *For further information, Circle 97 on the TSP Request Card.*

Inquiries concerning rights for the commercial use of this invention should be addressed to the Patent Counsel, NASA Resident Office-JPL [see page 16]. Refer to NPO-17051.

Position and Force Control for Multiple-Arm Robots

The number of arms can be increased without introducing undue complexity.

NASA's Jet Propulsion Laboratory, Pasadena, California

A strategy and a computer architecture have been developed for the simultaneous control of the positions of a number of robot arms manipulating the same object and of the forces and torques that the arms exert on the object. The scheme will enable coordinated manipulation of the object, causing it to move along an assigned trajectory and be subjected to the assigned internal forces and torques.

The basic principle is illustrated by the simplified example of a one-dimensional, frictionless system with a mass in contact with two actuators (see Figure 1). The servocontrol loop causes the actuators to apply forces F_1 and F_2 to the mass in an attempt to make it accelerate at a desired rate. The control imposes the condition that the total actuator force, $F_1 + F_2$, must equal F, the force necessary to produce the desired acceleration of the total system mass, which is the sum of the point mass plus the effective work-space masses of the actuators.

The control algorithm imposes the specified relationship between F_1 and F_2. For example, if it is desired to squeeze the object with a force F_p while accelerating it, then the control system will continually strive to readjust F_1 and F_2 to make $F_1 - F_2 = F_p$. If the object is constrained against moving, then F_1 and F_2 can be set to arbitrary values or subjected to an arbitrary criterion.

In the general case, n robot arms make contact with a body of finite size (see Figure 2). In this case, the body rotation and the linear motion of a point G on the body are specified, and the control algorithm apportions the forces, or torques, or both among all n arms. Of course, the equations of motion and the specifications of constraints (planes of contact and sliding, axes of rotation, robot-joint configurations, and the like) are more complicated in the n-arm case: In general, a dedicated microprocessor would be required to solve continually the motion and control-force equations for each arm.

Each of the n arms is considered to be attached rigidly to the object. A portion of the object in contact with each robot arm is treated, for control-algorithm purposes, as the last link in that arm. Thus, a portion of the mass and of the inertia tensor of the object is mathematically assigned to each arm.

As in the one-dimensional example, the equations of motion are solved for the force and torque that must be exerted by each arm to obtain the desired motion. In this case, however, the sum-of-forces (and/or torques) condition applies to all n arms. The difference-of-forces (and/or torques) condition is distributed among all arms so that each arm cooperates with the other arms to produce the desired internal forces or torques.

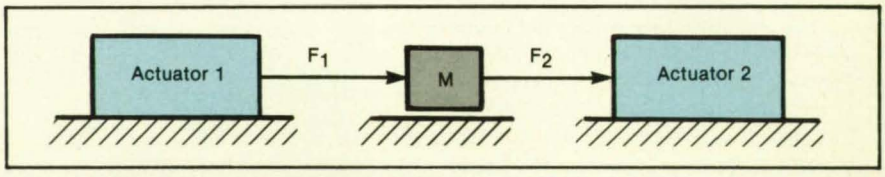


Figure 1. A **Mass, M, on a One-Dimensional Track** is pushed and/or pulled by either or both of two actuators. The control algorithm for this system imposes forces F_1 and F_2 subject to specified conditions on the motion and the squeezing or stretching of the object.

Instead of a difference-of-forces (or torques) condition it is possible to impose other arbitrary force/torque conditions, as long as the total forces and torques continue to satisfy the equations of motion. For example, one can require that a weighted

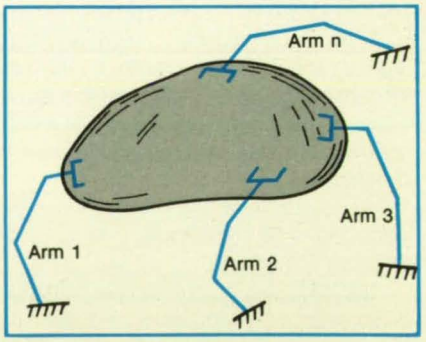


Figure 2. A **Number of Robot Arms** cooperate in manipulating an object. The control scheme apportions the contact forces and torques among the arms to produce the desired motion of the object, and the desired forces and torques inside the object.

sum of squares of forces, or some other performance index, be minimized.

The control scheme is well suited for a distributed computer architecture. Because the number of microprocessors required increases only linearly with the number of robot arms, in principle the finite nature of computing resources imposes no limit on the number of robot arms.

This work was done by Samad A. Hayati of Caltech for **NASA's Jet Propulsion Laboratory**. *For further information, Circle 6 on the TSP Request Card.*

In accordance with Public Law 96-517, the contractor has elected to retain title to this invention. Inquiries concerning rights for its commercial use should be addressed to

Edward Ansell,
Director of Patents and Licensing
Mail Stop 301-6
California Institute of Technology
1207 East California Boulevard
Pasadena, CA 91125

Refer to NPO-16811, volume and number of this NASA Tech Briefs *issue, and the page number.*

Lightweight Video-Camera Head

A separate optical assembly weighs only 80 grams.

Lyndon B. Johnson Space Center, Houston, Texas

A compact, lightweight video camera head has been constructed by remounting the lens and charge-coupled-device (CCD) image detector from a small commercial video camera in a separate assembly. Such a camera head could be useful in robotics, artificial vision, and vision guidance systems, where minimum size and weight are often important criteria. The camera head was designed to be mounted on the visor of a helmet to monitor the motions of eyes in experiments on vestibulo-ocular reflexes; even the smallest conventional one-piece video camera would have been too massive and bulky for this application.

The camera head measures 41 by 31 by 44 mm and weighs approximately 80 g. The cable that connects the camera head to the camera electronic circuitry is made with a specific wire-bundle twist to reduce line capacitance and to shield against external electromagnetic and radio-frequency interference. The cable can be up to 6 ft (1.8 m) long.

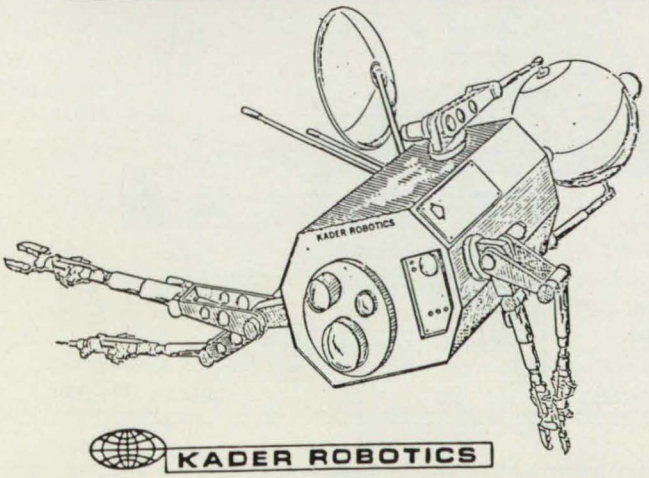
The main camera body and video-synchronization-separator circuit boards are mounted on a 127-by 102-mm mother board. The main camera body contains a power unit and video interface. The genlock and video-synchronization circuits make it easy to connect the camera to existing external television circuitry. The camera requires 12 Vdc at 425 mA.

The CCD image detector is sensitive to radiation from the visible to the near infrared and provides good image contrast. The detector sensitivity peaks at a wavelength of 920 nm. In the visible spectrum, the camera requires a minimum light intensity of 3 lux. A ring-shaped light source that surrounds the lens has been developed to provide uniform infrared and visible illumination over a circular region.

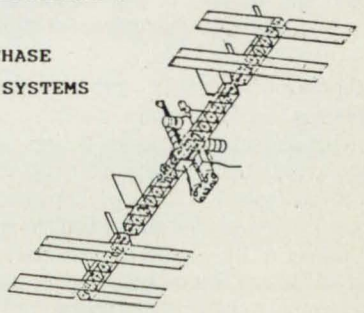
This work was done by David R. Proctor of Technology Inc. for **Johnson Space Center**. *No further documentation is available.*

MSC-21246

CONGRATULATIONS
NASA
25 YEARS
OF
EXCELLENCE



TOMORROW'S...
ORBITAL ROBOTICS IN EVA...
* SATELLITE REPAIR, REFUELING & MAINTENANCE
* DEBRIS CAPTURE & CHASE
* PLATFORM ERECTION SYSTEMS



KADER ROBOTICS
• Aerospace Systems •
P.O. Box 9954 Birmingham, AL 35220
(205) 854-6820

Television-and-Laser Range-Measuring System

Triangulation enables the measurement of distances from 1 to 200 ft (0.3 to 60 m).

Lyndon B. Johnson Space Center, Houston, Texas

A triangulation system measures the angle between two lines of sight to a point on an object, thereby determining the distance to the object. Unlike older triangulation-type ranging devices, this system is amenable to automation.

The system (see figure) is mounted on an optical platform. A charge-coupled-device (CCD) camera views the object along two lines of sight emanating from the opposite ends of a stereo arm. The lines of sight are oriented by two rotatable mirrors, the angular positions of which are controlled by stepping motors. A light beam from a helium/neon laser is directed by mirrors and a beam splitter along the line of sight in optical channel 1. Thus, the reflection of the laser light from the object, as seen in channel 1, appears at the center of the CCD image at any range. The laser reflection is also seen through channel 2, but initially it may not be at the center.

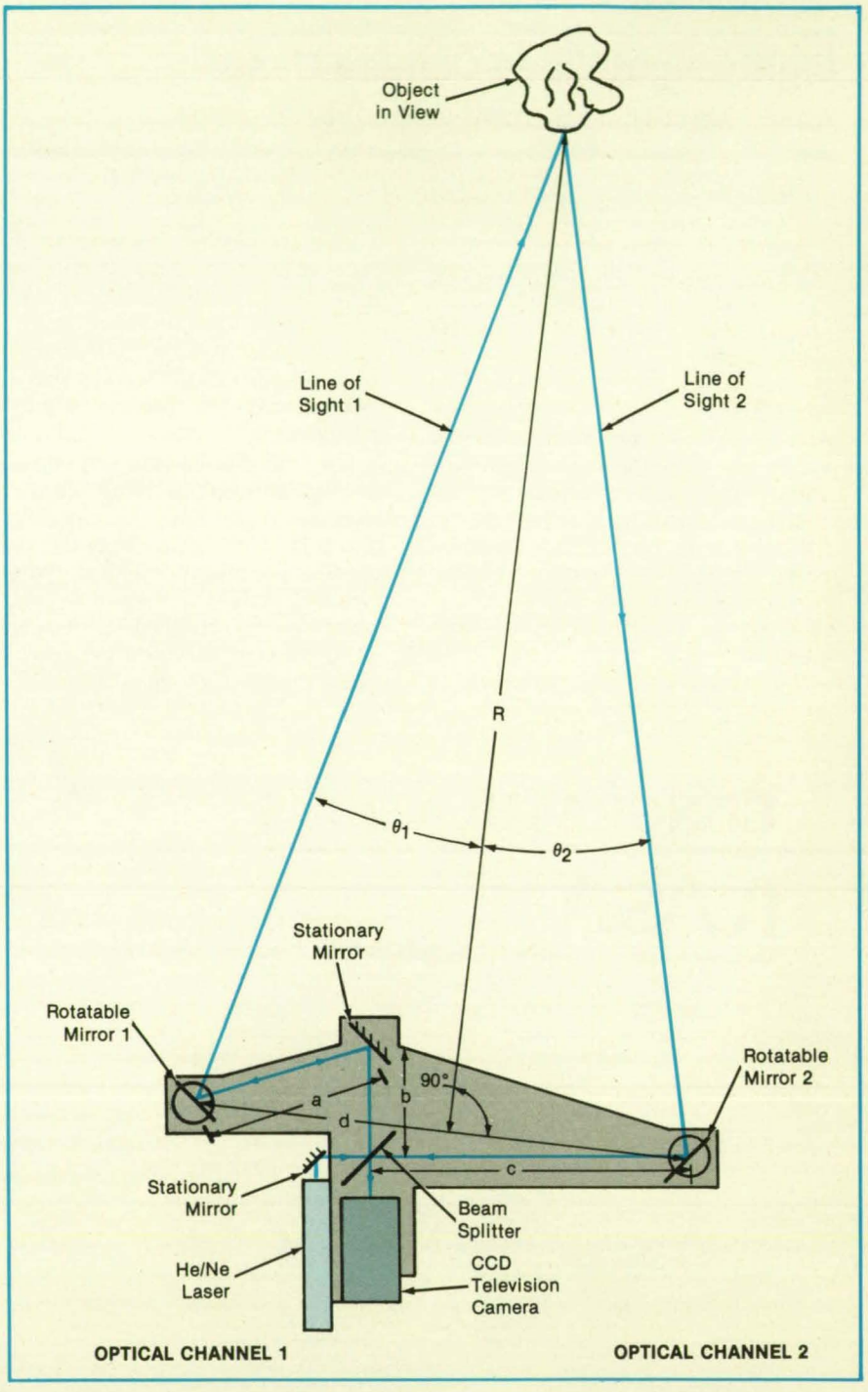
The optical platform is rotated to bring the object into the view of the CCD in both channels. A 633-nm narrow-band-pass filter placed over the central portion of the CCD allows only the laser light to figure prominently near the center. The rotatable mirrors are adjusted alternately until the lines of sight intersect, as indicated by the convergence of both laser spots at the center of the CCD. The stepping-motor sequence is automatically controlled to vary the convergence angle, $\theta_1 + \theta_2$, in increments of 0.001°, and so that θ_1 does not differ from θ_2 by more than 0.001°.

The camera is focused automatically. A servocontrol loop samples the video signal from the picture elements in the central region and activates a camera-focusing stepping motor to maximize the signal peak at the center.

Since the automatic control system continues to aim the platform and mirrors to maintain convergence, the system provides a continuous reading of the half convergence angle, $\theta = \theta_1 = \theta_2$. Then the distance, R, between the object and the optical center of the stereo arm is given by $R = (d/2) \csc \theta$, where d is the length of the stereo arm as shown on the figure. The approach or recession speed, V, of the object can also be calculated in terms of θ_1, the rate of change of θ, using $V = -(d/2)\,\theta \cot \theta \csc \theta$.

This work was done by J. Kevin Russell of Lockheed Engineering and Management Services Co. Inc., for **Johnson Space Center**. *For further information, Circle 101 on the TSP Request Card.*

This invention is owned by NASA, and a patent application has been filed. Inquiries concerning nonexclusive or exclusive license for its commercial development should be addressed to the Patent Counsel, Johnson Space Center *[see page 16].* *Refer to MSC-20867.*



The **Triangulation System** includes automatically aimed rotatable mirrors and a laser beam to define one of the lines of sight. The system adjusts itself automatically to bring the two lines of sight into convergence at a common point on the object.

Books and Reports

These reports, studies, handbooks are available from NASA as Technical Support Packages (TSP's) when a Request Card number is cited; otherwise they are available from the National Technical Information Service.

Minimum-Time Control for Robotic Manipulators

Current theories are examined critically.

A report surveys the state of the art in the theory of minimum-time control of robotic manipulators. It discusses some of the promising developments, pointing out, however, that the optimal-control problem in its full generality remains unsolved. It compares the various solution methods, indicating their merits and flaws.

The discussion begins with a brief overview of the field. Because analytic solutions are not possible except for the simplest of robot configurations, many approaches based on iterative/gradient-type algorithms have been proposed. Each is based mainly on one of the following ideas:

1. Analyze the two-point boundary-value problem derived from the maximum principle.
2. Assume some parametric form of the solution and optimize the parameters.
3. Iteratively modify the performance index so that the solutions of the easier optimization problem converge to the optimal one.

To date, none of these algorithms has exhibited consistent convergence over a wide class of robots. This situation has given rise to suboptimal solution methods based on linearization of the nonlinear dynamic equation.

The report discusses some qualitative aspects of the minimum-time control problem. It begins by applying the variation principle to obtain the equation of motion in generalized-momentum form. After stating the control objective in terms of time optimality, it presents derivations of four theorems, including simpler derivations of two key results that have appeared recently in the literature.

Next, the report reviews the variety of computational approaches that have been applied to the optimal-control problem. The author notes that the source of difficulty has been the possible existence of singular arcs and that the singular-perturbation approach offers promise as a remedy.

This is followed by a review of suboptimal algorithms. Special mention is accorded to the double-integrator algorithm based on the exact linearizing transform. The advantages of this scheme are the following:

1. It computes efficiently the exact linearizing torque.
2. The travel time is computable a priori and can be used to size the actuators.
3. The scheme is robust against sampling delay in control and against modeling errors.

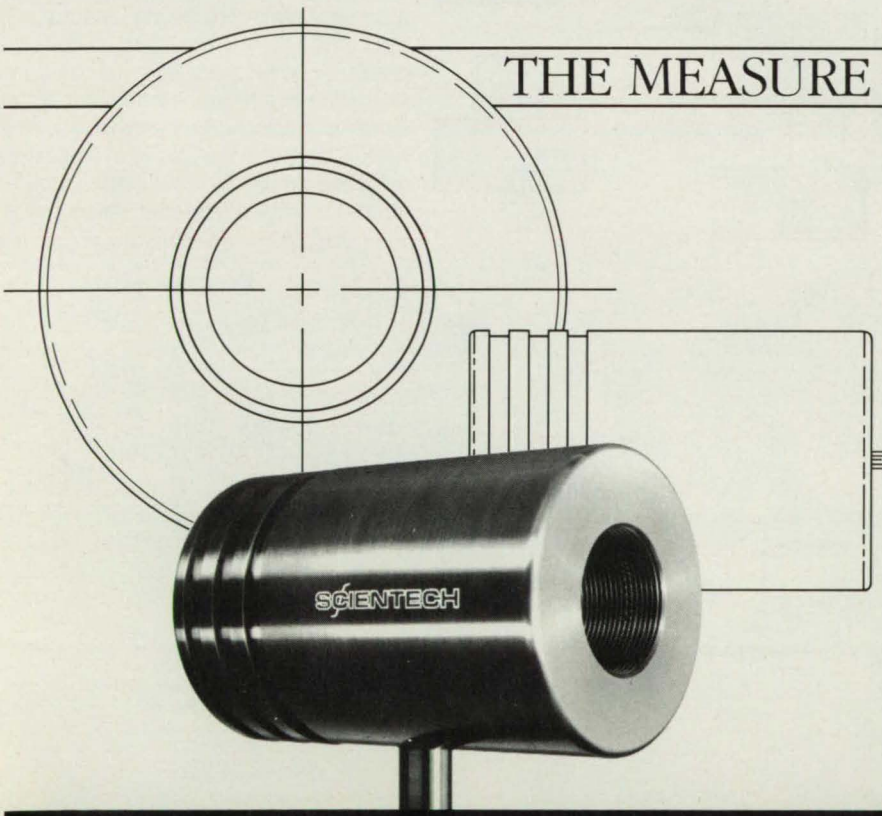
This work was done by John T. Wen of Caltech for **NASA's Jet Propulsion Laboratory**. *To obtain a copy of the report, "On Minimum Time Control for Robotic Manipulators," Circle 118 on the TSP Request Card.*

NPO-17070

Are you reading someone else's copy?

Get your own copy by filling in the qualification form bound in this issue.

THE MEASURE OF CONFIDENCE



SCIENTECH LASER POWER AND ENERGY METERS SET THE INDUSTRY STANDARD

Scientech has defined the standards for laser measurement for over 18 years. Based on an NBS design, our technology has evolved into a complete line of time tested, precision instruments unequaled for accuracy and reliability.

Calibration and performance verification utilize electric substitution—a standard Scientech feature with all our meters.

Scientech measurement systems are designed for a wide range of applications with 1", 2", 4", and 8" models. 1mW to 5KW CW and beyond—up to 100 gigawatt pulses—are measured with long-term linear precision better than 1%. Analog and Digital Watt/Joule Indicators are available with interfaces for oscilloscopes, chart recorders, printers, and computers.

For information on laser power and energy measurement applications, please call Scientech.

Toll Free: 800-525-0522

SCIENTECH®

Physical Sciences

Hardware, Techniques, and Processes

58 **Modulated-Voltage Metastable-Ionization Detector**

59 **Locating Residual Wax in Coolant Channels**

Computer Programs

68 **Program Reads Weather-Data Tapes From Aircraft**

73 **Estimating Geophysical Parameters From Gravity Data**

Modulated-Voltage Metastable-Ionization Detector

The range of measurable gas concentrations is extended.

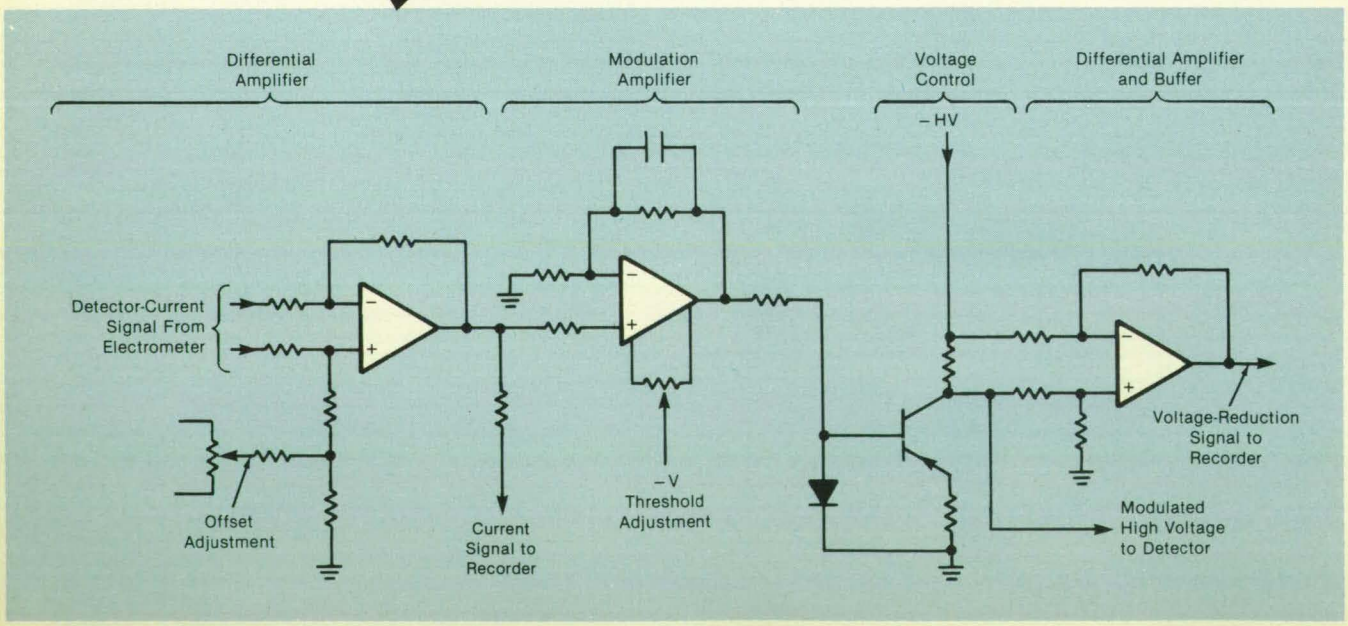
Ames Research Center, Moffett Field, California

A voltage-control feedback circuit extends the range of sample concentrations that can be measured by a metastable-ionization detector coupled to a gas chromatograph. A conventional detector measures concentrations from parts per billion to parts per million but saturates at higher values. The new detector retains the sensitivity of conventional ones but automatically reduces its voltage to prevent current saturation at higher values, thereby enabling the quantitative determination of relative concentrations approaching 100 percent.

In a metastable-ionization detector, the chromatography carrier gas (usually helium) is exposed to an electric field and energetic electrons from a radioactive source. This combination raises the carrier-gas atoms to a metastable state, which, in helium, has an ionization potential of 19.8 eV. Sample constituents having lower ionization potentials are ionized and collected at the electrodes that form the electric field.

At low concentrations, the collected current, less the background current due to the radioactive source, is proportional to the concentration of the sample constituents in the carrier gas. At high concentrations, an arc discharge forms, and the detector current saturates at a current limited by a protective resistor.

To prevent saturation, the improved detector (see Figure 1) includes a voltage modulator controlled by the detector output current. In the modulator circuit, the detector-current signal from the electrometer is fed to a differential amplifier, offset by an amount that compensates for the background, and then fed to a modulation amplifier. When the modulation-amplifier input exceeds the preset value corresponding to the threshold current, the



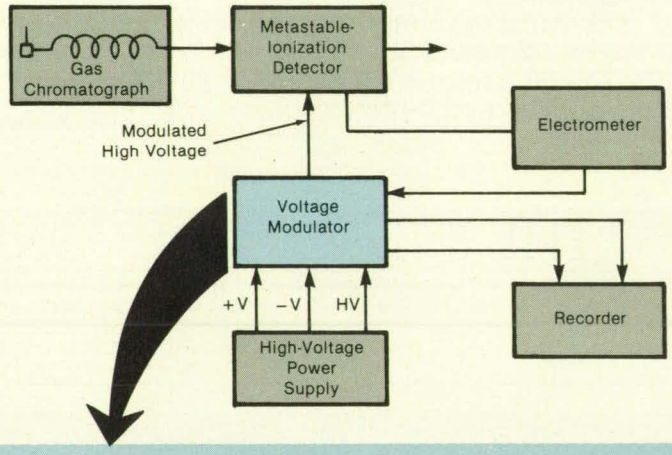


Figure 1. The **Modulated-Voltage Metastable-Ionization Detector** includes feedback circuitry to prevent current saturation. When the detector current begins to exceed a threshold, the detector high voltage is reduced to keep the current from rising much more.

modulation-amplifier output turns on the transistor in the transistor/resistor voltage-control amplifier.

The amplifier gains are chosen so that the high voltage is reduced by the amount needed to keep the detector current from rising significantly above the threshold. At sample concentrations above the threshold, the reduction in voltage is used as the measure of concentration. This voltage reduction is detected by a differential buffer amplifier and fed to the recorder. The relationship between the voltage reduction and the concentration is not linear; a calibration curve must be obtained empirically for each sample constituent.

Figure 2 shows an example of recorder output from a gas chromatograph fed with a helium carrier containing four sample gases at various concentrations. The nitrogen current peak just exceeds the threshold and is therefore followed quickly by a small voltage-reduction peak. The argon current peak greatly exceeds the threshold and so is quickly followed by a large voltage-reduction peak. The methane and krypton current peaks are below the threshold and cause no voltage reduction.

This work was done by Glenn C. Carle, Daniel R. Kojiro, and Donald E. Humphry of **Ames Research Center**. *For further information, Circle 77 on the TSP Request Card.*

This invention is owned by NASA, and a patent application has been filed. Inquiries concerning nonexclusive or exclusive license for its commercial development should be addressed to the Patent Counsel, Ames Research Center [see page 16]. Refer to ARC-11503.

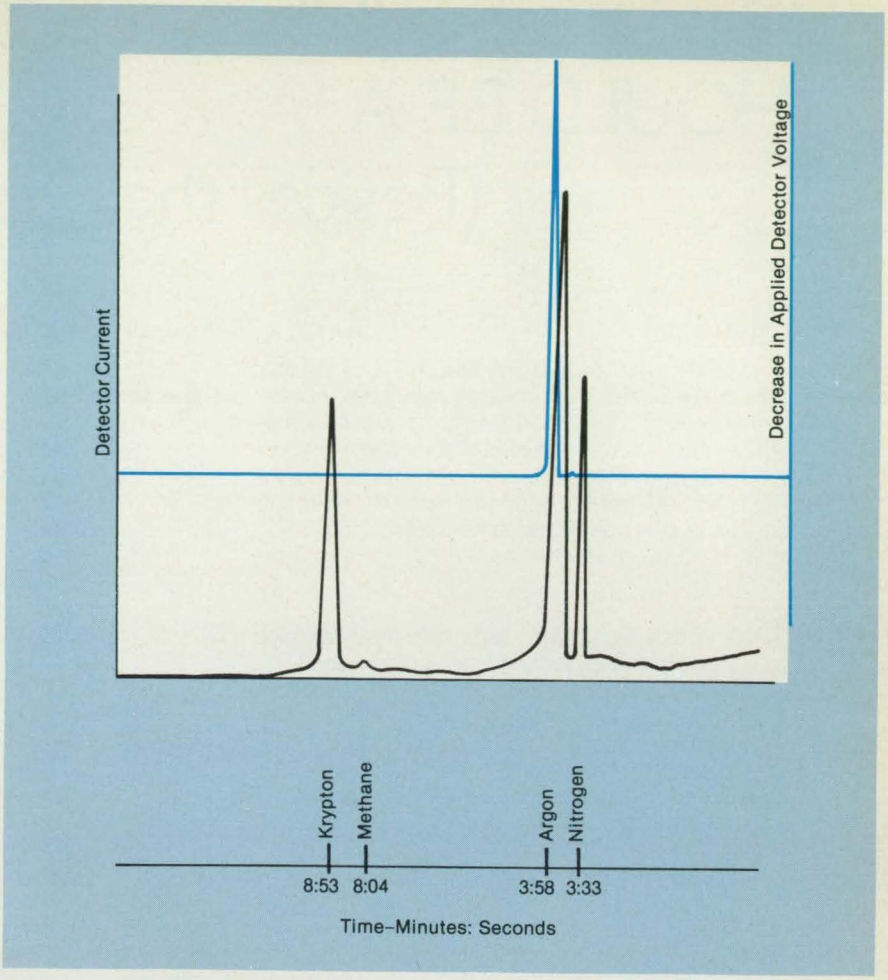


Figure 2. This **Recorder Output** shows the detector-current and voltage-reduction signals from a gas mixture with constituents both above and below the threshold concentration. Those above the threshold cause both current and voltage-reduction peaks. Those below the threshold give rise to current peaks only.

Locating Residual Wax in Coolant Channels

Neutron inspection finds deposits and defects invisible to x rays.

Marshall Space Flight Center, Alabama

Residues of machining or plating wax that block internal channels in heat exchangers or other metal parts are readily detected by neutron radiography. The technique has been used to inspect the coolant channels in the Space Shuttle main combustion chamber. However, it is also useful for finding such other hidden nonmetallic deposits as core material in turbine-blade coolant passages, braze "stop-off" in injector orifices, internal voids in rubber parts, flaws in metal-to-polymer seals, and voids in encapsulating compounds surrounding cables or electronic components. Such defects are usually not revealed by conventional x-ray inspection.

Previously, residual wax in hidden channels was detected by infrared chemical analyses of samples of effluent perchloroethylene, which had dissolved small amounts of the wax during passage through the channels. The method depended on operator skill in doing the test and processing the sample and often gave incorrect or uncertain results. Another infrared technique — one that measures relative heat-transfer rates by image analysis — is of little use because it does not give the exact locations of channel restrictions.

Unlike x-radiography, neutron radiography readily detects many low-density materials even when they are surrounded by larger quantities of denser materials. Materials with similar properties and densities often appear quite different when viewed by neutron radiography.

A beam of low-energy neutrons, produced by fission in a nuclear reactor, is directed at the part to be inspected. Some neutrons pass through the part unaffected, whereas others are deflected or absorbed by nuclei, depending on the nature of the local material. Those that pass through produce short-term radioactivity in a scintillator screen that is used to expose photographic film.

The technique gives a comprehensive view of the hidden channels. Several film exposures are made from different points of view, so that triangulation can be used to determine the locations of residual wax deposits. From densitometer readings and parallax exposures, partially blocked channels can be distinguished from completely blocked ones. Machining wax in channels 0.1 in. (2.5 mm) thick can be easily detected even when shielded by 0.5 in. (1.3 cm) of Inconel* nickel/iron alloy, with no significant damage to the metal part.

*Inconel is a registered trademark of the Inco family of companies.

This work was done by Douglas M. Guthrie of Rockwell International Corp. for **Marshall Space Flight Center**. *No further documentation is available.*

MFS-29212

10 REASONS WHY YOUR ADA COMPILER SHOULD BE A JANUS/ADA COMPILER (Besides the Price!)



1. **We're fast**
Compilation and development speed mean a lot when you're working on a large program; every minute you have to wait is time and money wasted. A Janus/Ada compiler has an average compilation speed of 400 lines per minute with a 6 MHZ 8086; over 500 lines per minute with an 80186; 1100+ lines per minute on an 8 MHZ 80286, and nearly 1900 lines per minute on PC Limited's 386.



2. **We work on any XXX86 machine.**
Not everybody can afford the newest technology and some of us can't afford the name brands . . . but with Janus/Ada, that doesn't matter. It doesn't need protected mode, 8087's, or PC-DOS. As long as you have an Intel 80X86 chip at the heart of your computer and some way to run or emulate MS-DOS 2.1 or higher, you can use Janus/Ada.



3. **Our product has been in use for over six years.**
We released our first compiler in 1981 and got our first review in 1982. The products we sell have had the scrutiny of customers and reviewers for over six years, changing to meet the increased sophistication of the technology and the user. Our customers come from every segment of the computing community; the government, Fortune 500, and academia. Users like yourself are able to benefit from the wide range of uses we respond to every day, as well as the built-in network of people working with Ada just like you.



4. **No copy protection.**
Our products come to you free of any form of copy protection and with a warranty insuring media replacement for defective media. We know you don't need the hassle of locking devices and other protective devices. We know you want to use Janus/Ada on your hard disk and network, and we make it easy to install, easy to maintain, and easy to use.



5. **Application programs written in Ada for as low as $12.00.**
We offer IBM graphic routines, window handlers, scientific libraries and many other application programs written in Ada. These programs come with complete source code and documentation and are user tested.



6. **We offer embedded systems capability, like rommable, reentrant code and licensing of our source code.**
Janus/Ada is designed to make your embedded processing easy . . . with features especially created for that environment. Our code is rommable, allowing you to "burn in" the applications you create. We make our source code available, in our Systems Package ("S" Pak), so you don't have to guess at the answer. If you would prefer to have us design and implement your code, we'll be more than happy to accommodate.



7. **Superior error handling.**
Nothing is more frustrating than an error in coding . . . except a bad error message which does nothing except confuse you. Our error messages tell you vital information, such as line location, cause of error and a full walkback including subprogram names. If you do a lot of development, or you just appreciate being fully informed, our error messages are sure to please!



8. **Support that won't let you down.**
Superior support services, such as the Janus/Ada bulletin board, the Janus/Ada BIX conference, a quarterly newsletter, as well as customized support services.



9. **Our compiler was developed on a micro, for a micro, in Ada.**
We have "bootstrapped" our compiler, version by version, so that we know it really works! Our compiler was developed on multiple XXX86 machines from different manufacturers, so that it would be a true microcomputer compiler. Our products are developed in Ada, demonstrating our commitment to the language and the capabilities it can bring to you.



10. **Self paced, low cost educational tutorials.**
The Janus/Ada Extended Tutorial offers a programmer's perspective on learning Ada. This tutorial was written expressly for novices in the Ada language, by a programmer, and includes a complete set of disk based quizzes to compliment the 150 page tutorial. You can determine how quickly you pace yourself, and you won't believe you did it for $99.95

JANUS/ADA PASSED VALIDATION 12/11/87 . . . AND IS STILL ONLY $99

CP/M, CP/M-86, CCP/M-86 are trademarks of Digital Research, Inc.
'ADA is a trademark of the U.S. Department of Defense
MS-DOS is a trademark of Microsoft
Copyright 1987 RR Software

Circle Reader Action No. 467



SOFTWARE, INC.

specialists in state of the art programming

P.O. Box 1512 Madison, Wisconsin 53701
(608) 244-6436 TELEX 4998168
1-800-722-3248

Materials

Hardware, Techniques, and Processes

61 Stronger Fire-Resistant Epoxies
61 Polyarylene Ethers With Improved Properties
62 Air Revitalization Using Superoxides

Books and Reports

63 Microstructure and Weld Cracking in Inconel 718*
64 Lubrication Handbook for the Space Industry
64 Optimization of Processing of Si_3N_4
64 Galvanic Corrosion in (Graphic/Epoxy) Alloy Couples
65 Temperature, Humidity, and Polymer Aging
66 Effects of Radiation on Insulators

Computer Programs

73 Strain-Energy-Release Rates in Delamination

Stronger Fire-Resistant Epoxies

A new curing agent improves mechanical properties and works at a lower temperature.

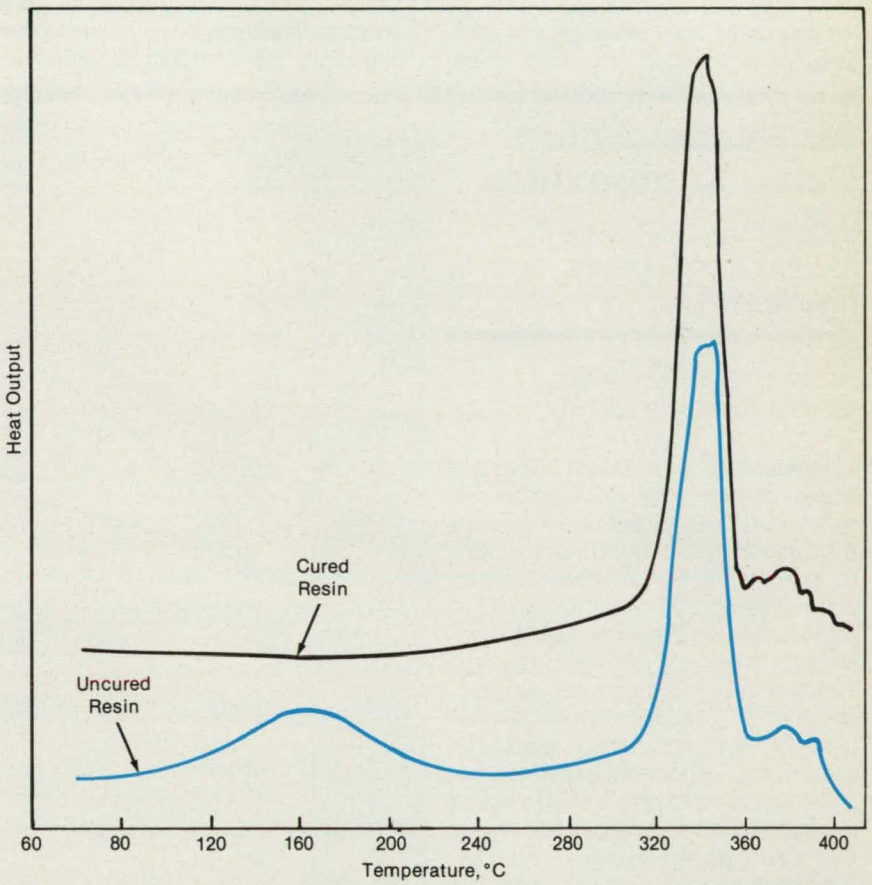
Ames Research Center, Moffett Field, California

The use of aminophenoxycyclotriphosphazene curing agents yields stronger, more heat- and fire-resistant epoxy resins. Because the epoxies can be cured without solvents, the formation of voids is suppressed. However, the new curing agents can be used with solvent if necessary; for example, for coating fabrics or casting films.

Curing proceeds in stages at temperatures of 120 to 125 °C and 175 to 180 °C, followed by postcuring at 225 °C. A tough, brown polymer results. The curing reaction has been monitored by Fourier-transform infrared spectrometry and by differential scanning calorimetry and is well understood (see figure).

The cured resins are thermally stable up to about 350 °C. When burned, the cured resins yield usually high amounts of char, which is highly desirable for fire-resistant applications. The char yields in nitrogen at 800 °C range from 42 to 55 percent; in air at 700 °C they range from 32 to 40 percent.

Graphite-fiber-reinforced epoxy resins cured with the new agents have properties superior to those cured with such conventional agents as diaminodiphenylsulfone. For example, a laminate made with one of the improved formulations exhibited a tensile strength of 72,080 psi (497 MPa), whereas a similar laminate made with a commercial resin cured by diaminodiphenylsulfone had a tensile strength of 51,639 psi (356 MPa).



Thermograms Made by Differential Scanning Calorimetry show one exothermic peak for the cured and two exothermic peaks for uncured epoxy resin containing the new curing agent. The peak at 163 °C indicates the polymerization reaction (that is, curing) whereas the peak at 330 °C indicates decomposition. The polymerization takes place at a lower temperature than it does with other curing agents.

This work was done by George M. Fohlen and John A. Parker of **Ames Research Center** *and Devendra Kumar of the National Research Council. For further information, Circle 7 on the TSP Request Card.*

Inquiries concerning rights for the commercial use of this invention should be addressed to the Patent Counsel, Ames Research Center [see page 16]. Refer to ARC-11548.

Polyarylene Ethers With Improved Properties

Ease of processability and mechanical properties generally exceed those of commercial materials.

Langley Research Center, Hampton, Virginia

As part of an effort to develop improved composite matrices for potential use on aerospace vehicles, a series of new polyarylene ethers (PAE's) were prepared from the reaction of activated dihalo compounds with various bisphenols. These

compounds exhibit excellent processability by compression molding, plus good mechanical properties.

The linear PAE's prepared are the polycondensation products from the reaction of either 1,3-bis(4-chloro or fluorobenzoyl) benzene or 1,4-bis(4-chloro or fluorobenzoyl) benzene with any one of the following bisphenolic compounds: bis(3-hydroxyphenyl) methane; bis(4-hydroxyphenyl) methane; 1,1-dimethyl-bis(4-hydroxyphenyl) methane; or 9,9-bis(4-hydroxyphenyl) fluorene. Measured number-average molecular weights for the PAE's range from 13,500 to 39,400 g/mole, and glass-transition temperatures vary from 114 to 243 °C. Ethynyl-terminated polyarylene ethers (ETPAE's) also were prepared by end-capping hydroxy-terminated PAE's with 4-ethynylbenzoyl chloride.

Composites, films, moldings, and adhesives were prepared. The physical and mechanical properties of the polymers were compared with those of commercially available PAE's. Some of the new PAE's exhibit high levels of thermoplastic flow and shear thinning and have use-temperature ranges that exceed those of commercially available materials. The fracture toughnesses of some PAE's are significantly higher than those of commercial materials. Some of the PAE's prepared are also insensitive to aggressive solvents and some have levels of crystallinity that should afford low coefficients of thermal expansion. The cured ETPAE's also exhibit excellent processability, high adhesive properties, and good resistance to hydraulic fluids.

All of the PAE's prepared are suitable for use as adhesives, coatings, films, membranes, and composite matrices. These materials show properties that make them potentially useful for both spacecraft and aircraft applications. The low coefficients of thermal expansion of some of the new PAE's should lead to improved dimensional stability for space structures, and their fracture toughnesses and excellent processability make them ideally suited for aircraft composites.

This work was done by Paul M. Hergenrother and Brian J. Jensen of **Langley Research Center** *and Stephen J. Havens of PRC Kentron, Inc. For further information, Circle 9 on the TSP Request Card.*

This invention is owned by NASA, and a patent application has been filed. Inquiries concerning nonexclusive or exclusive license for its commercial development should be addressed to the Patent Counsel, Langley Research Center [see page 16]. Refer to LAR-13555.

Air Revitalization Using Superoxides

$Ca(O_2)_2/KO_2$ pellets are superior to KO_2 pellets for air revitalization.

Ames Research Center, Moffett Field, California

Pellets made from powder mixtures of potassium superoxide, KO_2, and calcium superoxide, $Ca(O_2)_2$, have proven markedly superior to pellets of pure KO_2 for adding O_2 to and removing CO_2 from an atmospheric-pressure flow of humidified CO_2 in He. Superoxides have been used extensively to supply O_2 and scrub CO_2 in a variety of ambient-pressure life-support applications — including portable self-contained breathing apparatuses, spacecraft, and undersea submersible craft — and are attractive candidates for high-pressure air-revitalization applications because of their high O_2-storage density and high CO_2-absorption capacity and because of the potential simplicity of the total O_2-delivery/CO_2-scrubbing system.

Potassium superoxide releases O_2 and absorbs CO_2 through the following reactions:

1. $2KO_2 + H_2O \rightarrow 2KOH + 3/2\ O_2$
2. $2KOH + CO_2 \rightarrow K_2CO_3 + H_2O$
3. $KOH + CO_2 \rightarrow KHCO_3$

Unfortunately, upon exposure to the concentrations of H_2O and CO_2 existing in exhaled human breath, KO_2 tends to form fused, hydrated-hydroxide/carbonate coatings of low gas permeability on the exterior of the chemical granules. Once this product layer is formed, it limits the diffusion of H_2O and CO_2 reactants to the unreacted core of the KO_2 and results in poor utilization of the available O_2 and of the CO_2-scrubbing capacity. Moreover, the presence of the hydrated-hydroxide coating in conjunction with the exother-

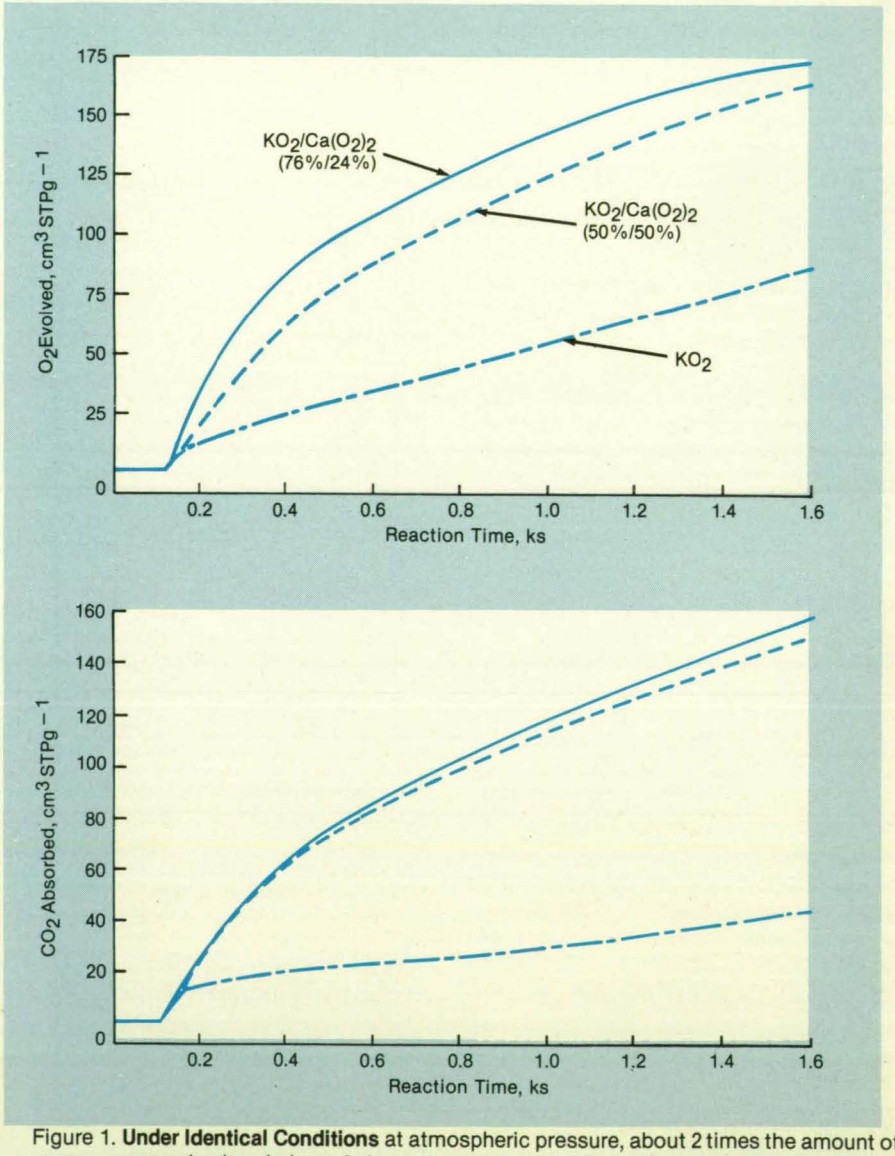


Figure 1. **Under Identical Conditions** at atmospheric pressure, about 2 times the amount of oxygen was evolved and about 3 times the amount of CO_2 was absorbed by $KO_2/Ca(O_2)_2$ pellets as by KO_2 pellets.

micity of reaction promotes intergranule fusion, making sections of the packed bed unavailable for reaction with the exhaled gas. The utilization of available O_2 is typically only 50 to 80 percent for KO_2 in portable breathing apparatuses. If reuse of a breathing apparatus is desired, the fusion of the superoxide bed also makes it difficult to remove the expended chemical from the breathing canister.

In 1-atm (0.1-MPa) flow tests, the deleterious coating effect encountered with KO_2 was alleviated using mixtures of KO_2 and $Ca(O_2)_2$ containing 24 or 50 weight percent of $Ca(O_2)_2$, without a significant sacrifice in the overall available O_2 and in the CO_2-scrubbing capacity (see Figure 1): the product coating on the superoxide-mixture pellets was permeable to H_2O and CO_2 reactants and was also hard and nonfusing. The expended superoxide material could be easily removed from the breathing canister: hence, re-use of the breathing device would be possible.

When individual pellets of 50 percent KO_2 and 50 percent $Ca(O_2)_2$ were reacted with humidified CO_2 in He at 10 atm (1 MPa), the rates of O_2 evolution and CO_2 absorption were one-third to one-eighth that exhibited by similar samples tested at 1 atm (0.1 MPa) (see Figure 2). It has been postulated that this drop in reactivity under hyperbaric conditions is caused principally by the decrease in the bulk diffusivity of the H_2O and CO_2 reactants in the high-pressure He, because the reactivity of the pellet was restored when the pressure was decreased from 10 atm (1 MPa) to 1 atm (0.1 MPa) while the other reaction conditions were held constant.

This work was done by Theodore Wydeven of **Ames Research Center** *and by Peter C. Wood and L. A. Spitze of San Jose State University. For further information, Circle 12 on the TSP Request Card.*

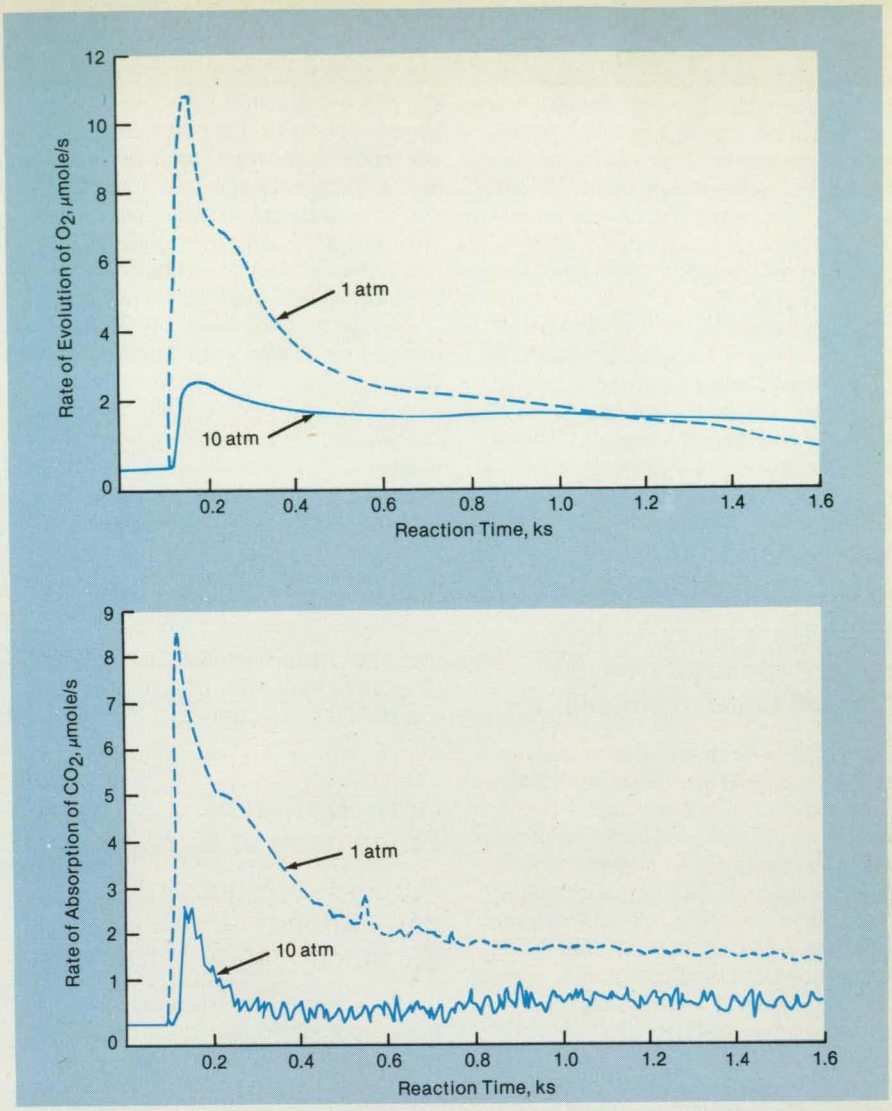


Figure 2. The **Rates of O_2 Evolution and CO_2 Absorption** are much less at 10-atm (1-MPa) pressure than at 1-atm (0.1-MPa) pressure.

Inquiries concerning rights for the commercial use of this invention should be addressed to the Patent Counsel, Ames Research Center [see page 16]. Refer to ARC-11695.

Books and Reports

These reports, studies, handbooks are available from NASA as Technical Support Packages (TSP's) when a Request Card number is cited; otherwise they are available from the National Technical Information Service.

Microstructure and Weld Cracking in Inconel 718*

Theories on the relationship between metallurgy and microfissuring are confirmed.

A report describes research on the effects of the microstructure on the cracking of heat-affected zones of welds in Inconel 718* alloy. In experimental studies, specimens were subjected to various combinations of time-varying thermal and mechanical stresses to simulate welding conditions and to identify the physical and chemical effects that cause microfissuring.

The report details specific correlations between microfissuring and grain size, Ni_3Nb (δ phase), hardness, $Ni_3(Al, Ti)$ (γ' phase), Ni_3Nb (γ'' phase), solution annealing heat treatment, and age-hardening heat treatment. Indirect correlations between microfissuring and impurity segregation are also presented.

The combined experimental results of this investigation and previous investigations appear to support a generalized theory of carbide liquation that explains the susceptibility to microfissuring. According to the theory, at sufficiently high temperature (but below the melting point of the alloy), liquid NbC forms along grain boundaries. The liquid NbC feeds Nb to the Ni-rich matrix, causing eutectic melting. Displaced by the additional molten material, the NbC spreads further along the grain boundaries, causing further melting. Under the strain imposed by welding, microfissures open to the liquid. When the alloy cools, Laves phases precipitate from the liquid along the microfissures.

The intergranular liquid distribution is controlled by the elements absorbed by the liquid from the grain-boundary region during the liquation and wetting process. Thus, the chemical composition of the grain-boundary region just before welding affects the susceptibility to microfissuring during welding. In particular, impurities appear to contribute to microfissuring. The susceptibility increases with the grain size because there is less grain-boundary area over which to spread the liquid, and the effect of the liquid is therefore magnified.

The chemical and microstructural alloy properties are determined by manufacturing processes and heat treatments. As a result of this research, the susceptibility to

microfissuring of an alloy part to be welded can now be evaluated on the basis of its metallurgical properties and process history. Because an intergranular-liquid mechanism also appears to cause hot cracking in the Nb-bearing 347 stainless steel, the generalized theory may be important to all Nb-bearing Ni or Fe alloys.

*Inconel is a registered trademark of the Inco family of companies.

This work was done by R. G. Thompson of the University of Alabama for **Marshall Space Flight Center**. *To obtain a copy of the report, "Effect of Microstructure on Weld HAZ Cracking of Inconel 718," Circle 159 on the TSP Request Card.*
MFS-27121

Lubrication Handbook for the Space Industry

Properties and application data are given for over 500 solid and liquid lubricants.

A 458-page handbook covers many of the solid and liquid lubricants used in the space industry. It will also be a useful reference in industrial and military applications of lubricants. Part A of the handbook is a compilation of data on the chemical and physical properties of over 250 solid lubricants, including bonded solid lubricants, dispersions, and composites. Similarly, part B covers over 250 liquid lubricants, greases, oils, compounds, and fluids.

Each part includes an introduction that describes the general characteristics of the various types of lubricants covered, a glossary, and tabulations of standard specifications (e.g., MIL, NASA, or ASTM specifications) and other test procedures. Part B also includes appendixes containing viscosity-conversion data, the international system of units, and conversion factors.

Lubricants and lubricant properties are arranged systematically so that designers, engineers, and maintenance personnel can conveniently locate data needed for their work. Cross-reference tables provide access to the data by types of lubricants, by applications, by product names, by manufacturers, and by specifications.

For each solid lubricant, the basic properties tabulated include compositions; suggested uses; compatibility with jet and other hydrocarbon fuels, solvents, liquid oxygen, and rocket fuels; and notes on such matters as usable temperature ranges, curing conditions, and tensile strengths. Also provided for many solid lubricants are data on methods of application, on resistance to radiation, on outgassing properties, on load capacity, on wear life, on coefficients of static and dynamic friction in air and vacuum, on electrical conductivities, on resistance to corrosion, and on weight losses in vacuum.

The properties listed for liquid lubricants vary from type to type. For lubricating oils, the properties listed generally include compositions (including additives), viscosities, specific gravities, flash points, fire points, pour points, stabilities under corrosion and oxidation, humidity-test results, neutralization numbers, evaporation percentages, carbon-residue percentages, colors, and precipitation numbers.

This work was done by Ernest L. McMurtrey of **Marshall Space Flight Center**. *Further information may be found in NASA TM-86556 [N86-31730/NSP], "Lubrication Handbook for the Space Industry."*

Copies may be purchased [prepayment required] from the National Technical Information Service, Springfield, Virginia 22161, Telephone No. (703) 487-4650. Rush orders may be placed for an extra fee by calling (800) 336-4700. The report is also available on microfiche at no charge. To obtain a microfiche copy, Circle 17 on the TSP Request Card.
MFS-27169

Optimization of Processing of Si_3N_4

Process changes are iterated under the guidance of x-radiography.

Silicon nitride is a prime candidate for heat-engine applications because of its resistance to oxidation and thermal shock and its strength at room and high temperatures. However, scatter in mechanical properties is a great disadvantage for design and reliability. This scatter is attributed to defects and inhomogeneities that occur during the processing of Si_3N_4 powder compositions or during the fabrication of silicon nitride parts.

In recent work at NASA Lewis Research Center, density gradients in sintered silicon nitride, characterized by x-radiography, were identified and appeared strongly dependent upon powder-processing and sintering conditions. A NASA technical memorandum describes a systematic investigation, based upon this preliminary work, of density-gradient/flexural-strength relationships as affected by processing.

The results of this program showed that a sintered Si_3N_4 composition containing approximately 6 weight percent each of Y_2O_3 and SiO_2, developed by NASA and designated NASA 6Y, was significantly improved. The improvement over baseline material was accomplished by the iterative utilization of conventional x-radiography to characterize structural (density) uniformity as affected by systematic changes in powder processing and high-pressure, nitrogen sintering parameters. A dense-case/less-dense-core structure, revealed by x-radiography of the baseline material, was eliminated by incorporating wet sieving of powders and increasing powder-grinding time and by increasing sintering time, minimizing BN (boron nitride) setter contact, and adjusting the sintering height in the furnace.

Four-point flexural strengths of 125,000, 79,000 and 67,000 psi (860, 540, and 460 MPa, respectively) at room temperature, 2,200 °F (1,200 °C) and 2,500 °F (1,370 °C), respectively, represent improvements of 56, 38, and 21 percent over baseline NASA 6Y properties. Improved material uniformity and reliability were demonstrated by a threefold reduction in the standard deviation and a fourfold increase in the Weibull modulus at room temperature. Accompanying the improvement in strength was a change in the type of flaw causing failure, from a more strength-limiting flaw to a less strength-limiting columnar β-Si_3N_4 grain.

This work was done by William A. Sanders and George Y. Baaklini of **Lewis Research Center**. *Further information may be found in NASA TM-87251 [N86-31729/NSP], "Correlation of Processing and Sintering Variables with the Strength and Radiography of Silicon Nitride."*

Copies may be purchased [prepayment required] from the National Technical Information Service, Springfield, Virginia 22161, Telephone No. (703) 487-4650. Rush orders may be placed for an extra fee by calling (800) 336-4700.
LEW-14456

Galvanic Corrosion in (Graphite/Epoxy)/Alloy Couples

Some alloys need protection against corrosion in salt water.

The effects of a galvanic coupling between graphite/epoxy composite material (G/E) and D6AC steel, 6061-T6 aluminum, and Inconel* 718 nickel alloy in salt water are described in a report. An introductory section of the report summarizes previous corrosion studies of G/E with other alloys. The details of sample preparation are presented along with photographs of the samples before and after immersion.

The tests were conducted in aqueous 3.5-percent NaCl solutions at 22 °C. In the experiments requiring electrical contact between the G/E and the alloy, bolts of a stainless steel previously found to be compatible with G/E were used to hold the G/E and metal specimens in contact.

The corrosion potentials of the alloys were measured with respect to a saturated calomel electrode. Galvanic currents were measured with a corrosion-measurement console. The corrosion rates of the alloy specimens were calculated from the weight losses and immersion times.

The measurements show that the steel

and aluminum alloys require protection against corrosion when they are galvanically coupled to G/E in salt water, while the nickel alloy is relatively unaffected and is compatible with G/E. The study also shows that the aluminum alloy is effective as a sacrificial anode, providing cathodic protection to the steel when both are galvanically coupled to G/E.

The report also describes six tests of methods of protecting the steel and aluminum alloys against galvanic corrosion. When the G/E is completely coated with paint or a paint/polyurethane resin combination, the steel is adequately protected by either a zinc-rich primer with a final coat of grease or by a primer/topcoat combination with a final coat of grease. The aluminum is protected by epoxy chromate primer/epoxy paint, with a final coat of grease. However, the grease may not be necessary in the case of the aluminum.

*Inconel is a registered trademark of the Inco family of companies.

This work was done by Merlin D. Danford and Ralph H. Higgins of **Marshall Space Flight Center**. *Further information may be found in NASA TP-2236 [N84-13263/NSP], "Galvanic Coupling Between D6AC Steel, 6061-T6 Aluminum, Inconel 718, and Graphite-Epoxy Composite Material: Corrosion Occurrence and Prevention."*

Copies may be purchased [prepayment required] from the National Technical Information Service, Springfield, Virginia 22161, Telephone No. (703) 487-4650. Rush orders may be placed for an extra fee by calling (800) 336-4700. The report is also available on microfiche at no charge. To obtain a microfiche copy, Circle 75 on the TSP Request Card. MFS-27055

Temperature, Humidity, and Polymer Aging

A theoretical basis is found for an empirical equation.

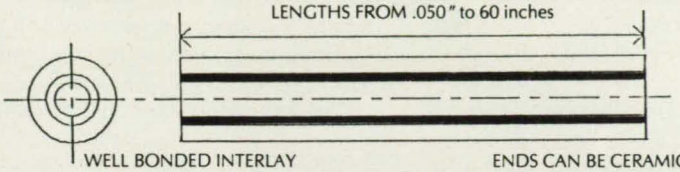
A report presents an analysis of experimental data on the electrical resistivity of a polymer (polyvinyl butyral) as a function of temperature and relative humidity. The resulting theoretical expression for the electrical resistivity (or its reciprocal, conductivity) resembles a generally accepted empirical law for the corrosion rate (or its reciprocal, lifetime).

The author begins by noting that experimentally the electrical resistivity at zero relative humidity obeys an Arrhenius relationship with an activation energy of 11.243 kcal/mole. Semilog plots of resistivity versus temperature at other values of relative humidity are found to be nearly parallel, and prompt an examination of the hygroscopic properties of the material in question. When replotted, the data show that at a given temperature the logarithm of resistivity decreases linearly with the

HIGH PERFORMANCE SUPERMATERIALS PLASMA SPRAYED OR SINTERED

We make tubes with a ceramic lining under compression, and an outer layer well bonded of almost any metal you would like to try, such as: Tungsten, Molybdenum, Nickel, Stainless Steels, Copper, Nickel-Chromium, Aluminum, Titanium and Tantalum. I.D.s of any ceramic oxide.

PLASMA DETONATION SPRAYED TUBES MADE ENTIRELY FROM POWDERS



TYPE "A" TUBE OR CYLINDER
O.D. = CERAMIC OR CARBIDE
I.D. = METAL OR CARBIDE

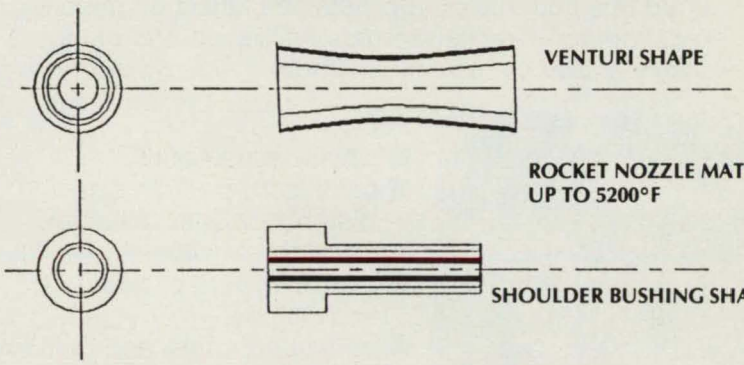
TYPE "B" TUBE
O.D. = METAL
I.D. = CERAMIC OR CARBIDE

TYPE "C"—3 layer sandwich of "A" or "B"

HOLES FROM .050" TO 12 INCHES
FINISHES FROM POLISHED OR GROUND 5 MICROINCH RMS TO 300 RMS

THERMAL BARRIER LININGS—O.D. & I.D. MATERIALS AVAILABLE TO RESIST UP TO 3000°F CONSTANT
CORROSION RESISTANT LININGS—O.D. & I.D.
WEAR RESISTANT LININGS—O.D. & I.D.

MANY MATERIALS AS TUBE STRUCTURES CAN BE IMMERSED IN MOLTEN METALS, SUCH AS: ALUMINUM, COPPER, STEEL AND OTHER METALS
SPECIAL TUBES OR CYLINDER SHAPES AVAILABLE



SIMPLE RING COUPON SETS QUOTED UNDER $1000, FAST DELIVERY

LIST OF MATERIALS AVAILABLE

The following is a partial listing of our high temperature materials, high and low purity metals and powders, rare earths, metal borides, nitrides, silicides, carbides, oxides, submicron powders, plasma spray powders, exotic metal powders, spherical powders, rods, wire, foils, Superconductor materials, and alloy materials. Commercial purities are much less costly than laboratory purities.

Alumina	Ceramics, various	Graphites	Nitrides	Tantalum
Aluminum	Cerium	Hafnia	Osmium	Tin
Antimony	Cermets	Hafnium	Oxides	Titania
Balls, various matls.	Chemical powders	Indium	Palladium	Titanium
Barium	Chromium	Iron	Platinum	Tungsten
Bauxite	Cobalt	Lanthanum family	Rhenium	Tungsten Carbide
Beryllium	Columbium	Lead	Rhodium	Vanadium
Bismuth	Copper	Magnesium	Selenium	Ytterbium
Boron	Diamond	Manganese	Silica	Yttria
Brass & Bronze	Gadolinium	Molybdenum	Silicon	Yttrium
Cadmium	Gallium	Neodymium	Silicon Carbide	Zinc
Calcium	Germanium	Nickel	Silver	Zirconia
Carbides, various	Glasses	Niobium	Steels, stainless	Zirconium
Carbon	Gold			

SUPERMATERIALS COMPANY

Suite 356 Statler Tower
1127 Euclid Avenue, Cleveland, Ohio 44115
Telephone (216) 861-0724

(An Affiliate of Carboride Corporation—world leaders in high performance ceramic composites)

Circle Reader Action No. 515

relative humidity, suggesting that the electrical resistivity decreases with increased water absorption.

The concentration of water absorbed in the polymer is assumed to be proportional to the vapor pressure of water in the air and to an Arrhenius temperature-dependence factor characterized by an activation energy for water-vapor absorption. Plots of resistivity versus water-vapor pressure at fixed temperatures have temperature-dependent slopes that can be fit by least squares to such an Arrhenius factor with an activation energy of 9.23 kcal/mole.

Next, the vapor pressure is expressed as the product of the relative humidity and the saturation vapor pressure, which is governed by yet another Arrhenius equation and the parameters of which are well known from previous measurements. This relationship is inserted in the equation that describes the plot of electrical resistivity versus water-vapor pressure. After a Taylor-series expansion about the absolute temperature of 273 K (0 °C) and neglect of small higher-order terms, the equation has the form

$$\ln \varrho(t,R.H.) = A - k_1 t - k_2 (R.H.)$$

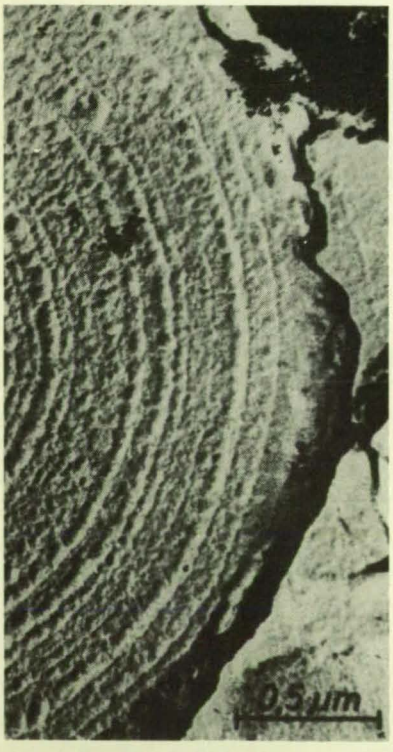
where ϱ = electrical resistivity, t = temperature in °C, R.H. = relative humidity, and A, k_1, and k_2 are constants.

The form of this equation is the same as that of the empirical equation for the corrosion lifetime. The author points out that this suggests a relationship between leakage currents and corrosion in insulating materials. It may be possible to define the corrosion lifetime as the time during which a specified amount of charge is transferred through leakage. In that case, the equation would be experimentally associated with the correlation among lifetime, relative humidity, and temperature.

This program was written by Edward F. Cuddihy of Caltech for **NASA's Jet Propulsion Laboratory**. *To obtain a copy of the report, "Aging Correlation Between Corrosion Lifetime and Relative Humidity and Temperature," Circle 20 on the TSP Request Card.*
NPO-16908

BASF
Carbonyl Iron Powders

- built layer-by-layer into minute (2-10 μm), highly spherical particles. BASF carbonyl iron powders are available in a range of grades which are widely accepted throughout industry. BASF powders are used in electronic core production, injection molding, electromagnetic interference, infiltration and other alloys and as an iron supplement.



For -
- unsurpassed purity
- consistent particle size distribution with optimum packing density
- over 60 years of accrued technology
- dedicated sales and delivery services, plus supporting laboratory facilities that keep us on the cutting edge of technical development.

Call or write: BASF Corporation, Chemicals Division, Inorganics, 100 Cherry Hill Road, Parsippany, N.J. 07054. Phone 1-(800)426-8702 or (201)316-3000 Ext. 3870

BASF Corporation
Chemicals Division

Intermediates & Fine Chemicals

BASF

Effects of Radiation on Insulators

Data have been compiled on a variety of thermosetting and thermoplastic polymers.

A report presents data on the responses of electrically insulating thermosetting and thermoplastic polymers to radiation. The lowest-threshold-dose (LTD) levels and the 25-percent-change levels are presented for such properties as tensile strength and electrical resistivity. Data on radiation-induced outgassing are also given.

The author notes that microscopic changes in insulators are indicated by changes in the macroscopic physical properties and that the LTD is an important indicator of the dose level at which the changes start to occur. For comparisons of the sensitivities of different materials to radiation, a consistent LTD should be used. The author proposes that the LTD be defined as that which produces a 1-percent change in the physical property of interest.

The tensile strengths of some insulators increase initially, even after the LTD is reached. The material becomes stronger because of cross-linking. In such cases, an "engineering-threshold-dose" can be used in comparing materials for design purposes. The author defines the engineering threshold dose as the dose that causes the property in question to decrease to a value 1 percent below the value before irradiation. LTD's sometimes vary with temperature or other condition of the insulating material.

Such effects as outgassing are known to be nonlinear even in the absence of radiation. This suggests that the LTD's for outgassing are probably nonlinear too.

This work was done by Frank L. Bouquet of Caltech for **NASA's Jet Propulsion Laboratory**. *To obtain a copy of the report, "Thresholds of Radiation Effects on Insulators," Circle 37 on the TSP Request Card. NPO-17032*

Interactive math with your IBM/XT/AT



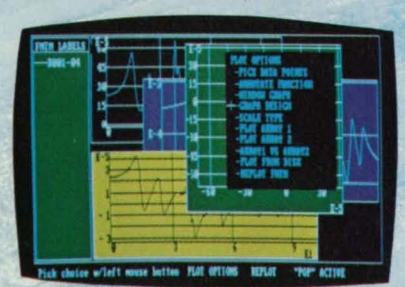
Over 40 preprogrammed functions are grouped into 7 menus for direct selection.



Powerful math options such as differentiate, integrate and FFT are executed in a couple of seconds with simple menu picks.



You can list data, edit, operate on, plot and store to disk. The function file directory allows easy access to stored data.



Select plot options in pop-up window using MOUSE or keyboard.

IAS
INTERACTIVE ANALYSIS SYSTEM

From the NASA Johnson Space Center environment comes breadth and depth of math functionality you've not seen on a Personal Computer.

Now, you have IAS, a main frame grade advanced menu driven system at a price accessable to everyone.

- Your choice: mouse, FNTN key, arrow key cursor pick, or type two-character commands
- New lookahead window and stacked menus with command trail
- More ways to generate math functions
- Pick preprogrammed functions directly from menu
- Keyboard x-y data entry
- Type algebraic equations
- Differential Equations. 1st, 2nd and 3rd order.
- Interpolation
- Curve fitting
- EQN, parameter and variable tables
- Extensive operations on functions, including FFT, differentiation, integration
- The other guys are eating their hearts out over IAS plot capability. No hoops to jump through, either.
- Matrix analysis
- Wireframe object eigenvector animation (vibration simulation)
- Breakthrough: User menu puts your program inside IAS
- External data interface menu
- Special picks for SDRC I-DEAS, Univ. of Cincinnati Universal Files and Lotus 1-2-3.
- EE's: Build your data acquisition system inside IAS
- Menu driven file management
- DOS command menu
- IBM XT/AT. 512K. 8087. CGA or EGA. Screen copy.
- 30 day moneyback guarantee

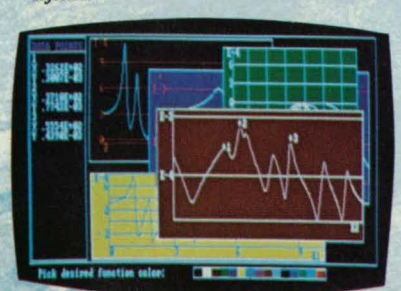
$149.00

VISA master charge

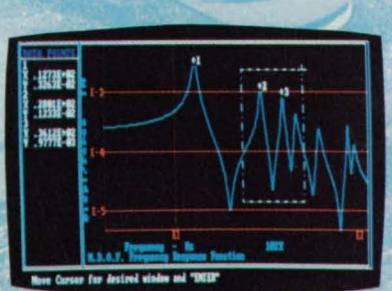
ATC ANALYSIS TECHNOLOGY COMPANY

3914 Miami Road
Cincinnati, Ohio 45227

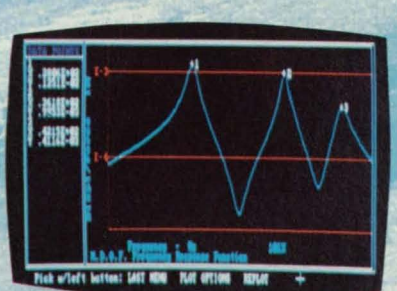
(513) 561-1100



Pick desired colors directly from color bar.



Rubber-banding box zooms on data you wish to magnify. Use MOUSE or keyboard.



Redisplayed data from zoom box. Data points are cursored for x-y values.

Circle Reader Action No. 546

Computer Programs

COSMIC: Transferring NASA Software

COSMIC, NASA's Computer Software Management and Information Center, distributes software developed with NASA funding to industry, other government agencies and academia.

COSMIC's inventory is updated regularly; new programs are reported in *Tech Briefs*. For additional information on any of the programs described here, circle the appropriate TSP number.

If you don't find a program in this issue that meets your needs, call COSMIC directly for a free review of programs in your area of interest. You can also purchase the 1987 *COSMIC Software Catalog*, containing descriptions and ordering information for available software.

COSMIC is part of NASA's Technology Utilization Network.

COSMIC® — *John A. Gibson, Director*, (404) 542-3265
Computer Services Annex, Univ. of Georgia, Athens, GA 30602

68 **Computing Radiation Characteristics of Phased Arrays**
68 **Program Reads Weather-Data Tapes From Aircraft**
73 **Estimating Geophysical Parameters From Gravity Data**
73 **Strain-Energy-Release Rates in Delamination**
73 **Analyzing Solar-Power Options for Spacecraft**
74 **Computer Program Predicts Turbine-Stage Performance**
74 **Computer Analysis of High-Speed Roller Bearings**
76 **Calculating Flows in Multiple-Blade-Element Cascades**
76 **Interactive Plotting Program**
76 **Tape-Certification Program**
78 **Locating Spaceborne SAR Imagery**
78 **Generating Cross-References Among Computer Routines**
78 **Designing Digital Filters**
78 **BASIC Programming in Water and Wastewater Analysis**

Computer Programs

These programs may be obtained at a very reasonable cost from COSMIC, a facility sponsored by NASA to make computer programs available to the public. For information on program price, size, and availability, circle the reference number on the TSP and COSMIC Request Card in this issue.

Electronic Components and Circuits

Computing Radiation Characteristics of Phased Arrays

Radiated powers, directivities, and radiation patterns can be calculated.

One of the most important radiation characteristics of an antenna system is the directivity. The accurate determination of this parameter is essential for the analysis and design of advanced antenna systems. In general, for most-commonly-used array elements like open-ended waveguides, horns, or microstrip patch antennas, an analytical expression of the $(\cos\theta)^q$ type can be used to tailor actual element patterns properly. Experimentally-measured element patterns could include mutual coupling, which may be significant in large arrays. Expressions for the directivity and radiation pattern of a single element and of a rectangular array using $(\cos\theta)^q$-type element patterns have been reported.

With the advent of monolithic microwave integrated circuits, phased arrays have become key components in the design of advanced antenna systems. Array-fed antennas are used extensively in today's multiple-beam satellite antennas.

A computer program was devised to generalize these results and obtain an efficient numerical technique for computing the directivity and the radiation pattern of the generalized array. The characteristics of the generalized array used in this program include arbitrary element locations; element patterns that are of the $(\cos\theta)^q$ type, analytically describable by other functions, or experimentally measured; and the polarizations and excitations of the elements.

The computer program is based on a very efficient numerical technique for calculating the radiated power (Romberg integration), directivity, and radiation pattern of a phased array. The formulation is very general and takes into account arbitrary element polarization, electric-field-plane and magnetic-field-plane element pattern, element location, and complex element excitation.

One of the advantages of this generalized array formulation is that it does not break down in special cases as might other approximations that use closed forms. Also, the formulation does not limit the observation of the pattern to the far-field zone. This can be very useful if the generalized formulation is going to be used with analysis programs for dual-reflector configurations. The program can be modified easily for use in the analysis of reflectors with phased-array feeds.

This computer program is one of the principal research tools at NASA Lewis Research Center for the analysis of advanced space-communication antenna systems. The generalized formulation and computer program provide complete flexibility in the analysis of array configurations and in the accurate analysis of experimental data. The program is written in FORTRAN IV and can be used on an IBM 370 computer.

This program was written by Roberto J. Acosta of **Lewis Research Center**. *For further information, Circle 163 on the TSP Request Card.*
LEW-14460

Physical Sciences

Program Reads Weather-Data Tapes From Aircraft

Data are analyzed and converted for further processing or display.

A computer program has been developed to help read and analyze the data gathered by airborne instruments for atmospheric research. By employing remote-sensing techniques, measurements of wind and wind stress can be obtained from airborne instruments in various locations and weather conditions.

The program was written to process data tapes from an airplane operated by the National Center for Atmospheric Research (NCAR). The tapes are in ½-in. (12.7-mm), nine-track, 6,250-bit/in. (2,461-bit/cm), 32-bit-word format and contain records of 19,840-bit length. There is one record per second of flight time. Each record contains samples of 98 parameters, sampled either 1 or 20 times per second.

The program reads the NCAR tape, optionally scales or averages the data, and stores (or appends) the results in a disk file. An error file is created if any records can-

not be successfully unpacked and converted to real numbers. The output from this program can be used as input to statistical-analysis programs for further processing or to plotting packages for graphical representation of the data.

This program is written in FORTRAN 77 for interactive execution and has been implemented on a DEC VAX-series computer operating under VMS. The program was developed in 1984.

This program was written by Mike Carlton and Carl A. Friehe of the University of California for **NASA's Jet Propulsion Laboratory**. *For further information, Circle 87 on the TSP Request Card.*
NPO-16744

Estimating Geophysical Parameters From Gravity Data

Features of planets are extracted from Doppler spacecraft- tracking measurements.

The ORBSIM program was developed for the accurate extraction of parameters of geophysical models from Doppler-radio-tracking data acquired from orbiting planetary spacecraft. The model of the proposed planetary structure is used in a numerical integration along simulated trajectories of the spacecraft around the primary body.

Using line-of-sight (LOS) Doppler residuals, ORBSIM applies fast and efficient modeling and optimization procedures that avoid the traditional complex dynamic reduction of data. ORBSIM produces such quantitative geophysical results as size, depth, and mass. ORBSIM has been used extensively to investigate topographic features on the Moon, Mars, and Venus. The program has proved particularly suitable for modeling gravitational anomalies and concentrations of mass.

The basic observable quantity for spacecraft-based gravity data is the Doppler frequency shift of a transponded radio signal. The derivative of this signal with respect to time carries information regarding the gravity field acting on the spacecraft in the LOS direction (the LOS direction being the path between the spacecraft and the receiving station — either Earth or another satellite). Many dynamic factors are taken into account, such as the rotation of the Earth, solar radiation, acceleration from planetary bodies, and adjustments of the location and time of the tracking station.

The actual trajectories of the spacecraft are simulated by the use of least-squares fits to conic motions. The theoretical Doppler readings from the simulated orbits are compared to actual Doppler observations, and another least-squares adjustment is made.

ORBSIM has three modes of operation: (1) trajectory simulation, (2) optimization, and (3) gravity modeling. In all cases, an initial gravity model of curved and/or flat disks, harmonics, and/or a force table are required input.

ORBSIM is written in FORTRAN 77 for batch execution and has been implemented on a DEC VAX 11/780 computer operating under VMS. The program was released in 1985.

This program was written by William L. Sjogren of Caltech and Ravenel N. Wimberly of Sterling Software for **NASA's Jet Propulsion Laboratory**. *For further information, Circle 59 on the TSP Request Card.*
NPO-16671



Materials

Strain-Energy-Release Rates in Delamination

Failures of composite laminates are analyzed under a variety of loads.

The Q3DG computer program was developed to perform a quasi-three-dimensional stress analysis of composite laminates that may contain delaminations. Delamination may result from low-velocity impacts, eccentricities in load paths that induce out-of-plane loads, or discontinuities in the structure that create out-of-plane stresses. Q3DG calculates the strain-energy-release rates for long, rectangular composite laminates containing delaminations and subjected to any combination of mechanical, thermal, and hygroscopic loading.

Q3DG uses a quasi-three-dimensional analysis in conjunction with concepts of linear fracture mechanics and fininte-element methods. Total strain-energy-release rates can be calculated by the use of the classical theory of laminated plates. Finite-element analysis is used to separate the total strain-energy-release rates into the three components associated with the three modes of fracture (opening mode, sliding mode, and tearing mode). Special eight-noded parabolic isoparametric elements are used to model the laminates. A rectangular-mesh and data-file-generator capability is included with the package. The input to Q3DG includes data on the geomerty, material, and loading of the composite object. The output includes nodal forces, nodal stresses, nodal displacements, stiffness matrix, and strain-energy-release rates for each fracture mode (including percentages and cross-terms).

The Q3DG program is written in FORTRAN V for batch execution and has been implemented on a CDC Cyber 170-series computer with a central-memory requirement of approximately 343K of 60-bit words. The mesh and data-file generator can be run interactively. This program was developed 1985.

This program was written by I. S. Raju of Analytical Services and Materials, Inc., for **Langley Research Center**. *For further information, Circle 13 on the TSP Request Card.*
LAR-13698



Machinery

Analyzing Solar-Power Options for Spacecraft

Costs, weights, and efficiencies are estimated.

The Solar Space Power Analysis Code, SOSPAC, was developed to examine the solar-thermal and photovoltaic power-generation options available for a satellite or spacecraft in low orbit around the Earth. SOSPAC is a software tool for the preliminary analysis of systems and enables the engineer to compare the areas, weights, and costs of several candidate electric- and thermal-power systems. The configurations studied include photovoltaic arrays and paraboloidal-dish systems to produce electricity only and in various combinations to provide both thermal and electric power.

SOSPAC has been used for comparison and parametric studies of proposed power systems for the NASA Space Station. The initial requirements are projected to be about 40 kW of electrical power and a similar amount of thermal power with temperatures above 1,000 °C. For objects in low orbits around the Earth, the aerodynamic drag caused by suitably-large photovoltaic arrays is substantial. Smaller paraboloidal dishes can provide thermal energy at a collection efficiency of about 80 percent but at increased cost.

SOSPAC enables an analysis of the cost and performance factors of five hybrid power-generating systems. The input includes electrical- and thermal-power requirements, durations of Sunlight and shade for the satellite, and the unit weights and costs of subsystems and components. The performance equations of the five configurations are derived, and the output tabulates the total weights of the power-plant assemblies, areas of the arrays, efficiencies, and costs.

SOSPAC is written in FORTRAN IV for batch execution and has been implemented on an IBM PC operating under DOS with a central-memory requirement of approximately 60K of 8-bit bytes. The program was developed in 1985.

This program was written by M. K. Selcuk of Caltech for **NASA's Jet Propulsion Laboratory**. *For further information, Circle 134 on the TSP Request Card.*
NPO-16855

Computer Program Predicts Turbine-Stage Performance

Complicated three-dimensional and dissipative effects are taken into account.

The MTSBL computer program for predicting the performances of turbine stages accounts for the effects of complex passage configurations. MTSBL is an updated version of the flow-analysis programs MERIDL and TSONIC coupled to the boundary-layer program BLAYER.

The method uses a quasi-three-dimensional, inviscid, stream-function flow analysis iteratively coupled to calculated losses so that changes in losses result in changes in the flow distribution. In this manner the effects of both the configuration on the flow distribution and the flow distribution on losses are taken into account in the prediction of the performance of a stage.

Boundary-layer analyses account for losses due to friction. Empirical loss models are used to account for incidence, secondary flow, disk windage, and clearance losses. Each boundary-layer analysis is performed using BLAYER. The results of the boundary-layer analyses are used to determine profile and end-wall friction losses. These losses, plus additional losses calculated from empirical models, are used to calculate the efficiencies of stators, rotors, and stages. The analysis has been applied to both axial and radial turbines.

This program has evolved over time, and a number of references should be consulted to determine the method used for the solutions. Also included is a reference that shows the specific application of the analysis to the design of a radial turbine and would be helpful in the analysis of a radial or mixed-flow machine.

The input required to analyze a blade row by use of MTSBL is only slightly more than is required to do the hub-to-shroud flow analysis for a blade row using the program MERIDL. A control block of information using a namelist input is entered prior to the data for MERIDL. The significance of all of the variables that can appear in the control block is described in the beginning of the program listing.

The program is written in FORTRAN IV for use on an IBM 3033 computer.

This program was written by Robert J. Boyle, Jeffrey E. Haas, and Theodore Katsanis of **Lewis Research Center**. *For further information, Circle 15 on the TSP Request Card.*
LEW-14218

Computer Analysis of High-Speed Roller Bearings

Performances of highly stressed bearings are predicted.

The engine performance that will satisfy the anticipated efficiency, speed, and specific-thrust requirements for aircraft in the coming decade places increased demands on the performances of engine components. Engines will be required to operate at high temperatures and speeds while maintaining low overall mass and high structural integrity. Bearings, in particular, emerge as critical elements of system design for the new engines.

The high-speed cylindrical roller-bearing analysis program (CYBEAN) was developed to compute the behavior of cylindrical rolling-element bearings at high speeds and with misaligned shafts. With CYBEAN, an accurate assessment of geometry-induced roller preload is possible for a variety of outer-ring and housing configurations and loading conditions. CYBEAN enables detailed examination of bearing performance and permits exploration of the causes and consequences of bearing skew. CYBEAN provides a general capability for the assessment of designs of bearings that support the main shafts of engines.

CYBEAN is structured as a software tool for the analysis of bearings, involving the coordinated execution of modules that perform specific analytic tasks. The bulk of the calculations performed by CYBEAN consist of the repetitive computation of displacements and forces resulting from solid/solid and solid/fluid interactions. These interactions are permitted to occur in a thermally varying environment and are viewed as part of a system in quasi-static thermodynamic equilibrium.

The system is defined by geometric and material descriptions of the bearing complement and the rheology of the lubricant used. The system is considered to be driven by external forcing functions that consist of a constant vector set representing definitions of shaft rotation, speed, and applied radial force. Additional system stimulation is accepted from heat gener-

NTB:BASE Research Center offers

12,000+ Solutions

NTB:BASE from NASA Tech Briefs

In minutes you can search 25 years of NASA Tech Briefs to find briefs related to your current project. NASA may have already found a solution or may suggest other ways of resolving the problem. On the way to space NASA has had to solve thousands of problems in all engineering fields under the most extreme conditions.

- **PC-Compatible** database. Can be used on IBM PC/XT/AT or compatible with 256k-memory, DOS 2.0 or higher, double-sided drive.
- **Subscription cost.** Each category costs $100.00. All six for $500.00. Annual updates $20.00 per category and $100.00 for all six.

Enclosed is check for $_____ (☐ for more than one category ☐ for all categories) covering the following:

☐ A Electronics
☐ B Physical Sciences
☐ C Mechanics
☐ D Materials
☐ E Fabrication Technology
☐ F 3-in-1 (Mathematics & Information Sciences, Life Sciences and Computer Programs)
☐ ★ ALL CATEGORIES

Name _____

Company _____

Address _____

City _____ State ____ Zip _____

Phone _____

NTBM Research Center
41 East 42nd St., NY, NY 10017-5391
212-490-3999

NTB:BASE from NASA Tech Briefs

4 breakthrough!

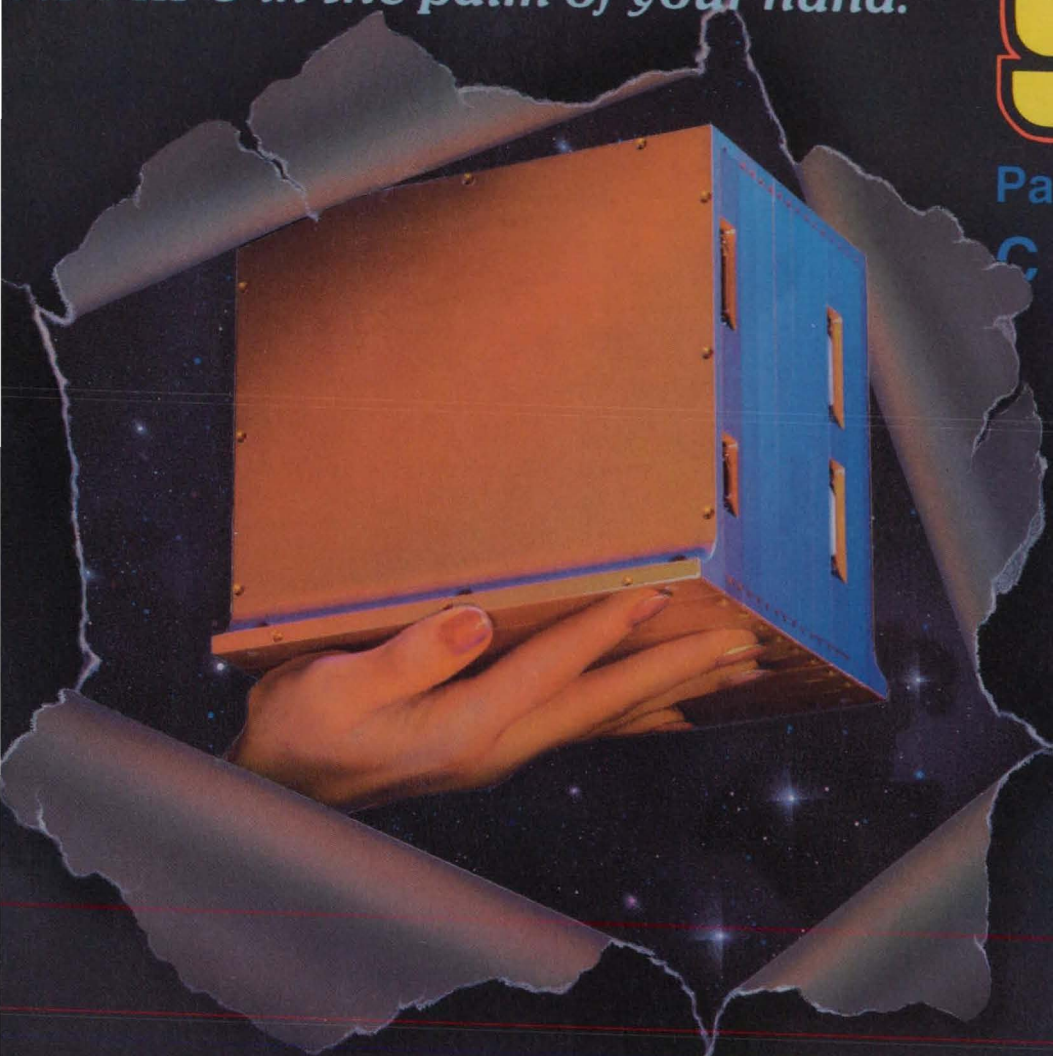
32 bit floating point
7.5 MIPS in the palm of your hand.

Honeywell

S5

Parallel Processing

COMPUTER



Typical Configurations

MODULES	MIPS	MEMORY KB	POWER WATTS	SIZE (IN^3)	WEIGHT (lb)
6	7.5	1152	30	180	6
10	17.5	1664	50	290	10
15	30	2304	75	420	15
20	37.5	3712	100	550	20

TECHNOLOGY TRANSFER BY SANDIA NATIONAL LABORATORIES UNDER CONTRACT TO DOE

Together, we can find the answers.

Honeywell

813/539-5820

Clearwater, Florida

Circle Reader Action No. 364

ated within the boundaries of the defined system volume.

Once the configuration and the material properties are defined, specific interaction mechanisms are used to determine the set of field equations for the equilibrium of forces. Solid/solid interactions are used to calculate contact stresses, contact sizes, and associated elastic forces. Solid/fluid interactions are used to determine raceway/rolling element tractions, flange/rolling element tractions, roller drags, and cage-related frictions. The completion of the detailed interaction mechanisms enables the generation of the equations of the equilibrium of quasi-dynamic forces. A Newton-Raphson iterative procedure is used to solve the equations. A Lundberg-Palmgren method is employed to compute the fatigue life of the bearing. Thermal effects on the system can be computed in either a steady or transient mode.

The input to CYBEAN consists of the bearing configuration, material properties, and imposed operating conditions. The output includes evaluated lubricant data, geometric and fit information, cage forces, speeds, maximum contact stresses, lubricant-film thicknesses, roller tilt and skew angles, and the temperature distribution for the complete nodal network.

The CYBEAN program is written in FORTRAN IV for batch execution and has been implemented on a UNIVAC 1100 computer operating under EXEC 8 with a segmented-memory requirement of approximately 91K of 36-bit words. CYBEAN has also been implemented on a CRAY series computer operating under COS. CYBEAN was developed in 1978. The UNIVAC version was last updated in 1981, and the CRAY version was released in 1986.

This program was written by H. Coe of **Lewis Research Center**. *For further information, Circle 96 on the TSP Request Card.*
LEW-14512

Calculating Flows in Multiple-Blade-Element Cascades

Blade shapes and spacings can be varied.

A computer code has been written to analyze flows on blade-to-blade surfaces of turbomachinery. The code can analyze rows that contain blades of several different shapes and/or spacings. This capability makes the code useful for calculating flows in centrifugal machinery with splitter blades or in mistuned blade rows, where the blade spacing varies.

The number of varying blade shapes that can be used in a blade-row design is not limited by the code. However, the amount of computer storage available does impose a practical limit on any problem. The code described here is dimensioned to handle from one to four bodies in cascade. After redimensioning, this same code can be used to calculate a flow problem with as many as 15 bodies.

The code solves approximate governing equations for blade-to-blade, steady-state flow problem in turbomachinery. The effects of compressibility, radius change, blade-row rotation, and variable streamsheet thickness are included. The working fluid is assumed to be inviscid, irrotational, and a perfect gas. The code can also handle flows of incompressible fluids. Overall, the code produces good results for subsonic flow, but the accuracy decreases for high subsonic and supersonic flows.

The multiple-body-panel code is written primarily in FORTRAN IV and uses double-precision arithmetic. Storage for the four-body version of the code is approximately 650,000 words when run in double precision. A typical running time for the code on the central processing unit (CPU) of the IBM 370/3033 computer at NASA Lewis Research Center is 25 s. A slightly different version of the code, which runs on the CRAY IS computer at NASA Lewis Research Center, requires less than 5 s of CPU time per run.

This program was written by Eric F. McFarland of **Lewis Research Center**. *For further information, Circle 19 on the TSP Request Card.*
LEW-14359

Mathematics and Information Sciences

Interactive Plotting Program

Plots can be edited before printing.

The Interactive Plotting Program (IAP) provides a fast and easy method of plotting data in a presentable format. Extensive plot editing can be done with the various IAP commands, which may be typed interactively from the terminal or read from batch command files. The ability to redirect output to a variety of devices enables the user to tailor plots with a graphics terminal before printing. IAP is designed to allow the addition or deletion of code for any type of terminal or plotting device.

Optional features are included to make the program as flexible as possible, but simple graphs can be made by using only two commands. Options include (1) a choice of 27 standard Hershey character sets; (2) labels, legends, and titles; (3) grids, scaling, and log axes; (4) pen color; (5) data sorting; (6) shrink factors; and (7) multiple overlays. All options in the program have default settings; i.e., labels, scales, character types, and plot symbols can be supplied automatically.

A user of IAP enters a series of commands to tailor the plotting of up to nine graphs on any graphics device attached to the computer. The plotting device is allocated only while being used, allowing other users to share the resources of the system. Data are read into the program from user-produced ASCII data files with a single X-Y point per record. IAP allows plottable sets of data of up to 2,048 points per set, with up to nine sets in one plot. Larger sets of data can be handled with the SAMPLE command to plot only every Nth data point. The HELP command delivers information on any IAP command. DCL commands can be executed from within IAP.

IAP is written in FORTRAN 77 and Assembler for batch or interactive execution and has been implemented on a DEC VAX computer under VMS. IAP currently has code for DEC VT125, VT240, HP 2648A, HP 7475, Tektronix 40XX, and Ramtek Colorgraphics terminals. Versatec 1200 and Grinnell devices are also supported but require the commercial Versatec or Grinnell graphics software packages. IAP was developed in 1986.

This program was written by Judith G. Moore of Wyle Laboratories for **Langley Research Center**. *For further information, Circle 95 on the TSP Request Card.*
LAR-13655

Tape-Certification Program

Magnetic tape is tested at various data densities.

A tape-certification program tests the usability of magnetic tape at different densities by writing test patterns and rereading them. The ability to certify tapes is important in computer systems that do large amounts of tape processing. A certification program is a cost-effective alternative to a tape-certification machine. TAPECERT is a VAX utility program for tape certification in use at the Jet Propulsion Laboratory Multi-Mission Image Processing Laboratory (MIPL), which processes data from such projects as Voyager and Galileo. MIPL maintains a library of some 80,000 tapes.

TAPECERT allows the user to select the tape density, the test pattern to use, and the number of allowed retries, and to decide whether to allow extended inter-record gaps to skip past bad spots on the tape. The program displays system error messages (parity errors, for instance) and record-count information with totals every 1,000 blocks. TAPECERT is designed so that command procedure can be set up

MOVE UP TO A NEW LINE

FROM HOUSTON INSTRUMENT

Prepare to be impressed. Meet the new line of high-performance plotters from Houston Instrument.™ HI's sleek new DMP-60 series is designed to impress even the most demanding CAD professional.

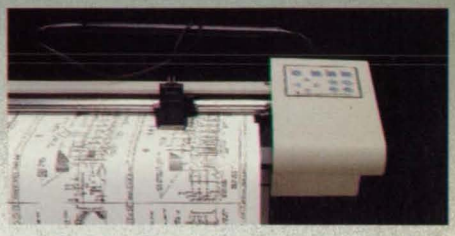
Discover unprecedented flexibility—blended with ultra-fine resolution, speed, and software compatibility. Benefit from HI's rigorous standards for quality, reliability, and service. All at prices starting from $4,695.*

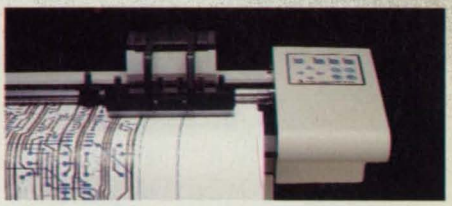
Watch the DMP-60 series double as a scanner with HI's unique SCAN-CAD™ option. Quickly produce multicolored drawings when you use the Multi-Pen adaptor. Plot several originals—without tying up your PC when you add HI's buffer expansion board.

Select media as small as 8½"×11" or as large as 36"×48". Load either DM/PL™ or HP-GL 758X-compatible software. Then watch as your plotter quickly produces a drawing polished to a precise resolution of 5 ten-thousandths of an inch. Smile when you see smoothly formed circles, curves, and lettering.

Explore HI's host of support programs including an overnight plotter-replacement service. And then relax, knowing that HI's new plotters rest on 27 years of engineering excellence.

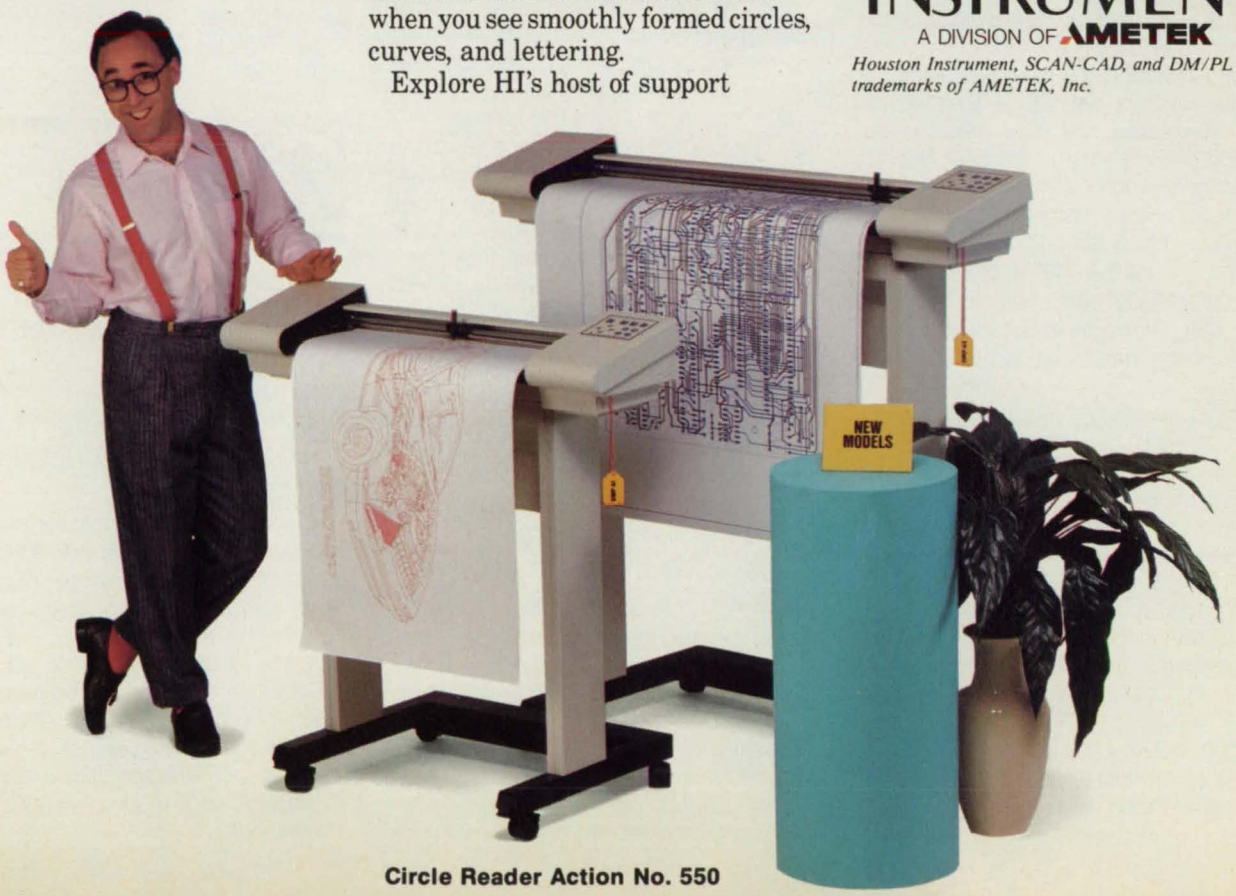
Move up. To a fine, new line. From Houston Instrument. Begin by calling 1-800-444-3425 or 512-835-0900 or writing Houston Instrument, 8500 Cameron Road, Austin, TX 78753. **U.S. suggested retail price.*





HOUSTON INSTRUMENT
A DIVISION OF AMETEK

Houston Instrument, SCAN-CAD, and DM/PL are trademarks of AMETEK, Inc.



Circle Reader Action No. 550

with defaults for different types of certification runs.

TAPECERT is written in FORTRAN 77 and utilizes standard VMS system services and run-time library routines. It has been implemented on DEC VAX-series computers operating under VMS levels 3.7 and 4.2. This program was developed in 1985.

This program was written by Scott E. Fullner of Caltech for **NASA's Jet Propulsion Laboratory**. *For further information, Circle 161 on the TSP Request Card.*
NPO-16876

Locating Spaceborne SAR Imagery

An arbitrary picture element can be located precisely.

The TLOCATE computer program was developed to determine the precise location of an arbitrary picture element (pixel) in a digital synthetic-aperture-radar (SAR) image. The approach requires no standard ground reference point and is independent of the attitude of the spacecraft. Traditional preprocessing of raw data into digital images may result in geometrically distorted pictures. TLOCATE will aid in unsupervised geometric rectification, location of pixels, and the combination of multiple image frames into mosaics. Locations predicted by TLOCATE using SEASAT and SIR-B images have been compared to high-precision topographical maps with an accuracy of approximately 200 m.

The location of a pixel in a digital image is determined by the intersection of the centroid plane of the radar beam and the surface of the planet. TLOCATE represents the intersection with (a) a model of the shape of the Earth, (b) the SAR Doppler equation that defines the plane of the radar centroid, and (c) the SAR range equation, which includes both signal-transmission properties and the rotation of the Earth.

TLOCATE can perform three major procedures: (1) determine latitude and longitude of the requested target pixel; (2) estimate such Doppler parameters as the centroid and the rate of change of frequency at the four corners of the image, the radius of the Earth, and the slant range; and (3) generate such postprocessing parameters as the swath velocity, the number of pixels to be deskewed, the center incidence angle, and the latitude and longitude of the four corners. These algorithms require the input of precise spacecraft ephemeris data (position and velocity) and operating characteristics of the SAR sensor.

TLOCATE is written in FORTRAN 77 for batch or real-time execution and has been implemented on a DEC VAX 11/785 computer operating under VMS 4.1 with a central-memory requirement of approximately 34K of 8-bit bytes. The program was developed in 1985.

This program was written by J. C. Curlander and S. Pang of Caltech for **NASA's Jet Propulsion Laboratory**. *For further information, Circle 92 on the TSP Request Card.*
NPO-16861

Generating Cross-References Among Computer Routines

This program helps a user search a library of computer programs.

The Cray Library Load Cross-Reference (CROSSREF) computer program is a tool that assists users in obtaining information about subroutines in a computer-program library. Maintaining a library of computer routines requires an understanding of the relationships between the modules of code. CROSSREF uses tables generated by the Cray operating system BUILD command to cross-reference the routines by tabulating routine names, EXTERNALS, COMMONS, and ENTRY POINTS.

CROSSREF creates alphabetized listings and tables that yield information about each member of the library. Summary tables, a table of contents, and library statistics are also produced. The user has the option to include or exclude Cray system EXTERNALS in the cross-reference lists. The output can be directed to either 132-character printer paper 11 or 8½ in. (27.9 or 21.6 cm) high or a cathode-ray-tube display. CROSSREF can accommodate libraries of up to 4,096 modules.

The CROSSREF program is written in FORTRAN IV for batch execution and has been implemented on a Cray X-MP 22-series computer (dual CPU) under COS. CROSSREF was developed in 1984.

This program was written by Clayton Guest of Informatics General Corp. for **Ames Research Center**. *For further information, Circle 50 on the TSP Request Card.*
ARC-11591

Designing Digital Filters

A computer program calculates a performance index from magnitude and phase errors.

The Digital Filter Design program presents a method to compare desired and designed digital filters by minimizing the sum-square error of the differences in magnitude and phase angles. Most filter-design techniques emphasize magnitude characteristics. Such techniques are adequate for a control system in which the phase angle of a filter imposes minor effects on the stability of the system. However, in a closed-loop feedback control system, a designed filter that introduces an excessive phase angle may distort the signal or push the system to instability. This Digital Filter Design program has been used to reshape the Space Shuttle pitch body-bending filter to provide more attenuation to flexible-vehicle-resonance modes without sacrificing the rigid-vehicle performance.

This program uses the Fletcher-Powell unconstrained-minimization method to calculate a performance index from the magnitude and phase errors. This index can then be used to measure the goodness of various filter designs. The input includes the number of second-order cascade sections in the designed filter, available frequency data points with desired phases and magnitudes, weighting factors for phases and magnitudes, initial estimates of filter coefficients and gain, and system sampling time. Subroutines are provided for printing and simple plotting of the response of the designed filter as a function of frequency.

This program is written in FORTRAN IV for batch execution and has been implemented on a CDC CYBER 830 computer operating under NOS with a central-memory requirement of approximately 76K (octal) of 60-bit words. The program was developed in 1983.

This program was written by Chiang Lin of McDonnell Douglas Corp. for **Johnson Space Center**. *For further information, Circle 55 on the TSP Request Card.*
MSC-20982



Life Sciences

BASIC Programming in Water and Wastewater Analysis

A collection of programs speeds routine calculations.

This collection of computer programs has been assembled for use in water-analysis laboratories. A number of calculations are necessary for many types of routine chemical analysis, especially in a laboratory that has few or no automated analyzers. In this case, a personal or small business computer can be a valuable tool. The necessary formulas for calculations can be found in the appropriate manual for the specified analysis (USEPA, 1983) (APHA, 1981).

Quality-control calculations are necessary in a laboratory to assure an acceptable degree of accuracy and precision in a given analysis. The first program calculates quality-control parameters used in routine water analysis. These are percent recovery (of spikes) and the industrial statistic (of replicates) (USEPA, 1979).

Curve fitting must be done to calculate unknowns from a number of standards of different concentrations. The second program calculates the line (or curve) of best fit for the standard concentrations and absorbances entered. It provides the slope (M) and the Y-intercept (B), the equation of the line, and the correlation coefficient. A plot of the points is provided to aid the user in the choice among a straight line, log curve, or power curve.

Once the choice is made, the M, B, and correlation coefficient are recalculated using the necessary log conversions, when the second least-squares routine is run. The transformed points can be plotted to show whether they produce a fairly linear relationship. Once the satisfactory relationship is established, the unknowns can be calculated by entering absorbance values. This program also contains a subroutine for the calculation of the quality-control parameters so that the control checks can be made without leaving the program.

The third program calculates the specific conductance from the conductivity measurement and the temperature at which the measurement is taken. This then corrects the conductivity to 25 °C, giving the specific conductance.

The fourth program calculates any one of four types of residue measured in water. The appropriate residue calculation is specified, and weights and volumes are entered to yield the results.

The fifth, sixth, and seventh programs calculate the results of titrations commonly performed on water samples. Normalities and volumes are entered to yield the results.

The eighth program converts measurements, made with a dissolved-oxygen meter that does not compensate for salinity, to the actual dissolved-oxygen concentration using oxygen-saturation values for fresh and salt water. The measured value, salinity, and temperature are entered to yield the actual oxygen concentration.

The ninth and tenth programs perform calculations of two other common titrimetric analyses. Again, normality and volumes are entered to yield the results.

The eleventh program calculates the oil and grease residue from a water sample. To yield the results, the samples are extracted, and the weights are entered.

The last two programs use spectrophotometric measurements of absorbance at different wavelengths and residue measurements. These are used to calculate the concentrations of chlorophyll *a* and phaeophytin *a* in phytoplankton and periphyton and the biomass and autotrophic index of periphyton. Absorbances and weights are entered to yield the results.

The programs included in this collection were written for a Hewlett-Packard 2647F in H-P BASIC. All but the plotting routines can be easily translated for other computers that use the appropriate BASIC language. In the case of the plotting routines, the graphics for another manufacturer's computer will be addressed differently.

This program was written by Thomas Dreschel of Bionetics Corp. for **Kennedy Space Center**. *For further information, Circle 18 on the TSP Request Card.*
KSC-11298

Is your subscription about to expire?

Check the expire date. If it is less than 6 months now is the time to fill out a new qualification form so that there is enough time before your subscription expires.

From Frogs To FMEA

National Technical Systems knows almost as much about a swamp as frogs and other amphibians do. It's part of the expertise we need to generate a Failure Modes & Effects Analysis(FMEA) on an armored amphibious troop carrier for the Marine Corps . . . or conduct an environmental profile on a SAM computer.

Test chambers simulate nearly every environment conceivable, while dynamic analysis features some of the world's most sophisticated equipment: a 40,000 force-lb. shaker, 1000 g's centrifuge, 20,000 g's pyroshock fixture, 5000 cu. ft. reverberent chamber capable of 165 dB. Also, testing of hazardous products, high-pressure/high-temperature gases and liquids, cryogenics, EMI/EMC, PCB/PWBs.

NTS — testing and analysis to better help you simulate the environment.

We Test Out.



NTS

National Technical Systems

Call National Technical Systems
In the west (714) 879-6110,
In the east (617) 263-2933 or write NTS,
1536 East Valencia Dr., Fullerton, CA 92631,
or 533 Main St., Acton, MA 01720

Circle Reader Action No. 358

Mechanics

Hardware, Techniques, and Processes

80 Holding X-Ray Film Inside Ducts
80 Heat Exchanger for Rotating Modular Structures
81 Laminar-Boundary-Layer Crossflow Sensor
83 Swivel Joint for Liquid Nitrogen
83 Simplified Analysis of Shock Waves
84 Acoustical Measurement of Mine-Shaft Length

Books and Reports

85 Analysis of Flow Across Cylinders
86 Calibrating Nonremovable Pressure Transducers

Holding X-Ray Film Inside Ducts

A simple, easy-to-use device speeds inspection.

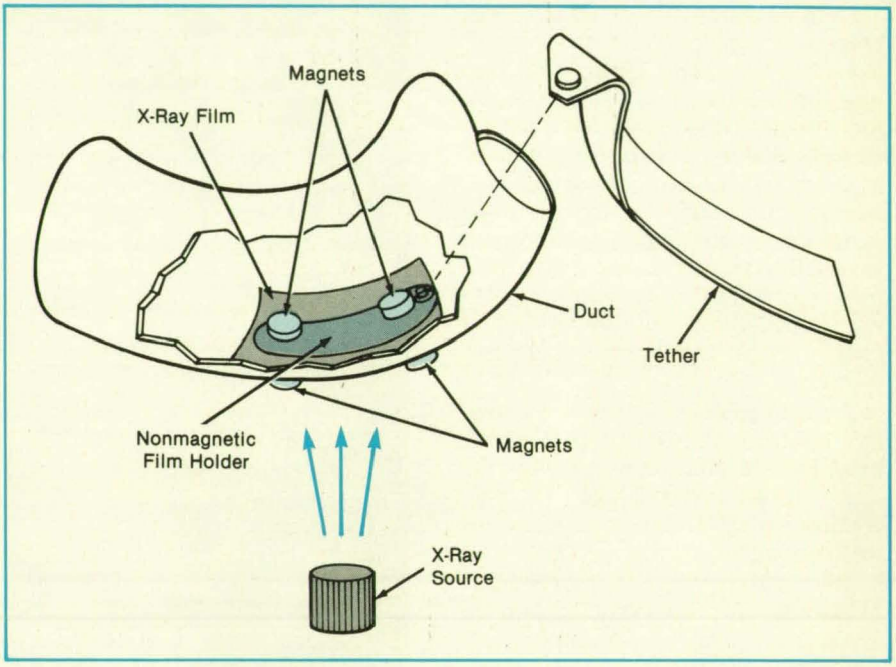
Marshall Space Flight Center, Alabama

Radiographic inspection of welds in the walls of nonmagnetic ducts is made easy by a new film holder. The holder enables the quick and accurate positioning of x-ray film inside a duct and presses the film securely against the inner wall for minimum image distortion and maximum sensitivity to irradiation by an x-ray source outside the duct.

Two pairs of opposed magnets are used to position the film (see figure). The magnets are strong, each having a holding force of 8 lb (36 N). Each is a disk of rare-earth/cobalt with a diameter of 0.75 in. (19 mm) and a height of 0.285 in. (7.2 mm). A pair of disks is bonded to a flexible, nonmagnetic film holder.

For an x-ray inspection, film is taped to the holder and placed inside the duct. The second pair of magnets is placed on the outside wall and oriented so that their poles attract the magnets on the holder, pressing the film tightly against the inside wall so that it conforms to the curvature of the duct. The exterior magnets indicate the position of the interior magnets and, therefore, of the holder and film. The holder can be repositioned easily by pulling its tether; the outside magnets will follow the inside ones.

The use of the holder avoids the need for mirrors and borescopes, saves time, and eliminates guesswork in the positioning of the film. It reduces inspection time by at least 90 percent.



X-Ray Film Inside a Duct is held by interior and exterior magnets. The tether is used to move the holder and to retrieve it from inside the duct.

This work was done by Ronald V. Bulthuis and Darryl Pierce of Rockwell International Corp. for **Marshall Space Flight Center**. *No further documentation is available.*

Inquiries concerning rights for the commercial use of this invention should be addressed to the Patent Counsel, Marshall Space Flight Center [see page 16]. Refer to MFS-29218.

Heat Exchanger for Rotating Modular Structures

Heat is transferred efficiently across plates without interstitial fillers.

Marshall Space Flight Center, Alabama

A heat exchanger transfers heat from one structure to another while accommodating rotary motion of the structures. Developed for modular space stations, the heat exchanger can be adapted to the transfer of fluids and heat across the joints of machine tools and robot arms and to the flow of coolant through portable electronic equipment.

In the heat exchanger (see Figure 1), the hot fluid from one structure flows through the middle one of the three heat-exchanger panels. The cold fluid from the second structure flows through the two outer panels. Fins inside the panels promote the transfer of heat between the circulating fluid and the panel surfaces. Thus, heat flows from the center panel to the outer panels and is carried off by the cold fluid.

Ordinarily, contacting surfaces must be very flat for efficient heat transfer between panels. Even when they are carefully manufactured for flatness, mechanical fasteners warp the surfaces when the panels are assembled, and the contact area may then be considerably smaller that of the surface areas. Often, interstitial materials such as

grease or foil have to be used to increase thermal conductance.

The new heat exchanger avoids these problems because the inner surfaces of the outer panels are flexible and act as diaphragms. When the fluid in an outer panel is pressurized even slightly, the pressure forces its working surface to conform to the mating surface of the middle panel. Any additional pressure in the outer panels merely increases the contact pressure, driving the contact thermal resistance down and increasing the rate of heat transfer across the interface. The heat-transfer rate can therefore be adjusted by changing the pressure of the fluid in the outer panels.

The cold fluid can be a two-phase medium that condenses in the outer panels. An increasing heat load causes the pressure in the outer panels to rise and thereby increase the contact conductance and the heat-transfer rate.

A rotating joint carries fluid to and from either the outer panels or the middle panel. The joint is an in-line axial-flow unit that can rotate freely (see Figure 2). The internal flow passages are concentric to the center of rotation, so that the same housing can accommodate both the supply and return flows.

Because the heat-exchanger panels can be disconnected from each other without disconnecting any fluid lines, the two connecting structures can be thermally coupled or decoupled without the loss of fluid. Before disconnection, it is necessary only to depressurize the outer panels to prevent the diaphragms from bursting. Once the panels are reconnected, they can be repressurized when heat transfer is needed.

This work was done by William E. Clark of Applied Technology Association for **Marshall Space Flight Center**. *For further information, Circle 137 on the TSP Request Card.*

In accordance with Public Law 96-517, the contractor has elected to retain title to this invention. Inquiries concerning rights for its commercial use should be addressed to

William E. Clark
Applied Technology Association
401 Hyder St., N.E.
Palm Bay, FL 32907

Refer to MFS-26037, volume and number of this NASA Tech Briefs *issue, and the page number.*

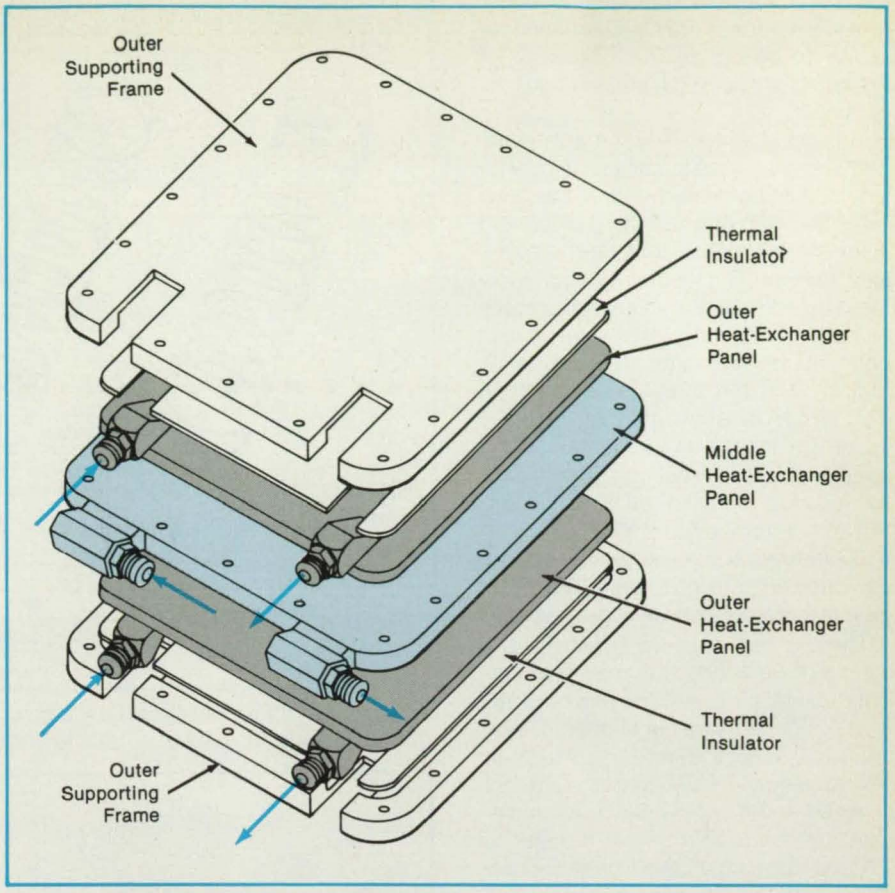


Figure 1. **Flat-Panel Heat Exchanger** passes heat from the fluid in its middle panel to the fluid in its outer panels. The diaphragmlike outer panels swell to conform to the surfaces of the middle panel, ensuring thermal contact.

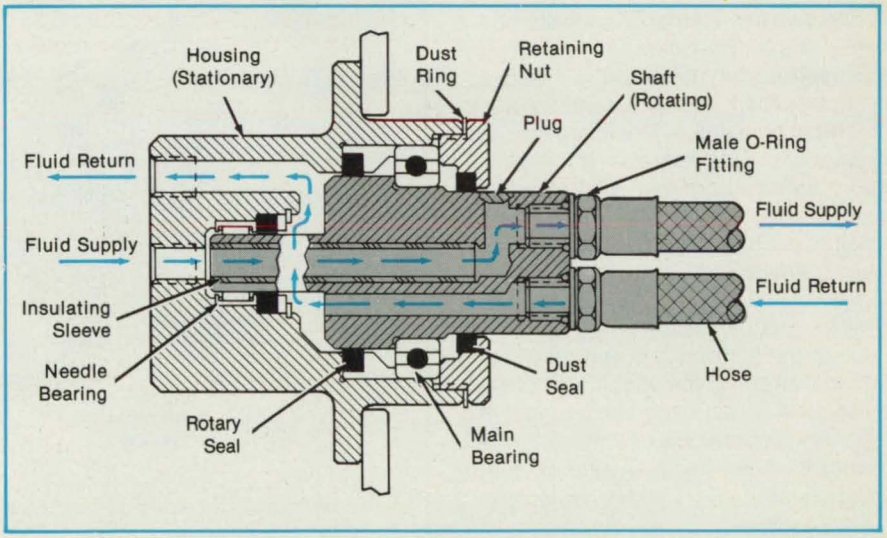


Figure 2. The **Rotary Fluid Coupling** provides a connection for both supply fluid and return fluid. The flexible hoses that carry fluid to and from the coupling accommodate the tilt of one structure with respect to the other.

Laminar-Boundary-Layer Crossflow Sensor

Crossflow vorticity is detected with nonintrusive electronic sensor elements.

Langley Research Center, Hampton, Virginia

The accurate determination of both the location and the cause of the boundary-layer transition from a laminar to a turbulent flow is important in basic research, for the validation of theory, and in developmental testing for validation

of design. The laminar-boundary-layer crossflow sensor provides a means for remotely detecting the presence of crossflow vorticity in a laminar boundary layer.

A boundary-layer flow on a three-dimensional surface (such as a wing with a sweep or nonaxisymmetric fuselage) is formed with one velocity component in the direction of and one normal to the external flow. The resultant velocity profile is inflected in a fashion that creates vorticity in the boundary layer. If this boundary layer is laminar, the vortexes that form in the streamwise direction can grow in strength, eventually causing transition to turbulence. Large variations in local heat transfer and skin friction exist in the lateral direction normal to the vortex cores. Crossflow vorticity, therefore, may be detected using a method for sensing these variations of heat transfer or skin friction.

The present technique provides a means of detecting the crossflow vorticity, using thin, surface-mounted arrays of hot-film sensing elements. One crossflow sensor (Figure 1) consists of several electronically heated elements exposed to the airflow. Since each element responds to the heat transfer in the boundary layer, the signal characteristics of an array of elements will display the spanwise variations in heat transfer resulting from the crossflow vorticity.

The array of elements consists of a series of thin-film nickel sensors with a polymer backing dissected to create a predetermined sensor geometry and electrical resistance. These are placed in an appropriate matrix on a thin polymer sheet and bonded with an adhesive. The resulting sensor thickness is small enough not to cause a boundary-layer transition to turbulence for most flight applications of interest. Silver-plated copper wires are soldered to the edge of the sensing grid and routed to terminal strips for the attachment of external lead wires. Each film element in the array is operated as a constant-temperature anemometer. At the time of measurement, the films are heated and the data taken.

The sensors may be installed in a staggered fashion or fabricated into one continuous multielement strip of sensors, providing for the streamwise measurement of crossflow vorticity (Figure 2). The device senses the crossflow continuously, allowing variable free-stream conditions during a single flight or wind-tunnel run. The hot-film anemometer signals respond in distinct ways to different boundary-layer phenomena. Since each phenomenon has a distinctive signal characteristic, the crossflow sensor can detect and measure the surface temperature, skin friction, transition, and relative vorticity amplitude, as well as resolve the characteristics of vorticity wavelength (vortex core spacing) in the crossflow pattern.

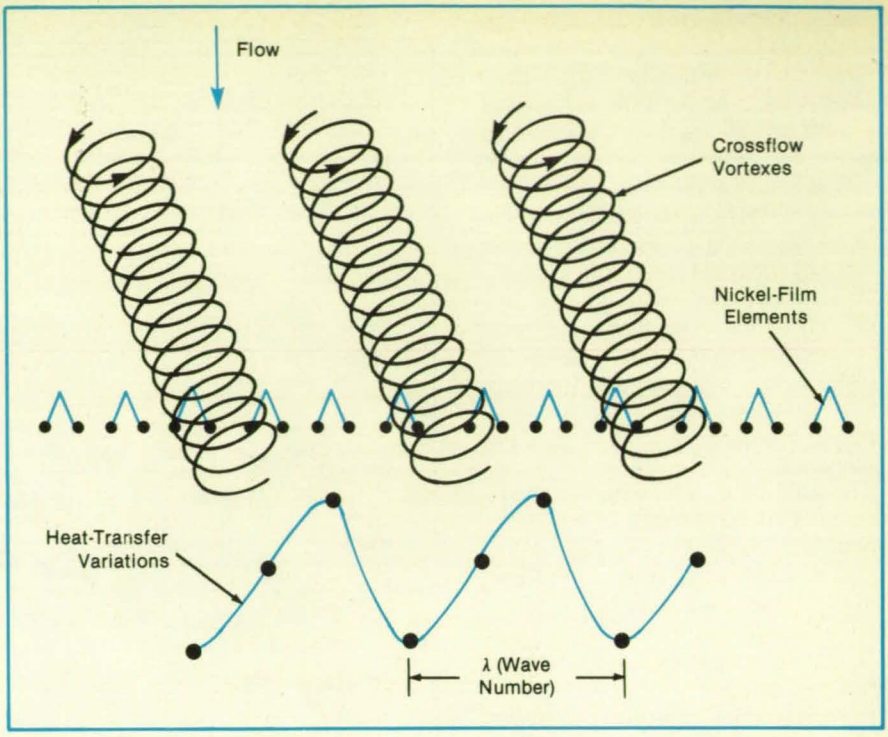


Figure 1. The individual **Crossflow Sensor** elements respond to the variation in heat transfer caused by laminar-crossflow vortexes.

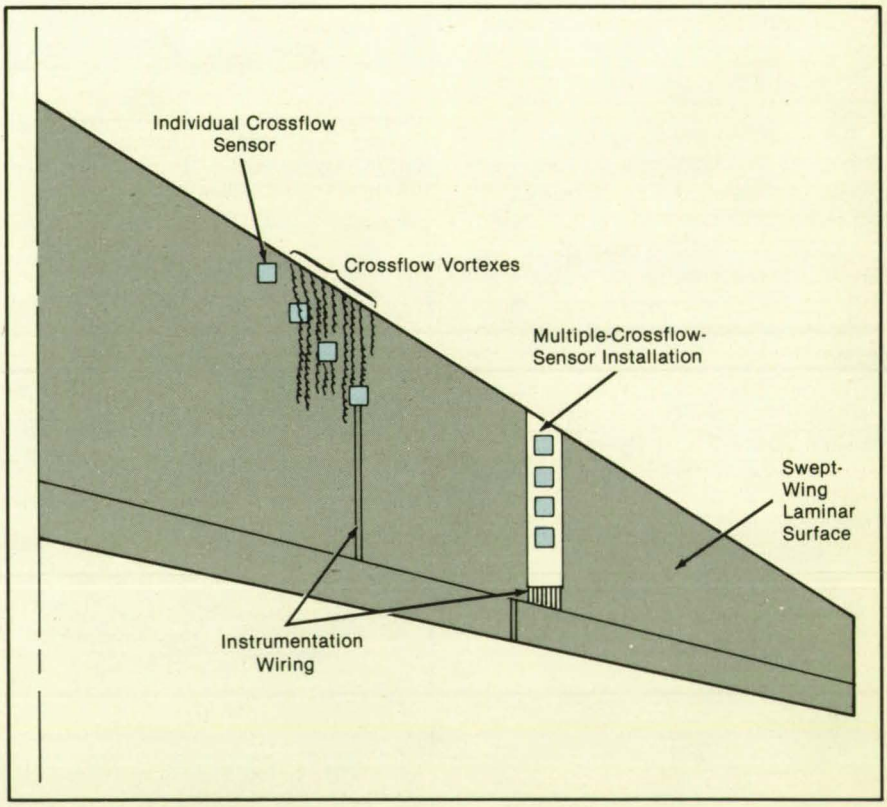


Figure 2. **Crossflow Sensors** can be installed in a variety of patterns, including staggered or combined into a continuous longitudinal strip.

This work was done by Bruce J. Holmes, Harlan K. Holmes, Thomas C. Moore, and Gregory S. Manuel of **Langley Research Center** *and Debra L. Carraway of Old Dominion University. For further information, Circle 165 on the TSP Request Card.*

This invention is owned by NASA, and a patent application has been filed. Inquiries concerning nonexclusive or exclusive license for its commercial development should be addressed to the Patent Counsel, Langley Research Center [see page 16]. Refer to LAR-13436.

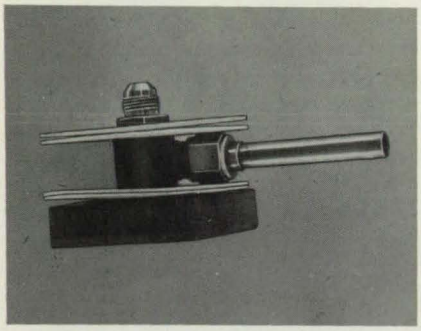
Swivel Joint for Liquid Nitrogen

The joint is compatible with hard foam insulation.

Lyndon B. Johnson Space Center, Houston, Texas

A swivel joint allows a liquid-nitrogen pipe to rotate through an angle of 100° with respect to a mating pipe. The joint functions without cracking the hard foam insulation on the lines.

The joint carries liquid nitrogen for cooling from the outside to panels on the inside of a hinged vacuum-chamber door (see Figure 1). The joint rotates when the door is opened or closed, without stressing the brittle insulating foam on the pipes and without significant leakage of nitrogen from the 40-lb/in^2 (280-kPa) pressurized line.



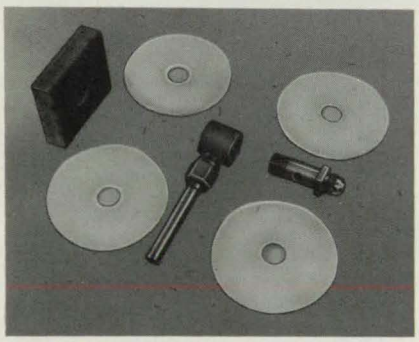


Figure 2. The **Pipe Joint Rotates** on disks so that mechanical stress is not transmitted to the thick insulation on the pipes. The inner disks ride on the fixed outer disks. The disks also help to seal the pressurized liquid nitrogen flowing through the joint.

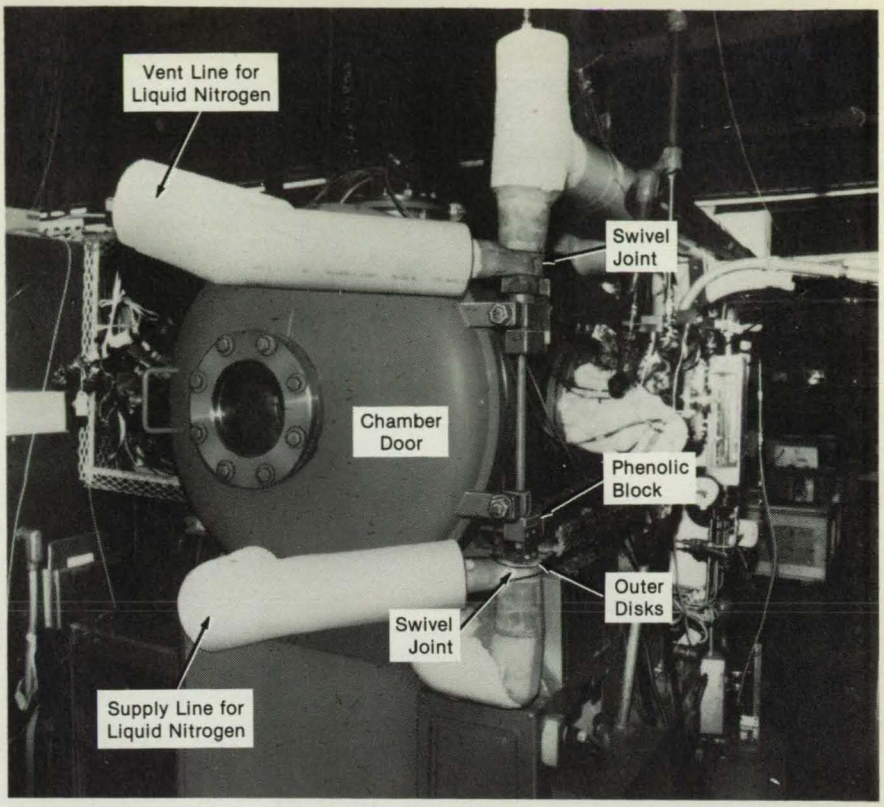


Figure 1. The **Pipe Joint Is Placed on the Hinge Line** of the door, enabling liquid nitrogen to flow between rigid, insulated pipes on the door and on the frame.

The swivel joint and pipes replace a flexible hose, which was unsatisfactory for several reasons. The soft foam insulation cracked after repeated opening of the door. Heat penetrating the cracks caused a significant loss of the cryogenic liquid. Frost accumulated in the cracks, eventually melted, and formed puddles on the floor. While the chamber was being filled or purged, the hose vibrated excessively.

The joint includes a stainless-steel bolt-and-connector combination of a standard type used in hydraulic systems (see Figure 2). The movable connector turns on the fixed bolt. Two pairs of large-diameter polytetrafluoroethylene disks — one pair at the top of the connector and one at the bottom — allow smooth, low-friction rotation to isolate the insulation from stress.

This work was done by James F. Milner of Rockwell International Corp. for **Johnson Space Center**. *For further information, Circle 130 on the TSP Request Card.*
MSC-21160

Simplified Analysis of Shock Waves

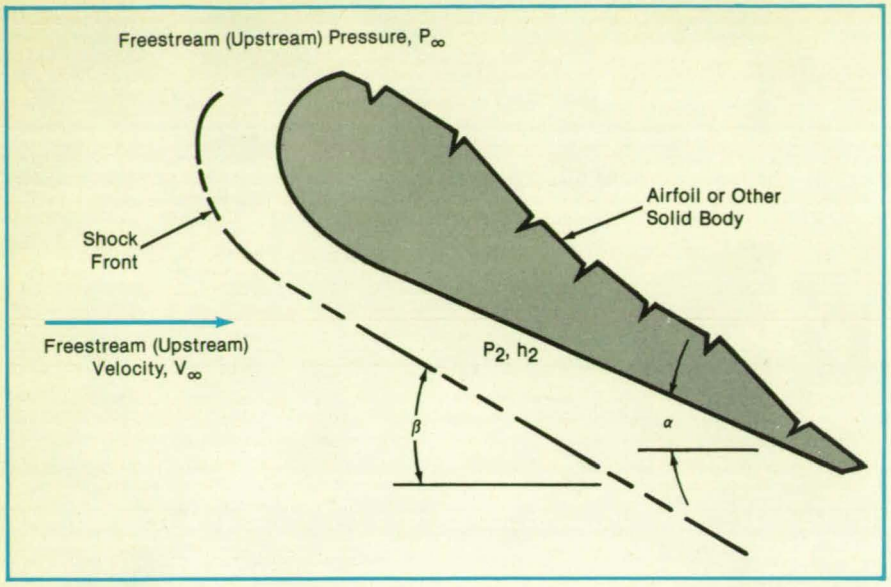
Semiempirical expressions and conventional analyses agree within about 3 percent.

Lyndon B. Johnson Space Center, Houston, Texas

A set of semiempirical formulas enables the direct calculation of supersonic and hypersonic shock-wave parameters without the use of iterative procedures. Formulas are provided for calculating shock deflection angle (see figure) and the downstream static pressure and enthalpy over the mach number range of 2 to 25. A relationship describing the thermodynamic behavior of partially dissociated air has also been developed.

Conventionally, such shock-wave parameters are determined by using iterative procedures to find a simultaneous solution of the continuity, momentum, and energy equations, the thermodynamic equation of state, and a shock-wave angle equation. The new formulas are derived from semiempirical data based on observations and experience and from comparisons with analytical data using conventional analysis techniques. Over a wide variety of flight conditions, results from the new equations agree with those from conventional analyses within about 3 percent. The new results also compare favorably with actual pressure data from a Space Shuttle orbiter flight.

The first of the new formulas gives the shock deflection angle as a function of the freestream mach number and the tangent of the angle of attack. The second formula gives the downstream static pressure as a function of the aforementioned quantities and of the freestream



The **Shock-Wave Parameters,** including the downstream pressure (P_2), downstream enthalpy (h_2), and the shock deflection angle (β), are approximated closely by semiempirical equations in terms of the upstream quantities and the angle of attack (α).

static pressure. The third formula gives the downstream static enthalpy as a function of the previously calculated shock deflection angle and the freestream airspeed. Finally, a set of four equations gives the relationships among the downstream temperature, kinetic specific heat, and dissociation level, as functions of the previously calculated downstream static enthalpy and pressure. The equations will be useful to the aircraft industry and in wind-tunnel and plasma-arc testing.

This work was done by Wilmer E. Neuenschwander of Rockwell International Corp. for **Johnson Space Center**. *For further information, Circle 150 on the TSP Request Card.*
MSC-20738

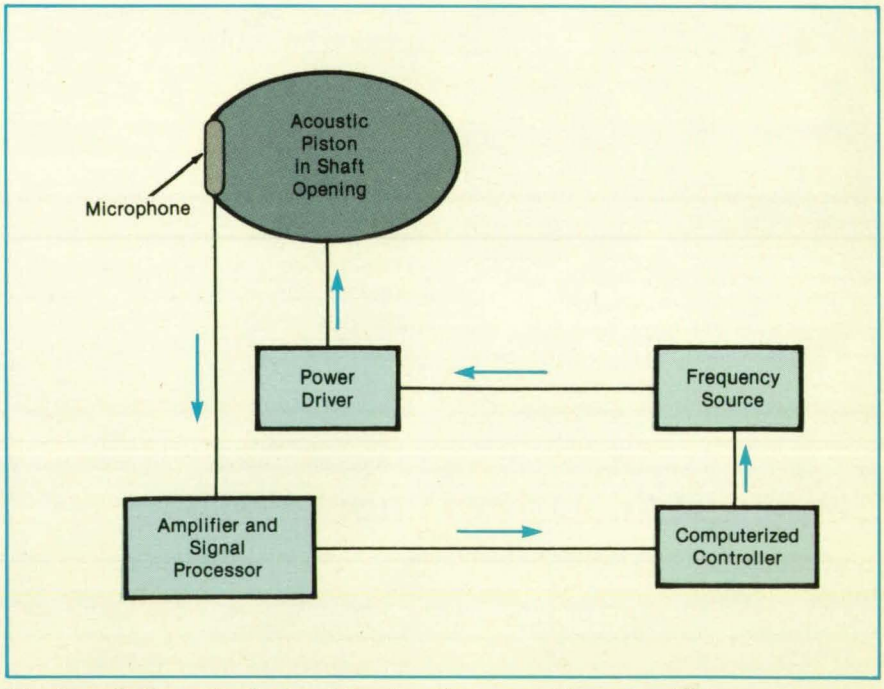
Acoustical Measurement of Mine-Shaft Length

The length is calculated from the measured resonant frequency.

Langley Research Center, Hampton, Virginia

An acoustical system (see figure) has been proposed to measure the depth of a "blind" shaft, such as a mined-out coal seam produced by boring machines, so that the amount of material removed can be determined. Direct optical measurements such as pulsed lasers do not work for shafts that are not straight. An acoustic wave, however, will be guided by the shaft and will provide an estimate of the shaft length, from which the volume can be estimated. This system can also be used for the measurement of any large cylindrical acoustic waveguide, such as a tunnel. The system is based on the generation of standing waves in the shaft, which acts as a waveguide for low-frequency sound waves. The frequency of resonance depends on the velocity of sound in the shaft, the harmonic number selected for measurement, and the length of the shaft.

An acoustic generator, such as a piston mounted on a shaker source, is directed at the accessible end of the mine shaft and set in motion at a specific frequency. A microphone at the source detects the sound from the shaft after the source has stopped. The frequency of the source is electronically adjusted to bring the device to the center of the mechanical resonance. This can be accomplished through a computer-controlled frequency source combined with an acoustic-amplitude detector or with a frequency-modulated source detecting the 180-degree phase shift that occurs at resonance. The frequency is recorded, and the computer-controlled device advances to the next harmonic, performs a measurement, and calculates the frequency difference between resonances, from which the shaft length is determined.



The **Acoustic-Generator System** determines the resonant-frequency difference to measure the shaft length.

The basic simplified equation for an open pipe is $F_m = mV/2L$ and for a closed pipe is $F_m = mV/4L$, where m denotes the harmonic number, F_m the resonant frequency, V the speed of sound, and L the length. If the frequency of the fundamental, F_1, is measured, then $L = V/4F_1$ for the closed shaft. If the difference in frequency between harmonics is measured, then $L = V/4(F_m - F_{m-1})$. Thus, the measured frequency difference determines the same information as does the fundamental resonance. With this system, either the fundamental or the frequency difference can be used to measure the length of the mine

shaft.

This work was done by Joseph S. Heyman of **Langley Research Center**. *No further documentation is available.*

This invention is owned by NASA, and a patent application has been filed. Inquiries concerning nonexclusive or exclusive license for its commercial development should be addressed to the Patent Counsel, Langley Research Center [see page 16]. Refer to LAR-13519.

Books and Reports

These reports, studies, handbooks are available from NASA as Technical Support Packages (TSP's) when a Request Card number is cited; otherwise they are available from the National Technical Information Service.

Analysis of Flow Across Cylinders

Despite its importance in engineering, the flow/cylinder interaction is understood poorly.

A report reviews various experimental, theoretical, and numerical methods of analysis of the interactions between a fluid and one or more cylinders across which it flows. This is a topic of extreme importance in engineering: tubes subject to crossflow are found in heat exchangers, chimneys, aircraft, offshore platforms, and marine towing cables, for example. The flows cause these structures to vibrate, and the vibrations alter the flow fields, so that the flows and the vibrations are strongly coupled. An understanding of flow/cylinder interactions is necessary for the prediction of vibration-induced failures and for design to avoid such failures.

The review begins with a discussion of the mechanisms that induce vibrations in nests of cylinders. The best understood mechanisms are vortexes, fluctuations of pressure caused by turbulence, and fluidelastic or aeroelastic instabilities, which are fully-coupled cooperative motions of the fluid and all the tubes in a structure. Other less-well-understood mechanisms include aeroacoustic noise, oscillating mean free-stream velocity, and jet switching. In connection with these mechanisms, there is a discussion of equations derived through physical arguments or mathematical modeling, with empirically determined coefficients; recent developments in the semianalytical/seminumerical modeling of vibrations due to multiple mechanisms; and accumulated experimental data that serve as guides for the design of banks of tubes.

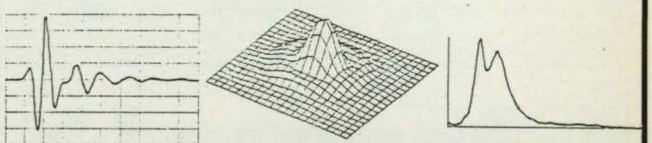
A major portion of the review is devoted to methods for the numerical analysis of flow/cylinder interactions. Numerical analysis is essential because the nonlinearities inherent in such interactions preclude closed-form solutions of the equations of motion. A typical approach would involve the numerical solution of the Navier-Stokes equations with an appropriate model for turbulence. This solution would include the pressure distribution and skin friction on the surface of the structure, from which one could solve iteratively the equations for vibration. The vibration-inducing mechanisms could be obtained as part of the numerical solution.

The discussion of numerical analysis

Instruments for the Measurement of Ultrasound

The AIMS-01 Acoustic Intensity Measurement System is a complete, stand alone, instrument with these normally very difficult to find features:

- XYZ positioner with 3200 step/in resolution
- Waveform digitizer with 50 MHz analog bandwidth
- Large, rugged tank, frame and cart assembly
- PC-AT based controller with EGA color graphics
- Easy to use, menu operated software that allows 3-D Beam profiles, intensity calculations, data archiving, hydrophone calibration, FFT spectral analysis and ...it is not expensive! **$16,500**



Digitized Pulse | 3-D Intensity | Spectrum

Broadband (40MHz) PVDF Hydrophones, both needle and membrane type with .5 and .25 mm apertures for high spatial resolution beam plots

Calibrated quartz ultrasound power standards

A full range of sound field absolute intensity measureing services with direct NBS tracebility

NTR Systems Inc. (206) 633-5684
1902 N. 34th St. Seattle, WA 98103

Circle Reader Action No. 539

LABORATORY PRECISION YOU CAN TAKE WITH YOU.



ESI's highly stable and transportable Resistance Standards allow routine calibration in the laboratory or in the field.

The SR1 individual resistance standards offer 0.005% long-term accuracy for most values from 1Ω to 10MΩ. Dekabox® DB877 Coaxial Dial and DB62 In-line Decade Resistors provide additional linearity checking capability with virtually continuous resistance between 0.01Ω and 12MΩ at 0.02% accuracy.

When you want to be sure your instruments are performing up to specifications, call ESI, the leading manufacturer of resistance standards traceable to the National Bureau of Standards.

Putting Precision To The Test.

esi®

Electro Scientific Industries, Inc.
13900 NW Science Park Drive • Portland, OR 97229

1-800-547-1863 (In Oregon call 503-641-4141)

Circle Reader Action No. 530

covers the following topics:

- Interactions between solid objects and laminar flows;
- Interactions between solid objects and turbulent flows;
- Mathematical models of turbulence;
- Vibrations in structures with small, large, or permanent deformations; and
- Flow through a nest of cylinders.

The author concludes that despite its importance in engineering and despite recent progress in numerical modeling, the understanding of the flow/cylinder interaction is still quite limited, and designs of banks of tubes still depend mostly on experiments or on equations with experimentally determined coefficients. A yet-to-be-developed numerical method powerful enough for the simulation of general flow/cylinder interactions will probably involve improved models for turbulence, finite-element and finite-difference computational techniques, nonlinear structural-analysis techniques, and existing analytical methods applicable to laminar and turbulent flow/solid interactions.

This work was done by Sang-Wook Kim of **Marshall Space Flight Center**. *Further information may be found in NASA CR-178996 [N87-18781/NSP], "A Critical Evaluation of Various Methods for the Analysis of Flow-Solid Interaction in a Nest of Thin Cylinders Subjected to Cross Flows."*

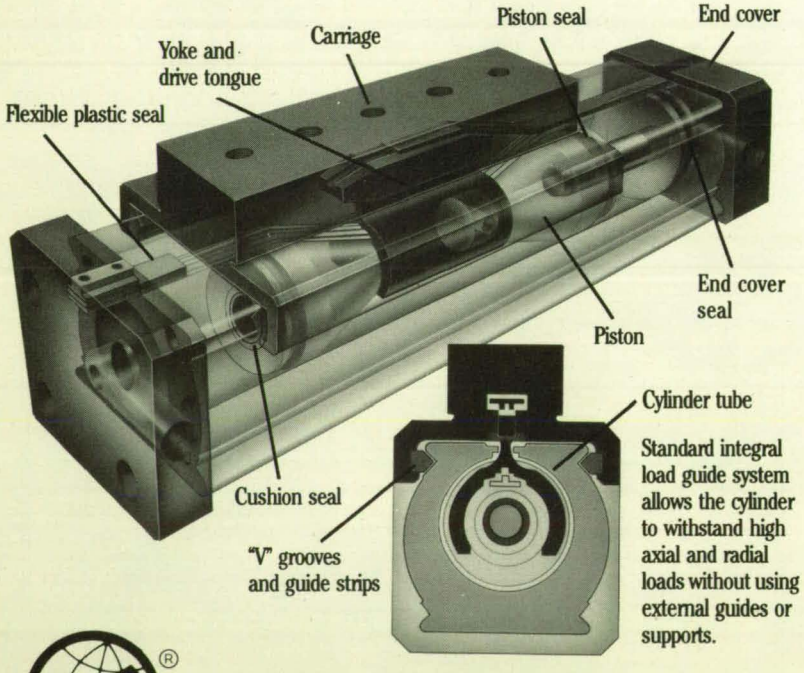
Copies may be purchased [prepayment required] from the National Technical Information Service, Springfield, Virginia 22161, Telephone No. (703) 487-4650. Rush orders may be placed for an extra fee by calling (800) 336-4700. MFS-27180

Norgren Lintra® Rodless Cylinders.

Lintra rodless pneumatic cylinders move materials or apparatus within their own length. That's why they're so compact. In fact, they require up to 50% less space than conventional cylinders. And their price is as compact as their size.

Thrusts: 65 to 425 pounds at 90 psig; five bore sizes: 25mm to 63mm; standard stroke lengths to 26 feet. For information on money-saving, space-saving Lintra rodless cylinders, contact Norgren.

Fully loaded at a compact price.



NORGREN®
THE WORLDWIDE GOLD STANDARD IN PNEUMATIC PRODUCTS.
5400 South Delaware, Littleton, CO 80120.
(303) 794-2611. Fax: (303) 795-9487. Telex: 45541.
For the name of the Norgren distributor nearest you, call toll-free 1-800-882-2626.

Calibrating Nonremovable Pressure Transducers

Units are calibrated en masse in a large pressure chamber.

A report describes a supplementary calibration procedure for pressure transducers. The method was developed for transducers that cannot be removed without damage — in particular, for transducers hard-mounted in a helicopter rotor blade for aerodynamic and acoustic measurements. The entire blade and its 188 pressure transducers are enclosed in a chamber in which their responses to known pressures and temperatures are measured.

The standard calibration procedure for pressure transducers is to place them individually in a small vacuum chamber and measure their responses. The new calibration supplements this initial calibration for units that cannot be recalibrated individually. In fact, it identified 15 units in the helicopter blade that had changed beyond acceptable limits.

The calibration was carried out in an environmental chamber 23 ft (7 m) long — 3 ft (0.9 m) longer than the rotor blade. A ribbon cable carried sensor signals through the seal around the chamber door. Leakage through the seal was compensated by pumping air out of the chamber at the rate at which air leaked in. A pressure range of 400 to 760 torr (53 to 101 kPa) could be achieved in the chamber with this arrangement.

The chamber was pumped down in 50-torr (6.7-kPa) increments. At each pressure step, readings of the transducer outputs were recorded manually by dialing through a rotary switch connected to the units through the ribbon cable. The numerical results were used as input for a computer analysis of errors.

This work was done by Michael E. Watts of **Ames Research Center**. *Further information may be found in NASA TM-88312 [N87-12830/NSP], "Supplementary Calibration Test of the Tip-Aerodynamics- and Acoustics-Test Pressure Transducers."*

Copies may be purchased [prepayment required] from the National Technical Information Service, Springfield, Virginia 22161, Telephone No. (703) 487-4650. Rush orders may be placed for an extra fee by calling (800) 336-4700.

Inquiries concerning rights for the commercial use of this invention should be addressed to the Patent Counsel, Ames Research Center [see page 16]. Refer to ARC-11792.

Machinery

Hardware, Techniques, and Processes

87 Engine-Monitoring Algorithm

88 Adaptive-Wall Wind Tunnel

88 Variable-Speed, Constant-Frequency Generation of Power

90 Designing a Transonic Nozzle for Efficient Cooling

Books and Reports

91 Minimum-Time Control for Robotic Manipulators

Computer Programs

73 Analyzing Solar-Power Options for Spacecraft

74 Computer Program Predicts Turbine-Stage Performance

74 Computer Analysis of High-Speed Roller Bearings

76 Calculating Flows in Multiple-Blade-Element Cascades

Engine-Monitoring Algorithm

Allowances are made for erroneous sensor readings.

Lewis Research Center, Cleveland, Ohio

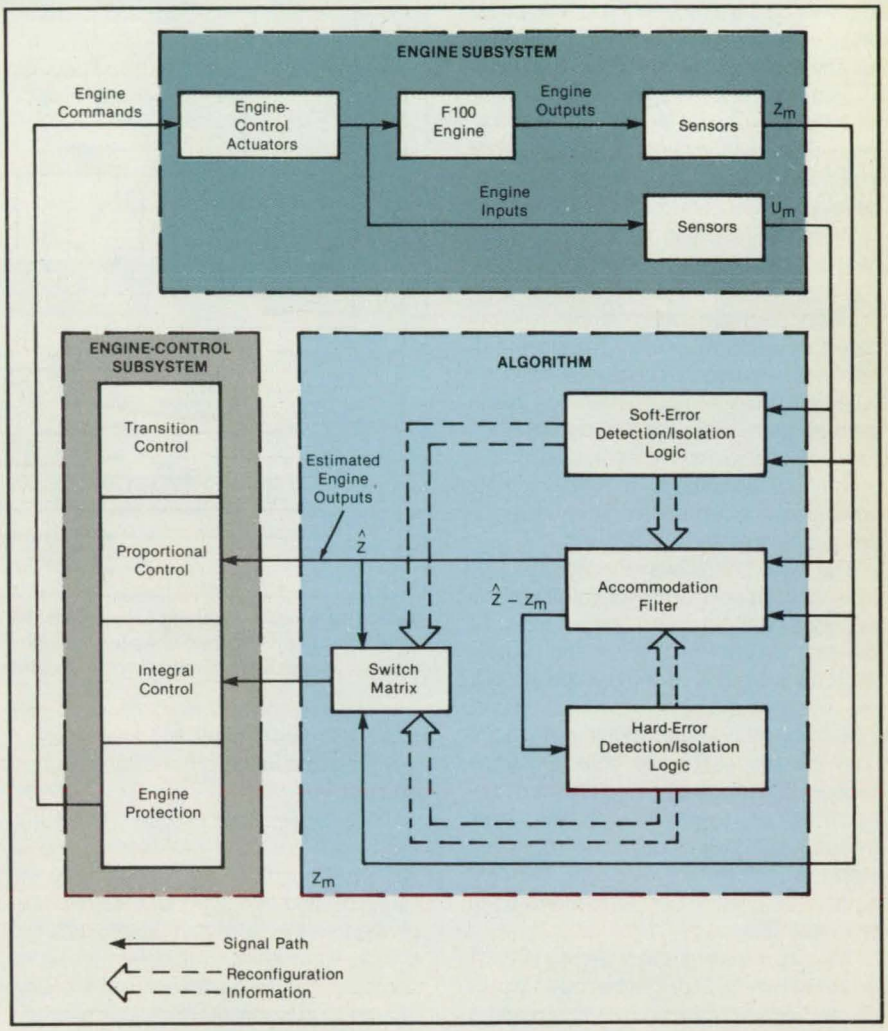
An algorithm has been developed to increase the reliability of digital electronic control systems for aircraft turbine engines: the algorithm detects, isolates, and accommodates failures or errors in engine sensors, which are typically the least reliable elements of engine-control systems. Heretofore, redundancy of sensors has been used in the effort to increase reliability. In contrast, the developmental algorithm is based on analytical redundancy, which uses a simplified mathematical model of the engine to interrelate the "normal" readings of different sensors: the algorithm determines whether the indication of a given sensor is consistent with those of the other sensors, within prescribed limits.

The inputs to the algorithm include the measured engine inputs $U_m(t)$, where t = time; the fuel flow; nozzle area; compresser-inlet-guide-vane angle; rear-compressor-variable-vane angle; and bleed flow. The inputs to the algorithm also include the measured engine outputs $Z_m(t)$, the fan and compressor speeds, burner and augmentor pressures, and fan-turbine-inlet temperature. The outputs of the algorithm are optimal (that is, as realistic as possible) estimates of the engine outputs, $\hat{Z}(t)$.

The algorithm consists of three elements (see figure): (1) logic for the detection of hard failures; (2) logic for the detection of soft failures; and (3) the accommodation filter, which contains the mathematical engine model and produces the estimates of the engine outputs. Hard failures are large out-of-range readings or bias errors that occur suddenly. These are relatively easy to detect via sudden large differences $Z(t) - \hat{Z}_m(t)$ between the accommodation-filter outputs and the sensor readings.

Soft failures are small bias errors or drift errors that accummulate slowly and are more difficult to detect. The soft-error-detection logic includes one normal-mode- and five failure-mode-hypothesis filters; these filters continuously track the sensor readings, searching for erroneous values. The performance of the algorithm is enhanced by the incorporation of integral action in a Kalman filter to improve the steady-state accuracy in the estimate of the fan-turbine-inlet temperature and by an adaptive error threshold that increases during commanded transients of engine operation to prevent false soft-error alarms.

The algorithm was tested in a computer simulation of the operation of an F100 turbofan engine. The algorithm performed well in tests of soft-error performance at seven operating points for all five sensed outputs. A test on a real engine has been scheduled.



As **Part of an Engine-Control System**, an algorithm generates engine-output estimates based on measurements of the inputs and outputs and detects failures of the input- and output-measuring sensors.

This work was done by Walter C. Merrill and John C. DeLaat of **Lewis Research Center**. *Further information may be found in NASA TM-87289 [N86-24697/NSP], "A Real-Time Simulation Evaluation of an Advanced Detection, Isolation, and Accommodation Algorithm for Sensor Failures in Turbine Engines."*

Copies may be purchased [prepayment required] from the National Technical Information Service, Springfield, Virginia 22161, Telephone No. (703) 487-4650. Rush orders may be placed for an extra fee by calling (800) 336-4700.
LEW-14514

Adaptive-Wall Wind Tunnel

Side vents are controlled automatically to compensate for interference by walls.

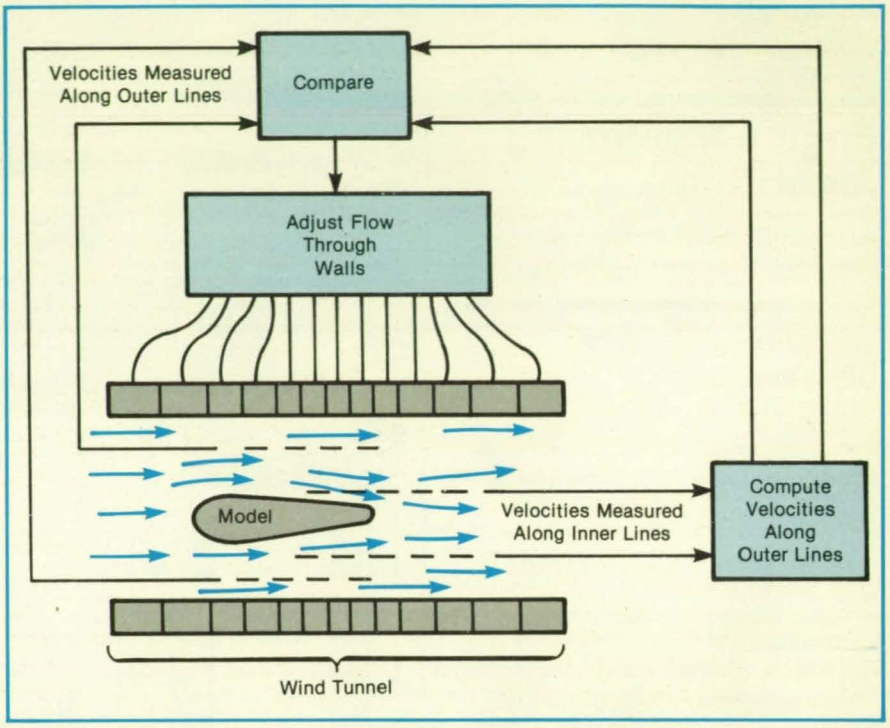
Ames Research Center, Moffett Field, California

An improved test station for the 2- by 2-Foot Adaptive-Wall Wind Tunnel at Ames Research Center is equipped for automatic sensing and correction of the effects of the walls on the airflow in the vicinity of the test model. The new facility is well suited for advanced research and development; for example, tests of airfoils in separated flows and flows with strong shock waves, tests of circulation-control rotors or other exotic airfoils, and detailed airfoil tests to develop computer codes for viscous flows.

Wall-interference-assessment algorithms (see figure) have been written to compute the flow velocities of the free air at designated control points and to compare them with measured velocities. Differences between the measured and computed velocities reflect interference by the walls and are used as control signals to set new wall conditions. The iteration of measurements, calculations, and adjustments continues until the wall-interference velocities are sufficiently small.

The wall conditions are adjusted by blowing air in or sucking air out at various locations on the top and bottom walls. To facilitate the control of inflow and outflow, each adaptive-wall assembly contains 32 cross-stream plenums of various widths. The smallest compartments are placed over the model for fine control. Partial-vacuum and compressed-air lines are connected to the plenums through slide valves that are positioned by computer-controlled stepping motors to provide the required amount of injection or withdrawal or to block the flow.

The side walls of the test section consist of schlieren-quality glass mounted in hinged frames. The window frames can be swung open to give access to the tunnel for installation of the model. A hole in each window is used to mount the model. The windows provide optical access for a fast-scan laser velocimeter and for a holographic interferometer to be installed subsequently.



Velocities Measured Along Lines Near the Model are used to calculate the velocities that would be observed along lines farther from the model if the model were in free air. These calculated values are compared with velocities measured along the farther lines.

The laser velocimeter system measures the velocities for the wall-interference-assessment algorithm. A 5-W argon laser and its associated optics on an external table generate a matrix of four beams with two colors. A transmitting scanner driven by computer-controlled motors aims the laser beams to position the measurement volume at each measurement point along the center line of the tunnel. For automatic alignment, the beam-steering mirrors are driven by motors in response to control inputs from light sensors. The light scattered from the measurement volume strikes a retroreflector, which returns it along the path of incidence to the optical table for color separation and processing.

This work was done by Daniel G. Morgan and George Lee of **Ames Research Center**. *For further information, Circle 119 on the TSP Request Card.*

Inquiries concerning rights for the commercial use of this invention should be addressed to the Patent Counsel, Ames Research Center [see page 16]. Refer to ARC-11717.

Variable-Speed, Constant-Frequency Generation of Power

Feedback of the stator power and reactive volt-amperes determines the rotor excitation.

Lewis Research Center, Cleveland, Ohio

A doubly-fed, wound-rotor generator can be used to provide a constant stator power, reactive volt-amperes, and frequency while the shaft speed varies. To accomplish this, it is necessary to control the rotor excitation; namely, the frequency, amplitude, and phase of the rotor current.

A prior method for accomplishing this type of operation has been to use a rotor excitation based on shaft speed. The disadvantage of this method is that, while the speed is adequate for the determination of the slip frequency, it is not adequate for the control of the power and of the reactive volt-amperes. When the speed is used as the controlling parameter, the rotor excitation lags the changes in the stator load. The fluctuations in the power and reactive volt-amperes in the stator are directly related to angular disturbances in the shaft.

The new method involves a control circuit that separates the rotor excitation into the generation of the slip frequency and the control of the amplitude and phase. In this control circuit, the speed determines the slip frequency, while the stator power and the reactive volt-amperes determine the amplitude and phase of the rotor current.

Small angular disturbances of the shaft



There's profit at the end of this tunnel. And it could be yours.

If your product, and profits, can be improved with wind tunnel testing, Boeing aerodynamic testing facilities are at your service through Boeing Technology Services. BTS specialists will work with you to understand your needs precisely, and then will help you tap into Boeing resources efficiently.

Boeing has subsonic, transonic, supersonic and hypersonic tunnels with on-line systems that deliver final plotted data within seconds. Our special services also include aeroacoustic testing, a captive trajectory system and a separate airflow calibration facility.

We can test your model. Or design and build one to your specifications. Or provide a complete package.

Boeing specialists also can help you develop a testing program to meet your technical requirements, timetable and budget. And we can handle projects that are classified or that require security for proprietary reasons.

For a full description of the Boeing aerodynamic testing facilities and services available to you, call Paula Royalty, Marketing Manager at (206) 277-4600. Or write to Boeing Technology Services, P.O. Box 3707, M/S 9R-28, Seattle, WA 98124-2207.

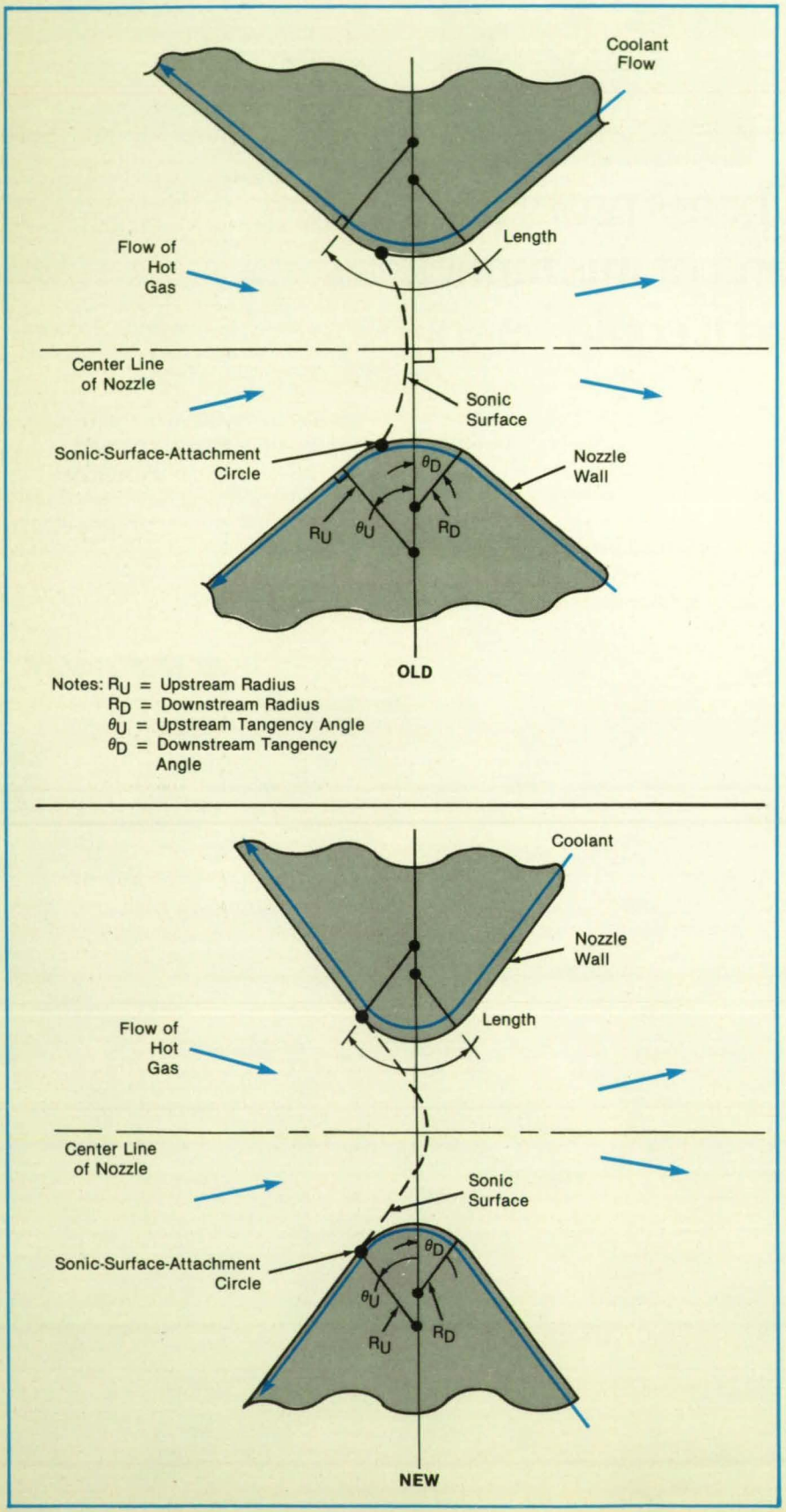
BOEING



Circle Reader Action No. 367

produce changes of phase in the induced stator voltage, causing large fluctuations in the stator power and reactive volt-amperes. To prevent this, the rotor-control circuit must respond quickly enough to change the phase of the rotor current. When the proper proportions of stator power and reactive volt-amperes are fed back to the rotor-control circuit to control the phase, the desired excitation is obtained.

This work was done by Frank J. Brady of **Lewis Research Center**. *No further documentation is available.*
LEW-14054



Designing a Transonic Nozzle for Efficient Cooling

Throat curvatures are adjusted to match maximum heat flux with maximum heat removal.

Marshall Space Flight Center, Alabama

A design for a high-pressure transonic-flow nozzle increases the effectiveness of the coolant flowing in passages in the wall of the nozzle. The revised curvatures of the nozzle wall provide a shortened transonic region and enable the selection of the approach- and discharge-wall angles for maximum cooling. As a result, the new nozzle design enables the wall to operate at a lower temperature, reducing thermal fatigue and increasing the life expectancy of the wall. It also enables the coolant to flow through the wall channels with lower pressure drop and, therefore, lower pumping pressure.

In previous designs, the upstream and downstream radii of the nozzle throat and the two tangency-point angles (see figure) were specified without regard to the position of the sonic point relative to the coolant-channel curvature. In the new design, the radii and the tangency-point angles are selected to give a shorter path for the high-velocity coolant through the channels.

Moreover, the sum of the angles is selected so that the coolant flow acquires a centrifugal-force component that is greatest in the vicinity of the sonic-surface-attachment circle. This means that the area of greatest heat flux from the gas flowing through the nozzle is also the area where the coolant can carry the heat away most effectively; the rate of heat transfer can be increased by as much as 50 percent.

This work was done by William R. Wagner of Rockwell International Corp. for **Marshall Space Flight Center**. *No further documentation is available.*
MFS-29224

The **New Nozzle Design** reduces the length of the coolant channels in the nozzle wall. At the same time, the greater curvature of the nozzle throat increases the centrifugal effect, and consequently the cooling capacity, without increasing the required pumping power.

Books and Reports

These reports, studies, handbooks are available from NASA as Technical Support Packages (TSP's) when a Request Card number is cited; otherwise they are available from the National Technical Information Service.

Minimum-Time Control for Robotic Manipulators

An existence theorem is proved for nonlinear systems.

A report discusses the mathematical requirements for the existence of a solution to the minimum-time control problem for a robotic manipulator that obeys nonlinear equations of motion. In essence, the problem is how to specify the sequence of manipulator-joint torques (within the allowable limits on those quantities) to move the manipulator from one particular position and orientation to another.

The authors begin by reviewing linear systems, for which the existence conditions for minimum-time control have been derived previously. Each such optimal control sequence is unique and is of the "bang-bang" type; that is, it involves the application of full torque to start or alter the motion, zero torque during each segment of the motion, and full torque to stop the motion.

Nonlinear systems are more likely to be encountered in practice and require more conditions for the existence of minimum-time solutions. The derivation begins with a statement of Fillipov's theorem, according to which the three conditions for minimum-time control are the following:

1. The trajectories generated by the admissible controls do not finitely escape during the interval to be minimized.
2. The final state is reachable in finite time using the admissible controls.
3. In the abstract control space, the control dynamics are convex over all admissible controls.

The third condition is satisfied in most of the applications envisioned by the authors. The second condition is not generally easy to satisfy; however, the reachability condition can be calculated for a nonlinear system that is feedback-equivalent to a linear system by calculating the condition for the equivalent linear system. The first condition can be checked using a Lyapunov-function approach. By constructing the energy Lyapunov function, the condition is shown always satisfied. Hence, for the robotic manipulators, the minimum-time control exists provided the available torque is large enough to overcome the gravity, thus satisfying the reachability condition. In the absence of gravity — for example, in space applications — the minimum-time control always exists.

This work was done by John T. Wen of Caltech for **NASA's Jet Propulsion Laboratory** *and Alan Desrochers of Rensselaer Polytechnic Institute. To obtain a copy of the report, "Existence of the Time Optimal Control for Robotic Manipulators," Circle 112 on the TSP Request Card.*
NPO-16919

Correction: In NASA Tech Brief MSC-20926 entitled Manual "Guillotine" Wirecutter which appeared in Vol. 10, No. 1 Pg. 110, the work done should have been credited to Orville K. Brack. Mr. Brack was at the Goddard Space Flight Center during the time he designed and developed this wirecutter. The wirecutter was installed and flew with the first Spartan system on STS 51G. The Spartan mission was completely successful. The wirecutter also flew with Spartan Halley on the ill-fated Challenger mission. Mr. Brack has since retired, lives in Barefoot Bay, Florida, and is a design consultant.

NASA WANTS YOU

to tell your fellow citizens how you have applied NASA research in your products or processes.

For more information, call:
Linda Watts
(301) 621-0241
NASA Spinoffs

12,000+ Solutions

25 YEARS OF NASA RESEARCH TECHNOLOGY AT YOUR FINGERTIPS

In minutes you can search 25 years of NASA Tech Briefs to find briefs related to your current project. NASA may have already found a solution or may suggest other ways of resolving the problem. On the way to space NASA has had to solve thousands of unique problems in all engineering fields; electronics, mechanics, materials, fabrication, etc., under the most extreme conditions. Each issue of NASA Tech Briefs contains about 50 to 70 briefs. Now with NTB:BASE you can examine over 12,000 briefs.

- **NTB:BASE**, a PC-compatible database. Can be used on an IBM PC/XT/AT or any IBM compatible equipped with: 256k-available memory or more; DOS 2.0 or higher; one double sided disk drive.
- **NTB:BASE** enables you to initiate a search by Subject Title, Author, Tech Brief Number or by Key Word or Phrase. You can review the abstract on your computer. The year in which the brief was published will be displayed with the abstract. You may order complete briefs for as little as $2.00 each.
- **NTB:BASE** offers 6 categories. They are **Electronics, Physical Sciences, Mechanics, Materials, Fabrication Technology** and **3-IN-1**, which includes Mathematics & Information Sciences; Life Sciences; and Pre-1976 Computer Programs. Each category subscription costs only $100.00, or subscribe to all 6 for only $500.00. Annual updates are $20.00 per category. All 6 for $100.00.
- **NTB:BASE** is transferable to hard disk drive for faster access and convenience. Handy User Guide comes with complete instructions.

Enclosed please find check for $_____ covering the selected categories ☐, or all categories ☐.

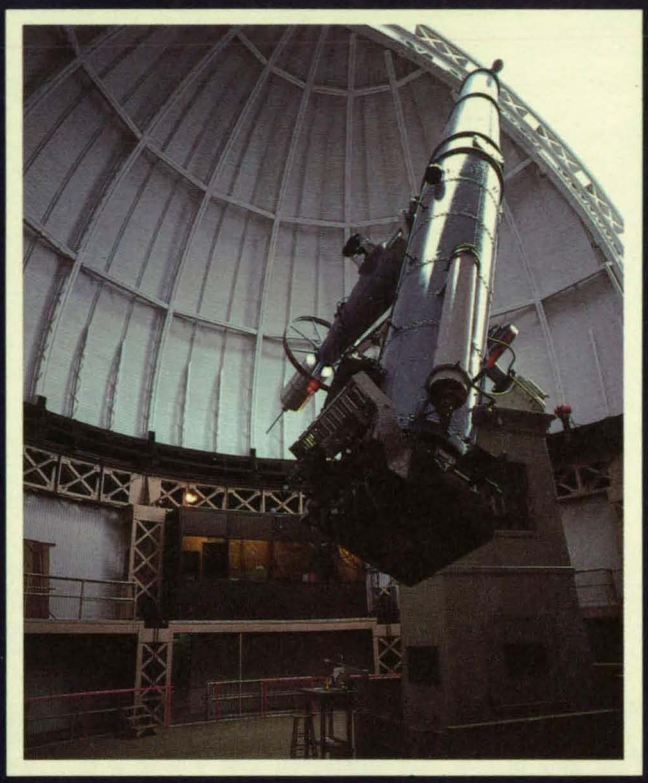
- ☐ A **Electronics**
- ☐ B **Physical Sciences**
- ☐ C **Mechanics**
- ☐ D **Materials**
- ☐ E **Fabrication Technology**
- ☐ F **3-In-1 (Mathematics & Information Sciences, Life Sciences and Computer Programs)**

NTB:BASE from NASA Tech Briefs

Name _____
Company _____
Address _____
City _____ State _____ Zip _____
Telephone _____

NTBM-Research Center, 41 East 42nd Street, Suite 921, New York, NY 10017-5391 212-490-3999

SCHOTT GLASS... HELPING OUR WORLD SEE OTHER WORLDS



Precision Optical Glass of uncommon dimensions.

When the University of Pittsburgh's Allegheny Observatory was developed around the turn of the century, Schott was the only company capable of making the lens blanks for the Observatory's refracting telescope. Three quarters of a century later, that telescope is still the third largest in the world.

Today, as the lenses of that refracting telescope are being replaced, glass from Schott Glass Technologies — a United States company — is the choice.

In fact, Dr. George Gatewood, director of the Allegheny Observatory, said that there wasn't much of a choice at all. "Schott is the only company in the world capable of producing the glass we need for our refracting telescope lenses."

He's not alone in his thinking. Because of Schott's world-wide involvement and award-winning Research and Development department, Schott glass has been chosen for use in many of the most advanced optical systems man has ever known. Including some of the world's biggest stargazers; like the University of Pittsburgh's Allegheny Observatory.

Schott Glass Technologies is a United States manufacturer of many types of glass. If you're involved in astronomy, space exploration, aerospace, precision measurements or optics, Schott can help you with the right glass for these and many other fields.



SCHOTT

SCHOTT GLASS TECHNOLOGIES INC.

400 York Avenue
Duryea, Pennsylvania 18642
(717) 457-7485 TWX 510-671-4535
Telefax (717) 457-6960

Fabrication Technology

Hardware, Techniques, and Processes

93 Tool Removes Arc-Light Reflectors
93 Truss-Core Corrugation
94 Field Repair of Thermoplastic Windows and Canopies
95 Protective Coating for Laser Drilling of Silicon

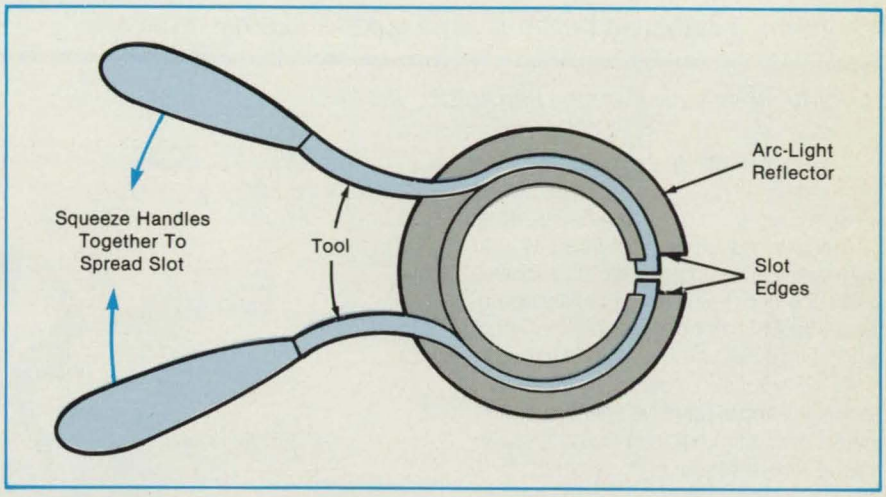
Tool Removes Arc-Light Reflectors

Self-clamping reflectors are easily removed from welding torches.

Marshall Space Flight Center, Alabama

A new tool makes the installation, adjustment, and removal of self-clamping arc-light reflectors on welding torches easy and simple. Normally, such a reflector clamps so tightly onto the end (gascup) of a welding torch that it is difficult to remove with bare hands. Usually, a screwdriver is wedged into a slot on the reflector to spread the clamping portion: this is an awkward operation that occasionally results in damage to the slot edges.

The tool, shown in the figure, consists of two arms that reach around from the back of the torch. A lip on each arm hooks into the slot of the arc-light reflector clamp. When the handles of the tool are squeezed together, the slot is spread, enabling easy installation, adjustment, or removal of the reflector without disassembly of the welding apparatus. At the same time, the tool grips the arc-light reflector firmly so that it can be positioned.



When the Handles of the Tool are squeezed together, the clamp of the arc-light reflector is spread, making the reflector easily removable without risk of damage.

This work was done by Stephen S. Gordon of Rockwell International Corp. for **Marshall Space Flight Center**. *No further documentation is available.*

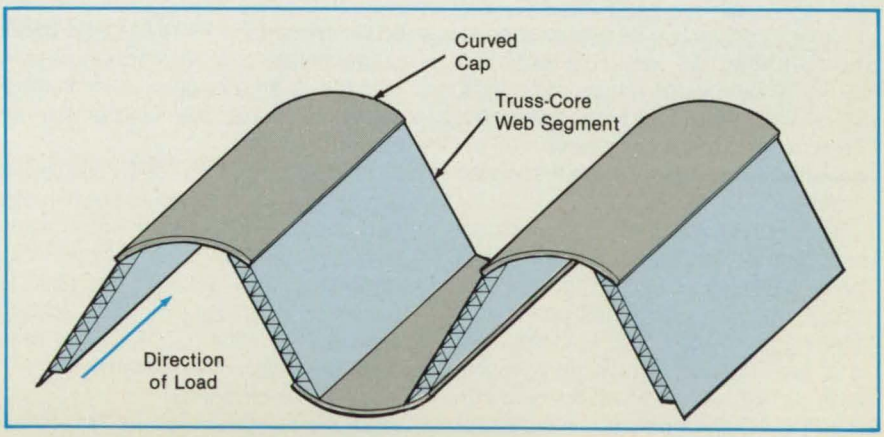
Inquiries concerning rights for the commercial use of this invention should be addressed to the Patent Counsel, Marshall Space Flight Center [see page 16]. Refer to MFS-29235.

Truss-Core Corrugation

The strength-to-weight ratio exceeds that of the beaded-web design by 60 percent.

Langley Research Center, Hampton, Virginia

The need for lighter and stronger primary structures for high-altitude, high-speed aircraft and for spacecraft motivates the search for minimum-mass fuselage and fuel-tank structures. Such craft normally require external protection systems; therefore, the underlying primary fuselage or tank structures need not be aerodynamically smooth. The limiting loads in such structures are primarily those that cause compression buckling of the wall sections. In this respect, corrugated structures offer the most attractive strength-to-weight efficiencies. A new corrugation design offers a significant weight saving over previous concepts for a wide range of loading. In this



The **Truss-Core Web** replaces the beaded web of previous corrugation designs.

design, the beaded web of prior concepts is replaced by a truss-core web, improving the strength-to-weight ratio over that of existing structures by as much as 60 percent.

The low-mass-fraction truss-core web design is shown in the figure. The truss-core web-to-cap joint provides rotational restraint for the cap, enabling the cap to carry its portion of the design load without edge rotation or premature local buckling. In the beaded-web corrugation, as much as 60% of the panel mass does not carry a load. The truss-core web is fully load carrying as are the caps, enabling the structure to support a much higher load at the same weight as that of the beaded-web, curved-cap corrugation.

Within the truss-core web, the cross-sectional properties are optimized to provide the web of lightest weight for the load to be carried. The truss-core corrugation and cap can be made of metallic or nonmetallic materials or appropriate combinations thereof. Structures of any width can be made by repeating any number of corrugation segments. Further, these sections can be repeated on curves to form the walls of such shell structures as cylindrical shells for fuselages and fuel tanks. Also, the cap strips can be extended and crimped over the truss-core webs, improving the damage resistances of the caps and further stabilizing the cap edges against rotation.

This work was done by Randall C. Davis and L. R. Jackson of **Langley Research Center**. *For further information, Circle 16 on the TSP Request Card.*

This invention is owned by NASA, and a patent application has been filled. Inquiries concerning nonexclusive or exlusive license for its commercial development should be addressed to the Patent Counsel, Langley Research Center [see page 16]. Refer to LAR-13438.

Field Repair of Thermoplastic Windows and Canopies

A hand-held induction heater makes quick and easy repairs.

Langley Research Center, Hampton, Virginia

Aircraft maintenance is currently the most challenging area of battlefield repair. When repairing aircraft windscreens, skins, or mainframes, structural integrity and high quality of repair are difficult to achieve under the constraints of battlefield operations. Repair under these conditions must be simple, quick, and durable. The repairs must be possible under severe weather conditions and in primitive shelters. Repair materials must remain stable and manageable at temperatures from 32 to 120 °F (0 to 49 °C). The use of induction-heating techniques and toroid bonding equipment developed at Langley Research Center has made these repairs relatively quick and easy.

Toroid bonding equipment is based on a self-tuning, solid-state power oscillator feeding 30- to 80-kHz power to a ferrite toroid. The toroidal shape introduces a uniform, concentrated magnetic flux into the materials to be bonded, causing eddy currents to flow in a ferromagnetic susceptor and/or paramagnetic adherends. These currents heat only the bond line or its vicinity. The power required to heat a bond area of 1 $in.^2$ (6.5 cm^2) to 800 °F (430 °C) within 1 min is less than 300 W, with most bonding temperatures requiring less than 200 W. Since no large fixtures are heated, the cooling rate is rapid, typically less than 2 min from the bonding temperature to the glass-transition temperature of the bonded material.

These toroid bonding techniques have been further developed to meet typical field-repair requirements. The induction-heating power supply has been engineered into a "ruggedized" solid-state unit, in a 1-ft^3 (0.028-m^3) package weighing 20 lb (9.1 kg). A hand-held bonding gun weighing 3 lb (1.4 kg) plugs into this power supply on a long cord. The maximum power required is 300 W. Lightly loaded repair bonds can be made in several minutes at an average power input of 150 W on metallic, polymeric, or polymer-matrix materials.



On-the-Spot Aircraft-Windscreen Repairs are made easily with a hand-held toroid bonding gun.

Field repairs were made by Langley Research Center personnel at the Hampton Aerospace Park on fighter-aircraft canopies (see photo). The patches were approximately 2 ft^2 (0.19 m^2) each and required 2 h from start to finish. In addition, repairs were made on .45-caliber bullet holes on a helicopter polycarbonate windscreen. Polycarbonate patches applied using the hand-held bonding gun formed effective doubler plates over the cracks emanating from the bullet holes, to restrain crack propagation. Each bond took less than 10 min per hole.

The toroid bonding field-repair technique provides repairs that are faster, simpler, and stronger than those using conventional techniques. The portable, ruggedized equipment and other equipment related to toroid induction are now available commercially as a result of this work.

This work was done by Robert L. Fox and James R. Tyeryar of **Langley Research Center**. *For further information, Circle 54 on the TSP Request Card.*
LAR-13525

Protective Coating for Laser Drilling of Silicon

Sodium silicate prevents spattered silicon from fusing with surrounding material.

NASA's Jet Propulsion Laboratory, Pasadena, California

The spattering of silicon during laser drilling or machining of a silicon wafer can be prevented from damaging the surrounding wafer or mask by forming a protective coating on the wafer before drilling or machining. To be effective in preventing such damage, a protective coating must have the following properties:

- Be easy to apply;
- Not react with the substrate or mask;
- Not be melted, penetrated, or destroyed by the spattered material;
- Not interfere with laser drilling or machining; and
- Wash off along with any spatters without damage to the mask or wafer.

The best coating materials found thus far come out of aqueous solutions as glasses. These include borates, phosphates, and silicates of the alkali metals. One material that can be applied satisfactorily is a dilute aqueous solution of "stabilized" sodium silicate (common "water glass"). The solution is stabilized by equilibrating it with powdered silica so that any excess alkali (which might react with the silica mask on the silicon wafer) is removed. Tests have not been run to determine whether the stabilization step is essential.

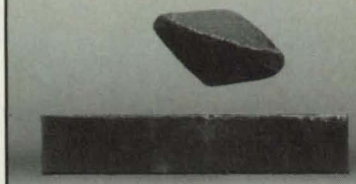
The sodium silicate solution can be applied to the wafer by dipping and draining or by spinning; presumably, application by spraying would also work. When dried in an oven, the solution leaves a thin coating of sodium silicate glass.

In a test, silicon wafers were partly coated with solutions of sodium metasilicate and sodium polysilicate and dried at 250 °C. A ruby laser was used to drill 0.003-in. (0.08-mm) holes in the coated and uncoated portions. The coatings were then removed by soaking in hot water for a few hours. The areas that had been coated were free of spatters. However, the coatings reacted with the laser beam to form rims of sodium silicate around the holes.

This work was done by Paul J. Shlichta of Caltech for **NASA's Jet Propulsion Laboratory**. *For further information, Circle 133 on the TSP Request Card.*
NPO-17148

SUPERCONDUCTORS
from
HiTc Superconco
High-temperature superconductors in production quantities!

Order your demo package today!



Package includes ceramic superconductor, magnet, petri dish and instructions for demonstrating Meissner effect.

- Custom and standard shapes, or powder
- Available today

For information, or to order your Superconductor demo package, call:

609-397-2900

HiTc Superconco
245 N. Main St. • P.O. Box 128 • Lambertville, NJ 08530
HiTc Superconco is a subsidiary of Lambertville Ceramic Manufacturing Co., manufacturer of ceramics and advanced ceramics for industry since 1947.

Circle Reader Action No. 544

"If a journey around the world changes a person, then a journey 200 times around the world at the speed that a spaceship travels changes a person even more." Joe Allen, astronaut

SEVEN DAYS IN SPACE
(A week aboard Space Shuttle "Discovery")

The first home-video documentary shot, almost entirely, in space.

- Background notes supplementing the video
- Footage never before seen by the public!
- 88 minutes of being there!



HV HALCYON VIDEO

With narration by the crew of mission 51-A

Launch into orbit on a tour of the Space Shuttle and its capabilites, guided by the astronauts and controllers of "Discovery," on the mission that returned two defective satellites to Earth. Become weightless, deploy new communications satellites, gaze back at your planet, strap on the Manned Maneuvering Unit and "Stinger," and take the ride men have dreamt of for thousands of years!

To order send name and address + check or money order for $29.95 + $3.00 for postage and handling to:
Halcyon Films and Video
110 Beach Road, Room 7B
Kings Point, New York 11024
or call
1-800-426-0582
Specify VHS or BETA

Circle Reader Action No. 532

Mathematics & Information Sciences

Hardware, Techniques, and Processes

96 Computer Scheduling of Airplane Arrivals
97 Generating Coordinates for Aerodynamical Calculations

Books and Reports

97 Knowledge-Acquisition Tool for Expert System
98 Determination of Grain-Size Distributions

Computer Programs

76 Interactive Plotting Program
76 Tape-Certification Program
78 Locating Spaceborne SAR Imagery
78 Generating Cross-References Among Computer Routines
78 Designing Digital Filters

Computer Scheduling of Airplane Arrivals

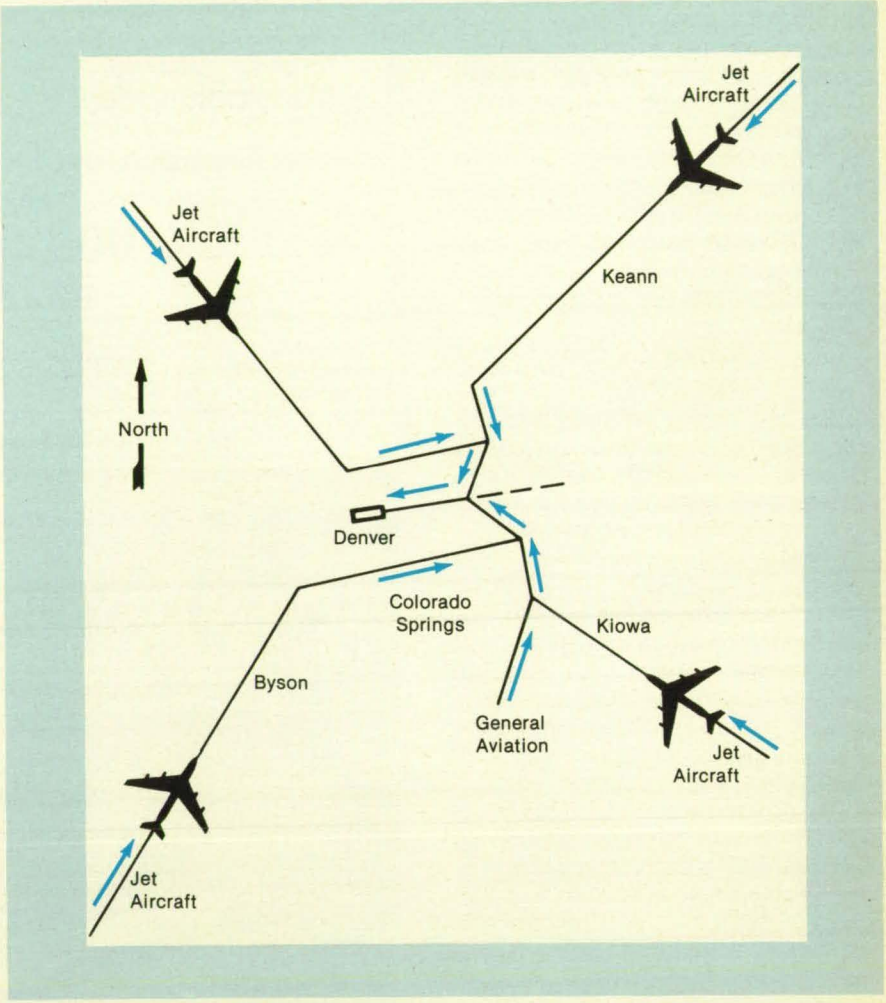
Controllers would be assisted in the coordination of many simultaneous flights.

Ames Research Center, Moffett Field, California

A prototype computer-based system has been developed to assist air-traffic controllers in scheduling the arrivals of many airplanes at an airport and at designated points along the approaches to the airport. The system is an evolving product of efforts to relieve the human controllers of routine tasks by incorporating as much as possible of their expertise into expert systems of computer programs. In recognition of the overriding requirement to promote safety, the system relies on the proved ability of human controllers to solve unforeseen problems and is therefore designed to be highly interactive: it explains its actions to the controllers, offers menus of commands, accepts modifications of flight plans, and incorporates special or temporary operating rules that the controllers may have to impose in specific situations.

The prototype system is designed to follow as many as 100 airplanes within a radius of 150 nautical miles (278 kilometers) of Denver, Colorado. Conventional jet-airplane traffic enters this Denver terminal area at four points called "feeder fixes" (see figure). For each new arrival, the system develops an admissible flight plan. As each airplane progresses through the terminal area, the system monitors the deviation of the airplane from its flight plan and provides advisory notices to return it to its assigned schedule. In cases of such disruptions as missed approaches and closed runways, the system revises the flight plans of all the aircraft in the terminal area.

The arrival time assigned to each airplane is based partly on the speed range of the airplane in standard flightpath calculations. The system also takes account of such requirements as the minimum allowable distances between consecutive airplanes on the same route, the different minimum-distance requirements for different classes of airplanes, and the prevention of conflicts with previously scheduled airplanes. For example, if none of these requirements can be satisfied for an entering airplane, the system will advise that it fly in a holding pattern at the feeder fix until the next available entry time.



Air Traffic Heading Toward Denver along four routes is scheduled by the prototype system. All airplanes are assumed to be on instrument flight rules, and all landings are assumed to take place at Denver Stapleton Airport on runway 26L.

The system operates on a Symbolics 3600 computer. The software is written in the Symbolics Zetalisp language, which accommodates component programs in compatible versions of the MRS, FORTRAN, and Lisp languages. The Lisp functions call FORTRAN programs to run when numerical subroutines are needed. MRS (Meta-level Reasoning System) is a logic-programming language used to treat facts, rules, backtracks in the search for alternative solutions, and other elements of planning.

The further development of the system is likely to require the acquisition of more expertise from the air-traffic controllers, research through simulation and field tests, and the incorporation of flight regulations. Issues that need to be addressed include the optimization of flightpaths (for example, for fuel-efficient descents), procedures to minimize deviations from schedules, and strategies to increase the capacities of airports.

This work was done by L. Tobias and J.

L. Scoggins of **Ames Research Center**. *Further information may be found in NASA TM-88234 [N86-28068/NSP], "Time-Based Air Traffic Management Using Expert Systems."*

Copies may be purchased [prepayment required] from the National Technical Information Service, Springfield, Virginia 22161, Telephone No. (703) 487-4650. Rush orders may be placed for an extra fee by calling (800) 336-4700.

Inquiries concerning rights for the commercial use of this invention should be addressed to the Patent Counsel, Ames Research Center *[see page 16].* *Refer to ARC-11742.*

Generating Coordinates for Aerodynamical Calculations

A mathematical method represents an aircraft surface as grids of variable spacing.

Ames Research Center, Moffett Field, California

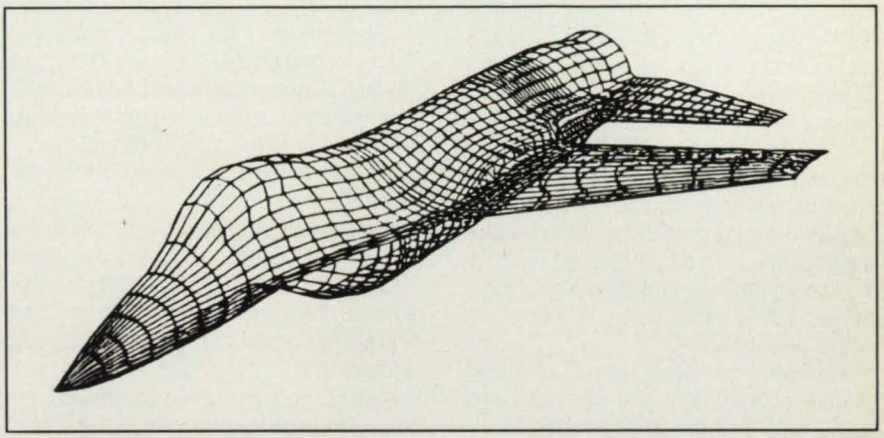
An elliptic method generates composite grids about a three-dimensional aircraft body. The realistic grids are useful in mathematical models of aerodynamic flow. A computer can generate the grids with little or no human intervention.

A body-conforming grid is first generated about the entire aircraft by the solution of Poisson's differential equation. This initial grid has relatively coarse spacing, and it covers the entire body. At boundary surfaces, the sizes of grid cells are controlled, and cell skewness is nearly eliminated, by the incorporation of the inhomogeneous Poisson terms, which are found automatically by the program. Certain regions of the grid — those in which high gradients are expected and which map into rectangular solids in the computational domain — are then designated for zonal refinement. Spacing in the zonal grids is reduced by adding points according to a simple algebraic scheme.

When flow-solver results require an adjustment to the size, location, or resolution of the fine zonal grids, the adjustment is usually made without any modification to the coarse grid and with simple changes to the subdivision that produces the zonal grids.

The method has been applied to a wing-and-body configuration based on the F-16 fighter airplane. The fuselage, including the canopy, the strakes, and the shelf aft of the main wing, has been fully modeled, as have been the main wing and the horizontal tail (see figure). The ventral inlet was faired over, and the vertical tail, the ventral fins, and the missile rails on the wing tips were deleted. A tapering sting of circular cross section was added to the rear.

The Poisson grid equations, including the side-condition equations that determine the inhomogeneous terms, were solved by a point-successive over-relaxation technique, which was chosen for its ease of programming and its flexibility with respect to boundary conditions. One hundred iterations, at about 1 second of central-processing-unit time per iteration, were required to generate the 37,000-point coarse global mesh.



Grid Lines on the Surface of the Wing and Body vary in spacing, depending on level of detail needed to model airflow accurately in the region. The grid intervals for a zone might be unchanged in one direction, halved in the second orthogonal direction, and reduced to much finer spacing in the third direction.

The coarse global grid was divided into 16 zones. The degree to which the coarse grid intervals were subdivided varied from no change at all to intervals as small as a thousandth that of a coarse grid layer; such small intervals are needed for the simulation of viscosity. A total of 300,000 points were used in the zones. The computer time to generate the zonal grids was insignificant.

Eventually, as grids become more realistic and complex, the entire flow field will have to be divided into several regions, with a coarse grid generated in each region. The ability of the new method to control the behavior of grids at boundary surfaces will make it easier to patch such regional grids together.

This work was done by Reese L. Sorenson of **Ames Research Center**. *Further information may be found in NASA TM-88240 [N86-31527/NSP], "Elliptic Generation of Composite Three-Dimensional Grids About Realistic Aircraft."*

Copies may be purchased [prepayment required] from the National Technical Information Service, Springfield, Virginia 22161, Telephone No. (703) 487-4650. Rush orders may be placed for an extra fee by calling (800) 336-4700.

Inquiries concerning rights for the commercial use of this invention should be addressed to the Patent Counsel, Ames Research Center *[see page 16].* *Refer to ARC-11732.*

Books and Reports

These reports, studies, handbooks are available from NASA as Technical Support Packages (TSP's) when a Request Card number is cited; otherwise they are available from the National Technical Information Service.

Knowledge-Acquisition Tool for Expert System

Digital flight-control systems will be monitored by a computer program that can evaluate and recommend.

According to a report, flight-systems engineers for advanced, high-performance aircraft will soon use a knowledge-acquisition tool (computer program) for an expert-system flight-status monitor that supplies interpretative data. An expert system is an artificial-intelligence (AI) system in which the knowledge of one or

more human experts has been put into a computer. The interpretative function is especially important in time-critical, high-stress situations because it can facilitate problem identification and corrective strategy. Conditions can be evaluated and recommendations can be made by ground-based engineers who will have essential knowledge for the analysis and monitoring of the performances of advanced aircraft systems.

Monitoring techniques available today supply system-status and -failure indications, but do not provide the interpretation function that is becoming increasingly necessary for advanced avionics and digital flight-control systems. Among the goals of development of the expert-system flight-status monitor is a hierarchical set of flight-monitoring capabilities. In this set, levels one and two represent the degree of flight-monitoring automation currently available. The third-level goal of expert interpretation includes the capability of putting information together and providing knowledge. Level three is expected to be operational within one year.

As a semi-intelligent "editor", the knowledge-acquisition tool is a computer program that enables easy access to the knowledge base of the expert system and that provides aid and direction in creating, modifying, and maintaining that base. Additionally, the onboard system maintains, corrects, and puts information into the expert system. Through help screens and online documentation, the knowledge-acquisition component of the expert-system flight-status monitor provides a coherent source of information. The subsequent use of the expert system reflects the logically consistent and complete knowledge base generated by the knowledge-acquisition tool.

The expert-system flight-status monitor processes the telemetry-downlink failure and status words, using a ground-based symbolic processor. The failure words are processed through a rule-based model of the failure-management system of the aircraft to arrive at an independent assessment of the state of the vehicle flight-control system. (For this purpose, a rule is a compact and manageable unit of knowledge that is reducible to an if/then expression.)

If the expert system detects any failures, the second level of rules is invoked to produce a high-level evaluation of the overall status of the aircraft. Any detected failure will be compared to the status-indicator words by the failure-management system of the aircraft. Rules yet to be developed are expected to resolve discrepancies between the onboard system and the expert system. Conditions that can adversely affect the safety of flight will cause cautions and warnings to be issued to the systems engineer, who will then be able to query the expert system for an explanation or to request a more detailed description of the aircraft state. The expert system will also be able to display messages or emergency procedures when necessary.

A structured, yet flexible, method enables easy modification of the knowledge base of the expert system. Because knowledge must be changed frequently, it cannot be hard-wired into the system. Instead, a means of forcing consistency in the rule base is established while the representation is deliberately kept simple and uniform enough to facilitate reading and manipulation of the knowledge base.

Some of the rules used by the knowledge-acquisition tool are in the form of traditional if/then (production) rules; others are defined in unusual formats to facilitate the definition of the knowledge base and to increase the execution speed of the inference mechanism in the expert system. In consideration of power and computational expense, production rules are eliminated whenever possible by partitioning the total system knowledge base into multiple knowledge bases that can be processed sequentially.

Using consistency and partitioning, the knowledge-acquisition tool provides a means of entering aircraft rules in an orderly manner. Consistency in rule entry is achieved by limiting the vocabulary through the use of certain basic words and previously defined clauses. The basic words are used to identify bits in the telemetry stream. Basic words, which are also considered to be rules, are either failure indications, status indications, or cross-channel-assessment indications. Unlike failure indications and status indications, cross-channel indications provide assessments of the computers that generate them.

The knowledge-acquisition tool is in current use on an advanced high-performance aircraft at the NASA Ames Dryden Flight Research Facility. As a side benefit, the tool provides automatic text generation of aircraft-system rules, creating systems-level documentation.

This work was done by James D. Disbrow, Eugene L. Duke, and Victoria A. Regenie of **Ames Research Center**. *Further information may be found in NASA TM-86802 [N86-16944/NSP], "Development of a Knowledge Acquisition Tool for an Expert System Flight Status Monitor."*

Copies may be purchased [prepayment required] from the National Technical Information Service, Springfield, Virginia 22161, Telephone No. (703) 487-4650. Rush orders may be placed for an extra fee by calling (800) 336-4700.

Inquiries concerning rights for the commercial use of this invention should be addressed to the Patent Counsel, Ames Research Center *[see page 16].* *Refer to ARC-11706.*

Determination of Grain-Size Distributions

Images of microstructures are analyzed by transform methods.

A report discusses the determination of the distributions of grain sizes by the analysis of images of microstructures. Such material properties as tensile strength, hardness, yield stress, fracture stress, and resistance to impact are influenced by grain-size distributions. Thus, analyses of material properties can benefit from detailed knowledge of grain-size distributions.

The shapes of grains are generally so complex that determination of grain-size distributions by current techniques are crude and imprecise. Estimates of the mean or average grain diameter can be determined from the grain-size distribution.

A theory is developed to relate the density of frequency components to the density of length components. The density of length components corresponds directly to the grain-size distribution function, from which the mean shape, size, and orientation of the grains can be obtained.

The two-dimensional gradient of a microstructure is tone-pulse encoded. The encoded image is subsequently Fourier transformed to determine the density of frequency components $F(s,\phi)$. The spatial density of length components $P(r,\phi)$ (grain-size distribution) can be determined directly from the density of frequency components $F(s,\phi)$ using the relation

$$|P(r',\phi)| = |F(s,\phi)|s$$

where ϕ is the angle of a point in polar coordinates; $s = 1/r'$; $r' = (x^2 \times y^2)^{1/2}$; and x and y are the horizontal and vertical coordinates, respectively.

Once $P(r',\phi)$ is determined, the mean grain size, shape, and orientation are obtainable from

$$D(\phi) \equiv \sum_{r'} |P(r',\phi)|r' / \sum_{r'} |P(r',\phi)|$$

Extensions of this work are continuing to examine porosity-size distributions in ceramics and fiber-spacing distributions in composites. The results of these studies may prove useful in the automotive, aerospace, aeronautical, nuclear, and construction industries.

This work was done by Edward R. Generazio of **Lewis Research Center**. *Further information may by found in NASA TM-88790 [N86-31065/NSP], "Determination of Grain Size Distribution Function Using Two-Dimensional Fourier Transforms of Tone Pulse Encoded Images."*

Copies may be purchased [prepayment required] from the National Technical Information Service, Springfield, Virginia 22161, Telephone No. (703) 487-4650. Rush orders may be placed for an extra fee by calling (800) 336-4700. LEW-14508.

MARTIN MARIETTA AERO & NAVAL SYSTEMS

PROVIDING THE FOUNDATION FOR FUTURE GROWTH

Martin Marietta has been providing technology to the United States Government for over fifty years and now has the most diversified contract portfolio of any major space defense contractor. Martin Marietta Aero & Naval Systems is experiencing tremendous growth applying advanced naval systems technology to a wide variety of projects and programs including the U.S. Navy's Vertical Launch System and the Army's Patriot Air Defense Missile Launcher.

Other current program activity includes work in:

- **Autonomous Underwater Vehicles**
- **Wide Aperture Array**
- **Advanced Lightweight Sonar**
- **Remotely Piloted Air Vehicles**
- **ASW Research & Technology**
- **Surface Weapons Systems**
- **Combat Systems Engineering**
- **MK 50 Torpedo**

Our continuing growth at Aero & Naval Systems has created immediate opportunities for these engineers with a technical MS/PhD or at least one year experience in:

Production Control Manager
- MRP II System
- Shop Floor Control Supt.

Systems Engineering
- Requirements Development
- Integration
- Test & Evaluation

Systems Analysis
- Operations Research
- Simulation & Modeling
- Mission Analysis
- Sensor Performance

Robotic Systems
- Telepresence
- Supervisory Vehicles
- Manipulator Design

Electronics Engineering
- Local Area Network
- Power Supply
- Electro/Mech. Pkg.
- Microprocessor Applications
- IR/EO Systems Design
- VLSI Design
- Radar Support

Mechanical Engineering
- Thermal Analyst

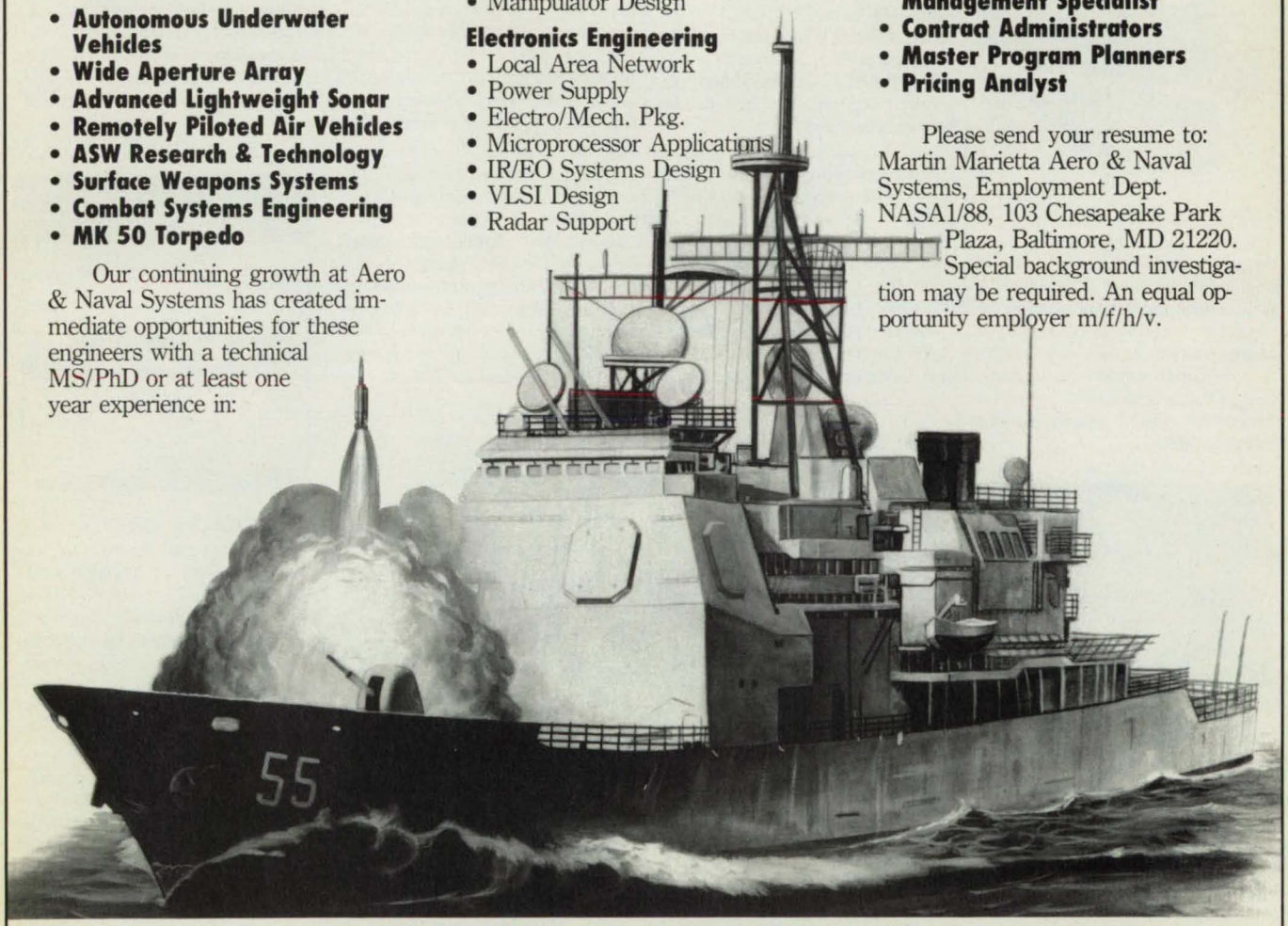
Logistics Engineering
- Reliability
- Systems Safety

Advanced Manufacturing Technologies
- Materials Engineers
- Test Engineers
- NDT Engineers

We also have opportunities for these professionals:

- **Sr. Subcontract Administrators**
- **Configuration & Data Management Specialist**
- **Contract Administrators**
- **Master Program Planners**
- **Pricing Analyst**

Please send your resume to: Martin Marietta Aero & Naval Systems, Employment Dept. NASA1/88, 103 Chesapeake Park Plaza, Baltimore, MD 21220. Special background investigation may be required. An equal opportunity employer m/f/h/v.



MASTERMINDING TOMORROW'S TECHNOLOGIES

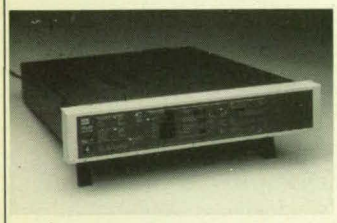
MARTIN MARIETTA

Circle Reader Action No. 440

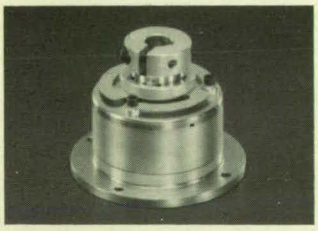
New on the Market



The **Industrial Encoder** Division of BEI's Motion System's Company (Goleta, CA) has a new Specifying Guide and General Product brochure. The 20 page document contains all mechanical and electrical parameters required to order from BEI's line of industrial optical encoders. Included are technical specifications on light, medium and heavy duty industrial position sensors as well as various encoder options, including count multiplication. **Circle Reader Service Number 581.**



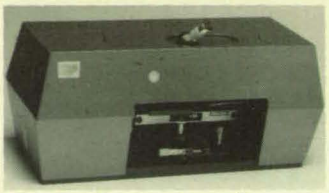
A 12 page color brochure from MTS Systems Corp, Minneapolis, MN, describes the firm's capabilities in engine simulation for **dynamic drive train testing and design**. MTS engine simulation systems allow the engineer to apply oscillating torque or motion to a specimen while it is spinning, thus simulating dynamic operating conditions. **Circle Reader Service Number 598.**



A line of **rare earth permanent magnet clutches and brakes** is now available from Electroid Company, Springfield, NJ. Available in either clutch or brake configurations, the units supply a torque to weight ratio five times greater than spring actuated designs. Typical torques and sizes include 1/6 to 2000 lbs-inches for clutches and ⅓ to 4000 lbs-inches for brakes. Both clutches and brakes can be built to fit user-specified size limitations and/or torque requirements. A brochure is available. **Circle Reader Service Number 596.**



Ioline Corporation, Lynnwood, WA, has announced that all models of the company's LP4000 and LP3700 **large pen format plotters** emulate the Hewlett-Packard Graphics Language. The Ioline subset of HP-GL output commands is designed to support a command set that is compatible with well-known computer aided design and drafting software programs like AutoCAD, VersaCAD, CADKEY and others. Existing Ioline plotters can be field-upgraded by users with the purchase of a ROM set available directly from the company. **Circle Reader Service Number 595.**



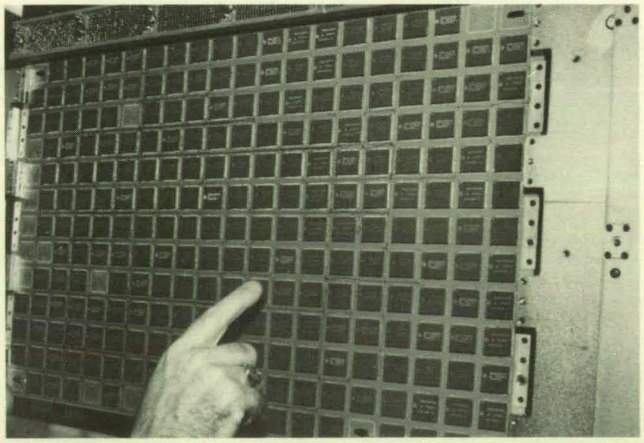
To test surface roughness for optics, silicon wafers, disks and magnetic tape, Photographic Sciences Corp., Rochester, NY, manufactures a quality non-contacting **surface profiler** that measures surface heights to an accuracy of one Angstrom (0.004 microinches) and a vertical measurement range of over five microns. Measurements can be made up to a length of 100 millimeters with a lateral resolution of approximately one micron. Applications include optics, disk, magnetic tape, silicon wafers, and machine surfaces. The profiler is insensitive to vibrations. **Circle Reader Service Number 599.**

A series of definitive bulletins covering ADVANCAP **TFE-capped seals** for MIL-G-5514F no-, one- and two-backup glands is now available from Advantec, Los Angeles, CA. Each bulletin describes six TFE-type cap materials, six energizer materials, dimensional information for 006 to 460 dash sizes, and a part numbering system to simplify ordering. Caps can be ordered separately. **Circle Reader Service Number 588.**

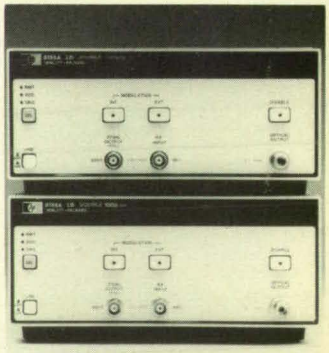
Art Gallery:Fantasy, a package of 140 pieces of **clip art** for use with Printmaster Plus and Newsmaster software, is available from Unison-World, Berkely, CA. The software includes 20 oversized graphics for the IBM version of Newsmaster. With Art Gallery I and II, Art Gallery:Fantasy brings the number of design elements up to 420. The package is not copy-protected. **Circle Reader Service Number 583.**

Interface Products, Inc., Oceanside, CA has announced a brochure containing complete information for selecting and specifying custom LCD modules. Views, block diagrams, isometric principle drawings and display capability illustrations are shown. Contents include features; applications; description; incandescent, electroluminescent and LED transillumination; electrical, environmental and lighting specifications. Dichroic and twisted nematic type displays are offered. IPI's LCD modules feature small size, low power and built-in electronics, and are available in alphanumeric or pictorial displays. **Circle Reader Service Number 589.**

Elxsi Corporation, San Jose, CA, manufacturer of the System 6400 mini-supercomputer has released a family of new **disk subsystems** that include an 823 megabyte disk drive and a high performance disk controller that offers a transfer rate of 2.4 megabytes per second. The controller will support eight 823 megabyte disk drives on a single controller or 6.6 gigabytes per controller. A two-controller system will allow disk striping and support up to 13.2 gigabytes of storage. Combined with an average positioning time of 16 milliseconds and a data transfer rate of 2.4 megabytes per second, the disk subsystem is an ideal choice for environments demanding high capacity and maximum performance. **Circle Reader Service Number 584.**



A new **supercomputer** from ETA Systems, Inc, St. Paul, MN, the ETA10 Model P, delivers true supercomputer performance for under $1 million, including the central processor, disk drive and software. ETA10 Model P is air-cooled, and can be installed in an ordinary office environment. Ranked as a Class VI supercomputer, the ETA10-P has a peak speed of 375 Megaflops, and is rated at 23 Megaflops on the Linpack (100 x 100, all Fortran) benchmark. ETA Systems also introduced their ETA10 Model Q, a faster processor priced at $1.2 million. **Circle Reader Service Number 597.**



Hewlett-Packard Company, Palo Alto, CA has introduced two new **laser-diode sources**, available in two wavelengths, using either a 1,300 nm or 1,550 nm laser diode. The stable optical-output power is typically -3dBm. High accuracy measurements of attenuation and loss are addressed by a short-term stability of +/– 0.003 dB for 15 minutes and a typical +/– 0.005 dB long-term stability for 12 hours. The LD sources can be modulated internally at 270 Hz or externally, either in the low-frequency range at 0 to 1 MHz or in the RF of 1 kHz to 850 MHz. The laser diode is modulated above the threshold with an extinction ratio of 10:1. Providing pulsewidth optical-output signals independent of the input-signal shape, these sources contribute to the test requirements found in fast telecommunication systems. **Circle Reader Service Number 582.**

Subject Index

A

ACOUSTIC MEASUREMENT
Acoustical measurement of mine-shaft length
page 84 LAR-13519

ADDRESSING
Blanket gate would address blocks of memory
page 36 NPO-16682

Electronic neural networks
page 42 NPO-16680

AERODYNAMIC CONFIGURATIONS
Generating coordinates for aerodynamical calculations
page 97 ARC-11732

AGING (MATERIALS)
Temperature, humidity, and polymer aging
page 65 NPO-16908

AIR PURIFICATION
Air revitalization using superoxides
page 62 ARC-11695

AIR TRAFFIC
Computer scheduling of airplane arrivals
page 96 ARC-11742

AIRCRAFT MAINTENANCE
Field repair of thermoplastic windows and canopies
page 94 LAR-13525

ALGORITHMS
Engine-monitoring algorithm
page 87 LEW-14514

ANTENNA ARRAYS
Computing radiation characteristics of phased arrays
page 68 LEW-14460

Wide-band, wide-scan antenna for circular polarization
page 26 NPO-16831

ANTENNAS
Dual-band microstrip antenna with reactive loading
page 26 MSC-21118

ANTIREFLECTION COATINGS
Coatings boost solar-cell outputs
page 27 NPO-16819

ARC JET ENGINES
Arc-jet power supply and starting circuit
page 22 LEW-14374

ARC LAMPS
Tool removes arc-light reflectors
page 93 MFS-29235

ARTIFICIAL INTELLIGENCE
Knowledge-acquisition tool for expert system
page 97 ARC-11706

AUTOMATIC CONTROL
Unified robot-control system
page 44 NPO-17134

B

BANDSTOP FILTERS
Designing a microwave band-stop filter
page 32 NPO-16945

BEARINGS
Computer analysis of high-speed roller bearings
page 74 LEW-14512

BLINDNESS
Public-facilities locator for the blind
page 49 MSC-21197

BOUNDARY LAYER TRANSITION
Laminar-boundary-layer crossflow sensor
page 81 LAR-13436

C

CALIBRATING
Calibrating nonremovable pressure transducers
page 86 ARC-11792

CAMERAS
Lightweight video-camera head
page 55 MSC-21246

CARBON DIOXIDE REMOVAL
Air revitalization using superoxides
page 62 ARC-11695

CAVITIES
Acoustical measurement of mine-shaft length
page 84 LAR-13519

CERAMICS
Optimization of processing of Si_3N_4
page 64 LEW-14456

CHEMICAL ANALYSIS
BASIC programming in water and wastewater analysis
page 78 KSC-11298

Modulated-voltage metastable-ionization detector
page 58 ARC-11503

CIRCUITS
Difference-equation/flow-graph circuit analysis
page 23 MFS-29245

COATINGS
Protective coating for laser drilling of silicon
page 95 NPO-17148

COMPOSITE MATERIALS
Strain-energy-release rates in delamination
page 73 LAR-13698

COMPUTER AIDED DESIGN
Designing digital filters
page 78 MSC-20982

COMPUTER GRAPHICS
Interactive plotting program
page 76 LAR-13655

COMPUTER PROGRAMS
Analyzing solar-power options for spacecraft
page 73 NPO-16855

Calculating flows in multiple-blade-element cascades
page 76 LEW-14359

Locating spaceborne SAR imagery
page 78 NPO-16861

Strain-energy-release rates in delamination
page 73 LAR-13698

COMPUTERS
The Mark III hypercube-ensemble computers
page 46 NPO-16772

CONTROL SYSTEMS DESIGN
Engine-monitoring algorithm
page 87 LEW-14514

CONTROL THEORY
Minimum-time control for robotic manipulators
page 57 NPO-17070

CONTROLLERS
Unified robot-control system
page 44 NPO-17134

CONVERGENT-DIVERGENT NOZZLES
Designing a transonic nozzle for efficient cooling
page 90 MFS-29224

COOLING
Designing a transonic nozzle for efficient cooling
page 90 MFS-29224

COORDINATES
Generating coordinates for aerodynamical calculations
page 97 ARC-11732

CORROSION PREVENTION
Galvanic corrosion in (graphite/epoxy)/alloy couples
page 64 MFS-27055

CORRUGATED PLATES
Truss-core corrugation
page 93 LAR-13438

CRACKING (FRACTURING)
Microstructure and weld cracking in Inconel 718*
page 63 MFS-27121

CRAY COMPUTERS
Generating cross-references among computer routines
page 78 ARC-11591

CROSS FLOW
Laminar-boundary-layer crossflow sensor
page 81 LAR-13436

CRYOGENIC EQUIPMENT
Swivel joint for liquid nitrogen
page 83 MSC-21160

CURING
Stronger fire-resistant epoxies
page 61 ARC-11548

CYBERNETICS
Programmable synaptic arrays for electronic neural networks
page 35 NPO-16674

CYLINDRICAL BODIES
Analysis of flow across cylinders
page 85 MFS-27180

D

DATA CONVERSION ROUTINES
Program reads weather-data tapes from aircraft
page 68 NPO-16744

DATA MANAGEMENT
Tape-certification program
page 76 NPO-16876

DATA TRANSMISSION
Dual-pilot-tone calibration technique
page 47 NPO-16930

Optical rotary joint for data transfer
page 20 MSC-21182

DELAMINATING
Strain-energy-release rates in delamination
page 73 LAR-13698

DIELECTRICS
Inspecting automatically thin ceramics for pinholes
page 49 MSC-21091

DIGITAL FILTERS
Designing digital filters
page 78 MSC-20982

DIGITAL SIMULATION
Computer analysis of high-speed roller bearings
page 74 LEW-14512

DUCTS
Holding x-ray film inside ducts
page 80 MFS-29218

DYNAMICAL SYSTEMS
Minimum-time control for robotic manipulators
page 57 NPO-17070

E

EDITING ROUTINES (COMPUTERS)
Knowledge-acquisition tool for expert system
page 97 ARC-11706

ELECTRIC FILTERS
Designing digital filters
page 78 MSC-20982

ELECTRIC GENERATORS
Variable-speed, constant-frequency generation of power
page 88 LEW-14054

ELECTRIC PROPULSION
Arc-jet power supply and starting circuit
page 22 LEW-14374

ELECTRICAL INSULATION
Effects of radiation on insulators
page 66 NPO-17032

ELECTRICAL RESISTANCE
Adjustable audible continuity tester for delicate circuits
page 18 GSC-13102

ELECTRICAL RESISTIVITY
Temperature, humidity, and polymer aging
page 65 NPO-16908

ELECTROCHEMICAL CORROSION
Galvanic corrosion in (graphite/epoxy)/alloy couples
page 64 MFS-27055

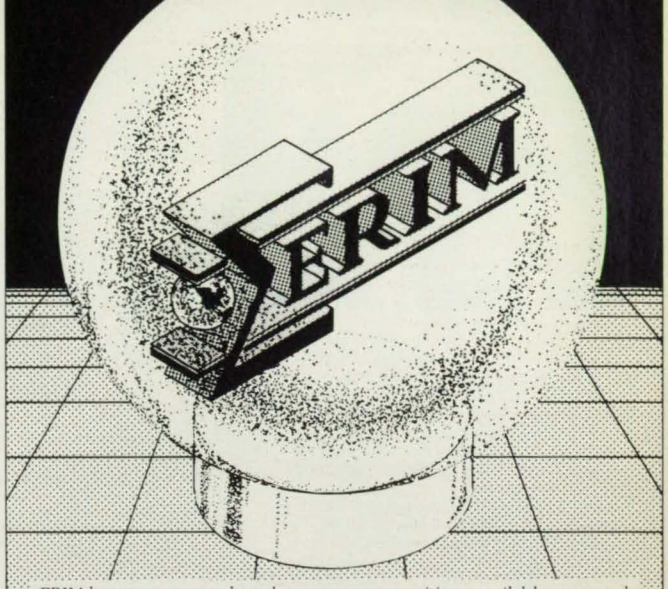
ELECTRONIC EQUIPMENT TESTS
Adjustable audible continuity tester for delicate circuits
page 18 GSC-13102

ELECTROPLATING
Locating residual wax in small coolant channels
page 59 MFS-29212

ENGINE MONITORING INSTRUMENTS
Engine-monitoring algorithm
page 87 LEW-14514

EPOXY COMPOUNDS
Stronger fire-resistant epoxies
page 61 ARC-11548

Our Image of the Future

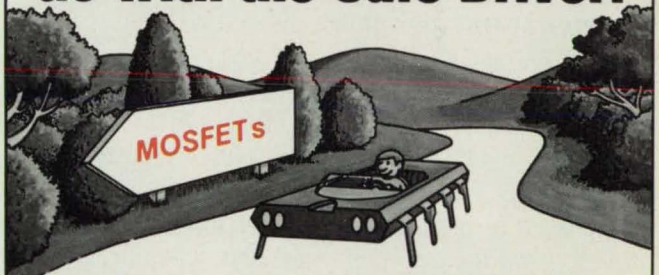


ERIM has many research and management positions available at several levels requireing a BS, MS, or PhD in engineering, physics, mathematics, or computer science, along with appropriate work experience. If you'd like to improve your future, send your resume to: *ERIM, Personnel Administration, Dept. IE, P.O. Box 8618, Ann Arbor, MI 48107-8618.*

U.S. Citizenship required. Equal opportunity employer

Circle Reader Action No. 475

Going to MOSFETs? Go with the Safe Driver!



ISO-GATE™ by DIONICS

- Opto-Isolated Input
- Photovoltaic Pure DC Out
- No Power Supply Needed
- Self-Generated Gate-Drive
- Self-Limited Gate Drive
- Single or Dual Floating Outputs
- The Safest Driver on the Road

STOP

- Risking Design Failure
- Costly Replacements
- Gate-Crashing Spikes
- Reckless Driving
- Needless Mosfet Slaughter

DIONICS 65 Rushmore Street, Westbury, NY 11590
(516) 997-7474 • Outside N.Y. 1-(800) DIONICS

Name _____ ☐ Please Send Literature

Company _____

Address _____ ☐ Please Telephone

_____

Telephone No. ( ) _____ EDN 121087

Circle Reader Action No. 548

SPACE CAMP®



YOU CAN ATTEND the exciting U.S. SPACE CAMP which inspired the hit movie "SpaceCamp".

*SPACE CAMP (grades 4-7) trainees enjoy Space Shuttle mission simulation, micro-gravity training, space food and model rocketry in 5-day program. February-August.

*SPACE CAMP-Florida (grades 4-7) offers 3 and 5-day programs near NASA's launch complex. April-November. Contact Huntsville address.

*SPACE ACADEMY Level I (grades 8-10) focuses on flight crew and mission control activities for full-size shuttle mission simulations in 5-day program. February-August.

*SPACE ACADEMY Level II is a 10-day college-accredited program for grades 11, 12 and college freshmen. Scuba course in Underwater Astronaut Trainer.

*ADULTS enjoy 3-day weekend sessions in the fall which feature astronaut speaker.

On-site accommodations and meals included. Major Eastern Airlines fare discounts available. For information, write SPACE CAMP '88, P.O. Box 1680, Huntsville, AL 35807. To register with credit card, phone:

1-800-633-7280

Circle Reader Action No. 538

EXPERT SYSTEMS
Knowledge-acquisition tool for expert system
page 97 ARC-11706

F

FEEDBACK CONTROL
Minimum-time control for robotic manipulators
page 91 NPO-16919

FINITE DIFFERENCE THEORY
Difference-equation/flow-graph circuit analysis
page 23 MFS-29245

FLAME RETARDANTS
Stronger fire-resistant epoxies
page 61 ARC-11548

FLOW DEFLECTION
Adaptive-wall wind tunnel
page 88 ARC-11717

FLUID DYNAMICS
Computer program predicts turbine-stage performance
page 74 LEW-14218

FLUID FLOW
Analysis of flow across cylinders
page 85 MFS-27180

Calculating flows in multiple-blade-element cascades
page 76 LEW-14359

FOURIER ANALYSIS
Determination of grain-size distribution
page 98 LEW-14508

G

GAS CHROMATOGRAPHY
Modulated-voltage metastable-ionization detector
page 58 ARC-11503

GAS HEATING
Arc-jet power supply and starting circuit
page 22 LEW-14374

GATES (CIRCUITS)
Blanket gate would address blocks of memory
page 36 NPO-16682

GEOPHYSICS
Estimating geophysical parameters from gravity data
page 73 NPO-16671

GRAIN SIZE
Determination of grain-size distribution
page 98 LEW-14508

GRAPHITE-EPOXY COMPOSITES
Galvanic corrosion in (graphite/epoxy)/alloy couples
page 64 MFS-27055

GRAPHS (CHARTS)
Interactive plotting program
page 76 LAR-13655

H

HEAT EXCHANGERS
Heat exchanger for rotating modular structures
page 80 MFS-26037

HYBRID COMPUTERS
Electronic neural-network simulator
page 35 NPO-17058

HYPERSONIC FLOW
Simplified analysis of shock waves
page 83 MSC-20738

I

IMAGE ANALYSIS
Determination of grain-size distribution
page 98 LEW-14508

IMAGE PROCESSING
Tape-certification program
page 76 NPO-16876

IMAGERY
Locating spaceborne SAR imagery
page 78 NPO-16861

INCONEL (TRADEMARK)
Microstructure and weld cracking in Inconel 718*
page 63 MFS-27121

INDUCTION HEATING
Field repair of thermoplastic windows and canopies
page 94 LAR-13525

INORGANIC PEROXIDES
Air revitalization using superoxides
page 62 ARC-11695

INSPECTION
Inspecting automatically thin ceramics for pinholes
page 49 MSC-21091

INTEGRATED CIRCUITS
Integrated circuit for simulation of neural network
page 38 NPO-17059

IONIZATION COUNTERS
Modulated-voltage metastable-ionization detector
page 58 ARC-11503

IONIZING RADIATION
Effects of radiation on insulators
page 66 NPO-17032

J

JOINTS (JUNCTIONS)
Optical rotary joint for data transfer
page 20 MSC-21182

L

LAMINAR FLOW
Laminar-boundary-layer crossflow sensor
page 81 LAR-13436

LASER DRILLING
Protective coating for laser drilling of silicon
page 95 NPO-17148

LASER RANGE FINDERS
Television-and-laser range-measuring system
page 56 MSC-20867

LIQUID NITROGEN
Swivel joint for liquid nitrogen
page 83 MSC-21160

LOGIC CIRCUITS
Programmable synaptic arrays for electronic neural networks
page 35 NPO-16674

LOGIC DESIGN
The Mark III hypercube-ensemble computers
page 46 NPO-16772

LUBRICANTS
Lubrication handbook for the space industry
page 64 MFS-27169

M

MACHINING
Locating residual wax in small coolant channels
page 59 MFS-29212

MAGNETIC TAPES
Tape-certification program
page 76 NPO-16876

MEMORY (COMPUTERS)
Electronic neural networks
page 42 NPO-16680

Blanket gate would address blocks of memory
page 36 NPO-16682

METEOROLOGICAL FLIGHT
Program reads weather-data tapes from aircraft
page 68 NPO-16744

MICROSTRIP TRANSMISSION LINES
Dual-band microstrip antenna with reactive loading
page 26 MSC-21118

MICROSTRUCTURE
Microstructure and weld cracking in Inconel 718*
page 63 MFS-27121

MICROWAVE ANTENNAS
Dual-band microstrip antenna with reactive loading
page 26 MSC-21118

MICROWAVE COUPLING
Three-waveguide beam and polarization splitter
page 40 NPO-16986

MICROWAVE FILTERS
Designing a microwave band-stop filter
page 32 NPO-16945

MICROWAVE RADIOMETERS
Millimeter-wave radiometer imager
page 50 NPO-17051

MINES (EXCAVATIONS)
Acoustical measurement of mine-shaft length
page 84 LAR-13519

MULTIPROCESSING (COMPUTERS)
The Mark III hypercube-ensemble computers
page 46 NPO-16772

N

NEURAL NETS
Electronic neural networks
page 42 NPO-16680

Electronic neural-network simulator
page 35 NPO-17058

Integrated circuit for simulation of neural network
page 38 NPO-17059

Programmable synaptic arrays for electronic neural networks
page 35 NPO-16674

NEUTRON RADIOGRAPHY
Locating residual wax in small coolant channels
page 59 MFS-29212

NICKEL ALLOYS
Microstructure and weld cracking in Inconel 718*
page 63 MFS-27121

NONDESTRUCTIVE TESTS
Locating residual wax in small coolant channels
page 59 MFS-29212

NONLINEAR SYSTEMS
Minimum-time control for robotic manipulators
page 91 NPO-16919

NUMERICAL FLOW VISUALIZATION
Analysis of flow across cylinders
page 85 MFS-27180

O

OHMMETERS
Adjustable audible continuity tester for delicate circuits
page 18 GSC-13102

OILS
Lubrication handbook for the space industry
page 64 MFS-27169

OPERATING SYSTEMS (COMPUTERS)
Generating cross-references among computer routines
page 78 ARC-11591

OPTICAL COUPLING
Optical rotary joint for data transfer
page 20 MSC-21182

OPTICAL RANGE FINDERS
Television-and-laser range-measuring system
page 56 MSC-20867

P

PHASE SHIFT KEYING
Dual-pilot-tone calibration technique
page 47 NPO-16930

PHASED ARRAYS
Computing radiation characteristics of phased arrays
page 68 LEW-14460

PHOTOMETERS
Compact sun-position sensor
page 30 ARC-11696

PHOTOVOLTAIC CELLS
Coatings boost solar-cell outputs
page 27 NPO-16819

PINHOLES
Inspecting automatically thin ceramics for pinholes
page 49 MSC-21091

PIPES (TUBES)
Swivel joint for liquid nitrogen
page 83 MSC-21160

PLANETARY STRUCTURE
Estimating geophysical parameters from gravity data
page 73 NPO-16671

PLANETS
Estimating geophysical parameters from gravity data
page 73 NPO-16671

PLASTICS
Polyarylene ethers with improved properties
page 61 LAR-13555

Temperature, humidity, and polymer aging
page 65 NPO-16908

PLOTTING
Interactive plotting program
page 76 LAR-13655

POISSON EQUATION
Generating coordinates for aerodynamical calculations
page 97 ARC-11732

POLARIZED ELECTROMAGNETIC RADIATION
Three-waveguide beam and polarization splitter
page 40 NPO-16986

Wide-band, wide-scan antenna for circular polarization
page 26 NPO-16831

POLLUTION
BASIC programming in water and wastewater analysis
page 78 KSC-11298

POLYMERS
Polyarylene ethers with improved properties
page 61 LAR-13555

POSITION SENSING
Position and force control for multiple-arm robots
page 54 NPO-16811

PRESSURE SENSORS
Calibrating nonremovable pressure transducers
page 86 ARC-11792

PROTECTIVE COATINGS
Protective coating for laser drilling of silicon
page 95 NPO-17148

R

RADIATION DISTRIBUTION
Computing radiation characteristics of phased arrays
page 68 LEW-14460

RADIATION EFFECTS
Effects of radiation on insulators
page 66 NPO-17032

RADIO TRANSMISSION
Dual-pilot-tone calibration technique
page 47 NPO-16930

RADIO WAVES
Wide-band, wide-scan antenna for circular polarization
page 26 NPO-16831

SCIENTIFIC/ENGINEERING GRAPHIC TOOLS

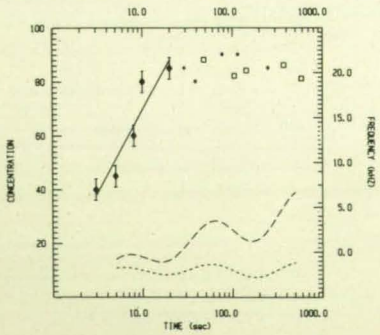
for the IBM PC and compatibles

FORTRAN/Pascal tools: **GRAFMATIC** (screen graphics) and **PLOTMATIC** (pen plotter driver)

These packages provide 2D and 3D plotting capabilities for programmers writing in a variety of FORTRAN/Pascal environments. We support MS, R-M, LAHEY FORTRAN and more. PLOTMATIC supports HP or Houston Instrument plotters. Font module available too!

Don't want to program? Just ask for **OMNIPLOT!** Menu-driven, fully documented integrated scientific graphics. Write or call for complete information and ordering instructions.

GRAFMATIC–PLOTMATIC–OMNIPLOT [S] & [P]



Microcompatibles, 301 Prelude Drive, Silver Spring, MD 20901

(301) 593-0683

Circle Reader Action No. 389

RADIOMETERS
Millimeter-wave radiometer imager
page 50 NPO-17051

RANGE FINDERS
Television-and-laser range-measuring system
page 56 MSC-20867

RECEIVERS
Public-facilities locator for the blind
page 49 MSC-21197

REFLECTORS
Tool removes arc-light reflectors
page 93 MFS-29235

REFRACTORY MATERIALS
Optimization of processing of Si_3N_4
page 64 LEW-14456

REMOTE MANIPULATOR SYSTEM
Minimum-time control for robotic manipulators
page 91 NPO-16919

REMOTE SENSORS
Millimeter-wave radiometer imager
page 50 NPO-17051

ROBOTICS
Minimum-time control for robotic manipulators
page 57 NPO-17070

ROBOTS
Position and force control for multiple-arm robots
page 54 NPO-16811

Unified robot-control system
page 44 NPO-17134

ROLLER BEARINGS
Computer analysis of high-speed roller bearings
page 74 LEW-14512

ROTATING BODIES
Heat exchanger for rotating modular structures
page 80 MFS-26037

ROTATING GENERATORS
Variable-speed, constant-frequency generation of power
page 88 LEW-14054

S

SATELLITES
Analyzing solar-power options for spacecraft
page 73 NPO-16855

SCHEDULING
Computer scheduling of airplane arrivals
page 96 ARC-11742

SERVOCONTROL
Position and force control for multiple-arm robots
page 54 NPO-16811

SHOCK WAVES
Simplified analysis of shock waves
page 83 MSC-20738

SIGNAL FLOW GRAPHS
Difference-equation/flow-graph circuit analysis
page 23 MFS-29245

SILICON
Protective coating for laser drilling of silicon
page 95 NPO-17148

SILICON NITRIDES
Optimization of processing of Si_3N_4
page 64 LEW-14456

SIMULATION
Integrated circuit for simulation of neural network
page 38 NPO-17059

SIMULATORS
Electronic neural networks
page 42 NPO-16680

Electronic neural-network simulator
page 35 NPO-17058

SOLAR CELLS
Coatings boost solar-cell outputs
page 27 NPO-16819

SOLAR POWER SATELLITES
Analyzing solar-power options for spacecraft
page 73 NPO-16855

SOLAR SENSORS
Compact sun-position sensor
page 30 ARC-11696

SOLID LUBRICANTS
Lubrication handbook for the space industry
page 64 MFS-27169

SPACE DETECTION AND TRACKING SYSTEM
Estimating geophysical parameters from gravity data
page 73 NPO-16671

STATORS
Computer program predicts turbine-stage performance
page 74 LEW-14218

STRESS ANALYSIS
Strain-energy-release rates in delamination
page 73 LAR-13698

STRUCTURAL MEMBERS
Truss-core corrugation
page 93 LAR-13438

SUBROUTINES
Generating cross-references among computer routines
page 78 ARC-11591

SUPERSONIC FLOW
Simplified analysis of shock waves
page 83 MSC-20738

SYNTHETIC APERTURE RADAR
Locating spaceborne SAR imagery
page 78 NPO-16861

T

TEMPERATURE CONTROL
Heat exchanger for rotating modular structures
page 80 MFS-26037

THERMOPLASTIC RESINS
Field repair of thermoplastic windows and canopies
page 94 LAR-13525

Polyarylene ethers with improved properties
page 61 LAR-13555

TOOLS
Tool removes arc-light reflectors
page 93 MFS-29235

TRACKING (POSITION)
Compact sun-position sensor
page 30 ARC-11696

TRAFFIC CONTROL
Computer scheduling of airplane arrivals
page 96 ARC-11742

TRANSDUCERS
Calibrating nonremovable pressure transducers
page 86 ARC-11792

TRANSMITTERS
Public-facilities locator for the blind
page 49 MSC-21197

TRANSONIC NOZZLES
Designing a transonic nozzle for efficient cooling
page 90 MFS-29224

TRUSSES
Truss-core corrugation
page 93 LAR-13438

TURBINES
Computer program predicts turbine-stage performance
page 74 LEW-14218

TURBOMACHINERY
Calculating flows in multiple-blade-element cascades
page 76 LEW-14359

V

VIDEO EQUIPMENT
Lightweight video-camera head
page 55 MSC-21246

W

WALL FLOW
Adaptive-wall wind tunnel
page 88 ARC-11717

WATER QUALITY
BASIC programming in water and wastewater analysis
page 78 KSC-11298

WAVEGUIDE FILTERS
Designing a microwave band-stop filter
page 32 NPO-16945

WAVEGUIDES
Three-waveguide beam and polarization splitter
page 40 NPO-16986

WEATHER DATA RECORDERS
Program reads weather-data tapes from aircraft
page 68 NPO-16744

WELDED JOINTS
Holding x-ray film inside ducts
page 80 MFS-29218

WIND TUNNELS
Adaptive-wall wind tunnel
page 88 ARC-11717

X

X-RAY INSPECTION
Holding x-ray film inside ducts
page 80 MFS-29218

Advertiser's Index

Alsys Inc.	(RAC* 341) ...41
Amco Engineering Co.	(RAC 498) 10
Analysis Technology Company	(RAC 546) 67
Ask Mr. Foster	(RAC 527) 37
Aurora Bearings	(RAC 413) 6
Automation Gages	(RAC 453) 14
BASF	(RAC 547) 66
Boeing Technology Corp.	(RAC 367) 89
Cincinnati Sub-Zero	(RAC 528) 15
Data-Control Systems	(RAC 371) 3
Dionics	(RAC 548) ...101
Electro-Scientific Industries	(RAC 530) 85
ERIM	(RAC 475) ...101
Fisher Pen Company	(RAC 451) ...104
Fluoramics Inc.	(RAC 541) 19
Gold Hill	(RAC 465) 45
Gould Inc., Recording Systems Division	(RAC 486) COV III
Grumman Data Systems	(RAC 363) ...8-9
Halcyon Films and Video	(RAC 532) 95
HiTc Superconco	(RAC 544) 95
Honeywell	(RAC 364) 75
Houston Instrument	(RAC 550) 77
IBM Scientific & Technical Division	(RAC 551) .24-25
Ioline Corporation	(RAC 472) 7
Kadar Robotics	(RAC 552) 55
Keithley Instruments, Inc.	(RAC 536) 17
Klinger Scientific Corp.	(RAC 368) 21
Martin Marietta	COV II-1
Martin Marietta Aero & Naval	(RAC 440) 99
McDonnell Douglas Corp.	(RAC 372) COV IV
Microcompatibles, Inc.	(RAC 389) ...102
National Technical Systems	(RAC 358) 79
Nicolet Test Instruments Div.	(RAC 350) 39
Norgren	(RAC 553) 86
Novespace	(RAC 554) 11
NTBM-Research Center	(RAC 500) .74, 91
NTR Systems Inc.	(RAC 539) 85
Oriel Corp.	(RAC 488) ...103
Panasonic Industrial Company	(RAC 380) 31
The Pittsburgh Conference	(RAC 537) 40
RR Software	(RAC 467) 60
Schott Glass Technologies Inc.	(RAC 383) 92
Scientech	(RAC 549) 57
The Space & Rocket Center	(RAC 538) ...102
Supermaterials Company	(RAC 515) 65
Tektronix Spectrum Analyzers	(RAC 329) .28-29
3M Comtal	(RAC 319) 43
Zitel Corp.	(RAC 555) ...4-5

***RAC** stands for **Reader Action Card.** For further information on these advertisers, please circle the RAC number on the Reader Action Card elsewhere in this issue. This index has been compiled as a service to our readers and advertisers. Every precaution is taken to ensure its accuracy, but the publisher assumes no liability for errors or omissions.

REMOTE POSITIONING to 0.10 μm...



With the ORIEL microprocessor based controller for operating up to 3 Encoder Mike DC motor drives.

The controller provides digital position read-out to 0.10 microns with resolution of up to 0.02 microns. Full RS232C built in interface allows easy operation with computers such as IBM, Apple, Hewlett Packard, etc. Constant speed scanning is easily accomplished with digital keyboard control of speeds from 0.5 to 200 microns/sec. If you need motorized positioning for alignment, remote control, scanning or point by point positioning, you should know about our 18011 Controller.



See pages 190-191 of Vol. 1, or contact us for information.

Canadian customers call us direct!

ORIEL CORPORATION

250 LONG BEACH BLVD., P.O. BOX 872, STRATFORD, CT 06497 • (203) 377-8282

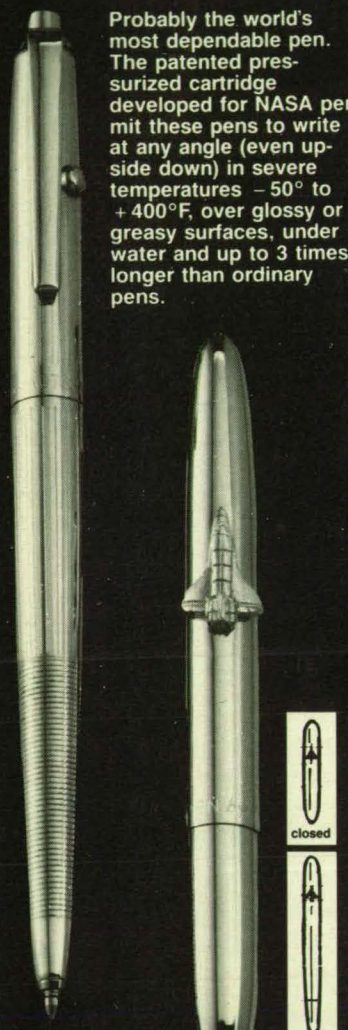
FRANCE UNITED KINGDOM

Circle Reader Action No. 488

fisher
SPACE PEN

...DEVELOPED FOR N.A.S.A.
...USED BY ASTRONAUTS ON SPACE FLIGHTS

Probably the world's most dependable pen. The patented pressurized cartridge developed for NASA permit these pens to write at any angle (even upside down) in severe temperatures −50° to +400°F, over glossy or greasy surfaces, under water and up to 3 times longer than ordinary pens.



Chrome Space Pen with flight button point retraction. Refills readily available.
$12.50

Chrome pocket/purse pen with distinctive Space Shuttle emblem. Unique compact design.
$17.50

Fisher Space Pens are available wherever better pens are sold. Corporate logos and emblems are available. You may order or request further information by contacting:

**743 Circle Avenue
Forest Park, IL 60130
(312) 366-5030**



Mission Accomplished

Through the technology transfer process, many of the systems, methods products pioneered by NASA are reapplied in the private sector obviating duplicate research and making a broad range of new products and services available to the public.

Donning the portable cooling suit, Stevie Roper tests out his new bicycle. The suit features a thermostat for temperature control during physical activity.

Ten year old Stevie Roper could only watch from the sidelines while other children played schoolyard games. Victim to a rare skin disease called hypohydrotic ectodermal dysplasia (HED), Stevie was born without the sweat glands needed to eliminate excess body heat. As a result, according to Dr. Ronald Reisner, head of UCLA's Dermatology Department, "any physical exertion or exposure to warm temperatures could induce heat stroke."

During a July, 1986 visit to his aunt, Sara Moody, Stevie became overheated while riding in a non air-conditioned car. "He was red in the face and gasping for breath," Ms. Moody recalled. "It was scary." Stevie was saved by a quick-thinking cousin who spotted a lawn hose, stopped the car, and doused him with cold water.

The incident prompted Ms. Moody to seek NASA's help."I was hoping NASA had some kind of air conditioned suit that would allow Stevie to live a more normal life," she explained. Moody, a Hampton, Virginia native, contacted NASA's Langley Research Center and explained the problem to Thayer Sheets, a Technology Utilization Specialist. Sheets spent "several days of non-stop telephoning" before locating a company that could help—Life Support Systems, Inc. (LSSI) of Mountain View, California.

A manufacturer of personal cooling gear, LSSI fabricated a child- sized version of its Mark VII Microclimate Cooling Suit. Presented to Stevie in October, the outfit consists of a helmet liner and vest that fit comfortably beneath the boy's clothes. An antifreeze solution cooled by a portable, battery-powered refrigeration unit is pumped through tubes to the garments, which are made from Flexitherm(TM), a temperature-sensitive fabric. The system can eliminate 40-60 percent of Stevie's stored body heat while lowering his heart rate by 50-80 beats per minute.

The Mark VII suit originated in a 1960's NASA program that produced a channeled cooling suit for astronauts. In 1971, the Acurex Corporation, under contract by NASA's Ames Research Center, adapted the technology to a liquid-cooled helmet liner for Vietnam helicopter pilots suffering from heat exhaustion. William Elkins, a key developer of the cooling system for Acurex, left the company in 1980 to form LSSI.

While the cooling suit is used mainly in industrial settings that require heavy protective clothing, such as nuclear power plants and steel mills, it has also found numerous military applications. The product has proven especially effective in reducing the fatigue of aircraft and armored vehicle personnel, according to Mr. Elkins.

In addition, race car drivers including Mario Andretti, A.J. Foyt, and Paul Newman (of motion picture fame) wear the cooling garment to alleviate cockpit heat stress.

LSSI recently initiated a pilot program with multiple sclerosis patients in Colorado designed to increase their exercising ability. "Like Stevie, these people are very sensitive to any rise in core temperature," explained Mr. Elkins. "By having them wear the suit during exercise, we hope to decrease exhaustion levels and thereby extend muscle control over longer periods." The goal, said Elkins, is to "have them become more productive."

For Stevie Roper, the cooling suit has already made a difference. "My sister (Cayce, age 12) and I can ride our bikes together now," he said.

'It's like a miracle," stated Mary Roper, Stevie's mother. "Whenever my son feels himself getting hot, he just puts on his suit."

"He's so much happier now," said Sara Moody, who has organized the HED Foundation to aid others with the disease. "When Stevie was fitted with the vest, he smiled at me and said, 'Auntie, now I can play football like the other kids.' I told him, 'Yes, Stevie, you can. You finally can.' " □

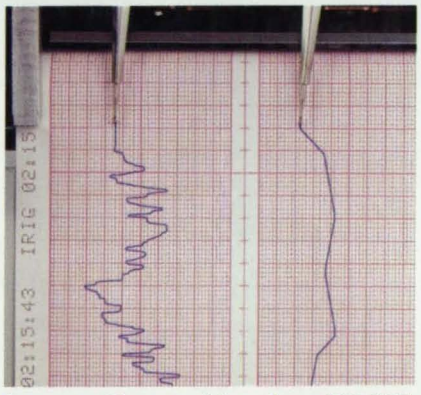
When he goes up to push the envelope, you don't have a split second to waste.



In a test pilot's critical world of action, that split second can mean the difference between life and death. When you're monitoring the parameters that keep test pilots flying, you can't afford the delays inherent to some recording systems.

Gould recording systems, such as the 3000 series and the new MK 200A, show what's happening on board, as it happens. No delay. No questions. A moving pen or video monitor informs you instantaneously about changes in pressure, temperature, pitch, vibration – all the human and mechanical parameters so critical to flight testing.

Highly reliable, rugged Gould strip chart recorders have been the standard in the aerospace industry



for over 40 years. More than 100,000 channels are currently in use.

Fully programmable and remote controllable, both the 3000 and the new MK 200A carry on this tradition, giving you matchless Gould trace quality, IRIG/NASA time code interfacing, and choice of configurations.

So, before you make a decision on telemetry display equipment, flight test the new MK 200A or the other Gould oscillographic strip chart recorders and emulators. They're built on the premise that you don't have a split second to waste.

For more information on real-time recording systems, call **1-800-GOULD-10,** or write Gould Inc., Test and Measurement, 3631 Perkins Avenue, Cleveland, Ohio 44114.

GOULD
Electronics

Circle Reader Action No. 486

THE X-30 IS KID STUFF.

To build higher and stronger. To shape an idea into reality that reaches the sky. For a kid, that's the stuff dreams are made of.

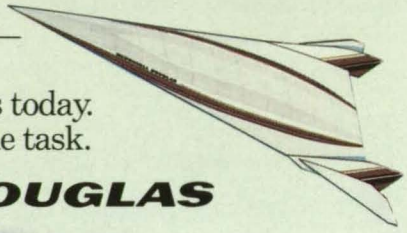
Kid stuff, because it's your kids, and ours, who will gain most from the advances in materials technology required to build the X-30 National AeroSpace Plane, forerunner of the Orient Express.

New materials will be needed to withstand the enormous heat and stress of X-30 flight. They'll be stronger materials, much lighter than those available today, with uses far beyond space flight.

The X-30 is kid stuff, because it is our children who will move from Earth to space and back at far less cost than we do today. And who will one day fly from Los Angeles to Tokyo in two hours aboard an Orient Express.

It is our children who will have—or not have—world leadership in aerospace as a result of our decisions today.

We can do no less than begin the task.



MCDONNELL DOUGLAS



Circle Reader Action No. 372